Oil & Natural Gas Technology

DOE Award No.: DE-FC26-05NT15478

Final Report

Project Title: "Technology on In-Situ Gas Generation to Recover Residual Oil Reserves"

Submitted by:
New Mexico Institute of Mining and Technology
801 Leroy Place, Socorro, NM 87801

Prepared for:
United States Department of Energy
National Energy Technology Laboratory

July 20, 2008

Office of Fossil Energy

National Energy Technology Laboratory

626 Cochrans Mill Road
P.O. Box 10940
Pittsburgh, PA 15236-0940

3610 Collins Ferry Road
P.O. Box 880
Morgantown, WV 26507-0880

One West Third Street, Suite 1400
Tulsa, OK 74103-3519

1450 Queen Avenue SW
Albany, OR 97321-2198

2175 University Ave. South
Suite 201
Fairbanks, AK 99709

Visit the NETL website at:
www.netl.doe.gov

Customer Service:
1-800-553-7681

U. S. Department of Energy Title Page Form Maker v1.0

Report Title: Technology on In-Situ Gas Generation to Recover Residual Oil Reserves		
Report Type: FINAL	Reporting Period Start Date: 10/01/1995 End Date: 02/29/2008	
Principal Author: Dr. Sayavur I. Bakhtiyarov		
Report Issue Date: 05/25/2008	DOE Award No.: DE-FC26-05NT15478	
Submitting Organization: New Mexico Institute of Mining and Technology 801 Leroy Place, Socorro, NM 87801		

Project Summary Page

Technology on In-Situ Gas Generation to Recover Residual Oil Reserves

Cooperative Agreement No.: DE-FC26-05NT15478

Contractor Names: New Mexico Institute of Mining and Technology, Socorro, NM

Award Date: October 1, 2005

Anticipated Completion Dates: February 29, 2008

DOE Award: $559,268.00

Principal Investigator: Dr. Sayavur Bakhtiyarov – New Mexico Institute of Mining and Technology

Program Manager: Traci Rodosta - National Energy Technology Laboratory

Type of Report: **Final Technical Report (revised)**

Date of Report: May 25, 2008

Reporting Period: **October 1, 2005 to February 29, 2008**

Table of Contents

List of Graphical Materials

Executive Summary

The project involved a final research and development in the United States a technology that was developed at the Institute for Geology and Development of Fossil Fuels in Moscow, Russia. Before the technology can be convincingly adopted by United States oil and gas producers, a preliminary laboratory research was conducted. In Phase I, the research team verified if the Russian formulations generate sufficient pressure and CO_2 concentration in-situ so that miscibility can be attained with typical oils. In the second phase of the project, the research team investigated an effectiveness of the foams generated by this process in order to improve sweep efficiency in porous rock with a range of permeabilities.

Background

The traditional CO_2 flood technology presents the following opportunities and challenges.
Advantages include:

- Dissolution of CO_2 (~5-10 %) in water results in:
  - Viscosity increase.
  - Reduction of mobility.
- Dissolution of CO_2 in oil results in:
  - Viscosity decrease.
  - Increase in oil recovery efficiency.
  - Reduction of surface tension between oil and water phases.
  - Increase both in oil production and sweep efficiency.

Disadvantages include:

- CO_2 breakthrough in producing oil wells.
- Small alterations of thermobaric equilibrium conditions result in reducing CO_2 concentration in oil and, consequently, a coagulation and deposition of asphaltenes and resins.
- Corrosion of oilfield equipment.
- Problems related to transportation of great volumes of CO_2 gas.
- Special equipment required for safe storage and transportation of CO_2 gas.
- High cost of the technology.
- Insufficient amount of CO_2 in many oil-fields.

The new in-situ CO_2 generation technology maintains all positive effects of traditional CO_2 flood method, and prevents the disadvantages of it.

Previous oilfield tests include the following:

- Samotlor oilfield, Tyumen Oil Co. (Russia), involving 121 operations from 1999 to 2001.
- Novo-Pokursky oilfield, Slavneft-Megionneftegas JSC (Russia), involving 56 operations from 2000 to 2004.
- Gunyuang oilfield (China), involving 20 operations covering 45 producing oil wells.

Project highlights include the following:

- Two experimental devices have been designed and built for measuring the pressure and the volume of the CO_2 gas generated according to the proposed new Russian technology.
- Preliminary experimental results on CO_2 gas pressure measurements demonstrated that the gas pressure increases with 1) polymer/surfactant addition, 2) decreasing temperature, and 3) increasing salinity of the system.
- At certain salinity values, the generated gas pressure starts decreasing.
- An alternative "gas-yielding" reactant was proposed and tested in order to optimize the reaction process.
- Injection sequence of the gas-forming and gas-yielding materials affects the reaction characteristics, but the total amount of generated CO_2 gas does not vary significantly.
- Regardless of the sequences of the injected solutions, the maximum attainable pressures are less than the calculated pressures due to the chemical equilibrium in the system.
- Slim tube and core flood experiments were conducted to define the sweep efficiency of the in-situ generated CO_2 gas.
- Three liquids (decane, crude and mineral oils) were used as fluids to be displaced in slim tube and core flood experiments. Distilled water and brine have been used as displacing fluids. The experimental data showed that a light mineral oil exhibited acceptable displacement efficiency (73.64%), and a cleaning of the system was easier and less time-consuming. Therefore, the mineral oil was chosen as a displaced liquid during the tests.
- The presence of the salt in the displacing liquid resulted in up to 7% increase in displacement efficiency (80.86%) if compared to that when distilled water was used as a displacing liquid.
- It has been observed that up to 3.3 % additional recovery obtained during injection of GY+GF reactants and 11.6% additional recovery during the injection of GY+GF system in combination with cationic surfactant.

Benefits

The new technology offers the following benefits:

- Enhanced resistance to injected water flow due to steady foamy barrier.
- Enhanced extraction of hydrocarbon components from porous media surface at certain thermobaric conditions of super-critical CO_2 gas.
- Increased sweep efficiency due to in-situ generated CO_2 gas.
- No need for additional pipelines and power supplies for CO_2 gas injection. Applicability in severe-climatic and remote zones.

Technology Transfer

Workshops and Professional Courses

- **Canadian Institute's Enhanced Oil Recovery Conference, Calgary, Alberta, Canada,** April 30 – May 2, 2008
- **Southwestern Petroleum Short Course,** Petroleum Industry of West Texas & Texas Tech University, Lubbock, TX, April 21-24, 2008
- **Workshop "Improved Oil Recovery"**, Society of Petroleum Engineers, Tulsa, OK, April 22-26, 2006
- **Workshop "PTTC DOE CO_2 Enhanced Oil Recovery"**, U.S. Department of Energy, Houston, TX, February 22, 2006

Publications

1. A. Kh. Shakhverdiyev, I. E. Mandrik, G. M. Panakhov, S. I. Bakhtiyarov and E. M. Abbasov, 2007, "Perspectives of Rheogazochemical Enhanced Oil Recovery Technology for Extraction Residual Carbohydrates Reserves", **Proceedings of Azerbaijan National Academy of Sciences, The Earth Sciences Series**, No. 3, pp. 38-47 (in Russian).
2. S. I. Bakhtiyarov, R. Grigg, R. Svec and O. Coskun, 2007, "Experimental Study of Salinity Effect on In-Situ Generated Carbon Dioxide", **International Journal of Manufacturing Science and Technology,** Vol. 1, No. 1, June, pp. 47-59.
3. S. I. Bakhtiyarov, A. K. Shakhverdiyev, G. M. Panakhov and E. M. Abbasov, 2007, "Volume and Pressure Measurements in Oil Recovery by In-Situ Gas Generation", **International Journal of Manufacturing Science and Technology,** Vol. 1, No. 1, June, pp. 1-11.
4. S. I. Bakhtiyarov and R. A. Overfelt, 2007, "A New Sand Fill and Compaction Method in Lost-Foam Process", **NASA Tech Brief**, MFS-31679-1.
5. G. M. Panakhov, S. I. Bakhtiyarov, A. Kh. Shakhverdiyev and E. M. Abbasov, 2006, "Kinetics of Gas Generation in Water Solution", **Transactions of Azerbaijan National Academy of Sciences. Issue: Mathematics and Mechanics Series of Physical-Technical & Mathematical Science,** Vol. 26, No. 4, pp. 239-246.
6. A. Kh. Shakhverdiev, G. M. Panakhov, E. M. Abbasov, I. E. Mandrik and S. I. Bakhtiyarov, 2006, "Integrative Efficiency of Bed Stimulation at Intrastratal Gas Generation", **Oil Industry Journal**, No. 11, pp. 76-78 (in Russian).
7. S. I. Bakhtiyarov, A. K. Shakhverdiyev, G. M. Panakhov and E. M. Abbasov, 2006, "Pressure and Temperature Measurements during Stoichiometric Reaction of In-Situ Carbon Dioxide Generation", **International Journal of Manufacturing Science and Technology** (accepted).
8. S. I. Bakhtiyarov, 2008, "Foam Stability in In-Situ CO_2 Enhanced Oil Recovery Technology" Proceedings, **ASME Fluids Engineering Division Summer Conference,** Symposium on Transport Phenomena in Manufacturing Processes, Jacksonville, FL, August 10-14, 2008 (submitted)
9. S. I. Bakhtiyarov, 2007, "A Novel Enhanced Oil Recovery Technology: In-Situ CO_2 Generation", Proceedings, **The 54th Southwestern Petroleum Short Course**, Lubbock, TX, April 25-26, 2007, pp. 228-238.
10. A. Kh. Shakhverdiyev, I. E. Mandrik, G. M. Panakhov, E. M. Abbasov and S. I. Bakhtiyarov, 2007, "Novel Rheogazochemical Technologies of Enhanced Oil Recovery", Abstracts of the **7th Scientific and Practical Conference "Geology and Development of Oilfields with Hard to Recover Reserves"**, Gelenjik, Russia, September 25-27, 2007, pp. 86-87 (in Russian).

11. A. Ghadimipour and S. I. Bakhtiyarov, 2007, "Slim Tube Studies of New CO_2 Enhanced Oil Recovery Technology", Abstracts of the **19th Annual Rio Grande Symposium on Advanced Materials**, Albuquerque, NM, October 9, 2007, p. 39.
12. S. I. Bakhtiyarov, 2007, "Effect of Surfactant on Volume and Pressure of Generated CO_2 Gas", SPE Paper No. 106902, Proceedings of **SPE Production and Operation Symposium,** Oklahoma City, OK, March 31 – April 3, 2007.
13. S. I. Bakhtiyarov, A. K. Shakhverdiyev, G. M. Panakhov and E. M. Abbasov, 2007, "Effect of Surfactant on Volume and Pressure of Generated CO_2 Gas" (Paper # 106902). **Proceedings of SPE Production and Operation Symposium**, Oklahoma City, OK, March 31 – April 3, 2007.
14. S. I. Bakhtiyarov, A. K. Shakhverdiyev, G. M. Panakhov and E. M. Abbasov, 2007, "Polymer/Surfactant Effects on Generated Volume and Pressure of CO_2 in EOR Technology", **6th Symposium on Transport Phenomena in Manufacturing Processes, 5th Joint 2007 ASME/JSME Fluids Engineering Summer Meeting**, San Diego, CA, July 30-August 2, 2007.
15. G. M. Panakhov, A. K. Shakhverdiyev, S. I. Bakhtiyarov and E. M. Abbasov, 2007, "Kinetics of Gas-Generation Processes in Liquid Solutions", Proceedings of **12th International Conference on Mathematics and Mechanics**, Baku, Azerbaijan.
16. S. I. Bakhtiyarov, R. Grigg, R. Svec and O. Coskun, 2006, "Experimental Study of Salinity Effect on CO_2 Flood", Proceedings of **6th International Scientific Practical Conference XAZARNEFTGASYATAG-2006**, Baku, Azerbaijan, October 12-14, 2006.
17. S. I. Bakhtiyarov, A. K. Shakhverdiyev, G. M. Panakhov and E. M. Abbasov, 2006, "Oil Recovery by In-Situ Gas Generation: Volume and Pressure Measurements", **ASME Joint U.S.-European Fluids Engineering Summer Meeting**, Miami, FL, July 17-20, 2006, Paper # FEDSM2006-98359.
18. O. Coskun, R. Grigg, R. Svec, D. A. Siginer and S. I. Bakhtiyarov, 2006, "The Effect of Salinity on In-Situ Generated CO_2 Gas: Simulations and Experiments", **Symposium on "Advances in Materials Processing Science", ASME International Mechanical Engineering Congress and Exposition**, Chicago, IL, November 5-10, 2006, Paper # IMECE2006-15703.
19. S. I. Bakhtiyarov, A. K. Shakhverdiyev, G. M. Panakhov, E. M. Abbasov and D. A. Siginer, 2006, "In-Situ Carbon Dioxide Generation for Oil Recovery: Experimental Study of Pressure and Temperature Variations during Stoichiometric Reaction", **Symposium on "Rheology and Fluid Mechanics on Nonlinear Materials", ASME International Mechanical Engineering Congress and Exposition**, Chicago, IL, November 5-10, 2006, Paper # IMECE2006-15708.

Presentations at Conferences and Symposia

1. **ASME Fluids Engineering Division Summer Conference,** Jacksonville, FL, August 10-14, 2008: "Foam Stability in In-Situ CO_2 Enhanced Oil Recovery Technology"
2. **Canadian Institute's Enhanced Oil Recovery Conference,** Calgary, Alberta, Canada, April 30 – May 2, 2008: "In-Situ CO_2 Flood Technology"
3. **Petroleum Short Course,** Petroleum Industry of West Texas & Texas Tech University, Lubbock, TX, April 21-24, 2008

4. **7th Scientific and Practical Conference "**Geology and Development of Oilfields with Hard to Recover Reserves**"**, Gelenjik, Russia, September 25-27, 2007: "Novel Rheogazochemical Technologies of Enhanced Oil Recovery"
5. **19th Annual Rio Grande Symposium on Advanced Materials**, Albuquerque, NM, October 9, 2007: "Slim Tube Studies of New CO_2 Enhanced Oil Recovery Technology"
6. **6th Symposium on Transport Phenomena in Manufacturing Processes, 5th Joint 2007 ASME/JSME Fluids Engineering Summer Meeting**, San Diego, CA, July 30-August 2, 2007: "Polymer/Surfactant Effects on Generated Volume and Pressure of CO_2 in EOR Technology"
7. **54th Southwestern Petroleum Short Course**, Lubbock, TX, April 25-26, 2007: "A Novel Enhanced Oil Recovery Technology: In-Situ CO_2 Generation"
8. **SPE Production and Operation Symposium, Oklahoma City, OK, March 31 – April 3, 2007:** "Effect of Surfactant on Volume and Pressure of Generated CO_2 Gas"
9. **SAMSON Technical Meeting, Midland, TX, February 21, 2007:** "In-Situ CO_2 Generation Technology"
10. **Trans-Pecos SPE Meeting, Odessa, TX, November 14, 2006: "**Reenergizing Reservoir"
11. **Engineers' Society of Tulsa, Tulsa, OK, October 2, 2006:** "Directing Unrecovered Oil to a Desired Destiny"
12. **6th International Scientific Practical Conference XAZARNEFTGASYATAG-2006, Baku, Azerbaijan, October 12-14, 2006:** "Experimental Study of Salinity Effect on CO_2 Flood"
13. **SPE Enhanced Oil Recovery Forum, Broomfield, CO, June 25-30, 2006:** "Enhanced Oil Recovery by In-Situ Generated CO2 Gas: Volume and Pressure Measurements"
14. **12th International Conference on Mathematics and Mechanics, Baku, Azerbaijan, June 2006:** "Kinetics of Gas-Generation Processes in Liquid Solutions"
15. **ASME Joint U.S.-European Fluids Engineering Summer Meeting**, **Miami, FL, July 17-20, 2006:** "Oil Recovery by In-Situ Gas Generation: Volume and Pressure Measurements"
16. **ASME International Mechanical Engineering Congress and Exposition, Chicago, IL, November 5-10, 2006:**
    1) "The Effect of Salinity on In-Situ Generated CO_2 Gas: Simulations and Experiments"
    2) "In-Situ Carbon Dioxide Generation for Oil Recovery: Experimental Study of Pressure and Temperature Variations during Stoichiometric Reaction"

Introduction

This final technical report covers the period October 1, 1995 to February 29, 2008. This chapter begins with an overview of the history of Enhanced Oil Recovery techniques and specifically, CO_2 flood. Subsequent chapters conform to the manner consistent with the Activities, Tasks, and Sub-tasks of the project as originally provided in Exhibit C1 in the Project Management Plan dated September 20, 1995. These chapters summarize the objectives, status and conclusions of the major project activities performed during the project period. The report concludes by describing technology transfer activities stemming from the project and providing a reference list of all publications of original research work generated by the project team or by others regarding this project.

Project Overview

The overall objective of this project was a final research and development in the United States a technology that was developed at the Institute for Geology and Development of Fossil Fuels in Moscow, Russia. Before the technology can be convincingly adopted by United States oil and gas producers, the laboratory research was conducted at Mew Mexico Institute of Mining and Technology.

The experimental studies were conducted to measure the volume and the pressure of the CO_2 gas generated according to the new Russian technology. Two experimental devices were designed, built and used at New Mexico Tech facilities for these purposes. The designed setup allowed initiating and controlling the reaction between the "gas-yielding" (GY) and "gas-forming" (GF) agents proposed by Russian technology. The temperature was controlled, and the generated gas pressure and volume were recorded during the reaction process. Additionally, the effect of surfactant addition on the effectiveness of the process was studied. An alternative GY reactant was tested in order to increase the efficiency of the CO_2 gas generation process.

The slim tube and the core flood experimental studies were conducted to define the sweep efficiency of the in-situ generated CO_2 gas. A set of core flood experiments were conducted to define effect of surfactant on recovery efficiency. The results demonstrated obvious advantages of the foamy system over the brine solution in order to achieve higher sweep efficiency and recovery coefficient. It is shown that a slug injection is not an efficient method for mixing GY and GF solutions and it can't generate considerable gas inside the slim-tube.
The project was implemented by a team including:

1. New Mexico Institute of Mining and Technology, Socorro, NM, USA
2. Institute for Geology and Development of Fossil Fuels in Moscow, Russia
3. Institute of Mathematics and Mechanics, Azerbaijan National Academy of Sciences, Baku, Azerbaijan

Acknowledgments

This research was performed under the Program of the U.S. Department of Energy (DOE), National Energy Technology Laboratory, Office of Fossil Energy, and contract number DE-FC26-05NT15478. The Contracting Officer's Representative is Traci Rodosta, with the DOE National Energy Technology Laboratory in Tulsa, OK.

The following individuals and companies provided valuable assistance to this project through participation on the project team or as consultants to the team:

New Mexico Institute of Mining and Technology, Socorro, NM, USA:
Dr. Sayavur Bakhtiyarov
Dr. Reid Grigg
Dr. Randy Seright
Robert Svec
Robert Sneider
Onur Coscun
Amir Ghadimipour
Murad Aliyev

Institute for Geology and Development of Fossil Fuels in Moscow, Russia:
Azizaga Shakhverdiyev

Institute of Mathematics and Mechanics, Azerbaijan National Academy of Sciences, Baku, Azerbaijan:
Geilani Panakhov
Eldar Abbasov

NOMENCLATURE

E_R	Recovery Efficiency (considering total pore volume)
E_R^*	Recovery Efficiency (considering slim-tube pore volume)
E_D	Displacement Efficiency
E_V	Sweep Efficiency
P	Pressure
ΔP	Pressure difference between inlet and outlet of slim-tube
P_{in}	Inlet pressure of slim-tube
P_{out}	Outlet pressure of slim-tube
$P_{dome\text{-}in}$	Nitrogen pressure on the dome of inlet BPR
$P_{dome\text{-}out}$	Nitrogen pressure on the dome of outlet BPR
V_P	Volume of production
Q	Flowrate
Q_{inj}	Injection flowrate
T	Temperature
K	Permeability
Φ	Porosity
μ	Viscosity
ρ	Density

LIST OF ABBREVIATIONS

ISCGT	In-Situ CO_2 Generation Technique
EOR	Enhanced Oil Recovery
ESP	Electrical Submersible Pumps
IOIP	Initial Oil in Place
MEOR	Microbial Enhanced Oil Recovery
IFT	Interfacial Tension
IGDFF	Institute for Geology and Development of Fossil Fuels
FVF	Formation Volume Factor
MMP	Minimum Miscibility Pressure
API	American Petroleum Institute (gravity unit)
WAG	Water Alternating Gas
GF	Gas Forming
GY	Gas Yielding
THF	Tetrahydrofuran
BPR	Back Pressure Regulator
psi	Pound per Square Inch
psia	Absolute psi
psig	Gauge psi
Mcf	1000 cubic feet
cp	centi-poise (viscosity unit)
v/v	Volume percent
ppm	Part Per Million
min	Minute

Activity 1. Slim Tube Experiments

1. INTRODUCTION

1-1- Introduction

A fast growth of worldwide oil demand and the subsequent surge in oil prices is intensifying the efforts to increase oil production. These efforts are classified in three categories: finding new oil reserves, developing proven reserves and improving the efficiency of oil production. The rate of new oilfield discoveries is in steady decline and most of the producing oilfields are in late stages of production which makes it most unlikely to have any breakthrough in the first two categories. But taking into account the fact that about two third of reservoir oil can not be recovered by conventional production methods, the importance of improving oil production efficiency by enhanced oil recovery techniques (EOR) can be acknowledged.

CO_2 flooding is the most commonly used EOR technique. A very good solvency property of CO_2 at high pressures in addition to oil swelling and reduction in oil viscosity caused by dissolved CO_2 in oil are main reasons behind the effectiveness of CO_2 flooding. But this method also has drawbacks. Very low viscosity and high mobility of CO_2 makes it to channel through the reservoir and leave large portions of reservoir untouched. Besides that, high cost of CO_2 transportation and compression makes this process relatively expensive and uneconomical especially for remote areas.

In-situ CO_2 generation technique (ISCGT) is designed to address CO_2 flooding method's shortcomings and makes CO_2 flood method economical in the places where CO_2 flooding is not feasible.

In this Activity 1 study, ISCGT is evaluated by the use of slim-tube displacement tests. Chapter 2 includes a summary and literature review about different EOR methods with more emphasis on CO_2 flooding. In chapter 3 ISCGT and the mechanisms involved in it are explained thoroughly. Chapter 4 describes the methods and liquids used in this study. The experimental setups and their operating procedure and also test results are detailed in chapter 5. The next chapter consists of the discussions and interpretations based on the experimental results of chapter 5 and finally concluding remarks are presented in chapter 7.

1-2- Study objectives and scope

1-2-1- Study objectives

1- Evaluation of the effectiveness of in-situ CO_2 generation technique as an EOR method by comparing it to brine-flooding and conventional CO_2 flooding.

2- Investigating the presence of free CO_2 in the system: CO_2 can be in two states in the system: (i) dissolved CO_2 in the oil and brine, and (ii) CO_2 in the form of free gas in the reservoir. There is free CO_2 in the system if the gas generation by this technique is enough to over-saturate the liquids (brine and oil), and therefore the excess CO_2 would be in the gas form. One of the requirements of having miscible flooding is to have CO_2 in the free form in the system. The generated CO_2 can become in contact with oil in two ways: as a free gas or by transferring from water to oil. But transfer of the dissolved gas from water to oil can't be large enough to make the gas and oil to reach miscibility. Hence, without a free gas in the system there would be no miscibility. On the other hand, surfactant can generate foam only in the presence of free gas. Therefore, it is of practical interest to investigate the presence of free CO_2 in the system.

3- Evaluation of the effectiveness of surfactant in foam generation and also in reducing the interfacial tension between water and oil
4- Evaluating the efficiency of different injection methods
5- Investigating the effects and awfulness of corrosion of the equipment caused by this process

1-2-2- Study scope

Our research is focused on evaluation of the efficiency of in-situ CO_2 generation technique to enhance oil recovery and also investigation of the corrosion effects on the equipment caused by this technology.

Because of the geometry of slim-tube (long and thin), the effect of viscous fingering in the experiments is low, which causes nearly perfect sweep efficiencies. Thus, the recovery efficiency evaluation is almost limited to the displacement efficiency study. Besides that, the homogenous glass beads used in the experiments canceled out the effect of heterogeneity in the study.

Also, generated heat by the exothermal chemical reaction between the reactants wasn't taken into account, because all the experiments were performed inside a temperature bath at constant temperature.

The oil used in the experiments didn't contain dissolved gas. Therefore, the effect of already dissolved gas on the interaction between oil and brine and also the change in CO_2 solubility in oil has been ignored.

2. BACKGROUND AND LITERATURE REVIEW

Oil Accounts for a large percentage of the world's energy consumption, ranging from 32% for Europe and 40% for North America up to a high of 53% for the Middle East [1], and despite all the investment on alternative energy resources in recent years, projections show that there will not be any considerable change in world oil dependency in the near future. [2]

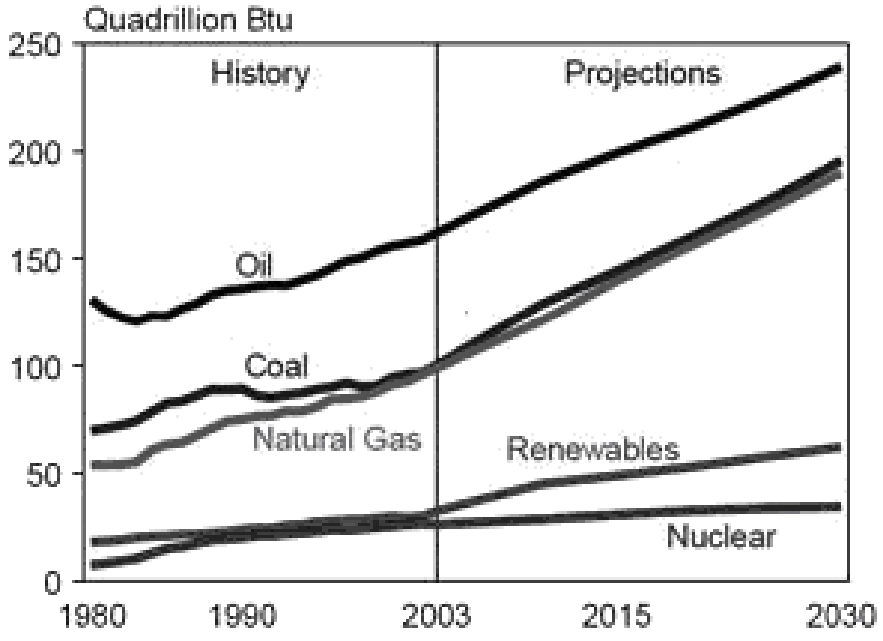

Figure 1. World marketed energy use by energy type, 1980-2030 [2]

Oil consumption is currently around 84 million barrel per day, and almost all of it is obtained by extraction from oil wells drilled in oil reservoirs. An oil reservoir is often thought of as being an underground lake of oil, but it is actually composed of hydrocarbons contained in porous rock formations.

2-1- Primary Recovery

After an oil well is drilled and made ready to produce oil, a collection of regulating valves called charismas tree, are installed on well bore and the production phase of oil well life begins. As long as the pressure in the reservoir remains high enough, the charismas tree is all that required to produce the oil. The production results in a pressure drop in the reservoir which follows by the expansion of the gas cap and aquifer, and in the generation of solution gas which pushes up the oil and helps to maintain the pressure and continue the production for a longer period of time. About 15% of the oil in reservoir is produced in this stage of production called primary recovery.

2-2- Secondary Recovery

After some time, the underground pressure falls to a point that it is insufficient to push the oil to the surface. The remaining oil is extracted using secondary oil recovery methods. Sometimes pumps, such as beam pumps and electrical submersible pumps (ESPs), are used to bring the oil to the surface. Other secondary recovery techniques increase the reservoir's pressure by water injection, natural gas reinjection and gas lift, which inject air, carbon dioxide or some other gas into the reservoir. The most common technique, water flooding, utilizes injector wells to inject large volumes of water under pressure into the hydrocarbon–bearing zone. As the water flows through the formation toward the producing wellbore, it sweeps some of the oil it encounters along with it. Upon reaching the surface, the oil is separated out for sale and the water is re-injected. While somewhat more expensive than primary production, water flooding can recover an additional 10 to 30 percent of initial oil in place (IOIP). [3]

2-3- Tertiary Recovery or Enhanced Oil Recovery (EOR)

Enhanced Oil Recovery (EOR) begins when secondary oil recovery methods are no longer enough to sustain the oil production, but only when the oil can be extracted profitably, which depends on the cost of extraction method and the current price of crude oil. Type of extraction method in turn depends on the reservoir characteristics. The EOR is a highly individualized process, specific to each field’s characteristics. Tertiary recovery allows another 5 to 15% of the reservoir's oil to be recovered. The EOR processes can be divided into four major categories: gas flooding, chemical flooding, thermal recovery and Microbial Enhanced Oil Recovery (MEOR).

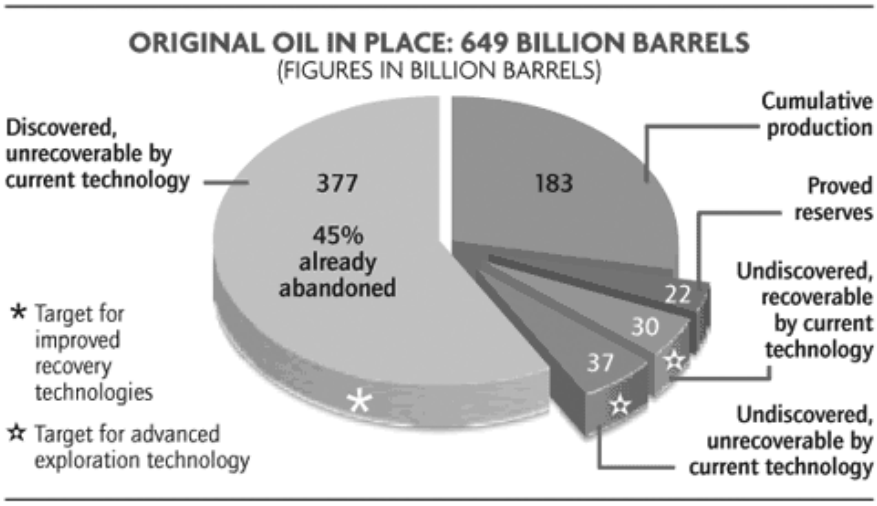

Figure 2. Distribution of world initial oil in place into produced, reserves, estimated undiscovered, recoverable and unrecoverable oil. [3]

2-3-1- Gas Flooding

Gas injection is the most commonly used EOR technique. Carbon dioxide, natural gas, flue gas and Nitrogen are injected in miscible or immiscible forms with the reservoir oil to enhance the production. Miscible gas vaporizes hydrocarbons, and enables oil to flow more freely and it is often followed by injection of water. When reservoir pressure is too low or the oil gravity is too dense, the injected gas remains physically distinct from the oil within the reservoir. However, it can still improve oil recovery by causing the oil to swell, reducing the oil's viscosity and improving its mobility [5]. Miscible CO_2 flooding can be attained in lower pressures comparing to other gases, but it's more expensive. Gas injection accounts for nearly 50 percent of EOR production in the United States [6].

2-3-2- Thermal Recovery

Thermal EOR methods include steam injection and in-situ combustion of hydrocarbons. A common principle of thermal EOR is to heat heavy oil, which reduces its viscosity sufficiently to enable it to flow readily and be economically recovered. Steam processes are generally applied to shallow heavy oil deposits [5].

In in-situ combustion part of the oil in the reservoir is set on fire, and compressed air is injected to keep it burning. Gases and heat advance through the formation, moving the oil toward the production wells [7]. Thermal techniques account for over 50 percent of U.S. EOR production, primarily in California [6].

2-3-3- Chemical Flooding

Chemical flooding technologies are subdivided into alkaline–surfactant–polymer processes. [3] The surfactant slug is injected primarily to lower interfacial tension (IFT) between the water and oil. A lowering of the IFT results in more efficient oil displacement and a significant reduction in oil saturation. [8] When there is gas in the displacing front, foamer agents are usually used in surfactants to decrease the mobility of displacing fluid and to enhance the production.

Polymers increase the viscosity of water front and improve its mobility. Occasionally polymers are injected as drive fluids behind the active surfactant slug to decrease the mobility of the front. [7] Less expensive alkaline chemicals are injected and react with organic petroleum acids in

certain oils to create surfactants in-situ to mobilize residual oil by lowering interfacial tension between oil and water. [10] However, high cost of surfactants and polymers has hindered the widespread use of chemical flood methods, but recent increase in oil prices has made these technologies look more promising.

2-3-4- Microbial Enhanced Oil Recovery (MEOR)

Any process that uses microbes to increase oil and gas production is called MEOR. The microbial gas processes are defined as: [9]

1- Permeability modification: Microbes alongside nutrients are injected into the reservoir to plug high permeability channels. The microbes flow into these channels and grow there partially plugging them. Subsequent water floods get diverted to unswept regions and recover more oil.
2- Oil bio-degradation: Certain bacteria attack hydrocarbons by feeding on them and convert them to smaller molecules that generally have lower viscosity.
3- Gas production: Two products of bacteria metabolisms are carbon dioxide gas and methane. They can help the oil production by dissolving in it and reducing its viscosity.

Microbial EOR is still in research phase with only one small R&D project reported, and no other projects are planned. [5]

2-4- Recovery Efficiency: [7, 10]

A key factor affecting the design of a flooding project is the recovery efficiency (E_R). It indicates the portion of initial oil in place that can be recovered by a flooding process.

$$E_R = \frac{Oil\ recovered}{Initial\ oil\ in\ place\ (IOIP)}$$

Recovery efficiency depends on two factors:

1) Displacement Efficiency (E_D): Displacement efficiency is the fraction of displaced fluid within the swept volume that has been displaced from the pores by displacing fluid. In other words, it is a measure how easily the oil can be removed from the rock pores.

$$E_D = \frac{Oil\ displaced}{Oil\ in\ place(OIP)\ of\ swept\ volume}$$

2) Sweep Efficiency (E_V): Sweep efficiency is the portion of the total reservoir volume contacted by injected displacing fluid.

$$E_V = \frac{Oil\ in\ place\ of\ swept\ volume}{Initial\ oil\ in\ place(IOIP)}$$

Recovery efficiency (E_R) is related to these efficiencies by,

$$E_R = E_D \times E_V$$

All of the enhanced oil recovery methods improve oil recovery by increasing one or both of these factors. Thermal flooding enhances displacement efficiency by decreasing the oil viscosity, gas flooding increases displacement efficiency by reducing interfacial tension (IFT) between displacing front and the oil and also by reducing the oil viscosity. Surfactant increases the displacement efficiency by decreasing IFT and if it contains foamer agents it also improves sweep efficiency by reducing the mobility of the displacing front. Therefore, the ultimate goal of all EOR techniques is to increase displacement efficiency and sweep efficiency as much as possible.

2-5- CO_2 flooding:

CO_2 flooding is the fastest growing EOR technique. In 2002, for the first time, the number of CO_2 projects exceeded the number of thermal recovery projects in United States. [11] Most of the CO_2 flooding projects are underway in United States. [5]

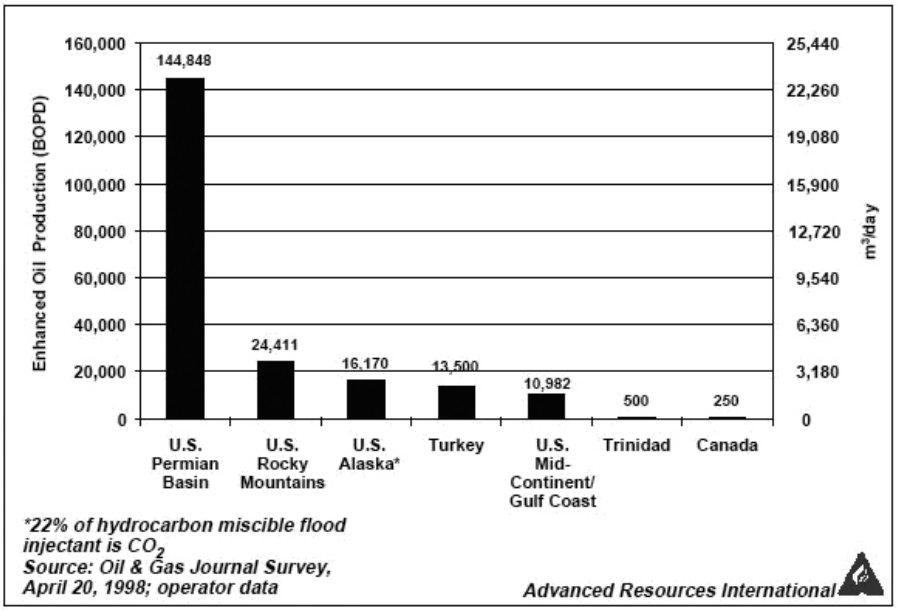

Figure 3. CO_2 flooding oil production (1998) [5]

Liu et al [13] mentioned following reasons for the increase in the use of CO_2 flooding:

- CO_2 remains a dense fluid over much of the range of reservoirs pressures and temperatures.
- CO_2 fluid is miscible or partial miscible with many hydrocarbon components of crude oil at reservoir conditions.
- Dense CO_2 has low solubility in water compared to oil.
- CO_2 in high pressures has higher viscosity comparing to other gases used in gas flooding.
- The US has CO_2 resources near many oil fields.
- CO_2 sequestration has environmental benefits by reducing green house gas effects.

CO_2 is a very compressible gas and at high pressures forms a phase whose density is close to that of liquid and with a higher viscosity comparing to other gases (although it remains low compared to that of liquids). Dense phase CO_2 has the ability to extract hydrocarbon components from oil more easily than if it were in the gaseous phase. [12]

In figure 4, density of carbon dioxide in different pressures and at 105°F is compared to other gases' densities used in gas flooding applications. It can be seen that Nitrogen and CH_4 density increases linearly with a slow rate but there is a big increase in carbon dioxide density after the pressure of 1000 psi.

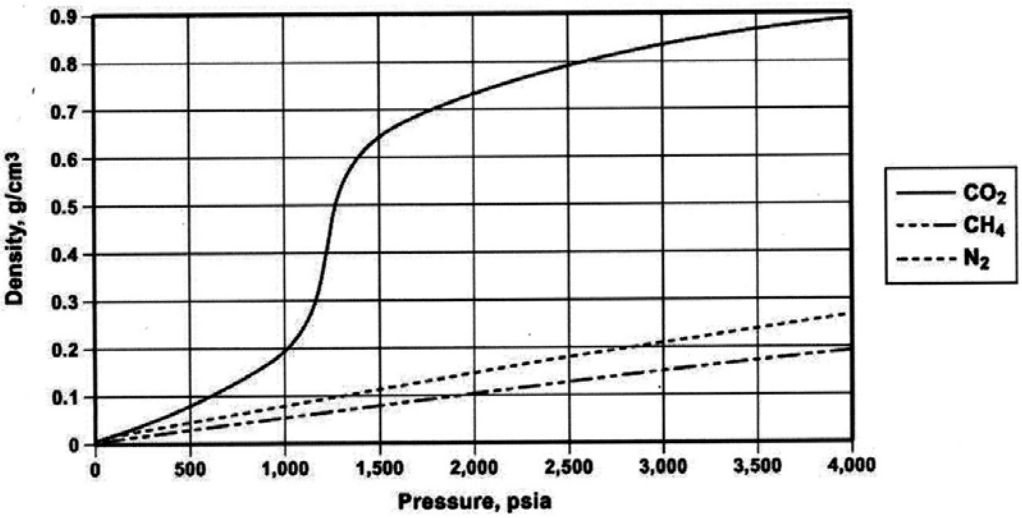

Figure 4. Variation of CO_2, CH_4 and N_2 densities at 105°F vs. pressure [12]

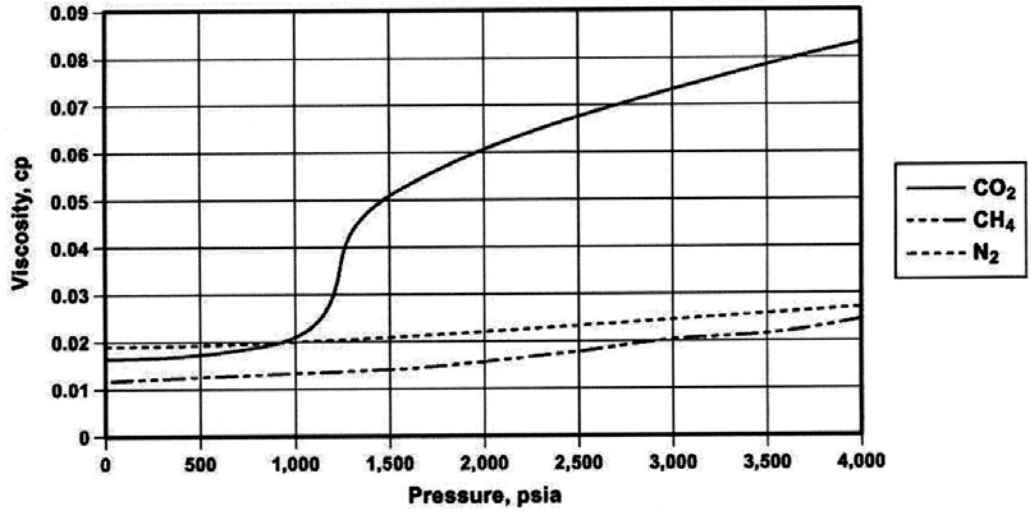

Figure 5. Variation of CO_2, CH_4 and N_2 viscosities at 105°F vs. pressure [12]

Carbon dioxide is much more soluble in oil than in water. Therefore most of injected CO_2 dissolves in oil and increases its viscosity and volume meanwhile there isn't a considerable change in viscosity and volume of the oil. Mungan [14] indicated that the change in viscosity and formation volume factor of water caused by the low-$C0_2$ solution can be shown to be less than 1 %. Chang et al [16] developed correlations for solubility of CO_2 in brine as well as for the effect of dissolved CO_2 in water FVF. Their simulations showed that when the water is present, only 5 to 10% of the carbon dioxide is dissolved in the water which reduces the oil recovery by 5%.

Sequestration of carbon dioxide is one of the options currently being studied that can decrease the amount of released CO_2 to the atmosphere. Depleted or partially depleted oil reservoirs are one of the geologic targets for carbon sequestration. [15] In this technique, carbon dioxide is captured and extracted from industries flue gases and transported and injected into suitable oil reservoirs to increase the oil production.

With high oil prices, this method can be an economical enhanced oil recovery application.

2-5-1- Minimum Miscibility Pressure (MMP):

The minimum miscibility pressure is the lowest pressure for which a gas can develop miscibility through a multi contact process with a given reservoir oil at reservoir temperature. Rao [18] has described MMP as the minimum pressure in which there is no interface separating the phases, or in the other words the pressure for which value of interfacial tension between two phases are zero.

When an oil field becomes a candidate for CO_2 flooding, a miscible or near- miscible process is considered to be the most desirable result. [19] Therefore it is very important to exactly measure minimum miscibility pressure. The industry standard of MMP measurement is slim-tube displacement test. [18]

Slim-tube is a long, thin stainless steel tube packed with very fine sand or glass beads. The reason for thin geometry is for minimizing the effect of viscous fingering in the slim-tube. The test begins with the slim-tube saturated with oil at reservoir temperature. Carbon dioxide is injected at a given pressure and oil recovery is measured. The displacement tests are carried out for a range of pressures and final oil recovery (or oil recovery at 1.2 hydrocarbon pore volume of CO_2 injection} is plotted versus pressure. The breakover point in the graph shows the minimum miscibility pressure (Figure 6). At pressures above MMP there is little increase in oil recovery because two phases have already achieved full miscibility.

Lighter oils usually have lower minimum miscibility pressure, because it's easier for carbon dioxide to extract lighter components of the oil. Contaminants such as methane and nitrogen significantly increase the CO_2 minimum miscibility pressure, and H_2S, C_2H_6 or intermediate hydrocarbons have the opposite effect.[28]

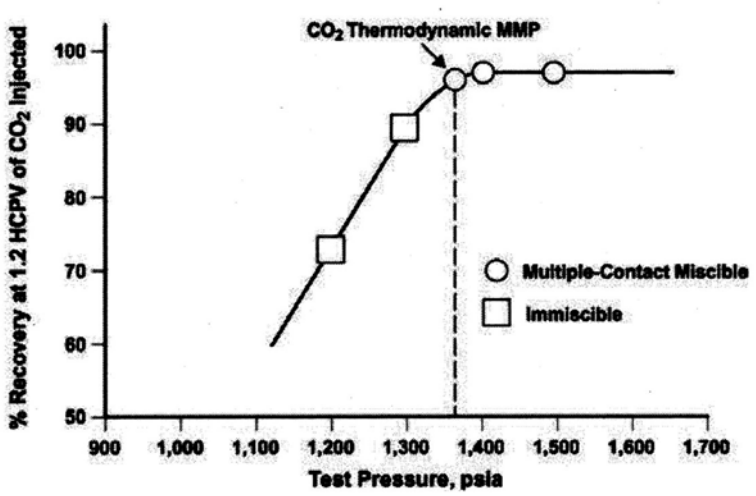

Figure 6. Slim-tube oil recoveries for fixed oil composition and temperature over pressure [12]

Improved oil recovery by CO_2 flooding results from:

- Vaporizing oil
- Stripping the light hydrocarbon ends out of oil
- Reducing oil viscosity
- Swelling the oil

- Lowering the interfacial tension between oil and water

In miscible flooding all the above phenomena are responsible for improving the oil recovery but the first two outweigh the rest. In immiscible flooding, in the absence of miscibility, oil production is enhanced by reduction in oil viscosity, oil swelling and decrease of interfacial tension between oil and water.

Miscibility between fluids can be attained through two mechanisms: first contact miscibility and multiple contact miscibility. When two fluids become fully miscible they form one phase and in a displacing application one can completely displace the other one. In multiple contact miscibility, which is the case in CO_2 flooding, full miscibility can not be achieved in the first contact but it needs many contacts in which the components of the oil and carbon dioxide transfer back and forth until the two phases can not be distinguished. [12]

2-5-2- Immiscible flooding

In reservoirs with low pressures (generally reservoirs with less than 1200m depth) [5] and with heavy oils (generally <27° API) [20], injected carbon dioxide remains physically distinct from the oil and can't reach miscible or near miscible state with the oil within reservoir, therefore the flood would be immiscible. Immiscible CO_2 still can improve the recovery by causing the oil to swell and reducing the viscosity of the oil and also (in the presence of water) by decreasing the interfacial tension between water and oil.

Holm has mentioned that "when carbon dioxide dissolves in the oil it expands that oil 10 to 60% and reduces its viscosity from 5 to more than 10-fold. If a CO_2 slug is injected ahead of water in any stage of a water flooding, the lower viscosity oil/CO_2 mixture flows more readily to production wells and the crude oil (swollen with CO_2) left behind could be only 90 to 40% of unswollen oil." [20]

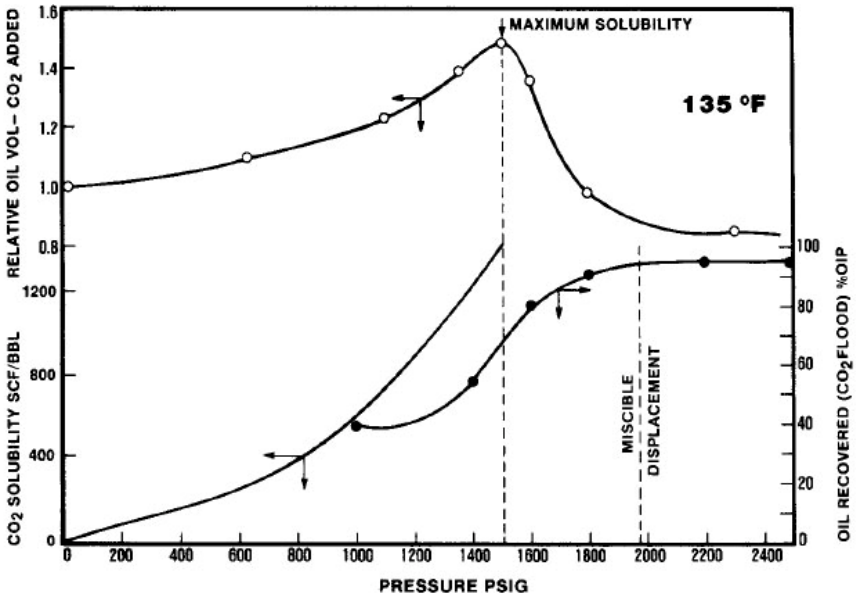

Figure 7. Variation of oil swelling in the presence of CO_2 over pressure in Mead Strawn crude oil [20]

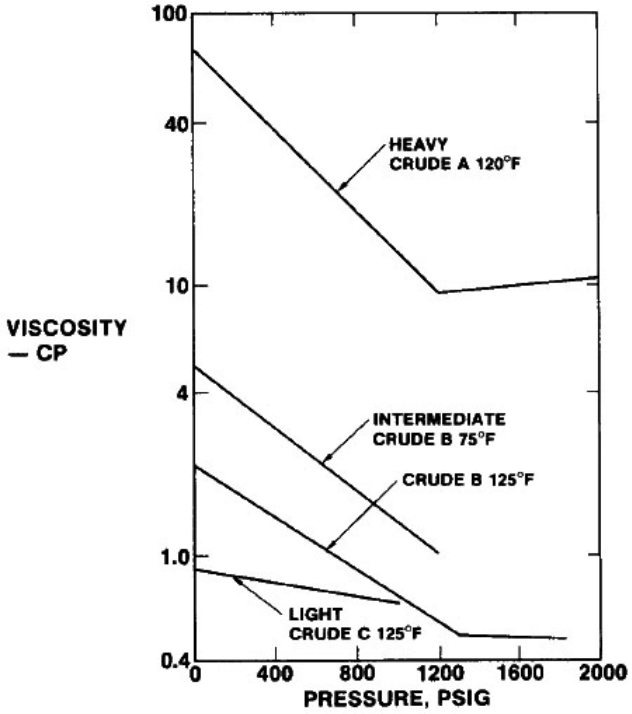

Figure 8. Variation of viscosity of different types of oil saturated with CO_2 over pressure [20]

The other parameter that is effective in improving oil recovery in immiscible brine/CO_2 flooding is reduction in interfacial tension between water and oil which leads to the formation of acidic brine-in-oil emulsions, and an increase in residual oil saturation. [21]

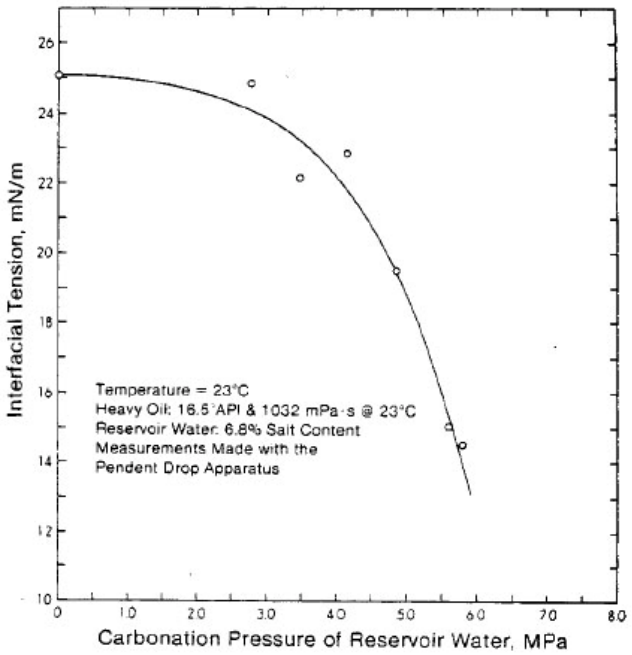

Figure 9. Variation of interfacial tension between carbonated water and Aberfeldy heavy oil over pressure [21]

2-5-3- Miscible flooding and near-miscible flooding

At pressures above the MMP of the CO_2 and reservoir oil (generally in reservoirs deeper than 1200m with oil lighter than 27° API) [5, 20] injected carbon dioxide will mix thoroughly with the oil within the reservoir such that the interfacial tension between these two phases disappears. Theoretically all contacted oil can be recovered under miscible conditions. [5]

In pressures below but close to MMP, the amount of dissolved CO_2 into the oil is not enough to vaporize sufficient reservoir oil into CO_2 therefore miscibility can not be achieved, but still it can help improve the recovery by vaporizing light oil components up to C_6. [12] This type of CO_2 flooding is usually called near- miscible flooding.

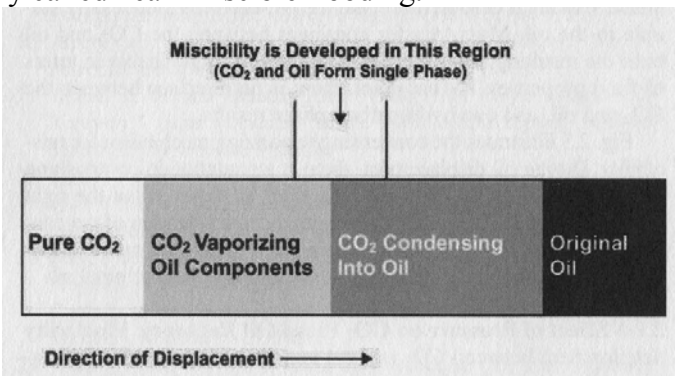

Figure 10. Schematic showing how CO_2 becomes miscible with crude oil through a multiple contact process [12]

2-5-4- CO_2 injection designs [2, 12]

Different CO_2 flooding design variations usually stem from the tendency to improve poor sweep efficiency of the gas flooding caused by very low viscosity of CO_2 comparing to liquids. There are five major injection process designs:

1) *Continuous CO_2 injection:* A predetermined CO_2 slug volume is injected continuously with no other interjected fluid or chase fluid. This approach usually is applied in non-water floodable reservoirs directly following primary recovery. Sometimes a different gas is used to drive the CO_2 through the reservoir.
2) *Continuous CO_2 chased with water:* It's the same as the continuous CO_2 injection method, except that chase water follows the continuous CO_2 slug and immiscibly displaces the mobile CO_2 oil bank to improve the mobility of gas slug and also reduces the cost of flooding by using a smaller volume of more expensive carbon dioxide. This approach is usually used in reservoirs with low heterogeneity.
3) *Conventional alternating CO_2 and water chased with water (WAG):* A predetermined slug of CO_2 is injected in cycles in which equal volumes of gas and water alternate (known as water alternating gas or WAG) at a constant gas/water ratio(WAG ratio). After the total CO_2 volume is injected, a chase of continuous water is started. One problem with the WAG is that some of the CO_2 is dissolved into the water and produces carbonic acid which has corrosive effects. [20]

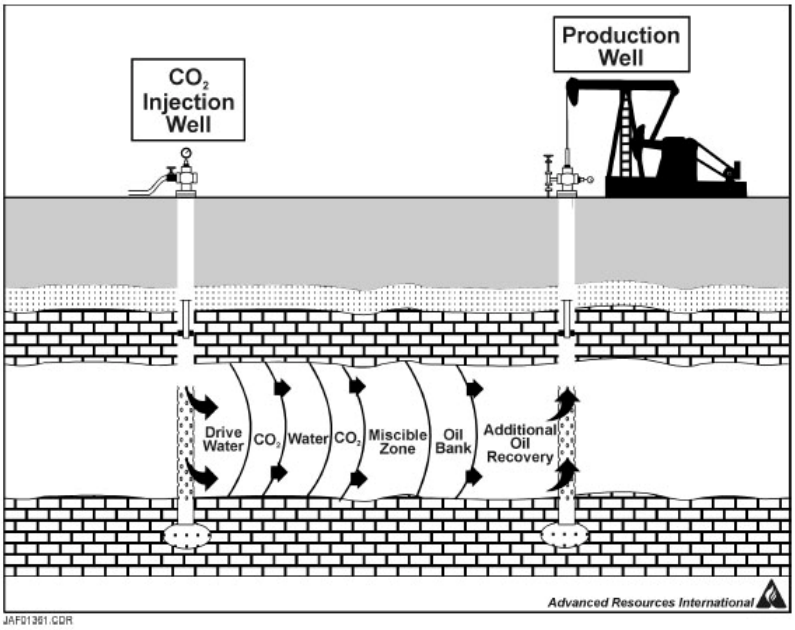

Figure 11. Schematic of the WAG process [5]

4) *Tapered alternating CO_2 and water (Tapered WAG):* CO_2 slugs are injected alternately with increasing water cycle lengths in tapered or unequal cycle volumes until the total CO_2 volume has been injected. Sometimes a chase of continuous water follows the taper. The objective is to reduce the total volume of CO_2 used in the flooding and decrease the cost of process
5) *Alternating CO_2 and water chased with gas:* It's a conventional WAG which is chased by a volume of less expensive gas after the total CO_2 volume has been delivered. The purpose of the chase gas is to maintain miscible displacement of the trailing edge of CO_2 slug while reducing the total CO_2 requirement.

2-5-5- CO_2 flooding drawbacks

1. CO_2 is expensive. Comparing to other displacing fluids (water, Nitrogen) carbon dioxide is relatively expensive (depending on sources from \$0.65/ MCF to \$3/MCF) [5] which makes CO_2 flooding uneconomical when oil prices are low.
2. Lack of supplies close to oilfields. The major deterrent to using CO_2 extensively to enhance oil recovery has been the distance between the oil fields and major supplies of CO_2 and the resultant cost of transporting it. During the past few years in the United States, pipelines over 400 miles long have been installed to transport CO_2 from naturally occurring deposits in New Mexico and Colorado to the oilfields in West Texas and surrounding areas. [23]
3. Low viscosity. CO_2 viscosity is very low compared to oil or water under the reservoir conditions. The viscosity ratio of crude oil to CO_2 usually exceeds 10 at ordinary reservoir conditions. [24] This low viscosity results in a much higher mobility of CO_2 comparing to the oil that is being displaced. Because of the high mobility ratio the displacing front is subject to viscous fingering and early CO_2 breakthrough. [13] As a consequence much of the oil reservoir is not contacted by CO_2 and can't experience swelling and viscosity reduction effects. Also, miscible displacement may not occur

except in small-volume channels and finger areas and injection of more CO_2 leads to excessive flow through areas already swept by carbon dioxide. [20] This unfavorable condition produces inefficient oil displacement.

2-5-5- CO_2 flooding mobility improvement methods

Several techniques for improving the mobility of CO_2 floods have been investigated: [20]

1. Installation of well packers and perforating techniques to isolate high permeability zones.
2. Shutting in production wells to eliminate low pressure sinks [25]
3. Alternate injection of water with CO_2 (WAG)
4. Addition of surfactant and foam producing chemical to water which is alternately injected with CO_2 to create a foam or emulsion in the presence of gas

The WAG process has been the most widely used mobility-control technique, but it's not without drawbacks. Holm mentioned that "although injected water invades the zones previously invaded by CO_2, subsequently injected CO_2 is not diverted completely to other zones. As a result, CO_2 channeling is reduced only temporarily. Because oil has been removed, CO_2 and water-invaded zones become more permeable, particularly to water, resulting in increased water-to-oil production ratios. If the amount of alternately injected water becomes large enough that the velocity of the water in the reservoir exceeds that of the CO_2, displacement efficiency is reduced severely. Thus, the gain recovery can be lost by lower displacement efficiency. This problem becomes more severe in CO_2 flooding of previously watered-out reservoirs." [20]

Also, dissolved CO_2 in the water decreases the amount of available CO_2 in the flood, traps the oil, increases water flow and decreases extraction of hydrocarbons by CO_2. [27]

Surfactant foams are usually injected after a water cycle. The surfactant flows to low permeability zones with water and when CO_2 is injected it forms a viscous foam in these layers which reduces the mobility of CO_2 slug or blocks low permeability zones. [12] Bernard et al has measured that when WAG injection is used with surfactant, CO_2 mobility is reduced 50% more than if plain WAG is used. [27]

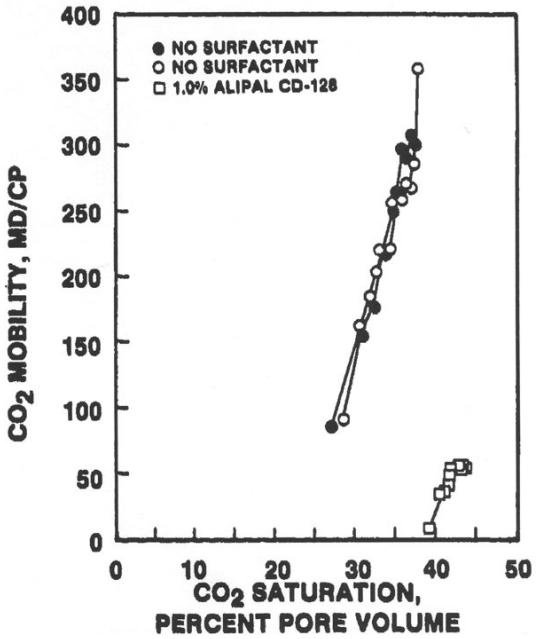

Figure 12. Variation of CO_2 mobility over CO_2 saturation with and without surfactant in a carbonate core [26]

2-5-6- CO_2 sources [12, 27]

Carbon dioxide supply can be of natural or industrial origin:

Natural CO_2: Carbon dioxide can be found in reservoirs in nearly pure form (98% CO_2) or as by-product in natural gas reservoirs in many parts of the world. Miscible flooding is sensitive to purity of CO_2 because some kinds of impurities can increase minimum miscibility pressure. Therefore in miscible flooding occasionally CO_2 concentration is required to be increased by processing to 90-98%. An immiscible flooding is not so heavily dependent on high quality CO_2.

Industrial CO_2: Carbon dioxide can be obtained as a side stream from industrial processes. These sources can be divided into the following main categories:

- Concentrated, high-pressure: from synthetic fuel plants and gasification combined-cycle power plants
- Concentrated, low-pressure: from ammonia plants
- Diluted, high-pressure: from hydrogen plants
- Diluted, low-pressure: from fossil-fuel power plants and cement plants

Natural CO_2 is cheaper but it's availability is less than industrial CO_2.

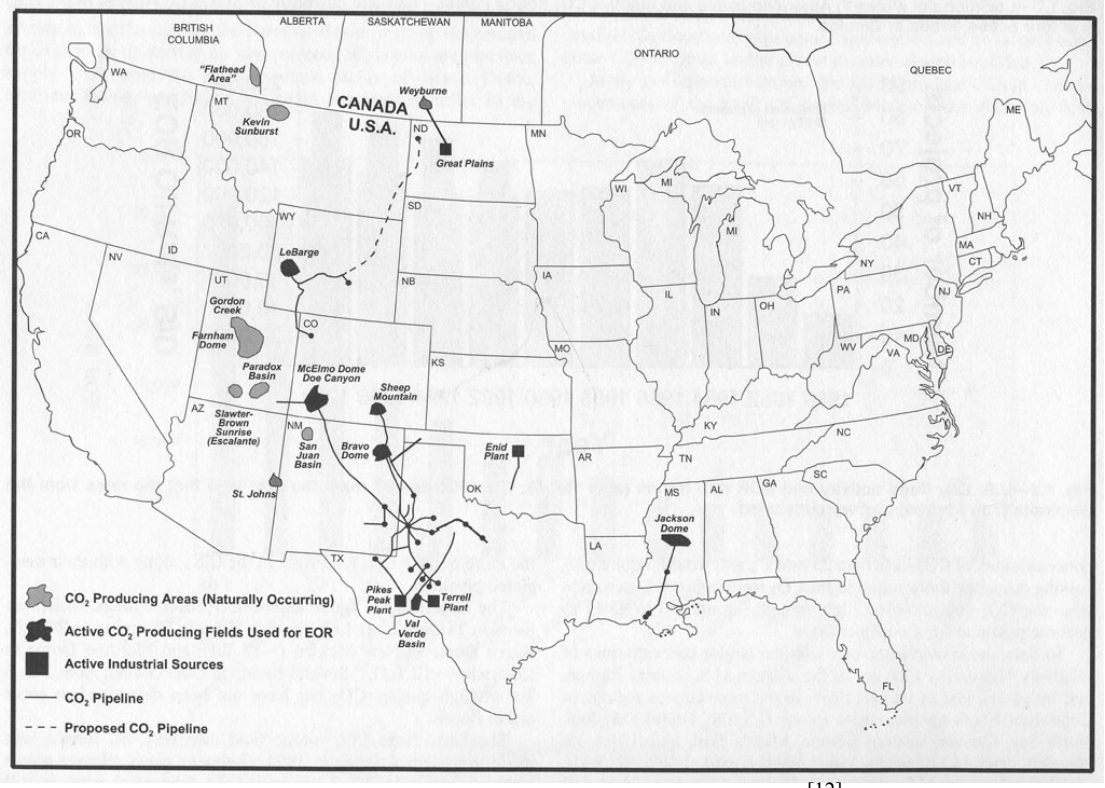

Figure 13. Location of CO_2 sources and pipelines in the U.S. [12]

3. IN-SITU CO_2 GENERATION TECHNIQUE

The research scientists and engineers at the Institute for Geology and Development of Fossil Fuels (IGDFF), Moscow, Russia in 1990s developed a new in-situ CO_2 generation technique to enhance oil recovery and to clean the wellbore zone. The concepts of the new technique were tested via the laboratory scale experiments followed by pilot tests in Western Siberian oilfields. This new technique is based on the injection of two (acid and base) aqueous solutions (gas-forming (GF) and gas-yielding (GY) solutions) of certain concentrations into the reservoir. Water-soluble foam generating surfactants can be added to these solutions. Chemical reaction between the injected liquids generates CO_2 gas and brine inside the reservoir according to the following reaction formulae:

$$GF + GY \leftrightarrow Salt + H_2O + CO_2$$

This EOR technology is developed to address major CO_2 flooding drawbacks: low viscosity of CO_2 which causes high mobility and early gas breakthrough, high cost of CO_2 flooding and problems with availability of CO_2 in remote areas.

Chemical reaction between GY and GF inside the reservoir leads to the generation of brine containing surfactant and carbon dioxide (as a free gas or dissolved in the brine and oil). Therefore, this method is expected to keep all the positive effects of conventional CO_2 flooding processes including swelling and reducing the viscosity of the oil and decreasing the interfacial tension between water and oil and also extracting the light hydrocarbons and achieving miscibility in near-miscible and miscible conditions.

In addition to CO_2 flooding effects, presence of water in the driving front improves the mobility of displacing fluid dramatically. Surfactant reduces the water-oil interfacial tension and in the presence of free gas, it can generate foam which in turn improves flood mobility by blocking low permeability channels and delaying the gas and water breakthrough.

The oil recovery enhancement by in-situ CO_2 generation technique can be categorized based on the improvements in displacement efficiency (E_D) and sweep efficiency (E_V):

Displacement Efficiency (E_D):

1. Dissolved CO_2 reduces the oil viscosity
2. CO_2 decreases oil-water interfacial tension
3. Surfactant decreases oil-water interfacial tension
4. In relatively high pressures, CO_2 extracts lighter oil components
5. In high pressures, CO_2 gets miscible with the oil and acts as a solvent

Sweep Efficiency (E_V):

1. Water improves the mobility;
2. Generated foam improves the mobility

On the other hand, this technology provides more adoptability and accessibility compared to conventional CO_2 flooding:

1. By using this technique there is no need for natural or industrial CO_2 sources. Containers of concentrated acid and base solutions can be carried out to the wellborn and get diluted on the location. Therefore, it's feasible for use in remote areas and also in regions with severe climatic conditions.
2. Less equipment is needed on the surface (compressors and power supplies) and there is no need for additional pipelines

3. This technique is less expensive compared to the conventional CO_2 flooding
4. Environmental impact is much less than traditional CO_2 flood technique, as a required amount of CO_2 is much less than that required for continuous CO_2 displacement. Dissolution of CO_2 in oil is accompanied by mass transfer process since CO_2 extracts the light fractions of oil dissolved in gaseous phase. During the flow in rock formations, CO_2 will be continuously enriched with light hydrocarbons (the concentration of the latter increases) and CO_2 content will decrease up to zero.

In-situ CO_2 generation technique is assumed to be applicable as a secondary recovery technique after the primary production of reservoir oil and also as the tertiary recovery after the water flood technique. This new technology was successfully applied at Samotlor (Tyumen Oil Co.), Novo-Pokursky (Slavneft Megionneftegas, JSC) and Gunyang (China) oilfields in 1999-2004. The application of this technology resulted in increased oil production, reduced water production, increased injectivity of wells and decreased injection pressure. However, the technology is not known in North America. The purpose of the reported project was a final research, development and evaluation of this promising technology in the United States. Before the technology could be convincingly adopted by the United States oil and gas producers, it was necessary to verify if the Russian formulations generate sufficient pressure and CO_2 concentration in-situ so that miscibility can be attained with typical domestic oils. Second, the project results must answer how effectively will the foams generated by this process in order to improve sweep efficiency in typical domestic porous rock.

4. METHODOLOGY

4-1- Methods used

Slim-tube displacements tests were performed to evaluate the In-Situ CO_2 Generation Technique (ISCGT). All the tests were run in the constant temperature of 80°C (except the first test). The temperature was chosen to produce an appropriate oil viscosity. Tests were performed at different operating pressures according to the objectives of the experiments. The first couple of tests were run to decide which oil is suitable for the experiments. The target was the oil with a high enough viscosity which could produce enough resolution in the results to make it easy to compare recovery efficiency of different methods. Also oil shouldn't be very high viscous because it becomes difficult to clean the system.

To investigate the efficiency of different methods of injection of GF and GY solutions, ISCGT flooding was conducted with simultaneous injection of the solutions and also with slug injection. The results were compared in order to select the optimal method of injection.

For evaluating an efficiency of the ISCGT as an EOR method, floodings were performed by distilled water, brine and ISCGT in different pressures. The purpose of distilled- water flooding was to investigate the effect of salinity of water by comparing its results to brine flooding results. The salinity and type of the salt of brine used in the brine flooding was similar to the produced brine by the chemical reaction of GY and GF solutions. This similarity was helping us to investigate the effect of presence of CO_2 alone by canceling out the influence of water salinity. Also, to inspect the surfactant effect on the flood performance, ISCGT flooding was conducted in presence and absence of surfactant at different pressures.

The efficiency of the ISCGT was also evaluated by "three-stage" flood experiments: flooding was run in the already brine-flooded system. Also, conventional CO_2 floodings were performed to measure the MMP of the CO_2 and oil at the given temperature (to investigate the miscibility of the floodings).

4-2- Materials used

Three oils were tested as a candidate fluid to be displaced from the slim tube: decane, crude oil and mineral oil. Decane is an alkane hydrocarbon with chemical formula $CH_3(CH_2)_8CH_3$, which is one of the components of gasoline and it's immiscible with water. Crude oil was from West Heidelberg field located at Cotton Valley (Louisiana). Mineral oil was a light paraffin provided by Fisher Scientific ^{TM} (gas chromatography results of mineral oil are presented in appendix B, Figure 84). Table 1 shows physical properties of the oils tested in the experiments.

Table 1. Physical properties of the oils used in the experiments (at 25ºC and atmospheric pressure)

Oil	Density, API(g/ml)	Viscosity, centistokes(cp)
Decane	62.1(0.727)	1.21(0.00087)
Crude oil	24(0.905)	74.4(0.067)
Mineral oil	33.9(0.851)	49.04(0.041)

Aqueous acid and base solutions with specific concentrations were prepared in the lab by diluting the preliminary concentrated solutions. Densities of GY and GF solutions are 1.114 g/ml and 1.0405 g/ml respectively.

Two types of surfactants were applied during the tests: CLS (calcium lignosulfonate), and an ionic surfactant. CLS is a cheap surfactant which is usually used as sacrificial agent. More surfactant is required to satisfy absorption on rock than it is used to create foam. To reduce the volume of required expensive surfactant, reservoir is initially saturated with cheaper sacrificial agents like CLS, and then the main surfactant is injected. [29] Experiments showed that the quantity and quality of generated foam by ionic surfactant is much better than that created by using CLS. The surfactants were added to GF solution with the concentration of 1% (v/v).

70,000 ppm (1.305 molal) concentration brine was used in the experiments. This concentration is calculated by considering the salt and water produced by the chemical reaction between GY and GF solutions and also the initial water presented in the solutions.

A commercial acid inhibitor was added to the acid solution to alleviate the corrosion damage to the system. An acid inhibitor provides a layer of coating on the stainless steel and hinders the acid from attacking it. On the other hand, it doesn't change the physical and chemical properties of the acid. Concentration of 0.1% (v/v) was chosen after inspecting the corrosion caused by acid solution containing different concentrations of acid inhibitor, at system operating temperature.

Tetrahydrofuran (THF) of concentration ~ 99% was used to clean the system and other lab equipment. THF is a very good solvent of oil and water. Pure CO_2 and nitrogen was provided in the high pressure tanks. Also, distilled water acquired from water distillation equipment in the laboratory.

5. EXPERIMENTAL SETUP, PROCEDURE AND RESULTS

5-1- Experimental Apparatus

Two slightly different experimental setups were used in the experiments. Apparatus A (Figure 14) was used for distilled water, brine and ISCGT flooding, and apparatus B (Figure 15) was used for conventional CO_2 flooding.

5-1-1- Experimental apparatus A

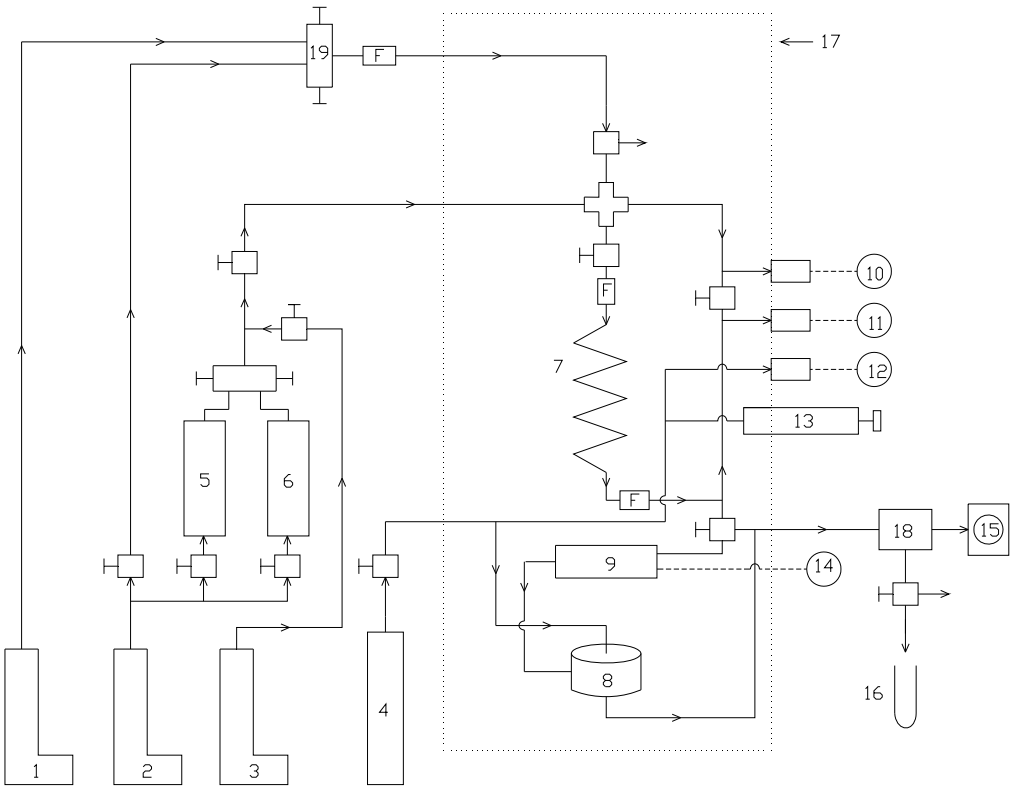

Figure 14. Schematic of experimental apparatus A: 1- ISCO^{TM} 500D syringe pump 2- ISCO^{TM} 260D syringe pump; 3- ISCO^{TM} LC5000 precision pump; 4-Nitrogen tank; 5- TEMCO^{TM} THF accumulator; 6- Temco^{TM} Oil accumulator; 7- Slim-tube; 8- TEMCO^{TM} BPR-50 Back pressure regulator; 9- PAAR^{TM} Densitometer; 10, 12- SENSOTEC^{TM} pressure transducers; 11- DIGITEC^{TM} pressure transducer; 13- HIP 50-6-15 hand operated pressure generator; 14- Density readout; 15- Scientific^{TM} GCA Precision Wet Test Meter; 16- Pyrex^{TM} vial sample collectors; 17- Eurotherm^{TM} temperature bath; 18- Liquid and gas separator; 19- Co-injection valve; F- 2-micron filter

Three pulseless ISCO^{TM} syringe pumps were used in the experimental setup A. Pumps 1 and 2 were high precision pumps with the accumulator capacity of 500 and 260 ml, respectively, and they were capable to operate at constant pressure or constant flowrate modes. The maximum operating pressures for pumps 1 and 2 were 3700 and 7000 psi, respectively. Pump 1 was used for injecting GF solution in ISCGT flooding. Pump 2 was used to inject distilled water, brine or GY solution in distilled water flooding, brine flooding and ISCGT flooding. It was also used to inject distilled water into THF and oil accumulators. The third pump was a low precision ISCO syringe pump with the accumulator capacity of 500 ml, used to fill out oil and THF accumulators with oil and THF. Two 1 liter TEMCO^{TM} accumulators were responsible for storing THF and oil

before injection into the system. In ISCGT flooding, the mixing point for GY and GF solutions was a HIP three-way / two-stem valve. The mixing valve was placed outside of the temperature bath to minimize the effect of corrosion in the system (because even in the presence of acid inhibitor, GF solution was corrosive at high temperatures). Therefore by mixing at the room temperature, we had only non-corrosive products of the chemical reaction inside the temperature bath. To increase the mixing efficiency of chemical reaction between GY and GF solutions, a 2-micron filter was placed right after the mixing valve. Also to reduce the effect of corrosion, it was tried to minimize the length of plumbing used between pump 1 and mixing valve. Two other 2-micron filters were installed right before and after the slim-tube to keep the permeability of slim-tube constant during the experiments. The slim-tube used in the experiments was a stainless steel vertical spiral tube filled with very fine glass beads. Two fine screens were placed in the inlet and outlet of the slim-tube to stop the loss of glass beads and a subsequent change in the permeability during the experiments. Table 2 shows the physical specifications of the slim-tube. The methods of calculating slim-tube pore volume, porosity and permeability are illustrated in Appendix A.

Table 2. Physical specifications of slim- tube.

Internal diameter, in.	0.125
Length, ft	40
Packing material	glass beads 200 mesh
φ, %	27.5
κ, darcy	6
PV, ml	106

Two pressure transducers were connected to the both ends of the slim-tube to measure the pressure difference between inlet and outlet. A PAAR™ densitometer was placed after the slim-tube to monitor the density of slim-tube products at the operating pressure and temperature in real time (the method of calculating density from densitometer readout is explained in the Appendix A). The operating pressure of the experiment was controlled by the use of a TEMCO™ BPR-50 back pressure regulator after the densitometer. A dome pressure of BPR was adjusted by nitrogen gas provided from a 6000 psi nitrogen tank and through a hand operated pressure regulator mounted outside the temperature bath. The SENSOTEC™ pressure transducer was showing the BPR dome pressure. After passing the BPR, products of the system were separated by a gas/liquid separator. The liquids were collected in 15 ml Pyrex™ vials and the gas was passed through a Scientific™ GCA Precision wet test-meter where its volume at ambient conditions was measured. Also, there was a liquid trap before the wet test-meter to stop liquids from entering wet test-meter. Slim-tube, densitometer and BPR were installed inside a Eurotherm™ temperature bath capable of providing temperatures up to 149°C.

All the equipment used in the system was made of stainless steel 316. Also the plumbing was 1/8″ Swagelok stainless steel 316 tubing. The total pore volume of the system (including slim-tube, equipment and plumbing) was 137 ml.

5-1-2- Experimental Apparatus B

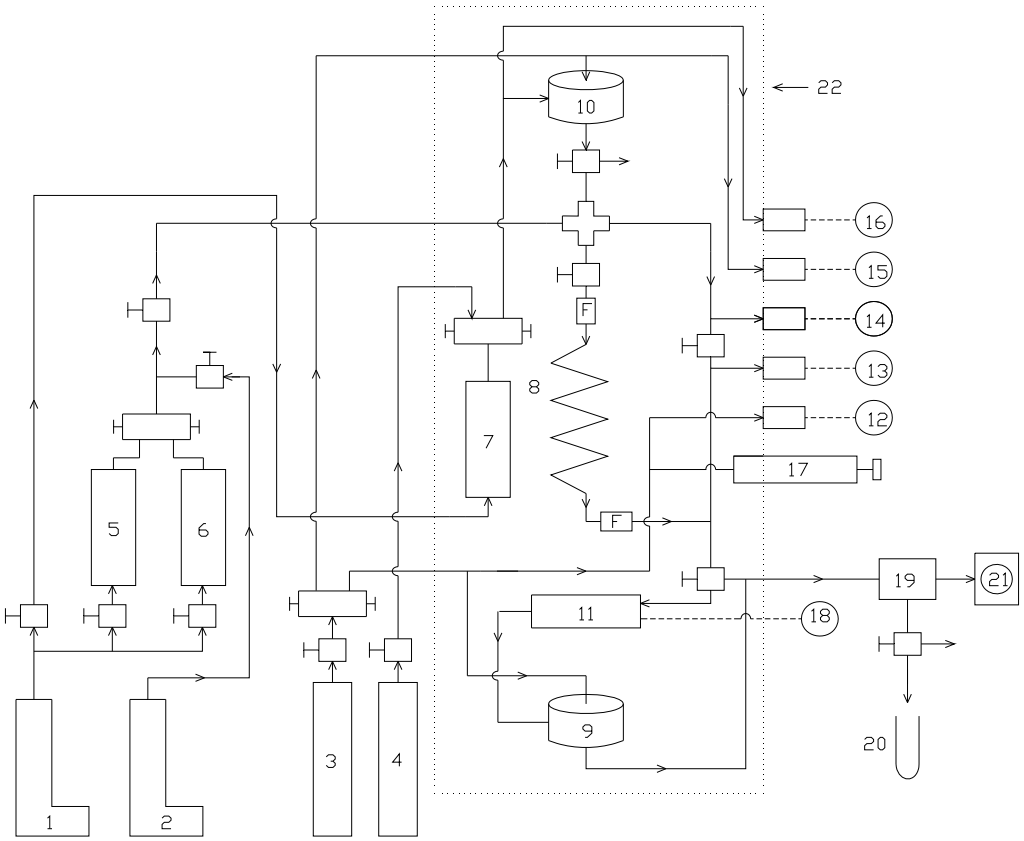

Figure 15. Schematic of experimental apparatus B: 1- ISCO^{TM} 500D syringe pump; 2- ISCO^{TM} LC5000 precision pump; 3- Nitrogen tank; 4- CO_2 tank; 5- TEMCO^{TM} THF accumulator; 6- - TEMCO^{TM} Oil accumulator; 7- - TEMCO^{TM} CO_2 accumulator; 8- Slim-tube; 9- TEMCO^{TM} BPR-50 Back pressure regulator; 10- TEMCO^{TM} BPR-50 Back pressure regulator; 11- PAAR^{TM} Densitometer; 12, 14, 15, 16- SENSOTEC^{TM} pressure transducers; 16- DIGITEC^{TM} pressure transducer; 17- HIP 50-6-15 hand operated pressure generator; 18- Density readout; 19- Liquid and gas separator; 20- Pyrex^{TM} vial sample collectors; 21- Scientific^{TM} GCA Precision Wet Test Meter; 22- Eurotherm^{TM} temperature; F- 2-micron filter

Two pulseless ISCO^{TM} syringe pumps were used in this experimental setup B. Pump 1 was a high precision ISCO^{TM} 500D syringe pump with the accumulator volume of 500 ml. It was used for injecting water into oil, THF and CO_2 accumulators. We used Pump 2 (ISCO^{TM} LC5000) for injecting THF and oil into the accumulators. A CO_2 tank with the pressure of 900 psi was used to provide CO_2 into the test tube. CO_2 was stored in an accumulator inside the temperature bath. A pressure transducer connected to CO_2 accumulator was showing the pressure of gas inside the accumulator. Also, a TEMCO^{TM} BPR-50 back pressure regulator at the inlet of the slim-tube was used in order to control the flow rate of CO_2 from accumulator to the slim-tube. The dome pressure of inlet BPR was directly controlled by the pressure regulator of nitrogen tank and it was measured by a pressure transducer connected to it. The rest of the system was similar to the apparatus A. Also, pore volumes of slim-tube and the system were the same as the setup A (106 ml and 137 ml, respectively). The CO_2 accumulator, the slim-tube, the BPRs and the densitometer were installed inside the temperature bath.

5-2- Experimental procedure

Experimental procedure for the tests done with apparatuses A and B are slightly different. Therefore, we have divided them into two sections.

5-2-1- Experimental procedure for apparatus A

1. Temperature bath was adjusted at the desired temperature and system was left for a couple of hours to achieve a thermal stability.
2. The pressure at the outlet BPR dome was adjusted to the desired operating pressure of the test.
3. The pump 3 was filled with 250-300 ml of oil.
4. Oil was injected into the oil accumulator.
5. The pump 2 was filled up with distilled water.
6. Water was injected to oil accumulator to inject the oil into the system.
7. After the system was filled out with oil, based on the type of injection, following procedure was performed:

For distilled water or brine flooding, the pump 1 was filled with distilled water or brine and it was injected into the system at a constant flow rate. The lower flowrates were favorable. But too low flowrates led to very long test time. Therefore, flowrate was optimized between low flowrate and short experiments time (40ml/hr for most of the tests). In ISCGT floodings, the pumps 1 and 2 were filled with GF and GY solutions, respectively. Then, the solutions were injected into the system at constant flowrates. GY and GF flowrates were determined by considering reaction stoichiometry ratio in order to maximize the generated gas and minimize the presence of GY solution and corrosive GF solution in the chemical reaction products. Also, in order to cancel out the variation of flowrate in the results and make it easier to compare the results of different floodings, we wanted to make the sum of GY and GF flowrates similar to distilled water and brine flowrates in water and brine floodings.

8. During the tests the pressure at the slim-tube outlet was kept similar to the desired operating pressure by using a manual pressure regulator.
9. At constant time intervals during the experiments the following parameters were recorded:
   - Temperature inside the temperature bath
   - Pressure at the slim-tube inlet
   - Pressure at the slim-tube outlet
   - Pressure of nitrogen at BPR dome
   - Density of slim-tube products
   - Volume of produced oil
   - Volume of produced water or brine
   - Volume of produced gas at ambient condition

Also at each time interval, a sample of produced liquid is collected by a Pyrex^{TM} vial. The length of time intervals was based on the injection flowrate and also the required resolution of data. For example, at the flowrate of 40 ml/hr, and considering the volume of vial (15 ml), time intervals of 15 minutes were used (approximately 10 ml of produced liquid per sample). Moreover, at certain times during the experiment more resolution was needed in the data than for the rest of the experiment (for instance, we needed more information around breakthrough phase than at the end of the experiment).

10. The experiments continued until the system stopped producing oil (or when the amount of the produced oil was negligible).
11. The system was cleaned thoroughly after the tests according to the following procedures.
    After distilled water or brine flooding:
    1) Pump 3 was filled with 300-400 ml of THF.
    2) THF accumulator was filled with THF.
    3) Pump 2 was filled with distilled water.
    4) Distilled water was injected into THF accumulator to inject THF into the system.

    After ISCGT flooding:
    1) Pump 2 was filled with 300 ml of distilled water.
    2) Distilled water was injected into the system (because ISCGT products are not soluble in THF so we need to flood the system with water to wash them out).
    3) The system was flooded with THF via the same procedure used after the brine flooding.
12. Sometimes produced water and oil were in an emulsion form which made it difficult to read their volumes. In that case, the samples were centrifuged to separate oil from water or brine and after that their volumes were recorded.
13. During the first ISCGT flooding tests, pH of a couple of liquid samples was measured to help us adjust GY and GF flowrates in future experiments.
14. The system was washed thoroughly by THF after distilled water or brine flooding, and by distilled water and THF after ISCGT flooding.

5-2-2- Experimental procedure for apparatus B

1. CO_2 accumulator was cooled down by using ice.
2. The valves connecting CO_2 tank to CO_2 accumulator were opened, and after a couple of hours (when enough CO_2 was condensed in the CO_2 accumulator to provide high pressures after the system was heated up) they were closed. Depending on the operating pressure, quantity of CO_2 inside the accumulator was enough for a couple of tests.
3. Temperature bath was adjusted at the desired temperature and system was left for a couple of hours to achieve a thermal stability.
4. Pressure at the outlet of the BPR dome was adjusted at the desired operating pressure of the test.
5. Pressure at the inlet of the BPR dome was adjusted at a pressure higher than the estimated maximum inlet pressure of slim-tube (for example, for the outlet pressure of 2000 psi, and the estimated maximum pressure difference of 700 psi across slim-tube, the dome pressure at BPR inlet was adjusted to be around 3000 psi).
6. The pump 2 was filled with 250-300 ml of oil.
7. Oil was injected into the oil accumulator.
8. The pump 1 was filled with distilled water.
9. Water was injected to oil accumulator to inject the oil into the system.
10. After the system was filled with oil, pump1 was filled with distilled water.
11. Distilled water was injected into CO_2 accumulator to inject CO_2 into the system.

For the comparison purposes, we tried to have the same flowrate of CO_2 in the slim-tube as we had for brine or ISCGT floods. Therefore, density of CO_2 in both slim-tube and the CO_2 accumulator (at thermobaric conditions) was calculated by using Supertrap^{TM} software, and proper flowrate of CO_2 injection from accumulator was estimated considering the same CO_2 mass flowrate in both the accumulator and the slim-tube.

12. During the tests, pressure at the slim-tube outlet was kept similar to the desired operating pressure by using manual pressure regulator.
13. At constant time intervals during the experiments the following parameters were recorded:
    Temperature inside the temperature bath
    Pressure at the slim-tube inlet
    Pressure at the slim-tube outlet
    Pressure of CO_2 inside the accumulator
    Pressure of nitrogen at the inlet of the BPR dome
    Pressure of nitrogen at the outlet of the BPR dome
    Density of the slim-tube products
    Volume of the produced oil
    Volume of the produced gas in ambient conditions

Also at each time interval, samples of the produced oil were collected by a Pyrex™ vial. After the CO_2 breakthrough, because of the big drop in the rate of oil production, fewer samples were needed to collect produced liquid. Therefore, we usually increased the duration of time intervals.

14. Experiment continued until the system stopped producing oil (or when the amount of the producing oil was negligible).
15. When the test was over, the system was cleaned by injecting 250-300ml of oil (step 6-9). Thus, there was no need of injecting solvent to clean the system and the system was cleaned by refilling it with oil.
16. Density of produced oil in different stages of production were measured to examine the effect of extraction of lighter components of oil by CO_2 (extraction made the later oil samples lighter).
17. After the volume of produced oil in each sample was recorded, vials were washed by THF.

5-3- Data processing procedure

1. Total produced oil and brine (or distilled water) at each time interval was calculated.
2. Total generated gas at each time interval was calculated.
3. Pressure difference along slim-tube at each time interval was calculated.
4. By calibrating the densitometer, density of the slim-tube products at each stage of production was calculated (the method of calibrating the densitometer and density calculations are illustrated in Appendix A).
5. Two recovery efficiencies were calculated:

Slim-tube recovery efficiency:

$$E_R = \frac{V_{Produced\ oil} - \left(V_{total} - V_{slim-tube}\right)}{V_{slim\ tube\ pore}} \times 100\%$$

or

$$E_R = \frac{V_{Produced\ oil} - 31}{106} \times 100\%$$

Oil recovery in "dead-volume" of the system (system volume without slim-tube volume) can be assumed to be perfect. Therefore, slim-tube recovery efficiency can be calculated by subtracting this volume (31 ml) from the total produced oil volume and by dividing the result to the slim-tube pore volume. This is the true recovery efficiency of the flooding and we used it to compare final recovery of different floodings.

System recovery efficiency:

$$E_R^* = \frac{V_{Produced\ oil}}{V_{total\ pore}} \times 100\%$$

Total pore volume of the system is 137 ml. We used this recovery efficiency whenever it was needed to know the real injected pore volume of the injecting fluid (for example, to compare the timing of incidents in the graphs of recovery efficiency to the ones in the pressure difference graphs).

6. The variation of recovery efficiency, pressure drop along slim-tube and product density over the pore volume of injected fluid were plotted.
7. The variation of produced oil, brine and gas over pore volume of the injected fluid were plotted.

5-4- Experimental Results

Table 3 shows the displaced and displacing fluid, the operating pressure and temperature, and the final recovery efficiency for all conducted tests in chronological order (operating pressure is the pressure at the slim-tube outlet controlled by BPR).

Table 3. List of all the performed tests, their final recovery efficiencies, operating pressures and temperatures, and the type of displaced and displacing fluids in chronological order.

Test No.	Displaced fluid	Displacing fluid	T, °F	P, psia	E_R , %
1	Decane	Distilled Water	122	1000	99.71
2	Crude oil	Distilled Water	176	1000	55.75
3	Mineral oil	Distilled Water	176	1000	68.01
4	Mineral oil	Brine	176	1000	77.54
5	Mineral oil	GY+GF	176	1000	73.30
6	Mineral oil	GY+GF	176	1000	77.92
7	Mineral oil	GY+GF+ Surfactant	176	1000	77.92
8	Mineral oil	Distilled Water	176	1000	65.66
9	Mineral oil	GY+GF	176	1500	73.67
10	Mineral oil	Brine	176	1000	68.86
11	Mineral oil	GY+GF(slug injection)	176	1000	71.88
12	Mineral oil	Brine	176	500	80.56
13	Mineral oil	GY+GF	176	500	65.94
14	Mineral oil	GY+GF+ Surfactant	176	500	69.81
15	Mineral oil	Brine	176	500	72.26
16A	Mineral oil	Brine	176	500	68.20
16B	Mineral oil	GY+GF	176	500	72.02
16C	Mineral oil	GY+GF + Surfactant	176	500	73.01
17	Mineral oil	CO_2	176	1000	50.47
18	Mineral oil	CO_2	176	2000	61.01
19	Mineral oil	CO_2	176	2000	66.13
20	Mineral oil	CO_2	176	3000	81.98

Overall, 20 slim-tube displacement tests were performed. All the tests, except test 16, were conducted as a regular (two-fluid) recovery method. It means, before each test the system was cleaned and refilled with oil and the effect of flooding in the oil filled system was examined. In the test 16 (three-stage flood), initially the oil-filled system was flooded with brine solution (test 16A). At the end of the oil production, without cleaning or refilling the system with oil, the system was flooded with GY and GF solutions to investigate the effect of flood on the residual oil (test 16B). After the production ceased, the system was flooded with GY and GF and surfactant to inspect the effect of ISCGT flooding containing surfactant on the residual oil (test 16C).

All the tests except test 1 were performed at the constant temperature of 176°F. Also, during ISCGT floodings, co-injection was used as the method of mixing GY and GF solutions with the exception of one test (test 11) in which we used slug injection to compare the efficiency of these two injection methods. During the first ISCGT flooding, chemical stoichiometry was used to determine the optimum injection flowrates of GY and GF solutions. After the first couple of ISCGT flooding tests, the pH of the produced brine was measured and the flowrates were slightly modified with the purpose of producing neutral pH or slightly basic product. By doing that, we were trying to maximize the gas production and also to protect the system from the acidic environment. During the experiment 11, consecutive slugs of GY and GF solutions were

injected into the system (1.8 PV of GY solution followed by 1.2 PV of GF solution followed by 1.0 PV of GY solution).

First three displacement tests were conducted to find the oil with proper viscosity for the following tests. In the first experiment we used decane and displaced it with distilled water at 122°F and 1000 psi. The recovery efficiency was very high (99.71%), which confirmed the fact that sweep efficiency in the system is almost perfect. But to evaluate the efficiency of ISCGT, we needed enough room for recovery efficiency improvement over water flooding. Therefore, it was decided to use heavier (more viscous) oil in the next experiments. In the second experiment, a heavy crude oil was displaced with distilled water at 176°F and 1000 psi. The recovery efficiency was in the proper range (55.75%). However, oil viscosity was so high that cleaning the system after the test was difficult. Thus, we decided to try lighter oil. A light mineral oil was used in the third test at similar thermobaric conditions. The recovery efficiency was still in the acceptable range (68.01%) and the cleaning of the system was easier and less time-consuming. Therefore, mineral oil was chosen for the following tests.

The rest of the tests involved injection of distilled water, brine and co-injection of GY and GF solutions with or without surfactant to displace the mineral oil at 176°F and different pressures. CLS surfactant was used during the test 7 at 1000 psi and the ionic surfactant utilized during the tests 14 and 16C at 500 psi. We should mention that the results of the test 12 are out of range when compared to other brine flooding results at 500 psi. This was probably caused by corrosion products left in the system after the test 11 (slug injection). Therefore, we decided to exclude test 12 results from the experimental analysis.

Finally, the experimental setup A was modified to the apparatus B and a couple of conventional CO_2 floodings (tests 17 - 20) were performed at 176°F and different pressures.

Table 4 shows the tests that will be used in chapter 6 to interpret the results (organized by the type of displacing fluid and operating pressure).

Table 4. List of tests arranged by operating pressure and type of displacing fluid (all experiments have been conducted at 176°F with the same mineral oil)

P, psia	Distilled water	Brine	GY+GF	GY+GF +Surfactant	CO_2
500		15-16A[1]	13-16B[1]	14-16C[1]	
1000	3-8	4-10	5-6-11[2]	7	17
1500			9		
2000					18-19
3000					20

The collected data of all tests are presented in Appendix C.

[1] Tertiary recovery tests

[2] Slug injection

6. DISCUSSIONS

In the first section of this Chapter 6-1, the experimental results have been organized and discussed based on the type of the test and also based on the operating pressure and the kind of displacing fluid in each test. In the second section of the chapter 6-2, the discussions and interpretations have been arranged considering the objectives of the study.

6-1- Secondary and tertiary recovery floods

Regular ("two-fluid") floods are the tests which were initiated when the system filled by oil. "Three-stage" recovery tests are the floodings that have been performed on the residual oil after the regular floods. Most of the performed tests have been done as a regular recovery flooding. Only one test (test 16) has been conducted as "three-stage" recovery method for slim-tube tests and it will be discussed at the end of this chapter.

6-1-1- Regular recovery

The discussion have been organized by the operating pressure of the tests (500 psi and 1000 psi) and also by the type of displacing fluid in each experiment (brine, co-injection of GY and GF, co-injection of GY and GF + surfactant and injection of CO_2).

6-1-1-1- Tests at 500 psi

Slim-tube outlet pressure was kept constant during these experiments. As a result, a pressure gradient along slim-tube length occurred, and its magnitude depends on the viscosity and relative permeability of different phases moving through the porous glass beads inside the slim-tube. Darcy's law describes a fluid flow through a porous medium by:

$$Q = \frac{-kA(P_b - P_a)}{\mu L}$$

According to Darcy's law, at constant flowrate and slim-tube specifications (permeability, cross-sectional area and length) pressure drop across slim-tube depends only on the viscosity of the flowing fluid. Figure 16 shows that in brine floodings, pressure difference along slim-tube drops continuously as lower viscosity brine displaces higher viscosity oil. Before a brine breakthrough, the rate of pressure drop is linear due to the constant injection flowrate. After the breakthrough, this rate decreases proportionally to the decrease in oil production, and finally pressure difference becomes steady when the system stops producing oil. During the GY and GF co-injection, an abrupt change in pressure difference can be observed right after a brine breakthrough. This is an excellent indication of presence of free CO_2 inside the system. A presence of gas phase to already existed oil and brine phases increases "a competition" for the pore space, and change in relative permeability of oil/brine/CO_2 system reduces the mobility of CO_2 and brine, and increases the resistance to the flow. [12, 30, 31, 32] Therefore, pressure across the slim-tube increases. Before a brine breakthrough, a presence of the large volume of oil with much higher ability to dissolve the generated CO_2, compared to that of brine, doesn't allow the produced CO_2 to exist in a free form. A decrease of oil volume after the brine breakthrough frees some of the generated gas into the slim-tube. It can be seen that a ΔP increase in the test 13 continues until 1.75 PV is injected, and then the pressure drops back again. This event follows by some oil production (2%) at ~ 2 PV of injection. Being easier to overcome the capillary forces at higher pressures and reducing the viscosity of residual oil by more dissolved CO_2 at elevated

pressures can be the reasons behind this late oil production which in turn, reduces the ΔP after 2 PV of injection.

During the tests with ISCGT + surfactant (test 14), a much larger ΔP was observed if compared to the ISCGT flooding without surfactant. It is due to the generation of foam in the presence of free CO_2 and surfactant, which increases the viscosity and considerably reduces the mobility of displacing front in the slim-tube. A mobility reduction by foam also is the reason behind a later brine breakthrough during the test 14 (Figure 18). This delay in a brine breakthrough and also reduced brine/oil IFT caused by surfactant are responsible for 4% increase in E_R compared to the test 13. A generation of foam in test 14 was confirmed by observation of large quantities of foam in the collected samples.

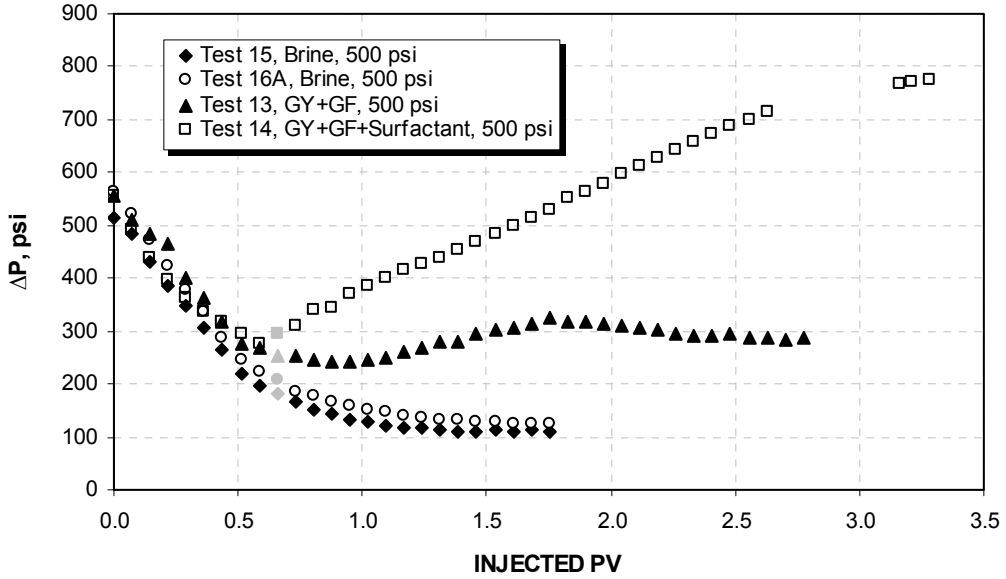

Figure 16. Variation of ΔP along slim-tube over injected PV for the tests performed at 500 psi and 176°F (brine breakthroughs are shown by gray symbols)

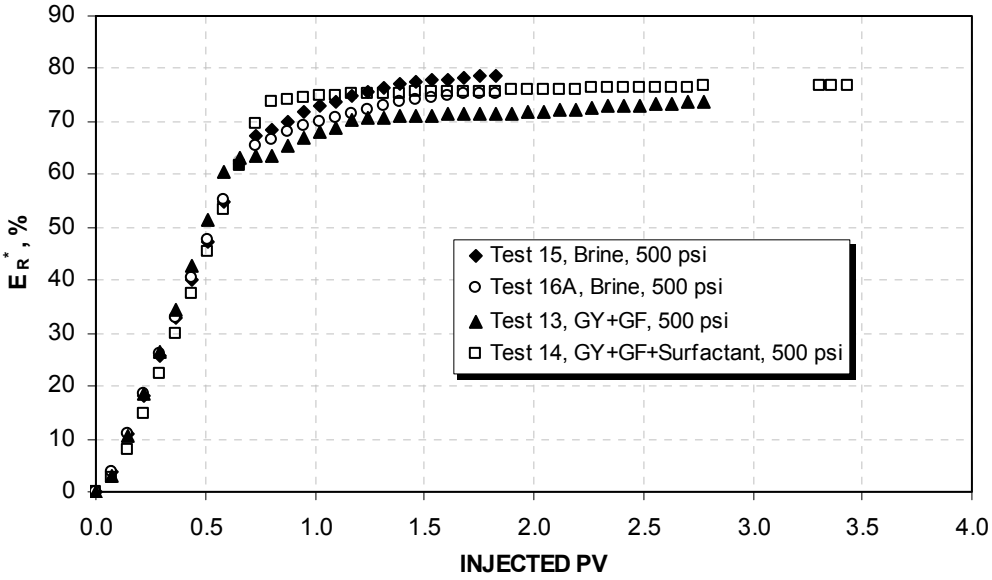

Figure 17. Variation of E_R^* over injected PV for the tests performed at 500 psi and 176°F

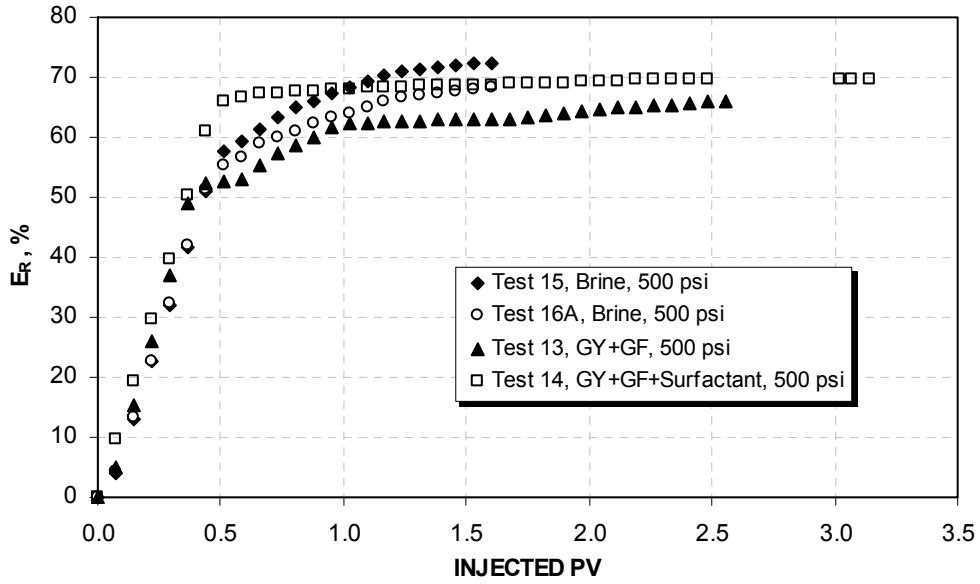

Figure 18. Variation of E_R^* over injected PV for the tests performed at 500 psi and 176°F

Figure 19 shows total liquid production (brine + oil) per collected sample (samples were collected every 15 minutes, i.e. at the constant flowrate of 40 ml/hr, 10 ml of liquid production was expected in each sample). The graph is useful for evaluating the effect of swelling caused by dissolved CO_2 in the brine and gas. As seen from this figure, during the brine flood a liquid production rate agrees well with the expected one. During the ISCGT flooding, the rate of liquid

production is 10 to 20% more than expected one. Swelling of oil and brine caused by dissolved CO_2 and also the volume occupied by free CO_2 in the system are responsible for increase in liquid production rate in ISCGT flooding. After 2 PV of injection, all the liquid inside the system becomes swelled and the swollen-liquid front reaches the slim-tube outlet and the system becomes steady, thus, the liquid production rate returns to the normal state.

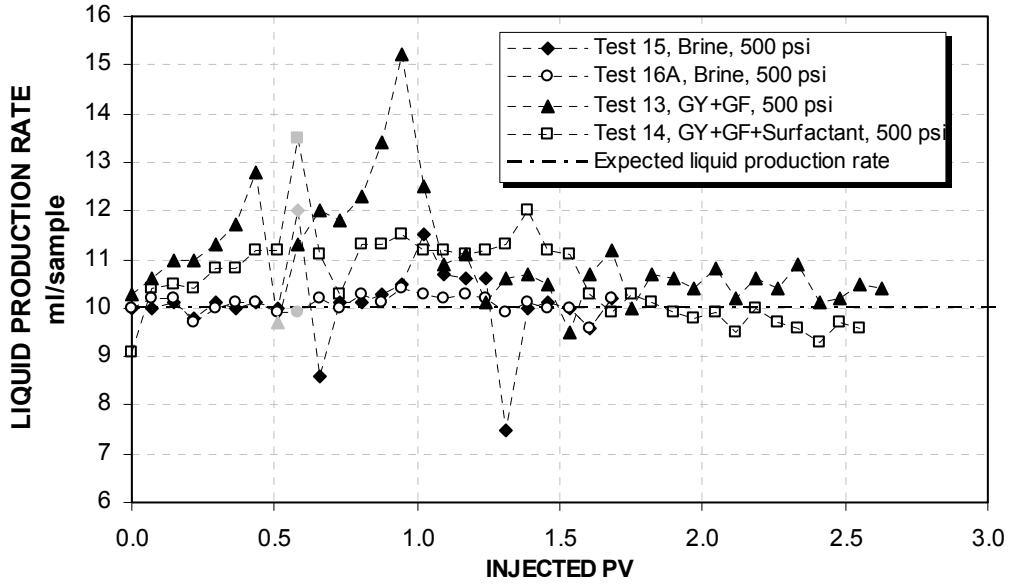

Figure 19. Variation of liquid production rate per sample versus injected PV for the tests performed at 500 psi and 176°F (brine breakthroughs are shown by gray symbols)

From Figures 20 and 21 it can be observed that gas breakthrough for ISCGT flooding occurs at about 1.5 PV of injection. This is about 1 PV behind a brine breakthrough and it corresponds well with the end of swollen liquid section in Figure 20. In the other words, gas breakthrough happens when all the liquid in the slim-tube is saturated and swollen with CO_2 and therefore, the free CO_2 front can reach the slim-tube outlet.

Moreover, presence of foam in the system (the test 14) reduces the mobility of CO_2 and delays the gas breakthrough by 0.5 PV compared to the test 13. It should be mentioned that a discrepancy between the gas production rate in the test 14 and the expected gas production rate (which is calculated considering GY and GF chemical reaction stoichiometry) is due to the presence of large volumes of foam in the product, and a fraction of the produced gas escapes before reaching wet test-meter.

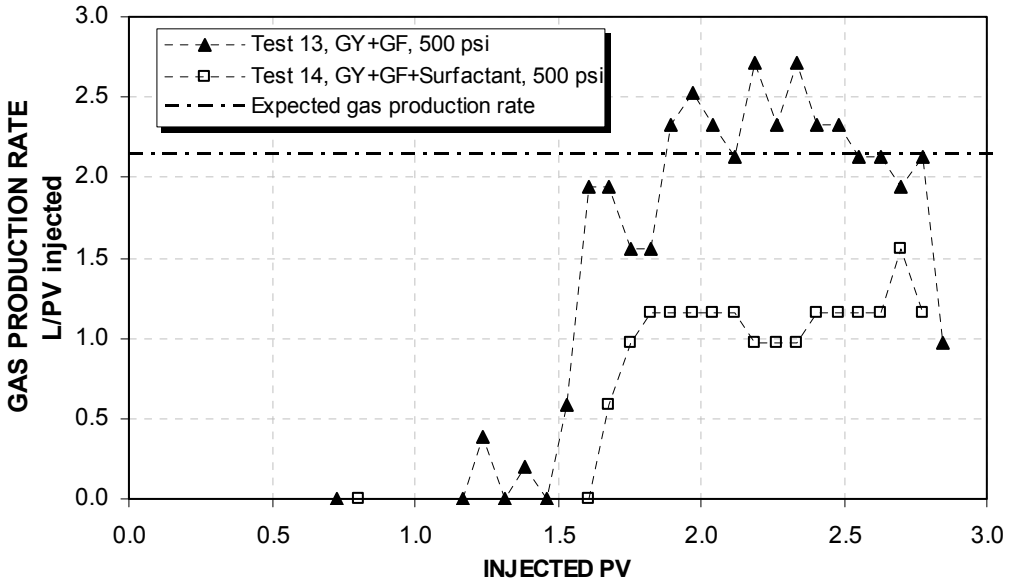

Figure 20. Variation of gas production rate (at ambient conditions) versus injected PV for the tests performed at 500 psi and 176°F (brine breakthroughs are shown by similar symbols on horizontal axis)

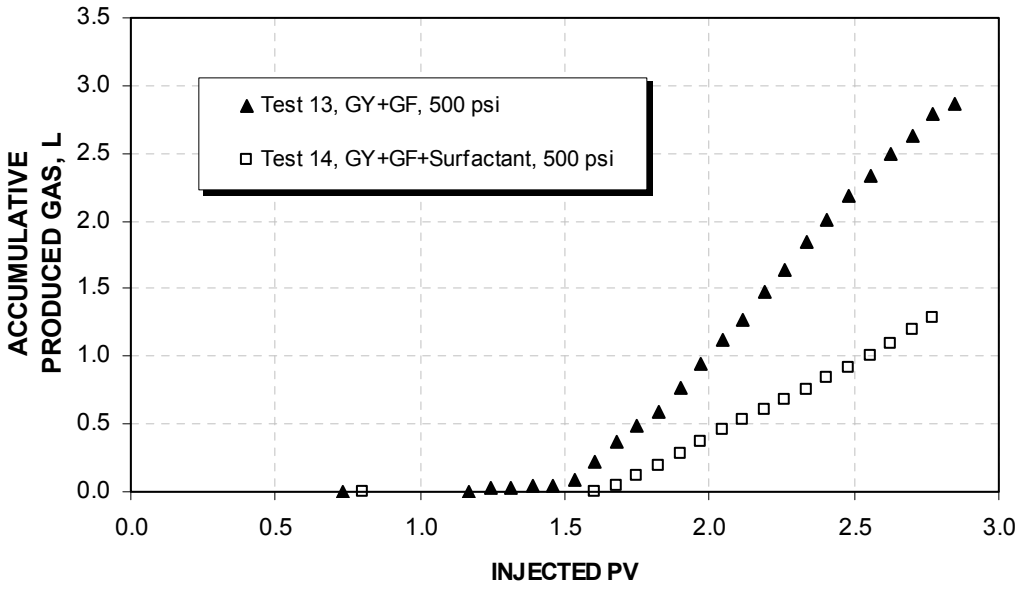

Figure 21. Variation of accumulative produced gas volume (in room conditions) versus injected PV for the tests performed at 500 psi and 176°F (brine breakthroughs are shown by similar symbols on horizontal axis)

6-1-1-2- Tests at 1000 psi

Figure 22 shows that at 1000 psi, for the brine flooding ΔP-PV curves are similar to the ones at 500 psi. But in ISCGT floods, there isn't any significant pressure increase after brine breakthrough and ΔP-PV curves are very similar to the brine ones. This indicates that the quantity of generated CO_2 inside the slim-tube is not enough to have a free CO_2 at 1000 psi, and a brine/oil system dissolves almost all the generated CO_2 (as seen from Figure 7, CO_2 solubility in oil increases by increasing the pressure). Therefore, there are only 2 phases (brine and oil) inside the slim-tube. However, there is a small bump in pressure drop curves for all ISCGT flooding right before brine breakthrough which almost coincides with an increase in oil production (Figure 23). This bump probably is caused by the presence of some free CO_2 in a small volume at the inlet of slim-tube. Then due to the more contact time between CO_2 and brine and residual oil, all generated gas dissolves in the liquids inside the system and therefore, the change in pressure drop remains small. The dissolved gas reduces the viscosity of the oil, and most probably it is a reason behind the increase in oil production at around 1 PV of injection.

After the test 4, the pressure difference increases from 100 to 200 psi along the slim-tube. This can be a result of a small decrease in permeability of the system caused by corrosion products of a failed test without the use of acid inhibitor.

Figure 23 indicates that after the fifth experiment, generally brine breakthroughs are occurring around 0.2 PV later. Again, change in the system parameters by corrosion products and also system wettability alteration by being in contact with brine for a long time can be responsible for the delayed brine breakthroughs.

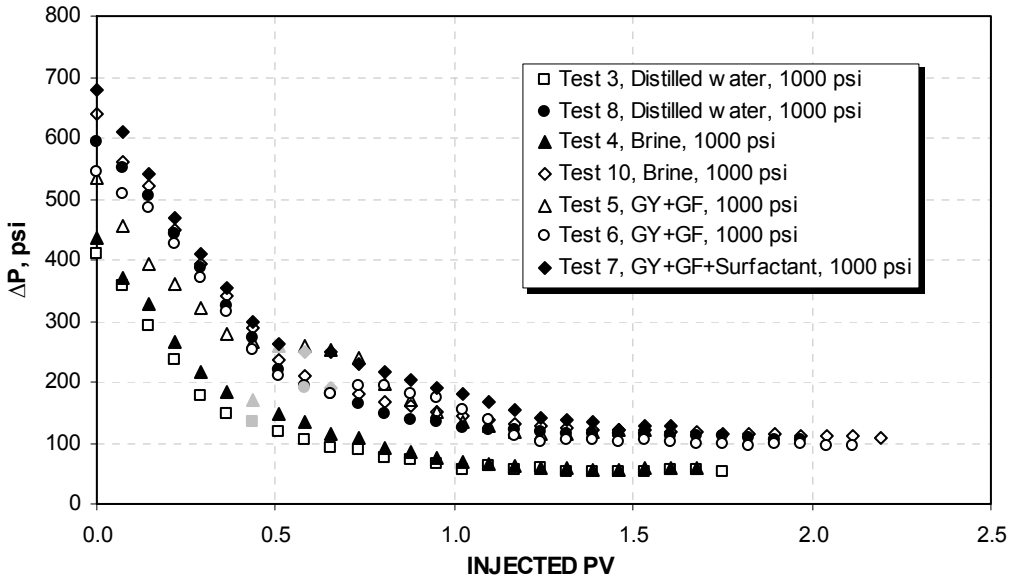

Figure 22. Variation of ΔP along slim-tube versus injected PV for the tests performed at 1000 psi and 176°F (brine breakthroughs are shown by gray symbols)

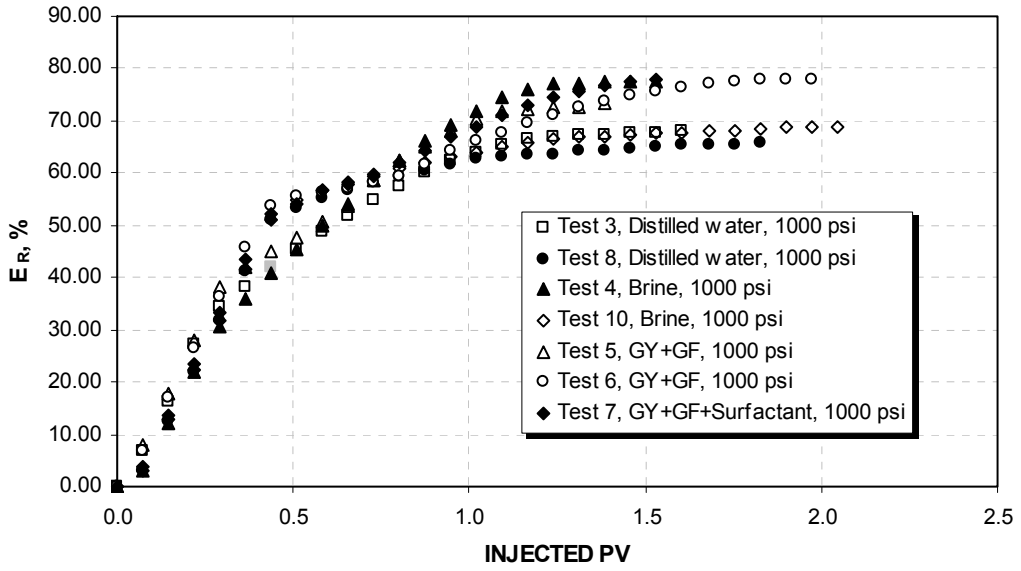

Figure 23. Variation of E_R versus injected PV for the tests performed at 1000 psi and 176°F

Figure 24 demonstrates that similar to the tests at 500 psi, there is a swelling effect caused by dissolved CO_2 in the system liquids (mainly oil) in all ISCGT floodings at 1000 psi.

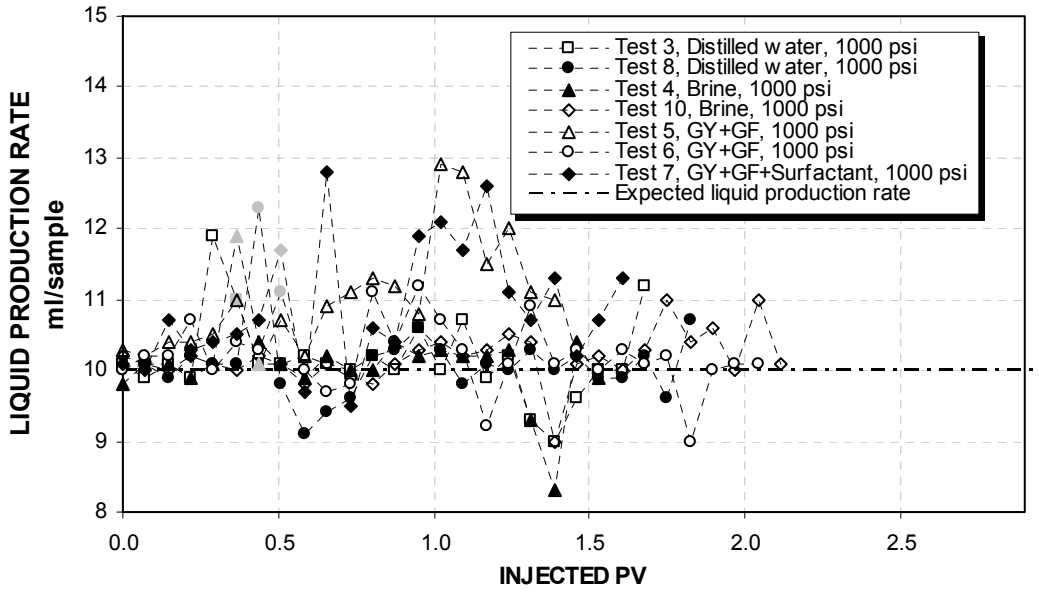

Figure 24. Variation of liquid production rate per sample versus injected PV for the tests performed at 1000 psi and 176°F (brine breakthroughs are shown by gray symbols)

Because of the absence of free CO_2 which in turn results in the absence of foam, addition of surfactant doesn't have any effect in delaying brine or gas breakthroughs at 1000 psi. It can be observed that in test 7, for unknown reasons, brine and gas breakthroughs occurred even slightly earlier compared to ISCGT floodings without surfactant.

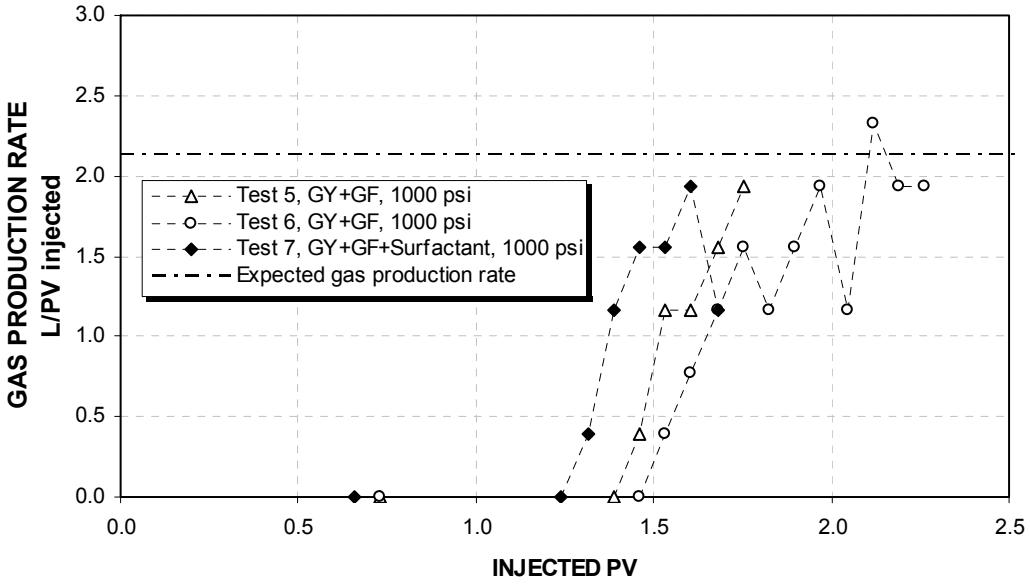

Figure 25. Variation of gas production rate (at ambient conditions) versus injected PV for the tests performed at 1000 psi and 176°F (brine breakthroughs are shown by similar symbols on horizontal axis)

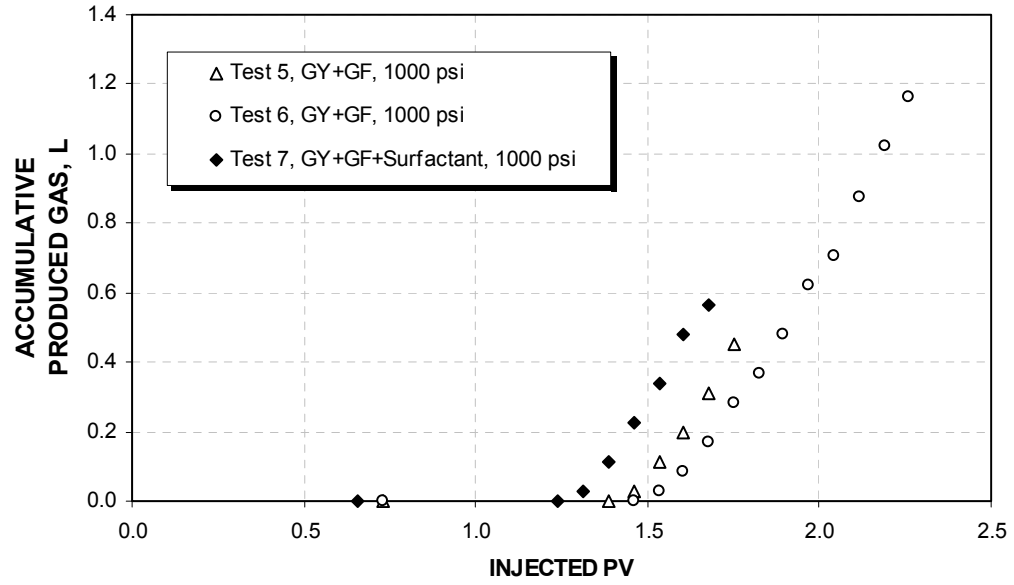

Figure 26. Variation of accumulative produced gas volume (in room conditions) versus injected PV for the tests performed at 1000 psi and 176°F (brine breakthroughs are shown by similar symbols on horizontal axis)

6-1-1-3- Tests with brine as displacing fluid

All the brine floodings at different pressures have the same ΔP decreasing pattern. No abrupt changes in pressure can be observed because there isn't any gas production inside the slim-tube

to generate a third phase in the system. For these reasons, a shift in pressure difference and also a later brine breakthrough can be seen after the test 4.

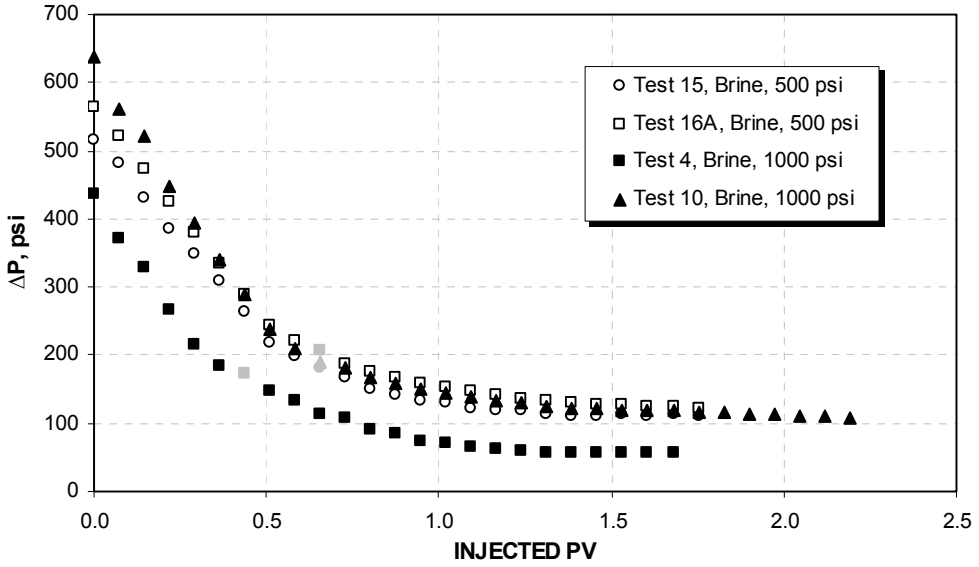

Figure 27. Variation of ΔP along slim-tube versus injected PV for the tests performed at 176°F and with brine as displacing fluid (brine breakthroughs are shown by gray symbols)

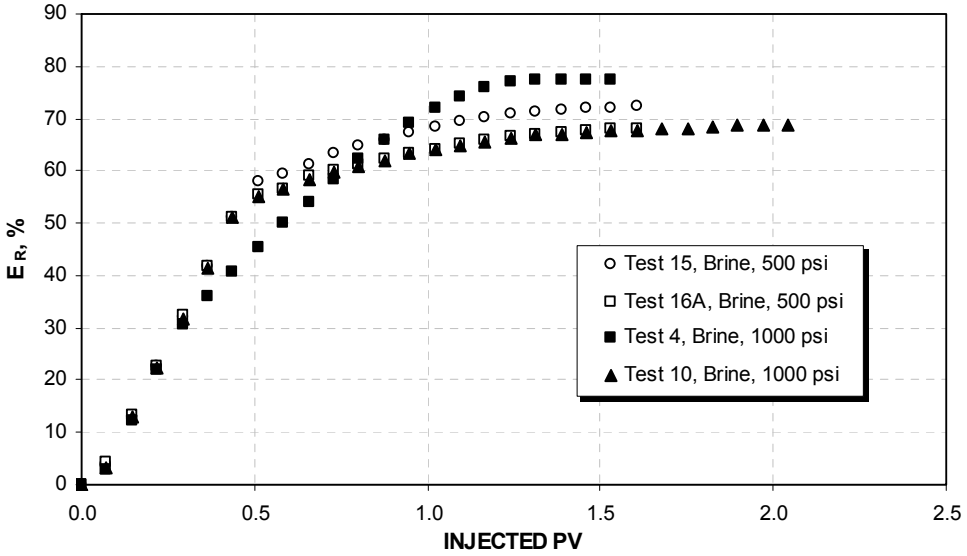

Figure 28. Variation of E_R vs. injected PV for the tests performed at 176°F and with brine as displacing fluid

Without a gas generation, a liquid production rate during brine floodings agrees well with the expected one, except some areas around a brine breakthrough.

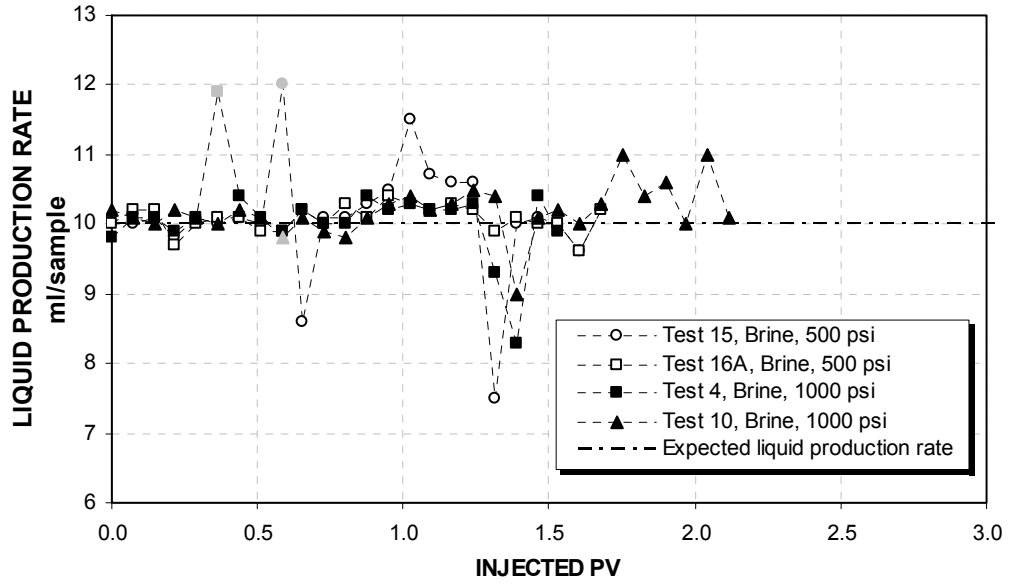

Figure 29. Variation of liquid production rate per sample vs. injected PV for the tests performed at 176°F and with brine as displacing fluid (brine breakthroughs are shown by gray symbols)

6-1-1-4- Tests with GY+GF as displacing fluid

This section analyzes all the ISCGT flooding tests that have been conducted without the use of surfactant. From Figure 30 it can be seen that for the tests performed at the pressures 1000 psi and 1500 psi, the ΔP-PV curves have exactly the same profile (decreasing with the increase of injected PV, with a bump right after the brine breakthrough). Only the test at 500 psi has a different ΔP-PV graph shape which is the result of presence of free gas inside the slim-tube. Thus, Figure 30 again confirms that there isn't any considerable amount of free CO_2 inside the slim-tube at the pressures more than 500 psi.

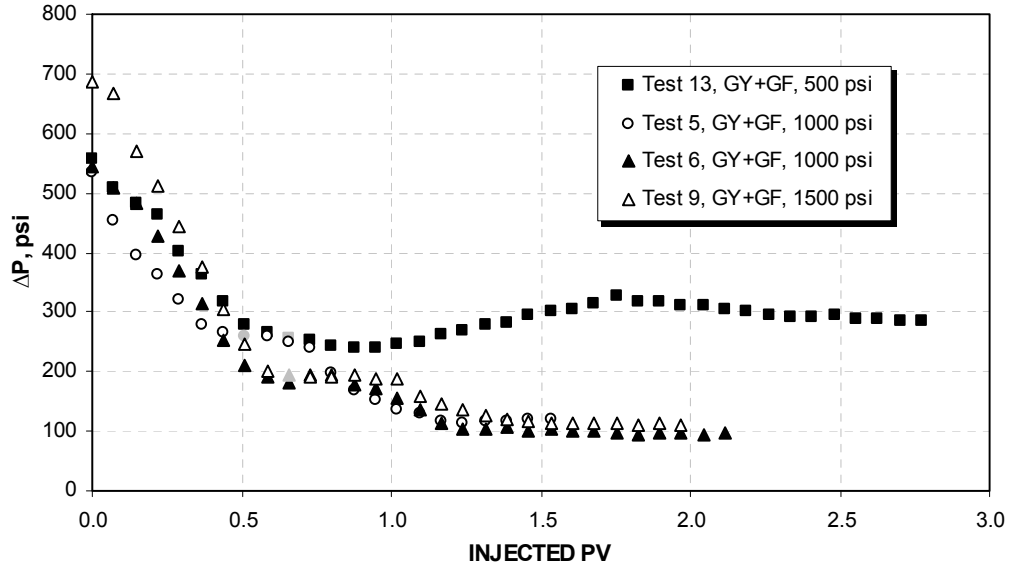

Figure 30. Variation of ΔP along slim-tube vs injected PV for the tests performed at 176°F and with GY+GF as displacing fluid (brine breakthroughs are shown by gray symbols)

Delay in brine breakthrough during the tests after the test 5 (Figure 31) probably is caused by the changes in systems parameters and wettability, as explained before.

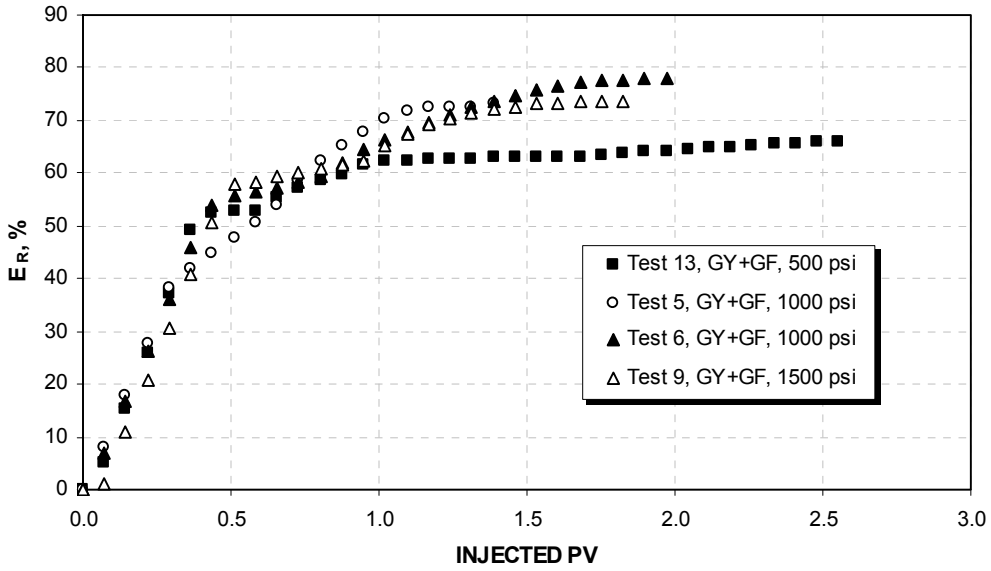

Figure 31. Variation of E_R vs. injected PV for the tests performed at 176°F and with GY+GF as displacing fluid

Figure 32 demonstrates that swelling has similar effects on liquid production rate at the pressures 1000 psi and 1500 psi. But at 500 psi, the increase in liquid production rate is much larger. It's because, at higher pressures only swelling of brine and oil caused by dissolved CO_2 is responsible for increase in liquid production rate, but at 500 psi, in addition to swelling, occupied volume by free gas also contributes to the rise in liquid production rate.

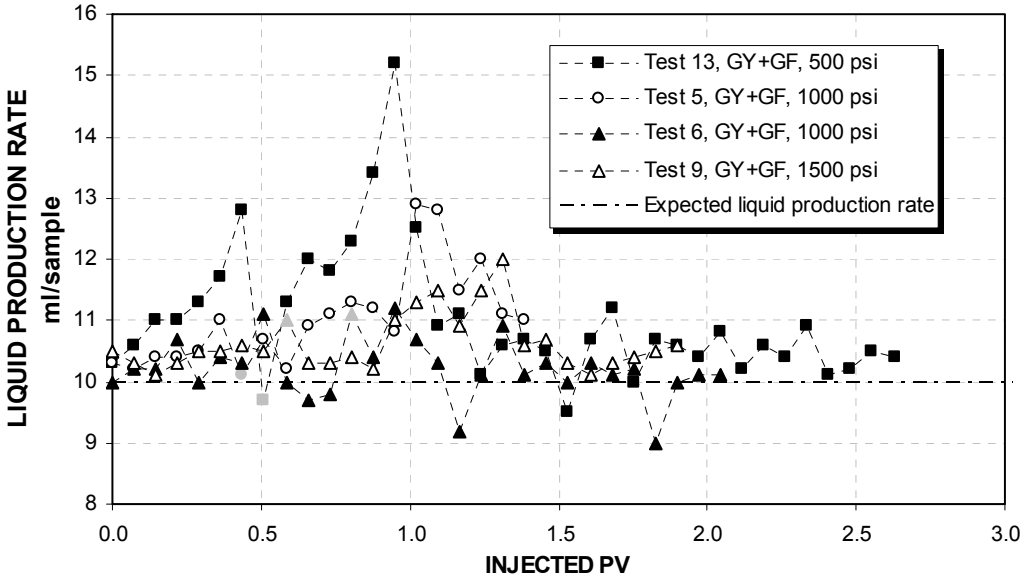

Figure 32. Variation of liquid production rate per sample vs. injected PV for the tests performed at 176°F and with GY+GF as displacing fluid (brine breakthroughs are shown by gray symbols)

As seen from the Figure 33, a gas breakthrough in all ISCGT floodings without a surfactant, occurs almost at the same time. This is reasonable if to consider a lack of foam in the system. Also, increasing the pressure slightly decreases the rate of gas production by increasing the solubility of CO_2 in the liquids system which leads to an increase in the volume of trapped gas inside the system.

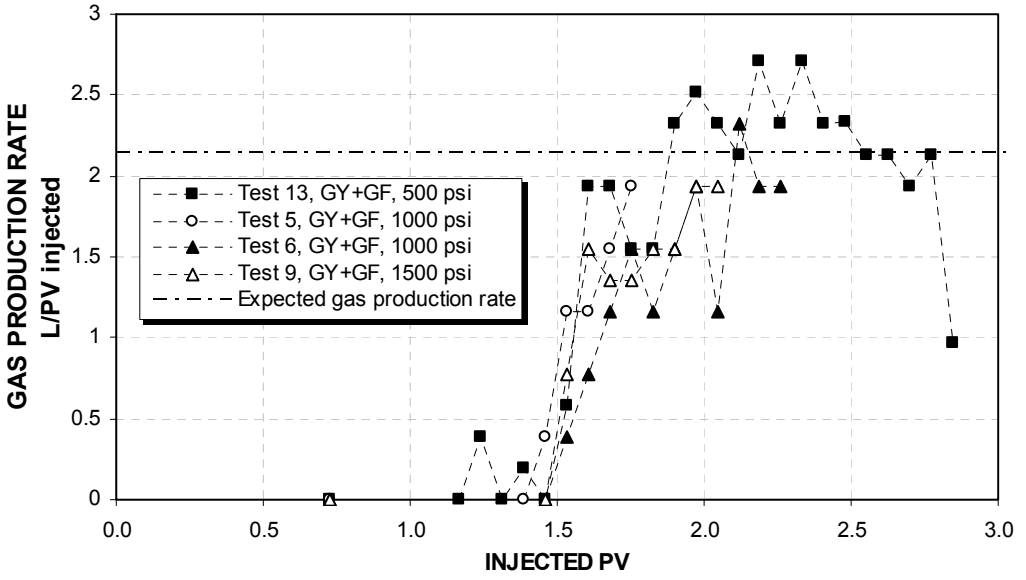

Figure 33. Variation of gas production rate (in room conditions) vs. injected PV for the tests performed at 176°F and with GY+GF as displacing fluid (brine breakthroughs are shown by similar symbols on horizontal axis)

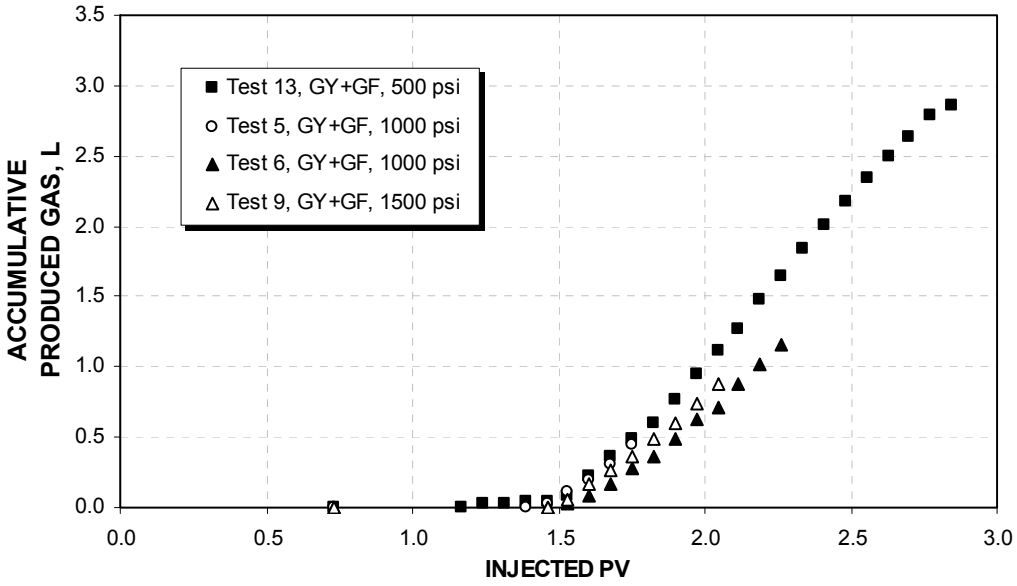

Figure 34. Variation of accumulative produced gas volume (at ambient conditions) vs injected PV for the tests performed at 176°F and with GY+GF as displacing fluid (brine breakthroughs are shown by similar symbols on horizontal axis)

6-1-1-5- Tests with GY+GF and surfactant as displacing fluid

Figure 35 is another indication of absence of free CO_2 gas inside the system at pressures higher than 500 psi. At 1000 psi, with no free gas available, surfactant can't generate any foam; therefore, there isn't any pressure increase after brine breakthrough. Generation of foam also delays brine breakthrough in test 14 by decreasing the mobility of displacing fluid.

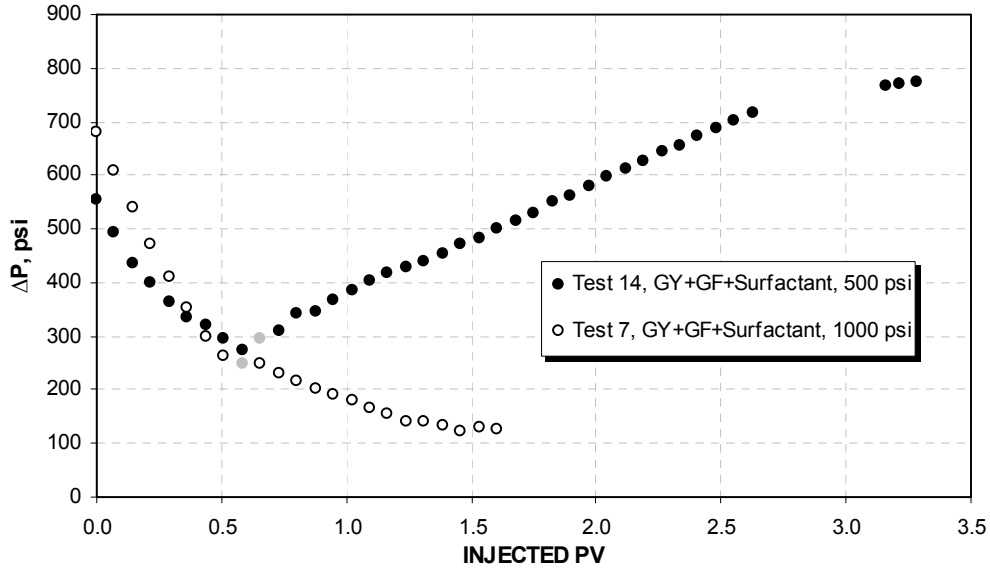

Figure 35. Variation of ΔP along slim-tube vs. injected PV for the tests performed at 176°F and with GY+GF and surfactant as displacing fluid (brine breakthroughs are shown by gray symbols)

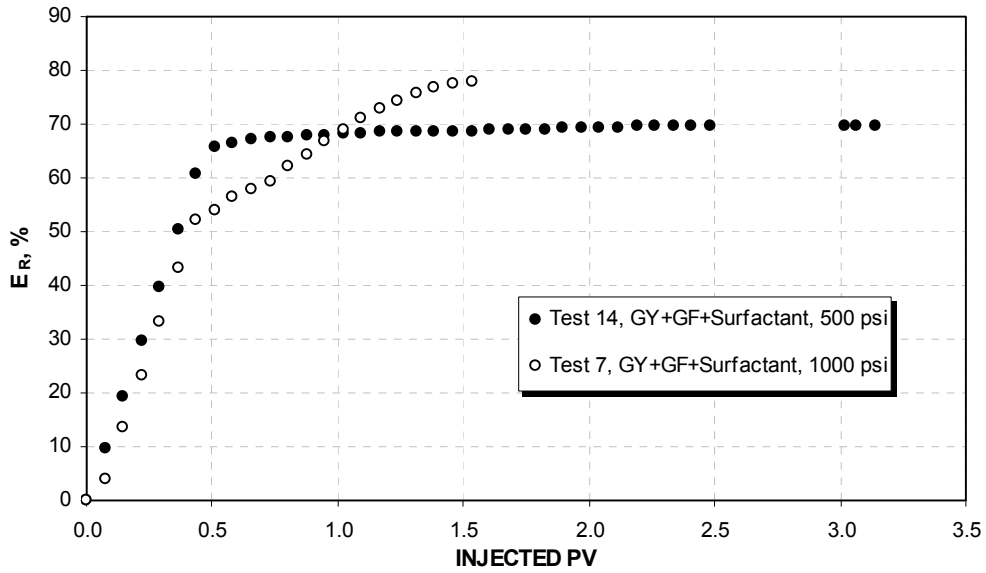

Figure 36. Variation of E_R vs. injected PV for the tests performed at 176°F and with GY+GF and surfactant as displacing fluid

There isn't much difference in liquid production rate in these two tests. It seems that increase in liquid production caused by presence of free CO_2 at 500 psi matches the extra oil swelling induced by more dissolved CO_2 at 1000 psi. In test 14, the drop in the liquid production rate after 1.75 PV can be explained by the difficulties of collecting liquid samples in the presence of large volumes of foam.

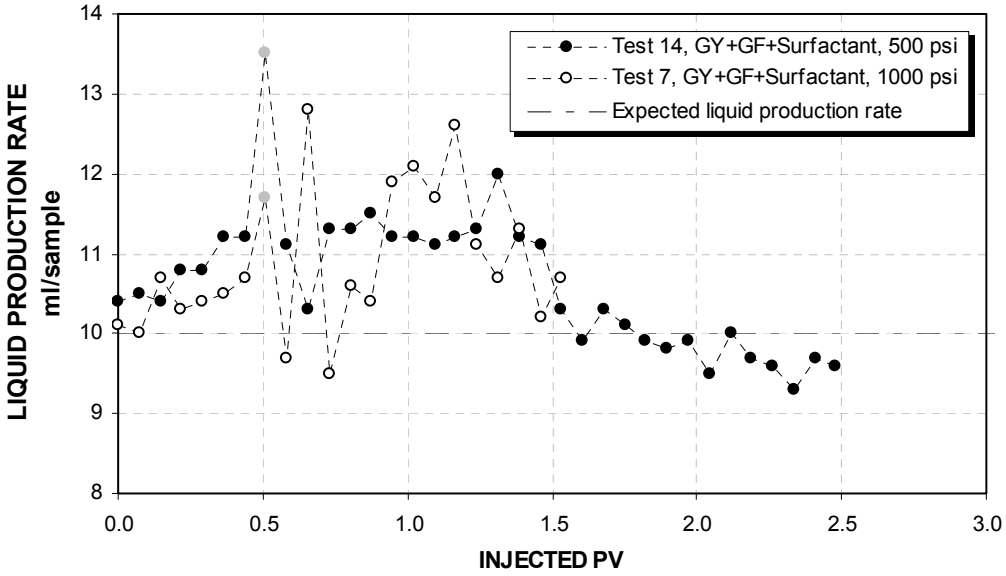

Figure 37. Variation of liquid production rate per sample vs. injected PV for the tests performed at 176°F and with GY+GF and surfactant as displacing fluid (brine breakthroughs are shown by gray symbols)

Again, a 0.75 PV delay in gas breakthrough caused by generation of foam during the test 14 as seen from the Figure 38.

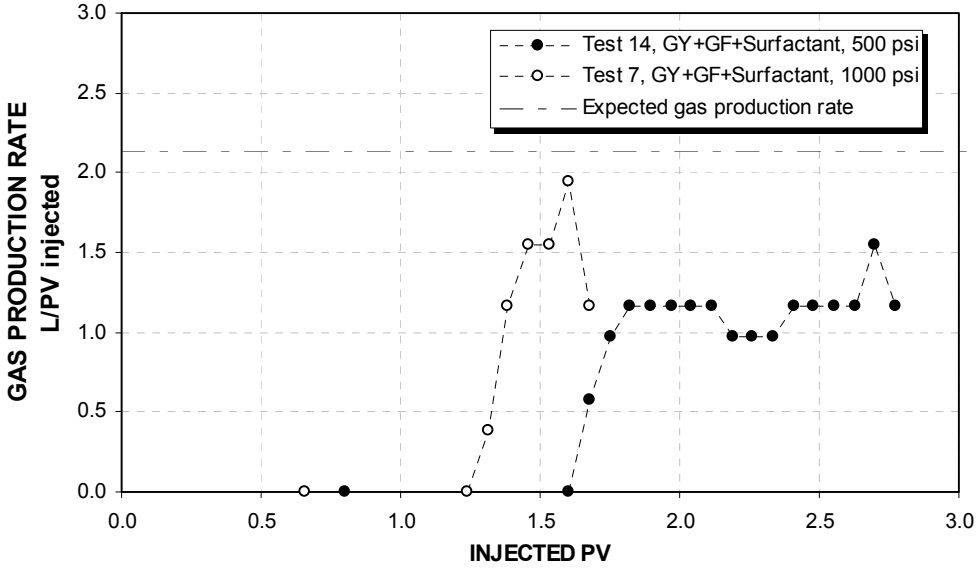

Figure 38. Variation of gas production rate (in room conditions) vs. injected PV for the tests performed at 176°F and with GY+GF and surfactant as displacing fluid (brine breakthroughs are shown by similar symbols on horizontal axis)

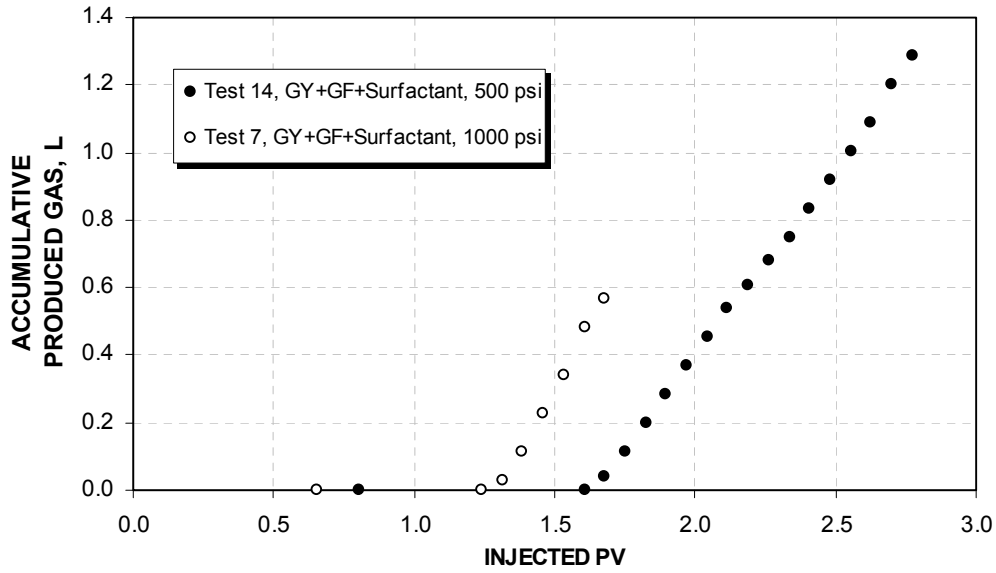

Figure 39. Variation of accumulative produced gas volume (in room conditions) vs. injected PV for the tests performed at 176°F and with GY+GF and surfactant as displacing fluid (brine breakthroughs are shown by similar symbols on horizontal axis)

6-1-1-6- Tests with CO_2 as displacing fluid

Table 5. Final E_R and E_R before gas breakthrough for CO_2 flooding tests

P, psi	E_R, %	Breakthrough E_R, %
1000	50.47	18.11
2000	61.01	36.41
2000	66.13	36.79
3000	81.98	46.50

CO_2 flooding at pressures of 1000 psi, 2000 psi (with a rerun) and 3000 psi were conducted. The results show that increasing the pressure improves oil recovery significantly. A high compressibility of CO_2 makes it a very dense fluid in higher pressures and decreases the mobility of displacing front considerably which in turn, improves oil recovery efficiency. Figure 41 clearly shows high pressure dependency of CO_2 density. By increasing the pressure from 1000 psi to 3000 psi, CO_2 density has become tripled but the density of oil has remained the same. Most of the E_R improvement at higher pressures occurs before the gas breakthrough (Table 5).

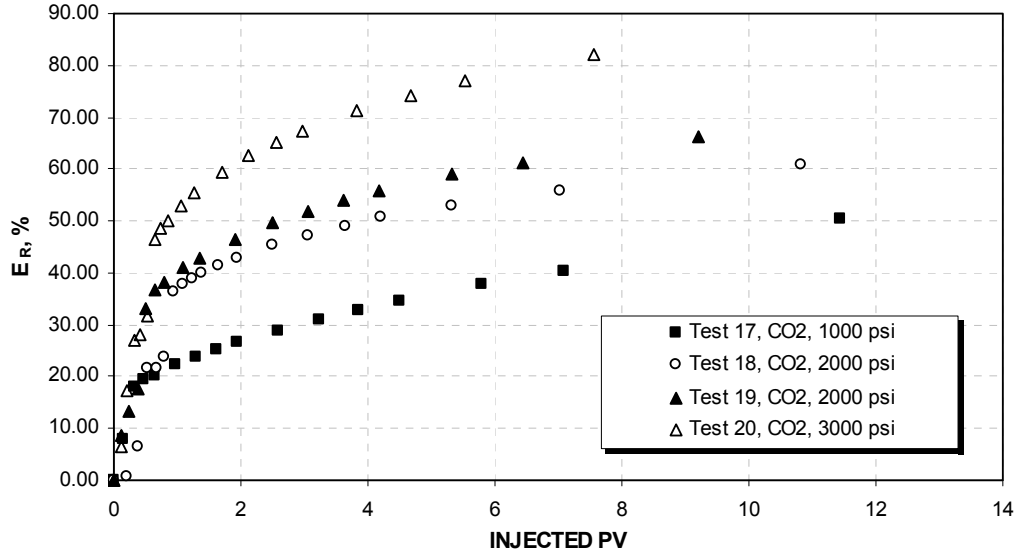

Figure 40. Variation of E_R vs. injected PV for the tests performed at 176°F and with CO_2 as displacing fluid

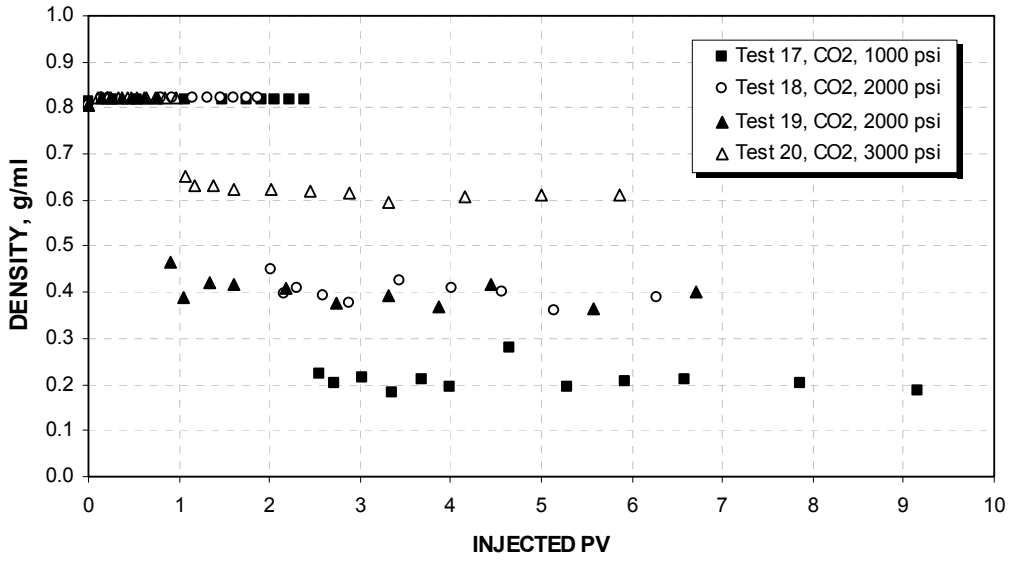

Figure 41. Variation of CO_2 density over injected PV for the tests performed at 176°F and with CO_2 as displacing fluid

To examine the extent of extraction of lighter oil components by generated CO_2, densities of three produced oil samples were measured at each pressure. Sample 1 was taken before gas breakthrough; thus, it was expected to have the same density as that of injected oil and can act as a baseline for comparing the density of other samples. Sample 2 was collected right after gas breakthrough and sample 3 was the produced oil at the end of production. If CO_2 extracts lighter components of oil, then latter collected samples should have lower densities.

Table 6 demonstrates the density measurements results. As seen from these data, at 1000 and 2000 psi, no considerable change in densities of different samples can be seen. Therefore, the pressure is too low to extract oil by CO_2. At 3000 psi, there is a slight decrease in the density of produced oil in second and third samples compared to the first one. It shows that there is a small extraction of oil components by generated CO_2 at 3000 psi, and CO_2 and oil are in near-miscible conditions at this pressure.

Table 6. Density of produced oil samples collected right before and after breakthrough and at the end of production during tests

P, psi (test#)	Sample 1 density, g/ml	Sample 2 density, g/ml	Sample 3 Density, g/ml
1000 (17)	0.8487	0.8486	0.8488
2000 (18)	0.8484	0.8483	0.8496
3000 (20)	0.8495	0.8482	0.8447

A CO_2 flooding at different pressures was conducted with constant flowrates inside the slim-tube. Because of the compressibility of CO_2, mass flowrate was larger in higher pressures and this led to larger gas production rates in room conditions at higher pressures (Figure 42).

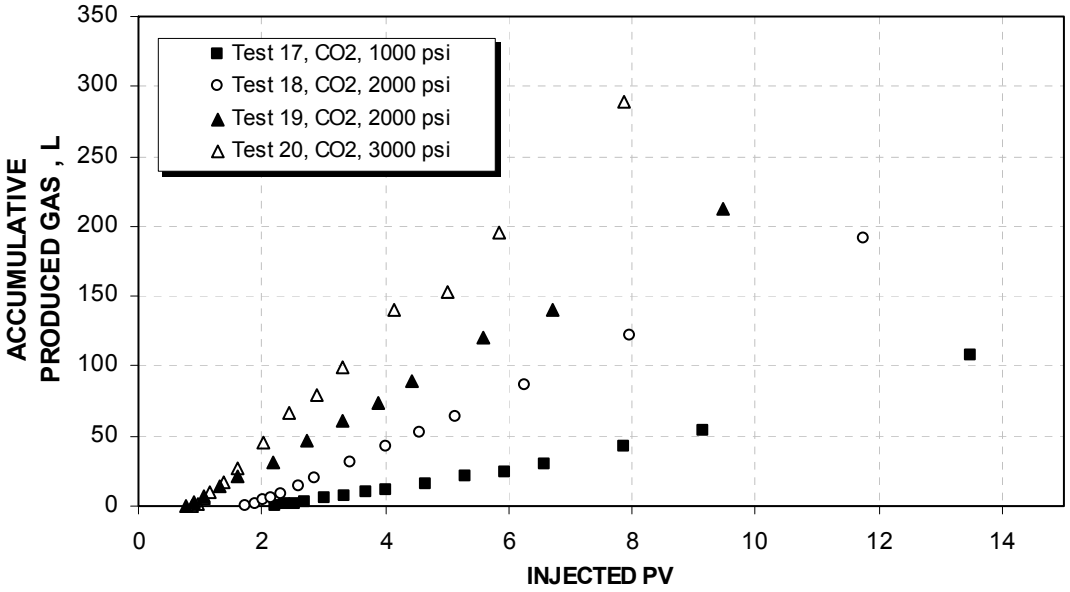

Figure 42. Variation of accumulative produced gas volume (at ambient conditions) vs. injected PV for the tests performed at 176°F and with CO_2 as displacing fluid

6-1-2- Three-stage recovery

To evaluate the effectiveness of ISCGT in extracting residual oil, the test 16 was conducted at 500 psi. Initially, system was flooded with brine (test 16A).Then it was flooded with GY and GF co-injection (test 16B), and the last stage was a co-injection of GY and GF solutions with the addition of surfactant. The second and third stages were started without cleaning residual oil from previous stages. All three stages were continued until the stop of oil production stopped. Pressure difference patterns for the first and second stages were similar to previous tests at 500 psi: the pressure difference is gradually decreasing during the brine flooding and it is slightly increasing in GY and GF co-injection because of the free gas generation. The only difference is that the increase in pressure difference starts right after the beginning of the second stage (instead of after brine breakthrough in regular flood tests). Small volume of residual oil- compared to regular recovery tests, which start with the system full of oil, dissolves less CO_2 and allows the free CO_2 to exist earlier in the system. For unknown reasons the amount of the observed foam at the outlet, and the pressure increase at the third stage were less than those of earlier tests involved a foam generation in the system.

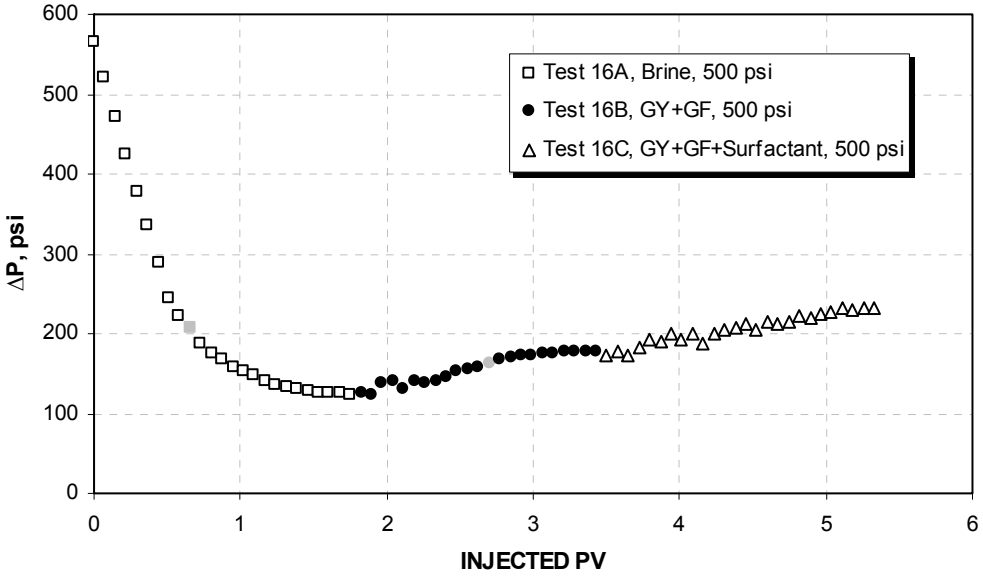

Figure 43. Variation of ΔP along slim-tube vs. injected PV for the tests 16A, 16B and 16C performed at 176°F and 500 psi (brine breakthroughs are shown by gray symbols)

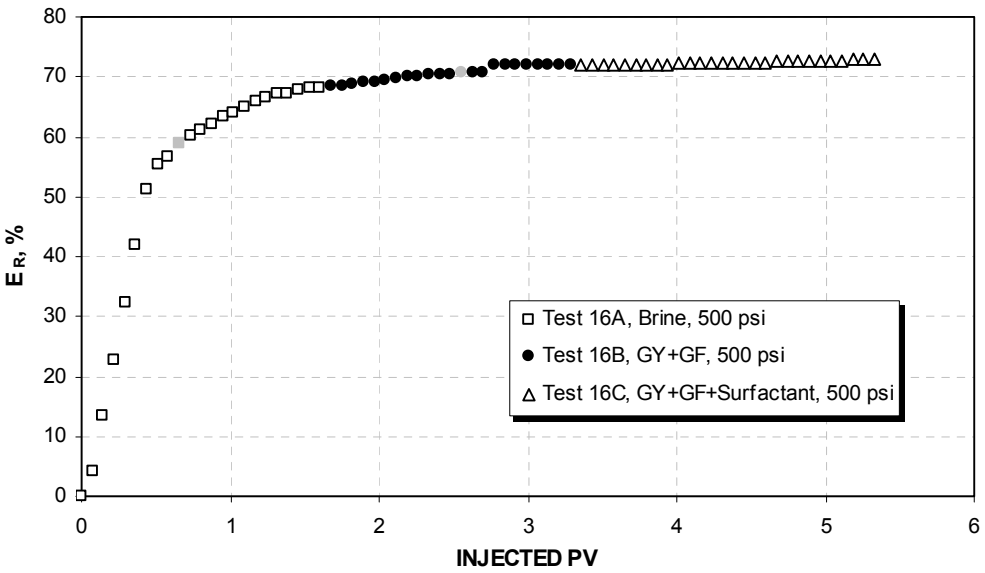

Figure 44. Variation of E_R vs. injected PV for the tests 16A, 16B and 16C performed at 176°F and 500 psi (brine breakthroughs are shown by gray symbols)

Swelling effect is similar to other ISCGT floodings at 500 psi. Increase in liquid production starts at the beginning of the stage 2 and continues for up to 1.5 PV injected. In the third stage, liquid production rate is close to expected rate (10 ml). The reason is that the system liquids are already swollen and the free gas is present inside the system. Therefore, during the test 16C the liquid production rate is actually the extension of that of the test 16B which is already back to the normal rate after 3 PV injection.

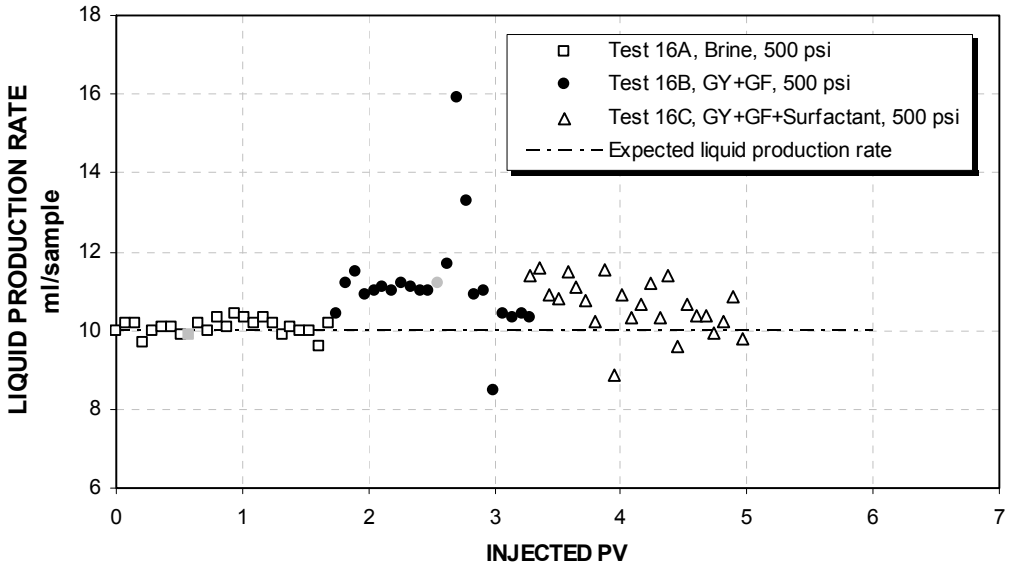

Figure 45. Variation of liquid production rate per sample over injected PV for the tests 16A, 16B and 16C performed at 176°F and 500 psi (brine breakthroughs are shown by gray symbols)

6-2- Discussions about study objectives

In this section, interpretations of the results are arranged by investigating the feasibility of achieving miscibility between CO_2 and oil in ISCGT, evaluation of effectiveness of this technique as EOR method, evaluation of different methods of injection (slug injection and co-injection), examining the effectiveness of surfactant and also investigating the severity of corrosion caused by this technique.

6-2-1- Miscibility

Big differences between oil recovery efficiencies and mechanisms involved in miscible and immiscible floodings make it essential to study the possibility of achieving miscibility between oil and CO_2 in ISCGT and the thermobaric conditions required for it.

From chapter 6.1, it was understood that the quantity of generated CO_2 by this technique is not enough to have considerable free CO_2 inside the slim-tube at the pressures higher than 500 psi (Figures 16, 22, 30 and 35) and at these pressures almost all the generated CO_2 is dissolved by system liquids (brine and oil). This was confirmed by PVTsim^{TM} simulator which predicted that considering the oil composition and thermobaric conditions, no free CO_2 can exist inside the system in pressures higher than 1100 psi.

To have miscibility between oil and CO_2, there should be many contacts between these two phases in which oil and CO_2 components transfer back and forth, and this process can't be done with the CO_2 in the dissolved form. Therefore, in order to achieve miscibility, free CO_2 should present inside the system.

Figure 46 shows the relationship between final recovery efficiency and operating pressure in four CO_2 flooding tests. The increase in E_R is linear, and considering section 2-5-1, all the points are in immiscible part of MMP graph and before breakover point. A pressure limit of the experimental setup didn't allow us to run CO_2 floodings at higher pressures and to measure MMP accurately. As seen from Figure 46, MMP of this mineral oil at the temperature of 176°F is

certainly more than 3500 psi. This indicates that miscible flooding can't be achieved in pressures less than 3500 psi and considering the fact that there isn't any free CO_2 at pressures higher than 1000 psi, it can be concluded that in ISCGT generated CO_2 and the specific mineral oil used in these experiments can not reach miscibility at 176°F and the flood would be immiscible.

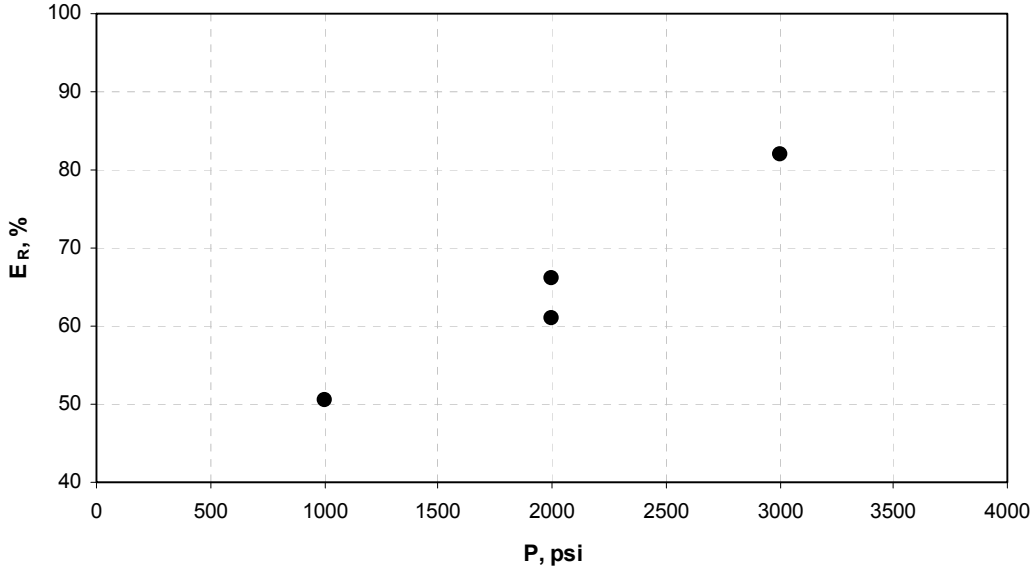

Figure 46. Variation of final E_R over operating pressure in CO_2 floodings conducted at 176°F

6-2-2- Evaluation of oil recovery efficiency

In the previous section, it was realized that the ISCGT is an immiscible flood. Therefore, this technique is expected to improve oil recovery by all the means of recovery improvement available in immiscible CO_2 floods (decreasing the oil viscosity and oil/water IFT and also oil swelling caused by dissolved CO_2). In addition, presence of surfactant and brine is expected to improve the recovery by improving the mobility of displacing front. Oil recovery efficiency resulted by this method is discussed in two types of experiments: oil recovery when ISCGT used to displace oil and three-stage oil recovery tests.

6-2-2-1- "Two-fluid" recovery tests

Table 7 shows final recovery efficiencies of all the tests performed with two-fluids. Gray cells show average recovery efficiencies in case there is more than one test in the same operating pressure and with the same displacing fluid.

At 500 psi, E_R attained with ISCGT without surfactant is about 4% less than that of brine flooding. By adding the surfactant, recovery of ISCGT becomes very close to that of brine flooding. It seems that presence of free CO_2 inside the system in the immiscible state decreases oil recovery by increasing the mobility of displacing front, and it outweighs the improve in oil recovery caused by dissolved CO_2 in the oil. However, generation of foam by surfactant improves the recovery and helps to reach brine flooding E_R.

At 1000 psi, brine flooding recovery has a 6-7% advantage over distilled water flooding. The reason behind this difference is probably wettability alteration in the slim-tube caused by brine. Brine makes the system more "water-wet", which means that the system inclines to imbibe water and expel oil, and this leads to easier extraction of oil out of pores and increase in oil recovery.

There is a 2% advantage for ISCGT flooding compared to brine flooding. This is caused by the fact that all the generated CO_2 is dissolved in the system liquids at this pressure, and it results in increase of the oil swelling effect, and also in reduction of oil viscosity compared to those at 500 psi in which some of the generated gas was in the free form. Addition of surfactant improves E_R by more than 2%. CO_2 flooding recovery at this pressure is 16-17% less than the other floodings. This large difference can be explained by very low density of CO_2 at 500 psi. As seen from Figure 41, CO_2 density is around 0.2 g/ml at this thermobaric conditions which is one fifth of the water density.

By increasing the pressure up to 1500 psi, no improvement in recovery of ISCGT flooding was observed. At pressures higher than 1000 psi, all the generated CO_2 is dissolved in the liquids system. Therefore, increasing the pressure can't increase the quantity of dissolved gas and it doesn't have any further effect on the oil swelling and viscosity of the oil.

Large density of CO_2 at higher pressures makes its recovery efficiency to surpass even the highest recoveries attained by ISCGT flooding.

Table 7. Final E_R of all the secondary recovery tests organized by operating pressure and type of displacing fluid (gray cells are calculated average numbers)

P, psi	Recovery Efficiency (E_R) of mineral oil displaced with different displacing fluids, %				
	Distilled Water	Brine	GY+GF	GY+GF +Surfactant	CO_2
500		72.26- 68.20	65.94	69.81	
		70.23	65.94	69.81	
1000	68.01- 65.66	77.54- 68.86	73.30- 77.92	77.92	50.47
	66.83	73.20	75.61	77.92	50.47
1500			73.67		
			73.67		
2000					61.01- 66.13
					63.57
3000					81.98
					81.98

6-2-2-2- "Three-stage" recovery tests

Final recovery efficiencies of different stages of test 16 have been shown in Table 8. In the second stage, co-injection of GY+GF can recover nearly 4% of IOIP. This equals to 12% of residual oil at the end of brine flooding. In the third stage, addition of surfactant recovers only 1% of IOIP or 3.5% of residual oil in place.

Table 8. E_R and residual oil E_R in the tests 16A, 16B and 16C

Test #	Displacing fluid	E_R, %	Residual oil E_R, %
Test 16A	Brine	68.20	68.20
Test 16B	GY+GF	72.02	12.01
Test 16C	GY+GF+ Surfactant	73.01	3.53

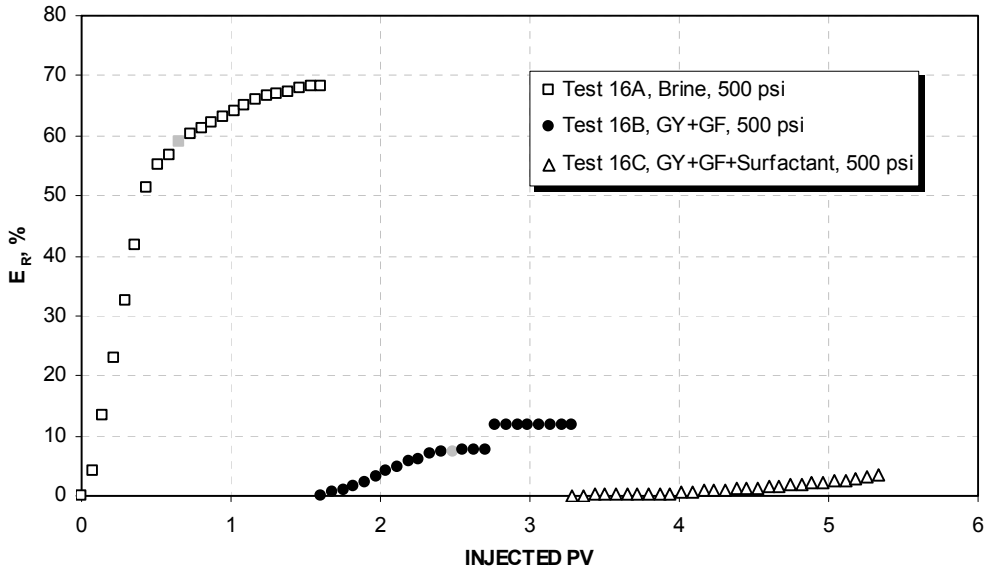

Figure 47. Variation of E_R of residual oil over injected PV for the tests 16A, 16B and 16C performed at 176°F and 500 psi (brine breakthroughs are shown by gray symbols)

6-2-3- Surfactant effectiveness

Addition of surfactant at 500 psi in "two-fluids" flood tests, improves E_R by nearly 4%. Reduction of displacing front mobility induced by the presence of foam, and decrease in brine/oil IFT caused by surfactant are the reasons behind this additional recovery. Also, presence of surfactant delays brine and gas breakthroughs by 0.2 PV and 0.1 PV, respectively (Figures 18 and 21). Both of these late breakthroughs make the flood more economical. A delayed brine breakthrough helps to produce more oil in a shorter period of time which is a more economical process considering high cost of production equipment lease, maintenance and also labor. A delayed gas breakthrough reduces the amount of required generated CO_2 for the same volume of the reservoir, and therefore decreases the volume of GY and GF solutions needed in thee flood. It also increases the contact time between generated CO_2 and oil.

At 1000 psi, presence of surfactant increases the recovery by 2%. The reason for smaller improvement in recovery compared to the one at 500 psi is due to the absence of foam in the system at this pressure, and surfactant can only enhance the recovery by decreasing the IFT between brine and oil. Moreover, there isn't any delay in brine and gas breakthroughs at 1000 psi, which again can be explained by the lack of foam in the system.

As the "three-stage" recovery at 500 psi (test 16C), for unknown reasons applying surfactant causes a very small improvement in E_R (~ 1%).

6-2-4- Effect of injection method

To examine the efficiency of the co-injection methods, the test 11 was performed by slug injection of GY and GF solutions. 1.8 PV of GY solution, 1.2 PV of GF solution and 1 PV of GY solution were injected consecutively. Table 9 shows that final oil recovery for the test 11 is less than the oil recoveries for the similar tests performed with co-injection method. Besides, from Figures 50 and 51 it can be seen that effects of both oil swelling and volume of CO_2 production is very small compared to those of the co-injection tests. Therefore, a slug injection is not an efficient method for mixing GY and GF solutions and it seems that it can't generate considerable gas inside the slim-tube. The reason of the slug injection inefficiency is a thin geometry of the slim-tube. It makes the mixing zone between consecutive slugs very small and therefore chemical reaction only happens in a small volume at the boundary of slugs.

The other problem with this injection method is corrosion. Even in the presence of high concentration of acid inhibitor, direct contact between corrosive GF solution and system at high temperature and for a long time is very corrosive.

Table 9. Final E_R and the injection method in the tests 5, 6 and 11

Test #	Displacing fluid	P, psi	Injection method	E_R, %
Test 5	GY+GF	1000	Co-injection	73.30
Test 6	GY+GF	1000	Co-injection	77.92
Test 11	GY+GF	1000	Slug injection	71.88

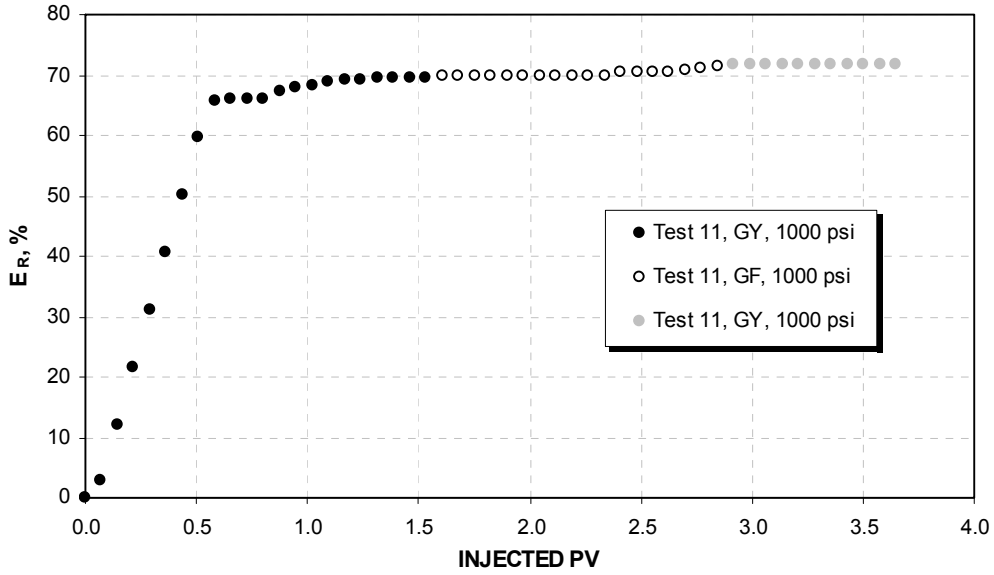

Figure 48. Variation of E_R over injected PV for test 11 performed at 176°F and 1000 psi and with GY+GF as displacing fluid and slug injection as the method of injection

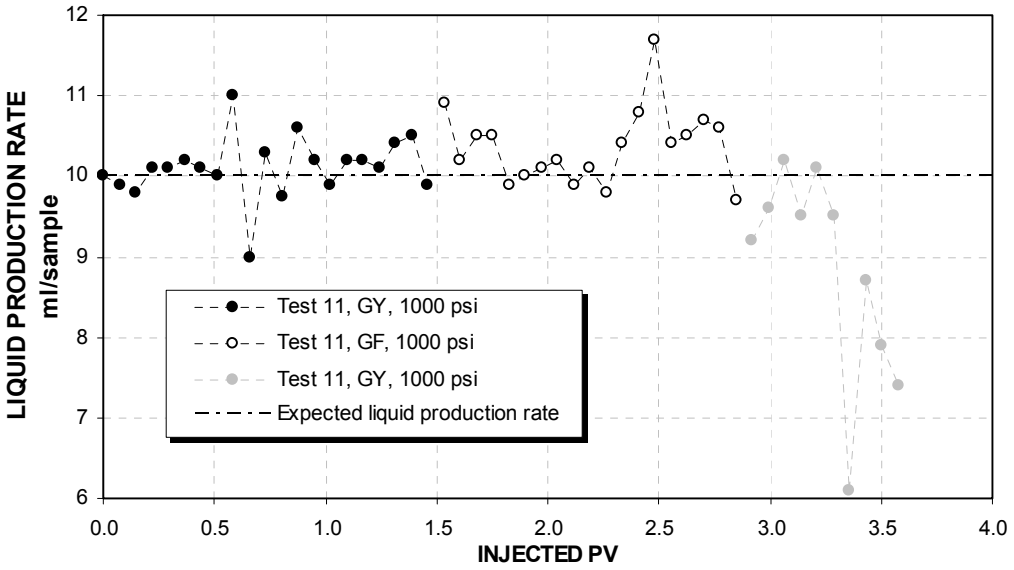

Figure 49. Variation of liquid production rate per sample over injected PV for test 11 performed at 176°F and 1000 psi and with GY+GF as displacing fluid and slug injection as the method of injection.

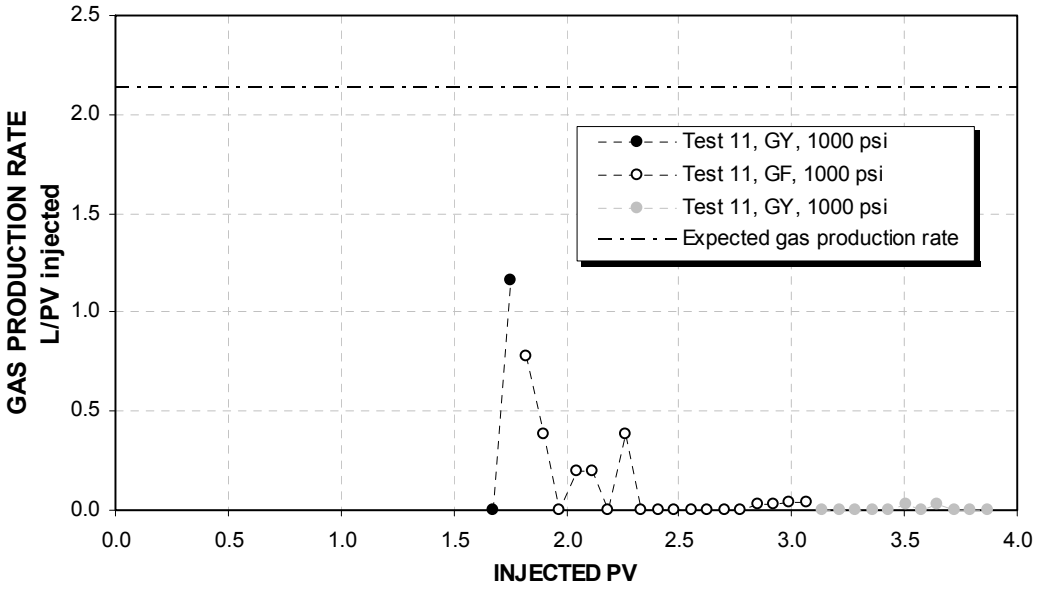

Figure 50. Variation of gas production rate (at ambient conditions) over injected PV for test 11 performed at 176°F and 1000 psi and with GY+GF as displacing fluid and slug injection as the method of injection.

6-2-5- Corrosion

There are two sources of corrosion during the ISCGT floods: carbonic acid and acidic GF solution. Dissolved CO_2 in water is in equilibrium with carbonic acid as follows:

$$CO_2 + H_2O \leftrightarrow H_2CO_3$$

Carbonic acid is a weak acid and it only exists in solution in equilibrium with CO_2, and its concentration is much lower than the concentration of CO_2. Acidic GF solution is another cause of corrosion in the system. Before reacting with GY solution in mixing valve, it's in the direct contact with the system. After the mixing, because of some inefficiency in the chemical reaction and mixing method, small concentrations of GF solution can exist in the system. To minimize the effect of corrosion in the system, following actions were considered during the tests:

- A commercial acid inhibitor was added to the GF solution. Acid inhibitor provides a coating on stainless steel and protects it from the acid.
- Mixing point of GY and GF solutions was placed outside temperature bath at room temperature. Considering very high temperature dependency of corrosion and very low concentrations of GF solution after the mixing point, corrosion effect was reduced considerably.
- The plumbing contacted GF solution before the mixing point was minimized.
- A contact time between GF solution and products of the chemical reaction with the system was minimized by reducing the duration of the test and also by flushing the system with distilled water and cooling down the system right after the experiment.
- To prevent a presence of GF solution in the products of chemical reaction, injection flowrate of GY solution was adjusted 5% more than the one calculated by chemical reaction stoichiometry ratio.

Even with all these measures, corrosion couldn't be prevented completely and there was a slight corrosion effects on the system and the pump used for injection a GF solution. Also, BPR diaphragm and Teflon ^{TM} and rubber O-rings had to be replaced after every couple of the tests. Teflon ^{TM} and rubber swelling caused by CO_2 also contributed to the O-rings degradation.

Activity 2. Generated CO_2 Gas Volume and Pressure Measurements and Core Flood Experiments

2.1. EXPERIMENTAL SETUP

As mentioned before, in this activity we performed two types of experiments. In this chapter, these sets will be introduced individually in the following sub sections: (1) chemical reaction tests in order to estimate the generated CO_2 gas volume and pressure, and (2) core flooding tests.

2.1.1. Chemical Reaction Experiments

The chemical reaction tests were performed on the experimental setup depicted in Figure 51. The reaction vessel was constructed by *Conoco Inc*., with a Teflon® compression cylinder. The vessel material is a combination of SS 304 and SS 316 grade stainless steels. It has 0.166" thick shell and 0.5" thick head, with a net volume of 512 mm, including the Teflon® cylinder. Its pressure rating is 2646 psig at 300˚F. A *Heise* pressure transducer with a pressure range between 0 and 5000 psia was used during the tests. The *Isco 500D Syringe pump* was used to inject the test solutions into the vessel. This pump allowed completely controlling the flow rate and the injection pressure of the test fluids. The *Hitachi* direct drive rotary vacuum pump was used to evacuate the reaction vessel before the injection of the test solutions. The experimental set up was installed inside the temperature bath, which allowed to maintain a constant temperature up to 250˚F.

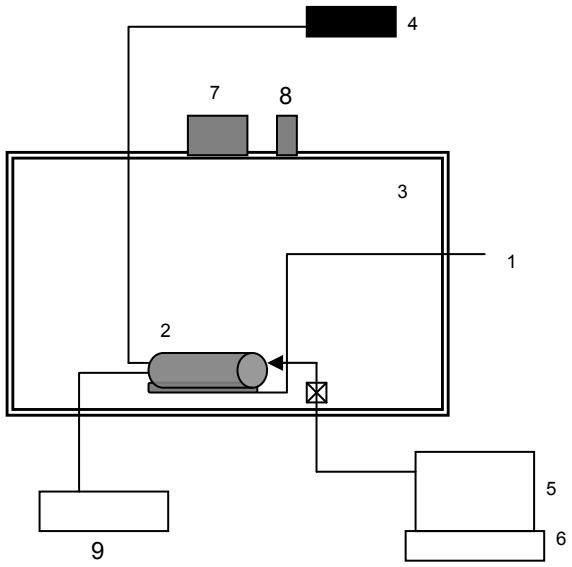

Figure 51. Experimental set-up: 1-Shaking mechanism, 2-Reaction vessel, 3-Constant temperature bath, 4-Pressure Transducer, 5-Syringe pump, 6-Pump control unit, 7-Heater, 8-Fan, 9-Vacuum pump.

2.1.2. Core Flooding Experiments

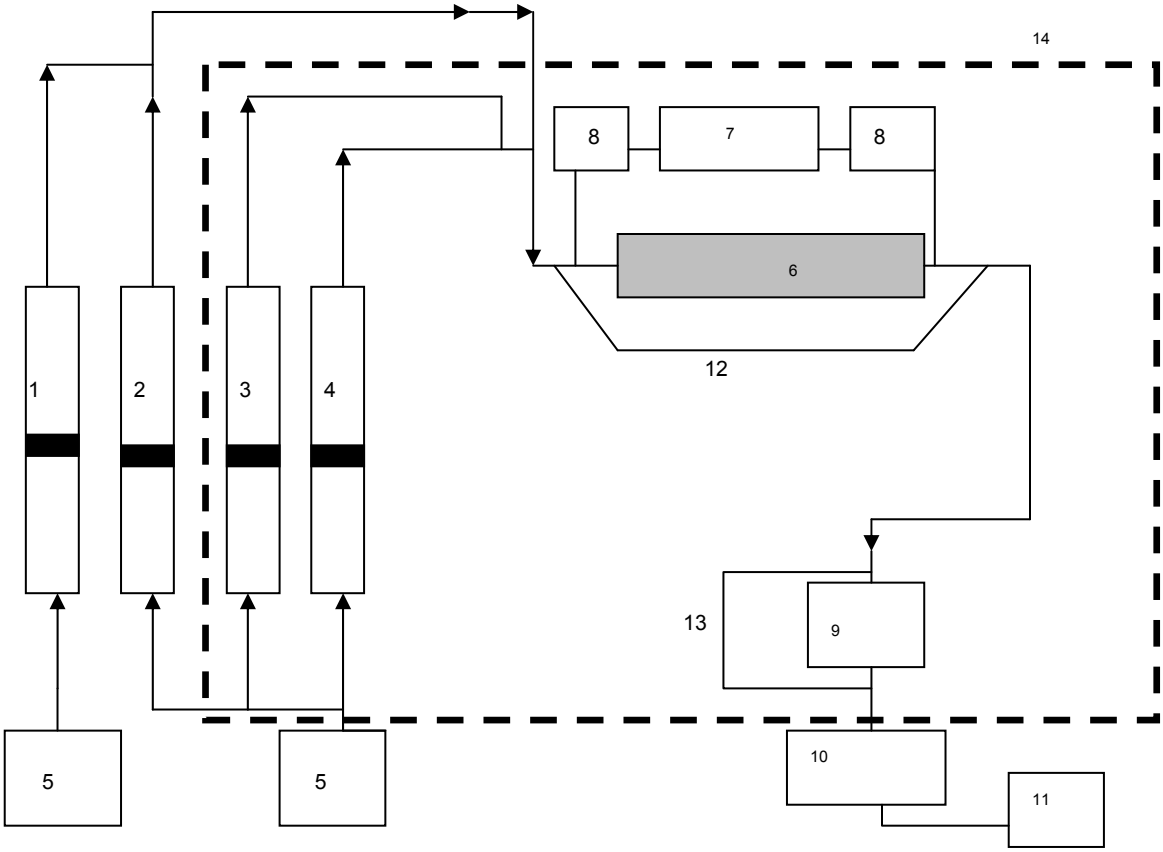

Figure 52. Experimental Set-up: 1.GY Accumulator, 2. GF Accumulator, 3.Oil accumulator, 4.Brine Accumulator, 5.Pumps (produced by Isco), 6.Core holder, 7. DAQ System, 8. Pressure transducers, 9. BPR, 10. Collector, 11. WTM, 12. Core holder by-pass, 13. BPR by-pass, 14. Constant temperature bath

The core flood tests were conducted on the experimental setup shown in Figure 52. Conaco and Temco accumulators, and Temco the core holder were used in the experiments. All accumulators and core holder are made of 316/304 grade stainless steel. The ISCO syringe pumps were used to deliver the test liquids in to the system. Computer controlled Sensotech (model TJF-2920-05) pressure transducers and NI Data acquisition system were used in the experiments. The pressure transducers were calibrated with the dead weight tester before starting the experiments. Pressure transducer had 1.0 psi resolution. A custom made back pressure regulator (BPR) and Ritter TG5 wet test meter (WTM) (model E2D2) were used during the tests. The experimental setup was placed in constant temperature bath (Omega Engineering) and it stabilized the inside temperature up to 250˚F. Liquid collector used in the system had a resolution of 0.2 ml.

2.1.3. Materials used

Several materials were used during these experiments: GY and GF solutions, Berea sandstone™ cores, light mineral oil, cationic surfactant (IGDFF1^{TM}), CLS, corrosion inhibitors, distilled water and brine. As mentioned before, GY and GF solutions posses basic and acidic properties, respectively. Berea Sandstone™ was used in the second part of these experiments as a core.

Berea Sandstone™ is a sedimentary rock whose grains are predominantly sand-sized and are composed of quartz sand held together by silica. The relatively high porosity and permeability of the Berea Sandstone™ makes it a good reservoir rock. The name a "split rock" is given to this sandstone due to the visible laminations in the rock, and it can be easily split along these laminations. Except for the laminations, some split rocks can be classified as a homogeneous porous cores and their permeability varies from 50 to 300 milidarcy. [41] Table 10 presents the generic composition and permeability range of Berea Sandstone™ cores used in our studies (data is obtained from the supplier).

White paraffin oil used in this study is obtained from VWR Scientific. It has a Saybolt viscosity of 180-190. HC2 cationic surfactant was supplied by Halliburton Energy Services.

Table 10. Chemical Composition of Berea Sandstone™ [41]

Silica	SiO_2	93.13%
Alumina	Al_2O_3	3.86%
Ferric oxide	Fe_2O_3	0.11%
Ferrous Oxide	FeO	0.54%
Magnesium Oxide	MgO	0.25%
Calcium Oxide	CaO	0.10%

2.2. EXPERIMENTAL PROCEDURE

2.2.1. Chemical Reaction Experiments

All experiments were conducted at constant temperature. First, a thermal stabilization of the reaction medium had to be provided. The caps of the vessel were tightened and a Teflon® ball (d = 1") was placed inside the vessel for increased mixing efficiency. Stirring of reactants are very important as the reaction rate and accuracy are highly dependent on the proper mixing. After sealing the vessel with caps, it was placed inside the temperature bath. All valves and pipe connections were tightened and checked for leaks. The bath gate was closed and the bolts have been tightened before the heating system was activated. Upon activation of the heating system, the bath was allowed to reach the desired constant temperature. The vacuum pump was connected to the system and operated until a desired constant temperature has been reached. Air was evacuated from the vessel before the reaction, and then the pump was disconnected from the system. After the air evacuation, the injection pump was flushed with 25 ml distilled water four times. Then the pump was flushed with 25 ml GF/GY solutions three times, and the pump was refilled with the desired volume of GF/GY solutions. Finally the pump was connected to the system and the entire volumes of GF/GY solutions were delivered to the vessel by the pump at a flow rate of 10000 ml/hr. Once the pump cylinder has been discharged, the flushing operation with 25 ml distilled water was repeated again four times. Then, the pump was flushed with 25 ml GY/GF solution three times, and the pump was refilled with the desired volumes of GY/GF solutions, and the pump was connected to the system. The pump run with a flow rate of 500 ml/hr while connected to the system. The flow was stopped at every 5 ml intervals, and the

pressure was stabilized while the reaction vessel was shaken for effective mixing of reactants. The experiment continued until the entire GY/GF solutions were delivered into the vessel.

2.2.1. a. Data processing for chemical reaction tests

All calculations are based on the following data obtained during the experiments: injected volumes of the GY or GF solutions, the generated CO_2 pressure in the reaction vessel, and the stoichiometric ratio of the chemical reaction as stated in Equation 1.1.1. Additionally, the initial pressure inside the vessel, the free volume of the vessel for the generated gas, densities of the solutions and the number of moles of CO_2 dissolved in the water for the injected unit volumes (5 ml) of reactants (predicted using the software "*PVTsim*") were measured and used during the calculations. Regardless the type of the initial solution in the vessel (GF or GY), the calculation procedure was the same. The calculations, described below, are for the injection of GY solution into GF solution. The GY solution is injected with the intervals of ~5 ml (V_{inj}). The injected number of moles of GY agent (n_{GYinj}) is calculated according to the equation:

$$n_{GYinj} = \frac{\left(V_{inj} \times \rho_{sol}\right) \times \left(weight\%\right)}{MW} \qquad (2.2.2)$$

The number of moles of GF agent (n_{GF}) reacted with injected GY (n_{GYinj}) was calculated from the stoichiometric ratio, where n_{GF} equals twice that of the $n_{GYinj.}$ According to the chemical reaction, the total number of moles of generated CO_2 (n_{CO2}) is equal to n_{GYinj}.

To calculate a theoretical pressure value, the generated gas is assumed to be an ideal gas (a compressibility factor z is taken as 1, and ideal gas law is used):

$$P = \frac{n \times R \times T}{V} / 14.22334 \qquad (2.2.3)$$

In this equation, R is the gas constant 0.082 atm×L/mol×K, T is the temperature in Kelvin scale, V is the free volume (l) in the reaction vessel, 14.22334 is the conversion factor, and n is the calculated number of moles of the generated CO_2. To calculate n, the number of moles of CO_2 dissolved in water (which is calculated with *PVTsim*) is subtracted from n_{CO2}.

For the concentration calculations, the amount of water in the system (n_{H2O} / V_{H2O}) at a specific time t must be known. There are two sources of water in the system: water introduced with the GF and GY solutions and water generated as a product of the reaction.

$$V_{H2O} = (V_{GF} \times \rho_{sol}) \times \frac{\left(1 - weight\%\right)}{\rho_{H2O}}, \quad (2.2.4)$$

where ρ_{H2O} is taken as 1 g/ml at the experimental conditions, and V_{H2O} is the volume of the water presented in the vessel before the reaction. In the above equation, replacing V_{GF} with V_{inj} will give us the volume of the water introduced to the system (V_{H2OA}) for the injected volume of the GY solution:

$$V_{H2OA} = (V_{inj} \times \rho_{sol}) \times \frac{\left(1 - weight\ \%\right)}{\rho_{H2O}} \quad (2.2.4)$$

Finally, the volume of the generated water (V_{H2OR}) produced due to the reaction, was calculated as:

$$V_{H2OR} = \frac{\left(n_{GYinj} \times 18\right)}{\rho_{H2O}} \quad (2.2.5)$$

Hence, the total volume of the water in the system (V_{H2OT}) for an injected volume of solution:

$$V_{H2OT} = V_{H2O} + V_{H2OA} + V_{H2OR} \quad (2.2.6)$$

$$n_{H2Otot} = \frac{\left(V_{H2OT} \times \rho_{H2O}\right)}{18} \quad (2.2.7)$$

To obtain the brine concentration in moles/liter, we divide the number of moles of salt, which is calculated from the reaction $\left(n_{GF} = n_{GY}\right)$ to V_{H2OT}:

$$\left[Salt\right] = \left(\frac{n_{Salt}}{V_{H2OT} \times 0.001}\right) \quad (2.2.8)$$

2.2.2. Core Flooding Experiments

The core flood experiments, which are the main focus of these studies, included the following steps: (i) conditioning of core, (ii) its porosity determination, (iii) saturation of core, and (iv) oil recovery.

2.2.2. a. Core Preparation and Porosity Determination:

The cores were drilled from the Berea Sandstone™ blocks. The ends of the cores were trimmed and they were dried at 120˚C for 24 hours. Dead volumes of the system were measured (connection and injection ends of core holder). Core #3 was inserted into core holder connected to the ISCO 500D syringe pump. The water at 2000 psi was injected into the core. The measured volumes of the end sections were subtracted from the injected water volume in order to obtain a pore volume. A bulk volume of the core with diameter of 1.5" and length of 15" was calculated. Following equation was used to find the porosity (ϕ=18.06%):

$$\frac{porevolume}{bulkvolume} = porosity = \phi \quad (2.2.9)$$

2.2.2. b. Saturation of Core

600 ml of the THF is injected into the accumulator. First 100 ml were injected into the core holder through the by-pass line, and the remaining 500 ml were injected into the core holder. After the completion of the THF injection, the brine was pumped into the accumulator. The concentration of the brine was 70000 ppm, which is equal to the concentration introduced to the system upon reaction of GF and GY agents. The gas in the accumulator was removed by connecting it to the service line. Initially, brine flow was first directed to the core holder through the by-pass line until no more THF is produced from the system. This was assured by the absence of the THF smell. Then the flow was directed to the core holder. 600 ml of the brine solution was injected into the system during the first run. Several pore volumes of the brine were

injected to the system to clean it completely and to saturate the core. The saturation criterion was a nonexistence of any gas phase in the effluent line. After the saturation of the core with the brine, the light mineral oil was pumped into the accumulator. ISCO pump was refilled completely with the distilled water. The core holder's inlet and outlet valves were closed. The flow was directed through the by-pass line and BPR. Flow was cut-off after injection of ~107 ml oil. The initial oil saturation depended on the type of the experiment. The non-graduated bottom part of the burette was filled with the brine (~10 ml), and the effluent from the core by-pass line was drained into the container. The downstream and upstream valves of the core holder were opened, and the flow was delivered into the core. Pump was refilled completely and the Wet Test Meter (WTM), the digital read out and the liquid trap were hooked up to the outlet of the system. As a general rule of the practice, three Pore Volumes (PV) of the oil were injected into the system and the flow was cut. As no additional brine displacement took place after ~3 PV of oil injections, it is assumed that the core is saturated with the oil.

2.2.2. c. Oil Recovery Tests

The oil recovery tests were performed according to the following steps (steps 1 through 11 will be skipped when the system is desired to be tested without water flooding):

1. The brine was pumped into the accumulator. The gas in the accumulator was removed by running the accumulator through the service line.
2. The brine flow was first directed to the core holder via the by-pass line in order to displace the residual oil in the by-pass line. Approximately 19 ml of oil were obtained from the by-pass line after injection of 100 ml brine to the line.
3. The pump was refilled.
4. The collection burette was flushed with THF and rinsed with the distilled water.
5. The flow path was set through the core and BPR.
6. The core's downstream and upstream valves were opened.
7. The brine solution was injected into the core to recover the oil. The brine injection for the recovery purposes included three runs with a total volume of 3 PV. After every run, brine was drained and the produced oil was kept in the burette. The volumes of the produced oil, brine and gas, and the water left behind in the pump were recorded. The heads of the oil and brine columns were recorded every 10 minutes.
8. A material balance was made for every recovery calculation.
9. The initial recovery was calculated according to the formulae:

$$\frac{V_{Oil\ \mathrm{Pr}oduction}}{IOIP} = \%Initial\ \mathrm{Re}\,\mathrm{cov}ery \qquad (2.2.10)$$

10. GY and GF solutions were sucked into the accumulators. GY, which was sent into the accumulator 2, contained 0.1% of the corrosion inhibitor *OCI* (to protect the equipment from corrosion).
11. The pumps were refilled.
12. The collection burette was flushed with the THF and rinsed with distilled water.
13. The flow path was set through the core and BPR.
14. The core's downstream and upstream valves were opened.
15. The flow rates of the chemicals are programmed on the pumps in order to satisfy stoichiometric ratios of the reaction.

16. Approximately 3 PV of the chemical agents were injected into the system to recover the oil.
17. The volumes of the produced oil, brine and gas, and the water left behind in the pump were recorded. The heads of the oil and brine columns were recorded every 10 minutes.
18. Material balance was made for the recovery calculations:

$$\frac{V_{Oil\,\mathrm{Pr}\,oduction}}{OIP} = \%\,\mathrm{Re}\,\mathrm{cov}\,ery \qquad (2.2.11)$$

2.3. RESULTS AND DISCUSSION

As mentioned before, this study consisted of two major sets of experiments described in the previous chapter. In addition to those, some additional tests were conducted to understand the character and effects of the new technology. These tests include chemical analysis of the reaction products, the permeability and corrosion estimation tests. Results of these tests were used for better understanding of oil recovery tests results.

Due to the acidic nature of the system, corrosion was an important issue to consider. There are many studies in the literature about corrosion problems on oil field equipment and their recommendations were taken into the account during our experiments.

2.3.1. CHEMICAL REACTION EXPERIMENTS

Figure 53 presents a variation of the generated CO_2 gas pressure with the total volume of the injected solutions. As can be seen from the graph, the injection sequences of chemical agents affect the gas generation capability of the system. When GY is added to GF (experiments 10, 14, 16, 17, 23, 24), generated CO_2 gas pressure increases linearly almost up to the end of the injection process. However, if GF is added to GY (experiments 15, 18, 22), practically no CO_2 generation was observed until the middle of the injection process. Also, the addition of the surfactant (IGDFF1^{TM}) does not have any significant effect on the pressure of the generated CO_2, in spite a foam formation was observed after the commencement of the experiment. As a result of chemical equilibrium, which will be explained later, when GY is injected into GF, the amount of the CO_2 pressure measured in the system is higher than that measured for the injection of GF to GY. Figure 54 compares the experimental results with the predicted ones for the experiments 15, 18 and 22. As seen from this figure, there is a big discrepancy between predicted and measured data.

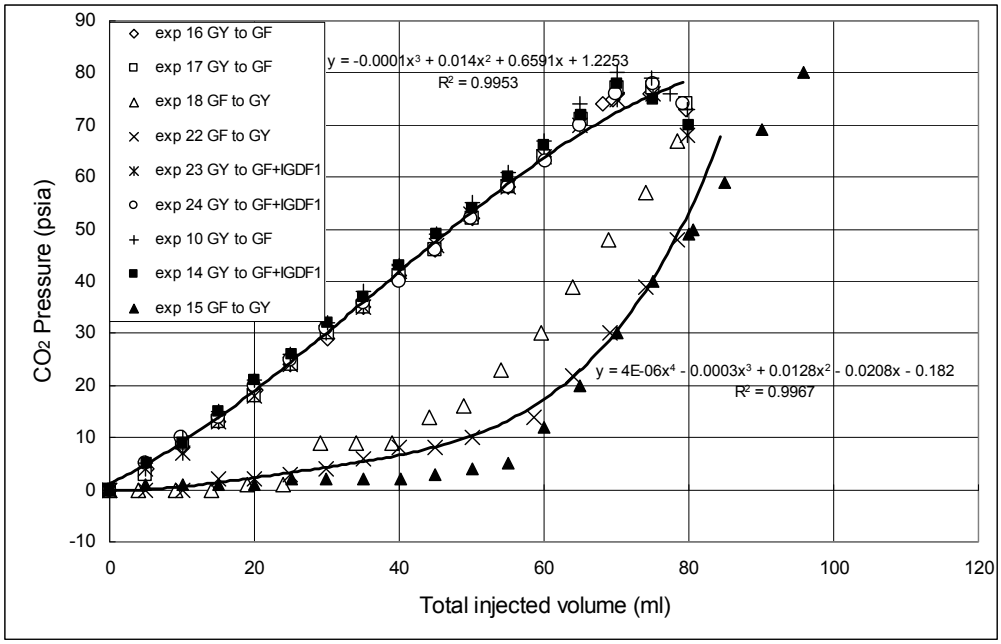

Figure 53. Generated CO_2 gas pressure vs. injected total volume of solutions.

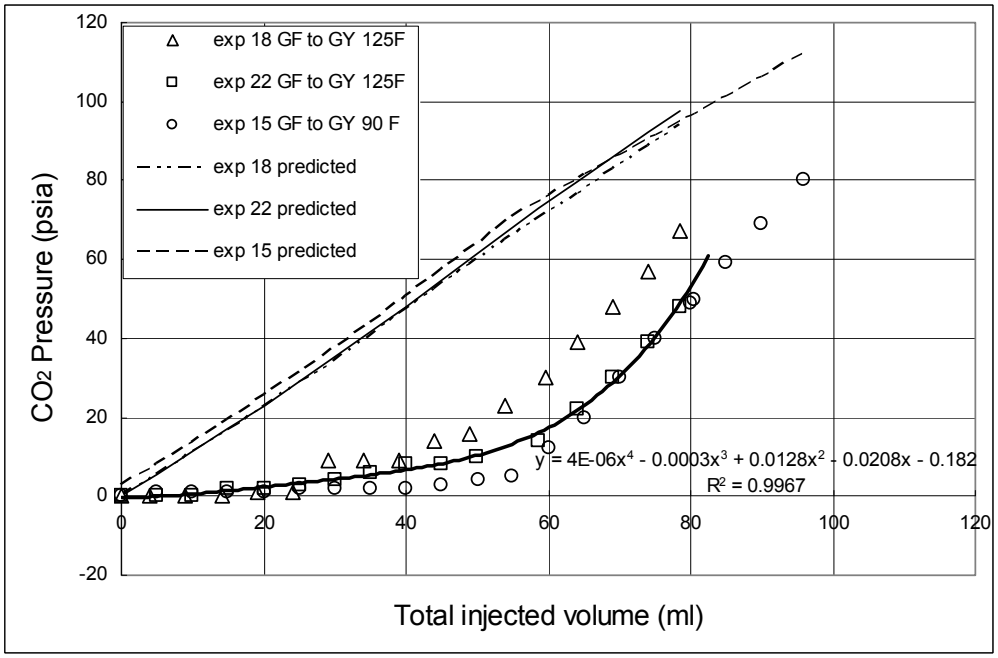

Figure 54. Variation of generated CO_2 gas pressure vs. total volume of injected reactants.

Figure 55 presents a variation of generated CO_2 gas pressure versus the %weight of the salt dissolved in the system. As seen from these figures, the generated gas pressure exponentially increases with salinity of the system. There is a similarity in the curves depicted in Figures 53 and 55, as salinity increases with the reaction between GY and GF solutions. Figure 56 compares experimental and predicted data for pressure variation versus salinity. Again, there is a significant discrepancy between experimental and predicted curves. In both figures (54 and 56),

the measured CO_2 values are much lower than the calculated CO_2 pressures (Appendix E, Table 38).

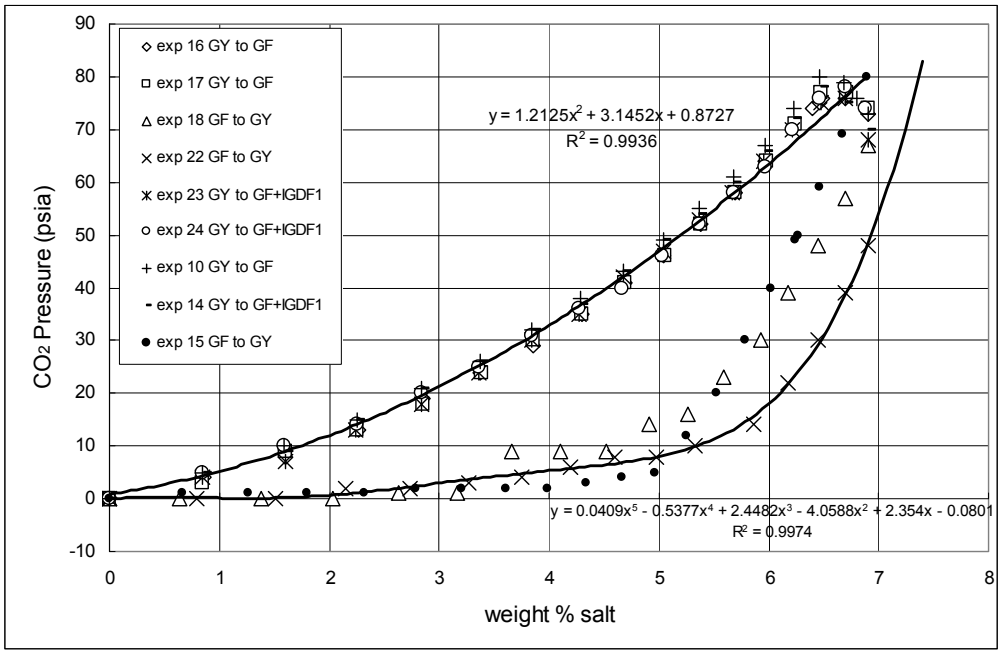

Figure 55. Variation of generated CO_2 gas pressure vs. %weight of salt in system.

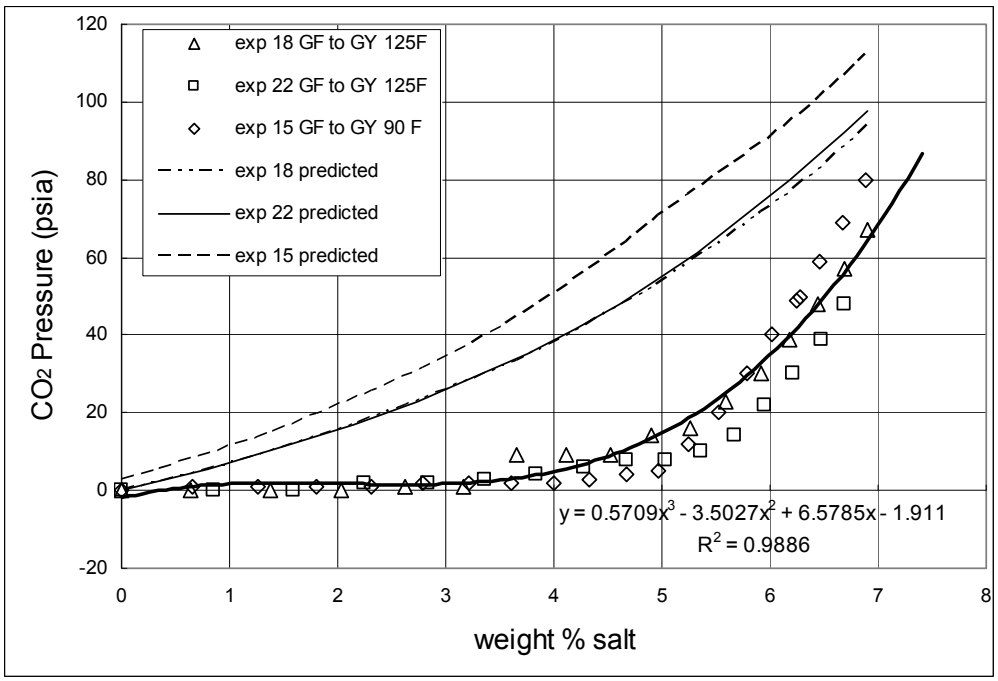

Figure 56. Variation of generated CO_2 gas pressure with weight % salt.

The observed phenomena (low pressure of the generated CO_2 gas) can be explained by the CO_3^{-2} equilibrium in the system. The GY reactant (Bronsted base) hydrolyses in two steps:

$$CO_3^{-2} + H^+ = HCO_3^- \qquad K_1 = \frac{1}{K_{a2}} \tag{3.1.1}$$

$$H_2O = H^+ + OH^- \qquad K_2 = K_W \tag{3.1.2}$$

$$CO_3^{-2} + H_2O = HCO_3^- + OH^- \qquad K = \frac{1}{K_{a2}} \times K_W = K_{b1} = 2.1 \times 10^{-4} \tag{3.1.3}$$

$$CO_3^{-2} + H_2O = HCO_3^- + OH^- \qquad K_{H1} = K_{b1} = 2.1 \times 10^{-4} \tag{3.1.4}$$

$$HCO_3^- + H_2O = CO_2 + H_2O + OH^- \qquad K_{H2} = K_{b2} = 2.3 \times 10^{-8} \tag{3.1.5}$$

At the beginning of the reaction, where initial $[CO_3^{-2}] = 1.29$ moles / liter, the following formulae will describe the reaction process:

$$CO_3^{-2} + H_2O = HCO_3^- + OH^- \tag{3.1.6}$$

The equilibrium concentrations of the reactants and the reaction products can be estimated according to the following equation:

$$Kb = 2.1 \times 10^{-4} = \frac{\chi^2}{(1.29 - \chi)} \quad \chi = 0.0164 = [HCO_3^-] = [OH^-] \tag{3.1.7}$$

$$-\log [OH^-] = 1.79 \quad \Rightarrow \quad pH = 12.2 \tag{3.1.8}$$

$$CT = [CO_3^{-2}]\left(1 + \frac{[H^+]}{K_{a1}} + \frac{[H^+]^2}{K_{a1} \times K_{a2}}\right) \tag{3.1.9}$$

$$CT = 1.29\left(1 + \frac{10^{-12.2}}{4.3 \times 10^{-7}} + \frac{(10^{-12.2})^2}{4.8 \times 10^{-11}}\right) \tag{3.1.10}$$

$$CT \cong 1.29 \Rightarrow \text{Total carbonate (mole/L)} \tag{3.1.11}$$

A concentration of the reaction products versus pH of the system is shown in Figure 57. As can be seen from this figure, at a pH value of 12.2, the $[H_2CO_3]$ is 1.29×10^{-11} and $[CO_2]$ is 2×10^{-8}. As we inject GF solutions into the vessel and decrease the pH of the system, $[H_2CO_3]$ and $[HCO_3^-]$ will increase and $[CO_3^{-2}]$ will decrease as pH reaches 10.33, according to the reactions stated below. At the point of pH = 6.35 where the second step of hydrolyses reaction is at equilibrium, $[H_2CO_3]$ will reach approximately the original carbonate concentration:

$$H_2CO_{3(aq)} = CO_{2(g)} + H_2O \qquad [CO_2]_{aq} = K_H \times P_{CO2} \tag{3.1.12}$$

$$H_2CO_3 + H_2O = HCO_3^- + H_3O^+, \qquad K_{a1} = 4.2 \times 10^{-7}, \quad pK_{a1} = 6.38 \tag{3.1.13}$$

$$HCO^- + H_2O = CO_3^{-2} + H_3O^+, \qquad K_{a2} = 4.8 \times 10^{-11} \qquad pK_{a2} = 10.32 \tag{3.1.14}$$

$(H_2CO_3)_{aq} - (CO_2)_g$ reaction equilibrates, around pH = 5, but we can not calculate K_H because of our concentrated solution and dynamic system with changing P_{CO2}.

As seen from the P_{CO2} - $[H^+]$ relationship, at pH < 6, P_{CO2} reaches detectible values. Figure 58 summarizes the relation of CO_2 pressure with pH of the system when GF solution is injected into GY solution.

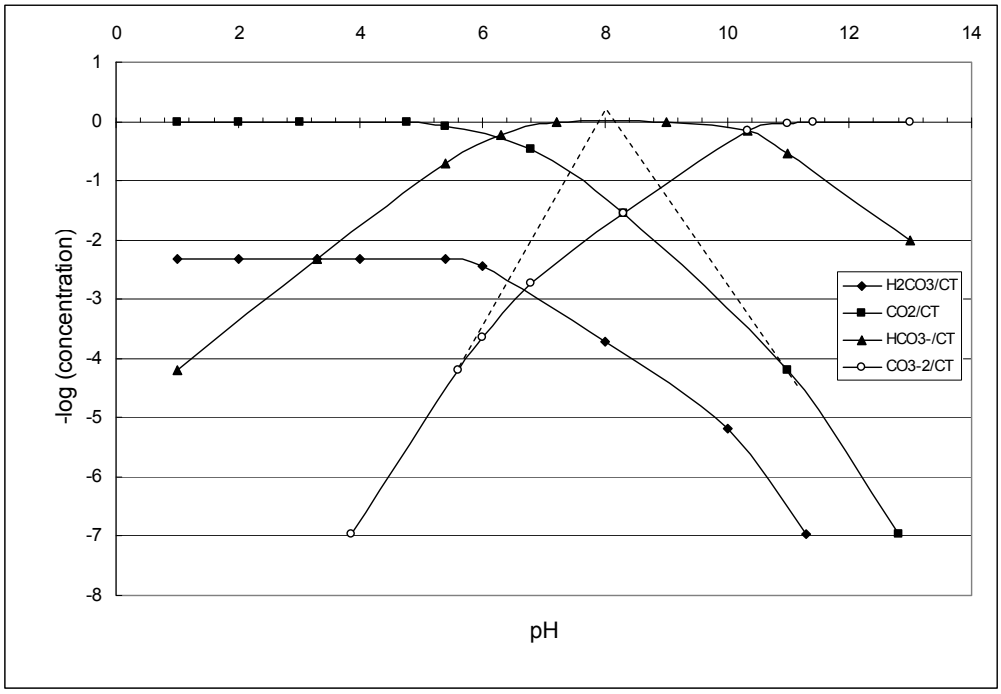

Figure 57. Concentration of reaction products with pH. [42]

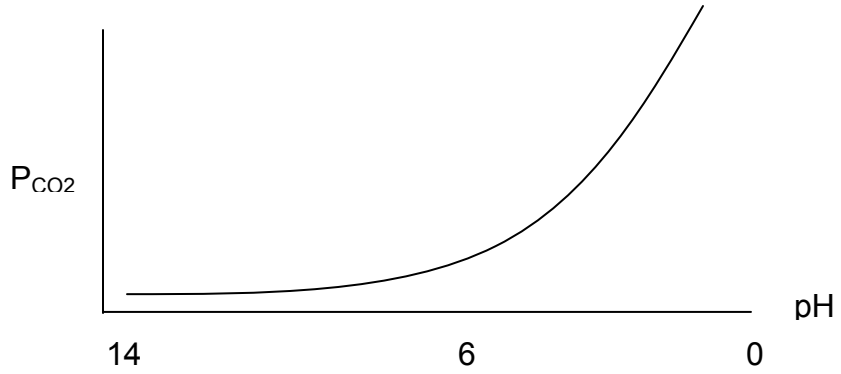

Figure 58. Variation of CO_2 pressure with system's pH.

The dynamics of the generated CO_2 gas pressure is quite different for the case where GY solution was injected into the GF solution. As seen from Figure 59, the pressure of the generated CO_2 gas linearly increases with the injected volume of the GY solution. Also, there is a good agreement between the predicted and experimentally obtained data. A decrease of the gas pressure at large volumes of GY solution (>70 ml) can be explained with the formation of HCO_3, which absorbs CO_2 gas from the system due to the excess GY. One can assume that in porous

medium we will not observe this phenomenon as the two aqueous solutions will be mixed more uniformly.

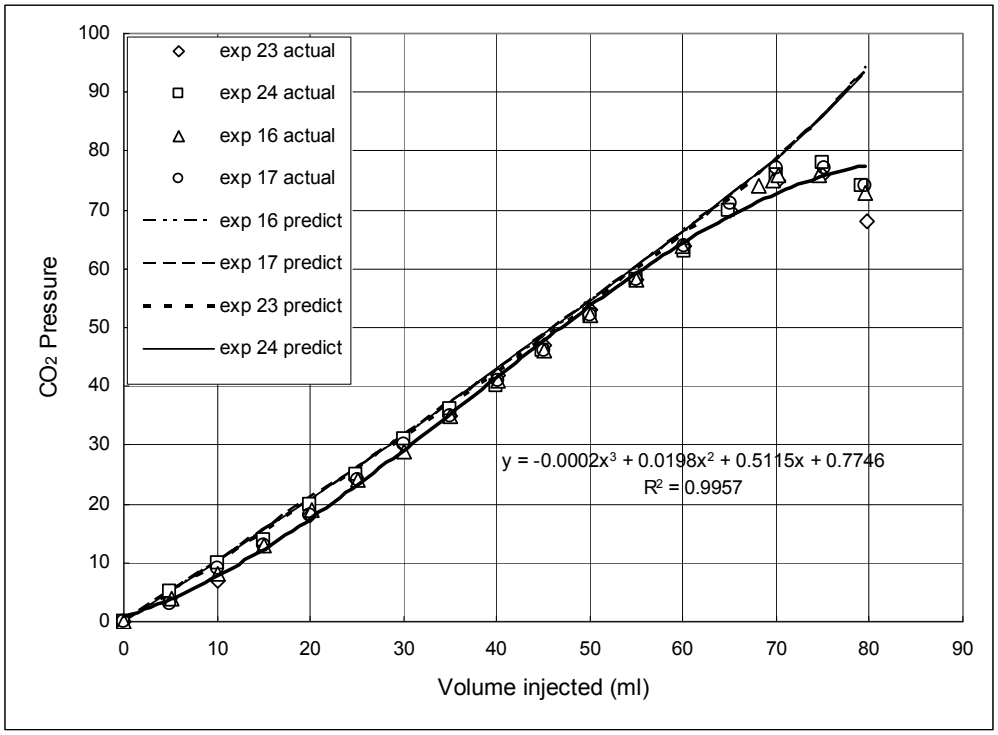

Figure 59. Variation of generated CO_2 gas pressure with injected GY reactant volume.

If we equate the second derivative of the pressure function shown in Figure 59 to zero, we can calculate the inflection point, where concavity

$$\frac{d^2 p}{dV^2} = -0.0012V + 0.0396 \Rightarrow p(V) \approx 33 \tag{3.1.15}$$

would correspond to the inflection point of the curve.

Based on the results shown above, we can conclude that, up to certain total volume of the injected liquids (33 ml) the pressure of the generated CO_2 gas increases linearly, above that level the pressure of the generated CO_2 gas increases exponentially, but it is still lower than the predicted pressure values, mainly, due to the CO_2 dissolution in the aqueous phase.

A variation of the CO_2 pressure versus salinity of the system when GY is added to GF, is shown in Figure 60. If we derivate the equation of the actual CO_2 pressure (p) - brine concentration (C_b) curve depicted in this figure in order to obtain the slope of the curve, one can observe that there is an increasing trend in the CO_2 gas generation with increasing the brine concentration of the system according to the following relationship:

$$\frac{dp}{dC_b} = -0.1752{C_b}^2 + 3.774C_b + 1.2414 \tag{3.1.16}$$

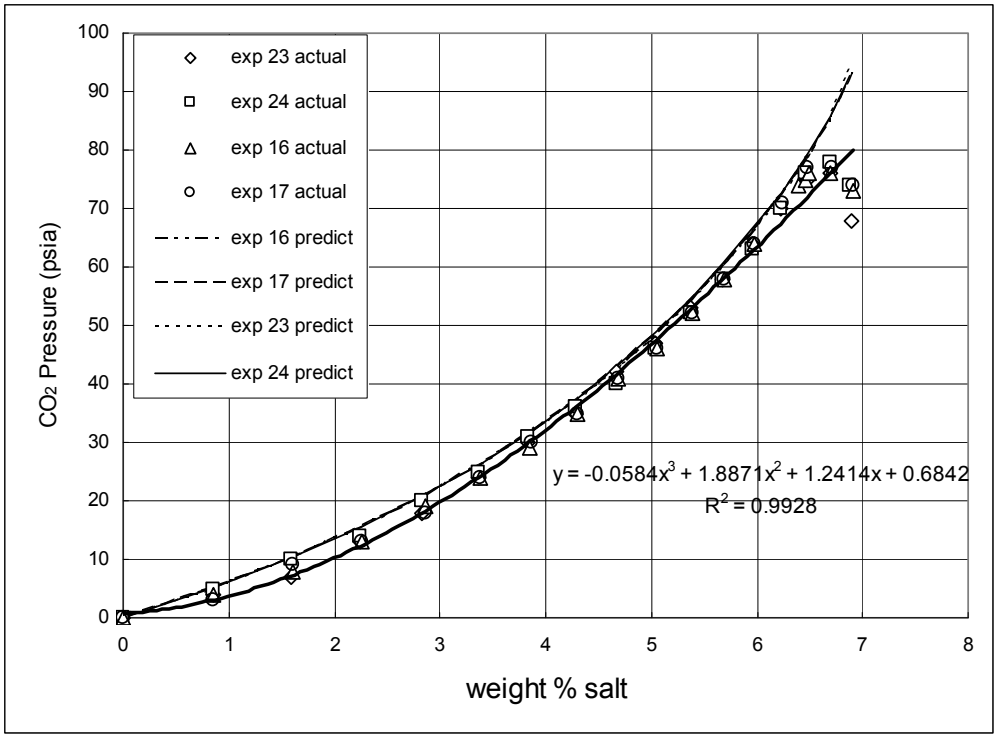

Figure 60. Variation of CO_2 gas pressure with salinity of the system (case: GY added to GF)

This phenomenon can be explained with the effect of brine concentration of the system on solubility of CO_2 gas in brine solution. If a presence of salt would not affect on CO_2 solubility, we could observe a linear relation between weight percent of salt and CO_2 pressure, which is a result of CO_2 generated, as both salt and CO_2 are the products of the same reaction. But in our case, increasing salt concentration decreases the CO_2 solubility in aqueous phase, so a less CO_2 dissolution in aqueous phase is leading to a higher CO_2 pressure. Previously, Duan and Sun determined that the solubility of CO_2 in water decreases with increasing concentration of brine in the aqueous solution [43]. Therefore, the volume of the free CO_2 gas, generated per injected volume of solution increases with increasing concentration of brine in aqueous solution. The results of studies by Chang *et all* [44] (Figures 61 and 62) and Masoudi *et all* [45] also support these findings and should be considered for further laboratory and field studies. As seen from Figure 62, solubility of CO_2 in water increases significantly with increasing the pressure. This increase is more pronounced especially between 0 and 2000 psi, which is the pressure range for majority of the core flooding experiments. Tables 38 and 39 (Appendix E) represent the CO_2 pressures calculated with "*PVT Sim*" software by Calsep.

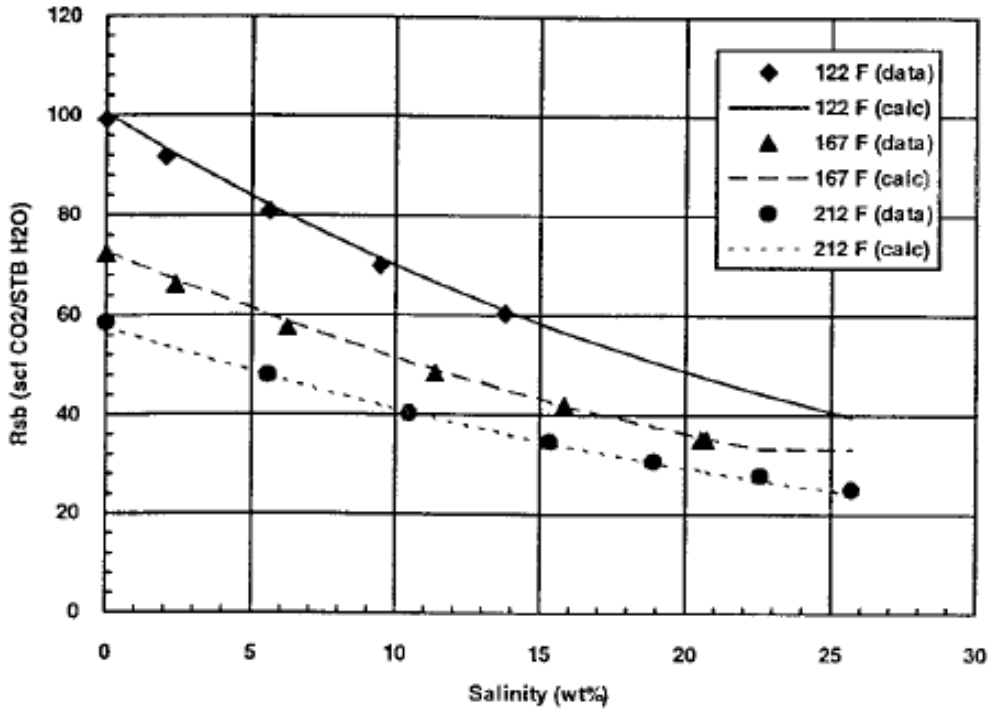

Figure 61. Comparison of measured and calculated CO_2 solubilities in brine at 695.5 psia. [44]

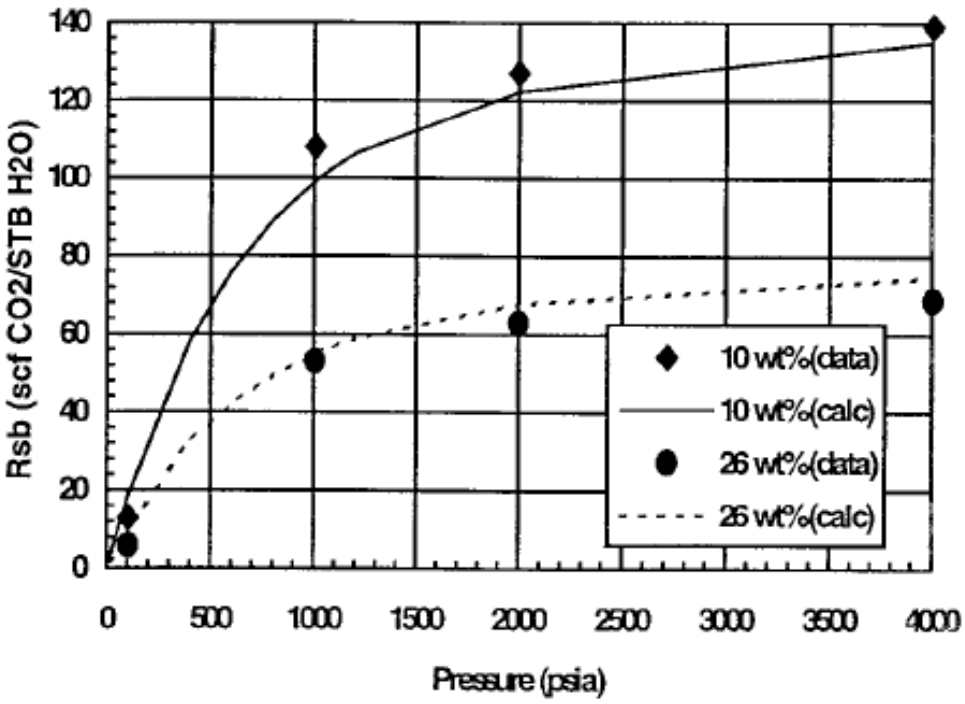

Figure 62. Comparison of measured and calculated CO_2 solubilities in brine at 100°F. [44]

2.3.2 CORROSION PROBLEMS

During these experiments the concerns regarding the corrosion effects of the process on the test system lead us to analyze a chemistry of the reaction products. Three samples were analyzed: (i)

GF to GY injection (experiment 18), (ii) GY to GF injection (experiment 17), and (iii) GY to GF+IGDFF1™ injection (experiment 23). As can be seen from Table 11, certain amounts of Fe, Ni, Cr and Mo elements exist in the solutions after the experiment. It should be noted that chemical solutions are prepared in glass beakers with distilled water and they did not contain any Group B metallic elements initially. Although the concentrations of metal ions are not high, but their presence in the system was a point of concern. Existence of metal ions shows that our vessel, which is made of SS 304 and SS 316, is corroded by the reaction solutions.

Table 11. Major ion concentrations in reaction products.

Identification	HCO_3 (mg/l)	Na (mg/L)	Fe (mg/L)	Ni (mg/L)	Cr (mg/L)	Mo (mg/L)
#17	7800	25000	135	18	0.30	1.2
#18	12200	28000	0.96	3.6	0.13	4.1
#23	9800	25000	255	34	85	6.5

There are two main factors originated from nature of our system which lead to corrosion on metallic components: (1) the GF agent of acidic nature, and (2) the CO_2 gas generated upon reaction and their combined effect with pressure and temperature (doubled at every 10˚C [46]).

The reports of CO_2 corrosion effects on oil field equipment have a history of more than 60 years. [47] In his study of CO_2 corrosion, Crolet claimed that pH of brine solution decreases with increasing partial pressure of CO_2. Further more, this decrease is more significant when there are bicarbonate ions (HCO_3^-) in the solution. Assumptions on relationship between CO_2 pressure and pH (see Figure 57), which are based on the experimental observations and basic chemistry knowledge are supported by these findings. Crolet proposed to use a high Cr content steels (>13%) which is below the Cr content in SS316 and SS304 used in our set up. However, it is appeared that both steel grades are subject to pitting and crevice corrosion in acid environment at elevated temperatures. As seen from Table 11, this chemical system dissolves Ni, Mo and Mo in the steel and we observe heavy corrosion.

Regarding the acid treatment and CO_2 gas injection processes in oil fields, only few researchers (Muller *et al* [48], Piccolo *et al* [49], Grinsven *et al* [50], Gunaltun [51], Chitwood *et al* [52]) conducted studies about corrosive effects of these chemicals. In many studies, researchers stated and explained the problem and proposed solutions to prevent corrosion (the popular ones are corrosion inhibitors, polymer based linings, and cathode protection).

After observing heavy corrosion in chemical reaction experiments, we searched for the methods to prevent or slow down corrosion during core flooding experiments. One of the first attemps was to change the design of experimental set up, position the chemical solution accumulators outside the air bath and cool them down up to ~10˚C with an external heat exchanger unit. However, this approach was not very effective. Corrosion took place even on the surface of the accumulators. The second approach was to remove the heat exchanger and to add a corrosion inhibitor. 1% weight of OCI corrosion inhibitor was mixed with GF solution. This approach was more effective to reduce corrosion in the accumulators.

In addition to the effects of corrosion on metal parts of the experimental set up, an alteration of the core properties as a result of contact with solution system must be considered too. For example, at the beginning of the experiments, pressure drop through the core was recorded as 100 psi at the brine flow rate 1000 ml/hr in a 18.56" long core. The calculated initial core permeability was 193 mD. Before the Experiment G, data in Table 12 were obtained during brine flooding tests. These data were used for permeability calculations. According to these data, the calculated permeability of sandstone is 7.3 mD for the brine solution with the viscosity 0.0011407 kg/m.s. Hence, the permeability of sandstone core decreased 26 times when the ISCGT system was used for oil recovery. We assumed that this was partially due to the plugging of core by corrosion products. Therefore, utilization of anticorrosion inhibitors are very crucial for this new technology.

Table 12. Variation of pressure drop along the core with flow rate.

Q (ml/hr)	Pin (psi)	Pout (psi)	ΔP (psi)
40	545	470	75
50	565	470	95
100	670	470	200
200	880	470	410

3.3. CORE FLOODING EXPERIMENTS

The core flooding experiments can be divided into categories:
1) ISCGT system or brine solution were used as secondary recovery method. The solutions were injected into the cores (1.5" diameter) that had not been previously water flooded.
2) A brine flooding was applied prior to the solution injection for oil recovery. This group of tests can be considered as tertiary recovery experiments.

In all core flooding experiments the pumps 1 and 2 were used to deliver GY and GF components, respectively.

3.3.1. ISCGT and brine injection as secondary recovery techniques

The experiments B, C, D, F and G can be considered of this category oil recovery. The B, C, and D experiments were conducted at 1500 psi +/- 10 psi BPR pressure, and the F and G experiments were conducted at 500 +/-10 psi BPR pressure. The bath temperature was set to107˚F for all experiments and it must be noted that oil was aged for 48 hours in the core before a recovery.

The experiment B was aimed to recover the initial oil in place with ISCGT system injected into already brine and oil saturated core. Table 40 (Appendix F) presents the original data obtained during the experiment B. A percent of recovery was calculated based on these data. In this experiment GY and GF flow rates were 28 and 25 ml/hr, respectively. IOIP was 58.5 ml in the core of 15.6" long with 18.1% porosity. One PV was equal to 81.7 ml, S_{oi} =71.7%.

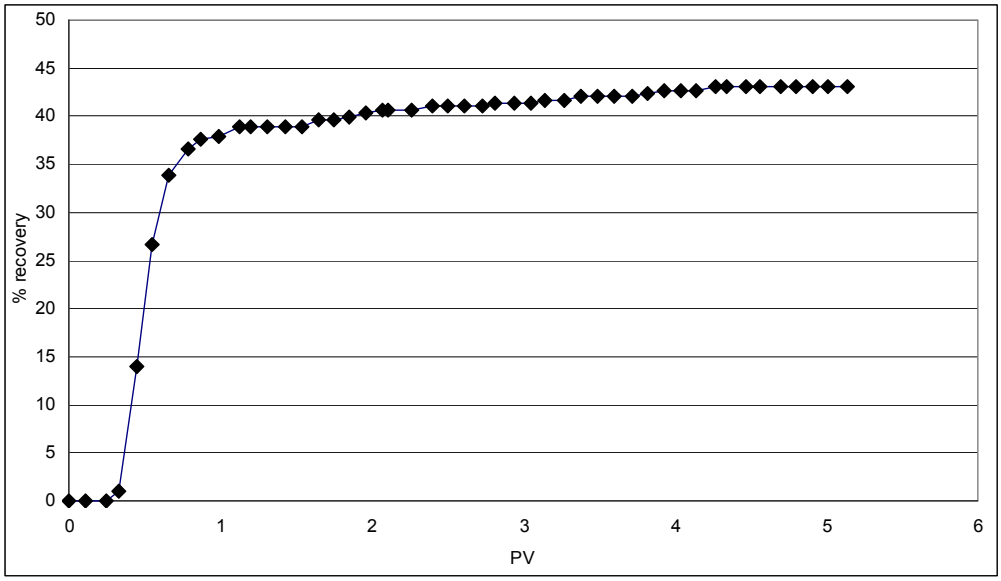

Figure 63. Variation of percent oil recovery vs. injected PV of ISCGT system for experiment B.

Figure 63 presents the recovery percent vs. injected PV of ISCGT system during the experiment B. During this experiment, we obtained 43.1% oil recovery. The results are close to those obtained during a brine injection of experiment A. One would assume this is due to the high pressure (3,000 psi) in the system, which prevents a generation of the free CO_2. At these circumstances, the system behaves like a carbonated water recovery application. According to Khatib *et al* [40] a carbonated water recovery provides up to 26% PV less residual oil saturation than brine flooding. Therefore, an oil recovery can't be higher. A higher recovery after the breakthrough might be due to the increased CO_2 gas generation at the later stages of the reaction process.

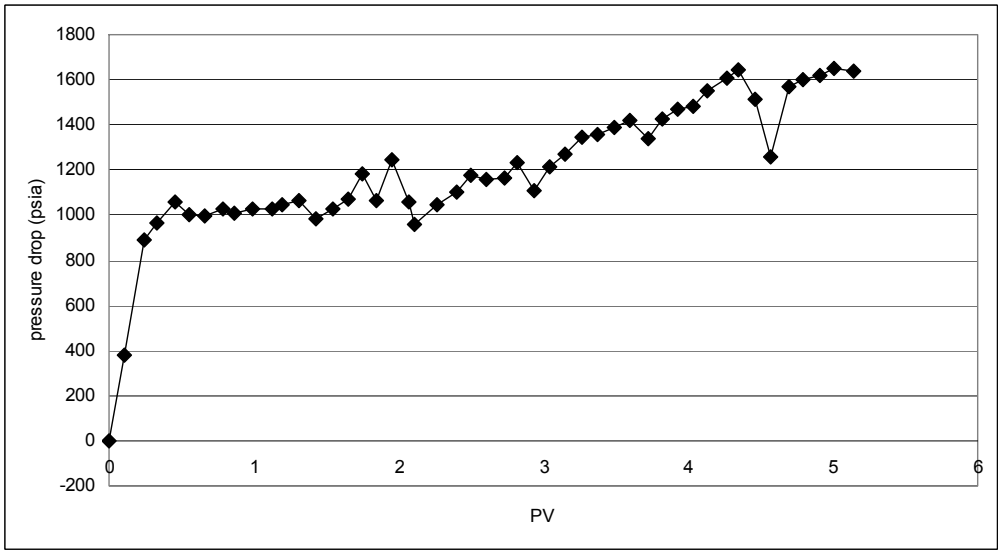

Figure 64. Variation of pressure drop with injected PV of ISCGT system for experiment B.

Figure 64 presents the pressure drop versus injected PV of ISCGT system during the experiment B. It must be mentioned that the BPR regulates the outlet pressure around 1500 psia, and the changes in the pressure drop also reflect the changes the pressure at the inlet. As seen from Figure 64, during the ISCGT system injection a breakthrough takes place at ~0.6PV. After the breakthrough, pressure drop through the core first stabilized (up to the 2 PV), and then gradually increased. However, the recovery was not affected by this behavior (Figure 63) and remained almost constant after the breakthrough. At such a high pressure this might be a result of the dissolution of the generated CO_2 gas in the aqueous phase rather than in oil.

Figures 65 and 66 represent the data obtained during the experiment C (oil recovery with ISCGT system + 3% wt. cationic surfactant. IOIP and Soi were 56.5ml and 69%, respectively. The obtained recovery was 36.6% at 107˚F, and 1 PV = 81.7 ml. The experiment was conducted at 1500 ±10 psi BPR pressure. A breakthrough occurred at ~0.75PV.

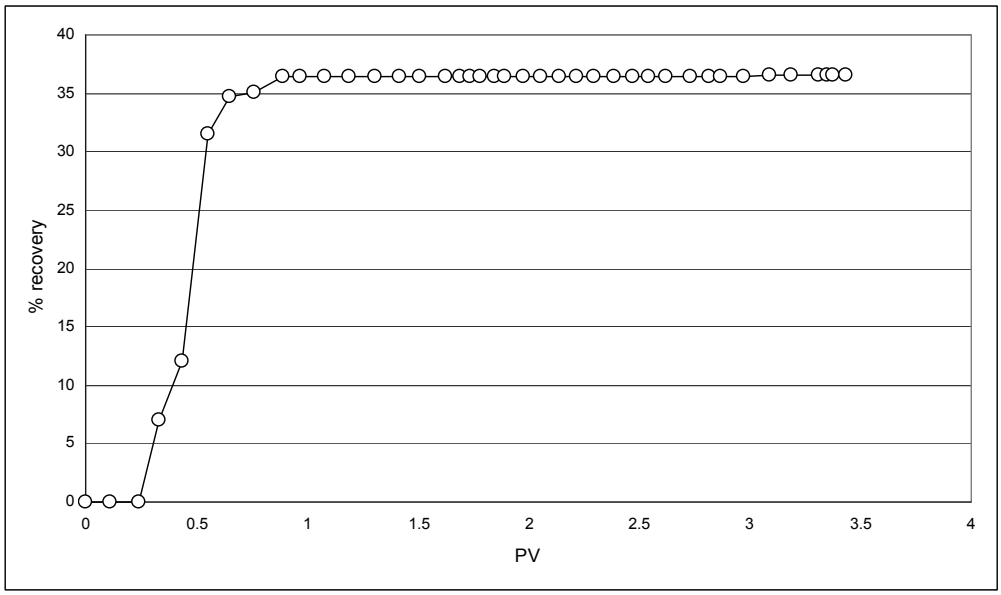

Figure 65. Variation of percent oil recovery vs. injected PV of ISCGT system during experiment C.

Figure 66 presents the pressure drop variations versus the injected PV of ISCGT system during the experiment C. A decrease of the pressure drop was observed twice at injected PV values (1.6 and 3.5). This was a result of the technical problems in precise controlling the pressure above 3500 psi. At the same time, we did not observe any abrupt increase in the pressure drop [16] which could be a result of the foam formation due to the lack of the sufficient free CO_2 gas in the system.

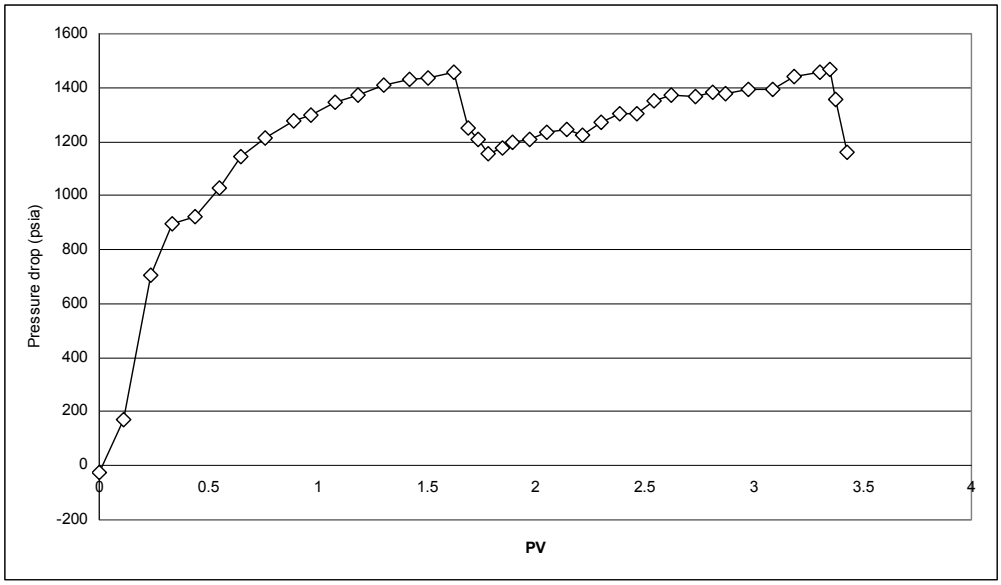

Figure 66. Variation of pressure drop with injected PV of ISCGT system during experiment C.

During the experiment D, the initial oil in the core was displaced by the injected brine solution. In this experiment the brine flow rate was 50 ml/hr. IOIP = 52.3 ml for the core of 14.2" long and 18.1% porosity (1PV = 74.2 ml and S_{oi} =70.5%). Figure 67 shows percent oil recovery versus injected PV during the experiment D. As seen from this figure, 38.2% of initial oil was recovered after 2.87 PV of brine injection as a recovery agent. Results of this experiment will be used to compare with other ISCGT oil recovery experiments.

During the Experiment F a light mineral oil was recovered by injection ISCGT system. Solutions are co-injected with the initial flow rates of 28 ml/hr for GY solution and 25 ml/hr for GF solution. GF solution included 1% wt. corrosion inhibitor to protect the setup system. IOIP is 53.7 ml which results in an initial oil saturation of 72.5% with a pore volume of 74.2 ml.

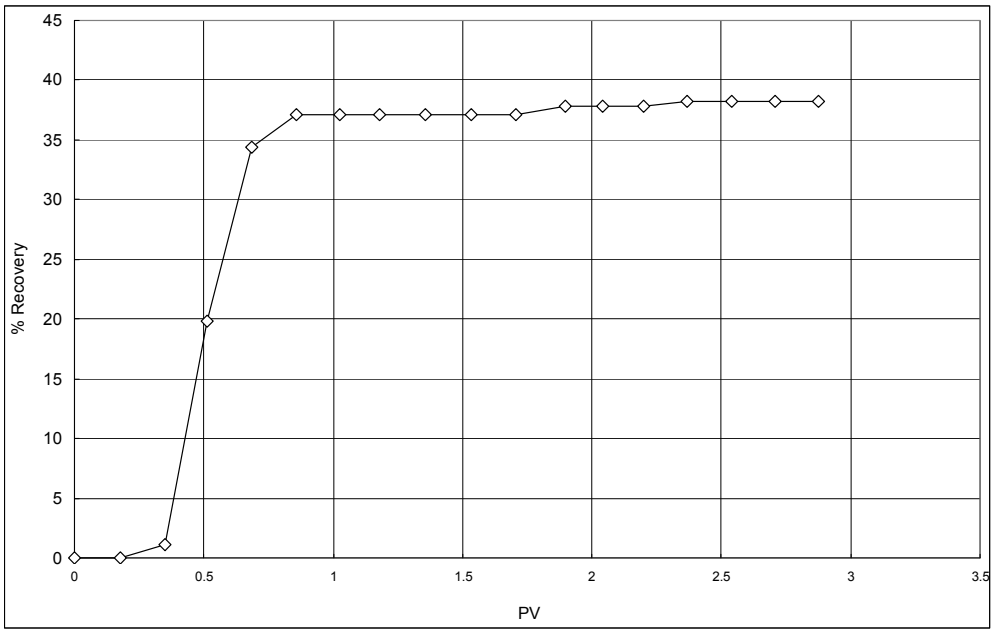

Figure 67. Variation of % oil recovery with injected PV of brine solution during experiment D.

During the Experiment F, after t=270 min (3.42 PV of displacing fluid is injected) from the beginning of the displacement process, injection was interrupted, flow rate was decreased ~75% (Q_{GF}=6.5 ml/hr and Q_{GY}=7 ml/hr), pumps were refilled and injection continued again after 25 minutes.

Slim tube experiments demonstrated that 1100 psi is the critical pressure value above which free CO_2 does not exist in a brine + CO_2 system. Therefore, in core flood experiments a pressure was kept less than or equal to 1100 psi in order to have free CO_2 in the system. As seen from the experimental data (Table 43, Appendix F), inlet pressure of the system was much higher than the bubble pressure of mineral oil at initial flow rates. Therefore, the flow rates were decreased in order to achieve more free CO_2 gas.

The variations of percent oil recovery and pressure drop versus injected PV of the displacing fluid for the Experiment F are shown in Figures 68 and 69, respectively. As seen from these figures, at 500 psi a recovery was comparable with that using brine solution (44% oil recovery was obtained with brine injection in Experiment E). At lower flow rates, the pressure drop significantly decreased along the core (~3.42 PV), and a slight increase in oil recovery was observed. After 3.42 PV injection of the ISCGT, ~1% additional oil was recovered.

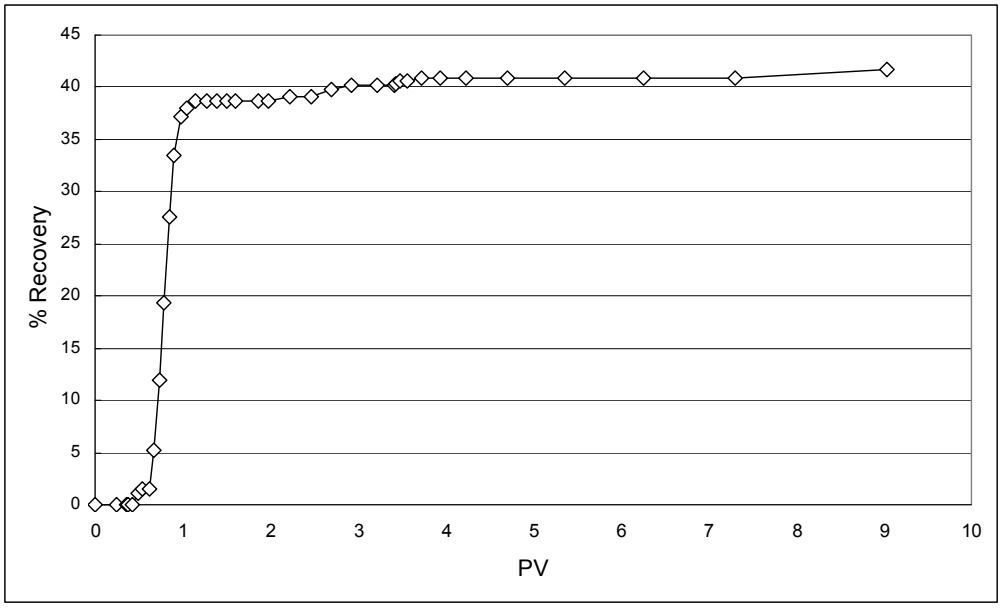

Figure 68. Variation of % oil recovery with injected PV of ISCGT system for experiment F.

Figure 70 shows the gas production (calculated from the slopes of flow curve) during the experiment F. As seen from this figure, a generated gas volume per PV of the injected ISCGT system increases with the injected PV. As was mentioned above, a sufficient CO_2 generation requires a sufficient quantity of GF component (higher pH) due to CO_2-Carbonate chemical equilibrium.

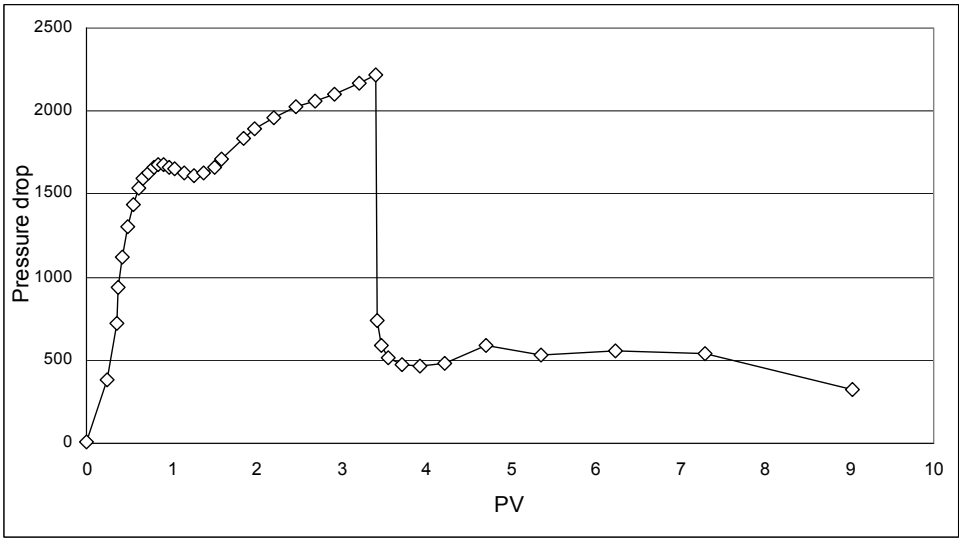

Figure 69. Variation of pressure drop with injected PV of ISCGT system for experiment F.

During the Experiment F a distance between mixing point of solutions and GY accumulator is 2.3 times shorter than the distance between mixing point and GF accumulator. Considering the stoichiometric volumetric flow rates, due to this difference, the solution with low pH values reaches the mixing point 29.8 seconds before the solution with high pH values. This injection

technique could protect the system against corrosion. Therefore, an alternative injection technique will be applied during the next tests (Experiment H).

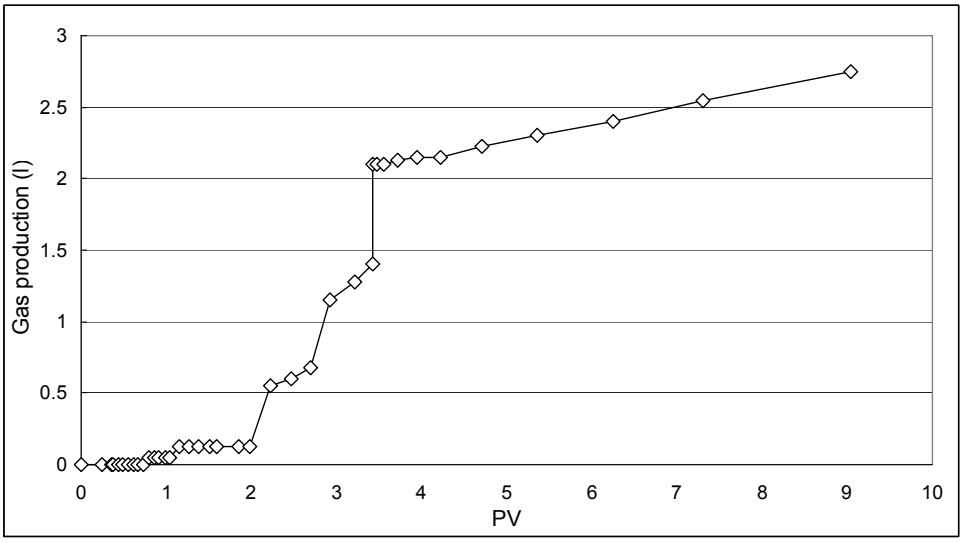

Figure 70. Gas production with injected PV of ISCGT system for experiment F.

The experiment G aimed recovery of light mineral oil from Berea sand stone core (14.2" long, 18.1% porosity) with injection ISCGT system. Components of the ISCGT system were co-injected with initial flow rates of 28 ml/hr and 25 ml/hr for GY and GF, respectively. GY component included 1% wt. corrosion inhibitor by weigh and 6% wt. cationic surfactant to form foam for mobility control. IOIP was 52.9 ml which resulted in an initial oil saturation of 71.4% with a pore volume of 74.2 ml. In this experiment, total oil recovery was 46.5%, which is significantly higher than that obtained in brine flooding and ISCGT injection at higher pressures. Figure 71 presents the increase in oil recovery with injected pore volume of the ISCGT system. It should be mentioned that after 35 minutes from the beginning of the injection process, Q_{GY} was decreased by 50%, and after next 5 minutes Q_{GF} was decreased by 50%. These manipulations of flow rates allowed to balance pH of the system and the pressure drop along the core between 0.46 – 0.5 PV, and finally, to increase free CO_2 generation. The dashed vertical red and blue lines on Figure 71 indicate the instances when the flow rates were reduced. Figures 72 and 73 represent variations of pressure drop and generated CO_2 gas volume versus injected PV of ISCGT system for the Experiment G. As seen from these figures, at PV = 0.5 a pressure drop decreases almost twice and produced gas volume doubles. Above 0.5 PV injections, system starts generating significant volumes of gas, mainly due to the cationic surfactant in the system.

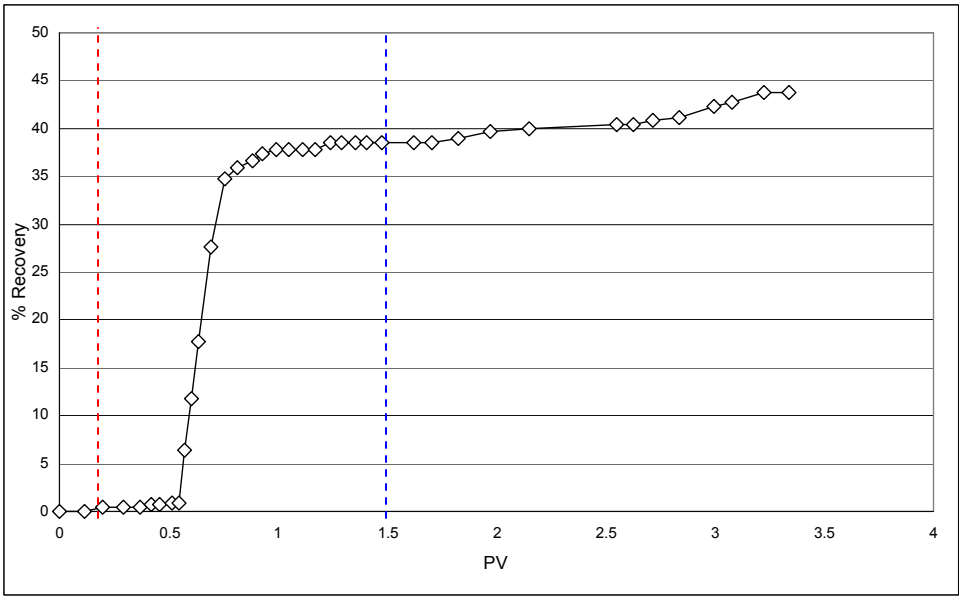

Figure 71. Variation of % oil recovery with injected PV of ISCGT system for experiment G.

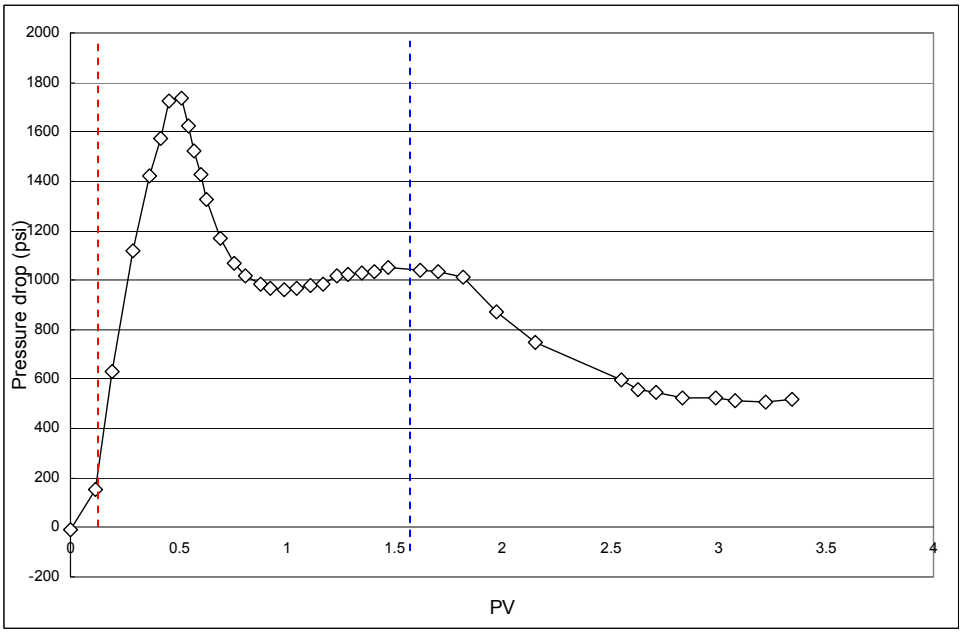

Figure 72. Variation of pressure drop with injected PV of ISCGT system for experiment G.

3.3.2. Tertiary recovery using ISCGT system

The Experiment A has been conducted in three stages:

1) recovery of mineral oil with brine,
2) recovery of residual oil with injection of ISCGT system into the already water flooded core, and
3) recovery by ISCGT system with 1% wt. cationic surfactant added to GF component.

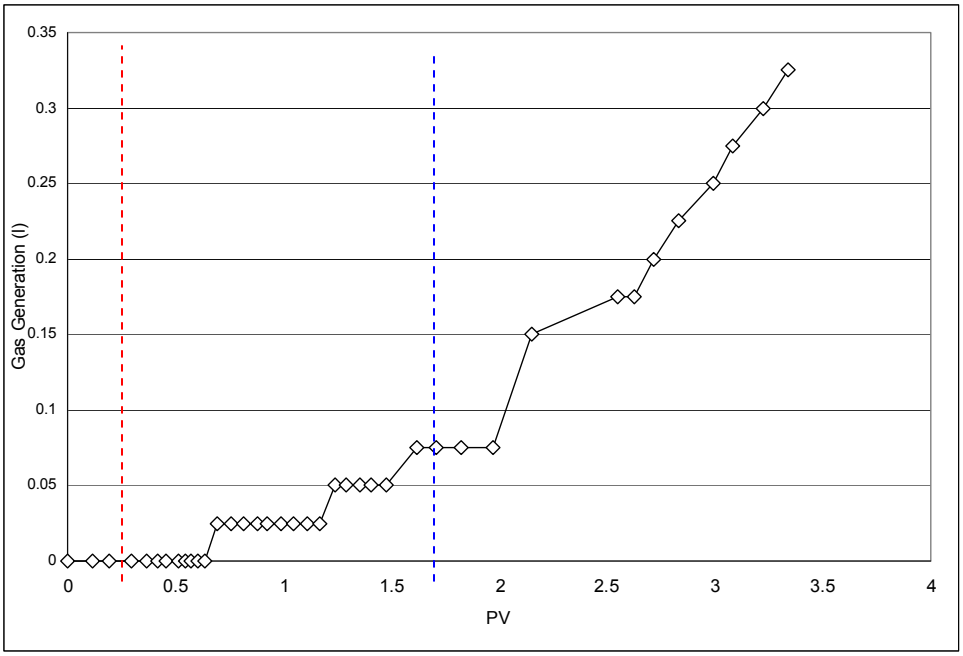

Figure 73. Gas production with injected PV of ISCGT system for experiment G.

Tables 45-47 (Appendix F) represent the original data obtained during all three stages of the Experiment A, respectively. From these data the percent recoveries were calculated (T = 107˚F, core of 15.6" long with 18.1% porosity, 1PV = 81.7 ml, P = 1,500 psi). During the first stage experiments, a brine flow rate was 50 ml/hr, OIP = 54 ml and S_{oi} =66%. The first stage of the process resulted in 44 % of oil recovery. During the second stage of displacement the flow rates of GY and GF components were 28 ml/hr and 25 ml/hr, respectively (OIP = 30.2 ml and S_{oi} =37%). In the third stage the flow rates of GY and GF components were 28 ml/hr and 25 ml/hr, respectively (OIP = 29.2 ml and S_{oi} =35.8%).

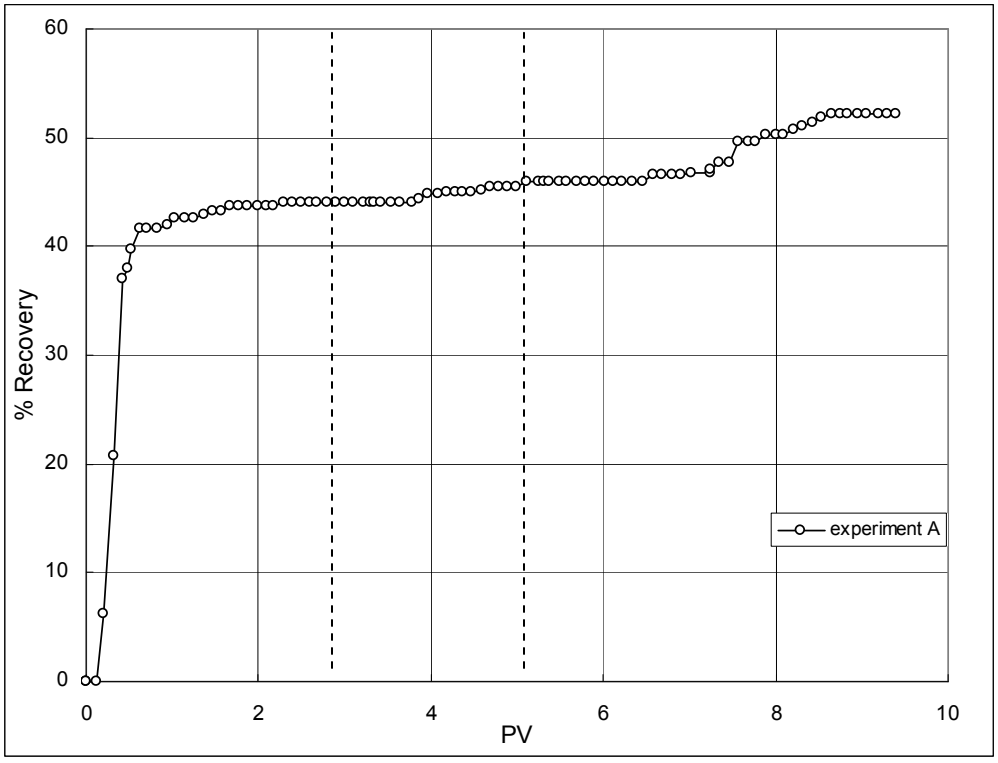

Figure 74. Percent of oil recovery versus PV of injected displacing fluids for experiment A.

Figure 74 presents the percent oil recovery versus PV of the displacing fluids during the Experiment A. The dashed lines indicate the commencements of second and third stages. As expected, second and third injection stages had lower recovery percentages in comparison to the first stage. Injection of the ISCGT system provides 3.3% additional oil recovery. Cationic surfactant addition to the GF component provides 11.6% additional recovery at 1500 psi.

Figure 75 presents the pressure drop versus PV of displacing fluids in Experiment A. It must be mentioned that the BPR controls the outlet pressure up to 1500 psia, and the changes in the pressure difference also reflects the changes of the inlet pressure. As seen from this figure, a breakthrough of the brine solution occurs after 0.42PV injection (50 min from the beginning of the recovery process). Further increase of the PV injection results in a stabilization of the pressure drop through the core, and therefore, recovery decreases.

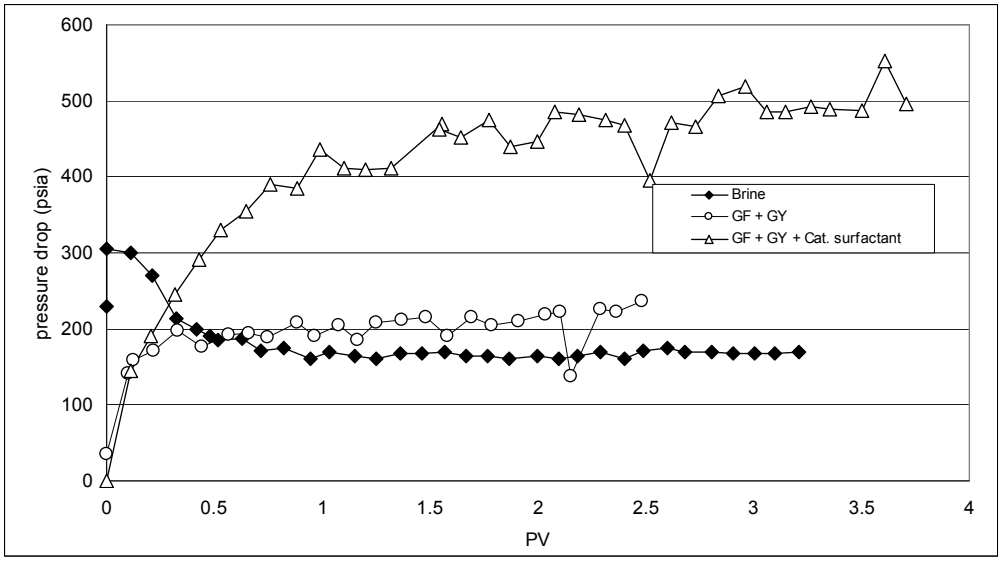

Figure 75. Pressure drop versus PV of displacing fluid for experiments A.

In contrast to the brine injection, a pressure drop fluctuates during ISCGT system injections. A pressure drop increases in oil recovery by either ISCGT or ISCGT + surfactant injections. In both injection schemes, with or without surfactant, we have an increase in pressure drop through the core. This increase in pressure drop results in additional oil recovery in later stages of the injections.

The Experiment E also was conducted in three stages (500 ± 10 psi):
1) recovery of mineral oil with brine,
2) recovery of residual oil with ISCGT system to the already water flooded core, and
4) recovery by ISCGT system with 1% wt. cationic surfactant added to GF component.

Tables 48-50 (Appendix F) represent the original data obtained during the first, second and third stages of the Experiment E, respectively. These data have been used to calculate a percent of the recovered oil (T = 107˚F, 14.2" long core, 18.1% porosity, 1PV = 74.2 ml). A brine solution flow rate at the first stage of the Experiment E was 50 ml/hr (IOIP = 43.7 ml in a core, S_{oi} = 58.98%). 44.4% oil recovery was obtained after the first stage of the recovery process. Flow rates of GY and GF components in the second stage of the experiment were 28 ml/hr and 25 ml/hr, respectively (OIP = 24.3 ml in a core, S_{oi} =32.8%). Additionally 9.9% of the residual oil was recovered. GY and GF flow rates during a third stage of the Experiment E were 28 ml/hr and 25 ml/hr, respectively (OIP = 21.9 ml, S_{oi} = 29.6%). After the third stage of the recovery process an 11.9% of the residual oil was additionally recovered.

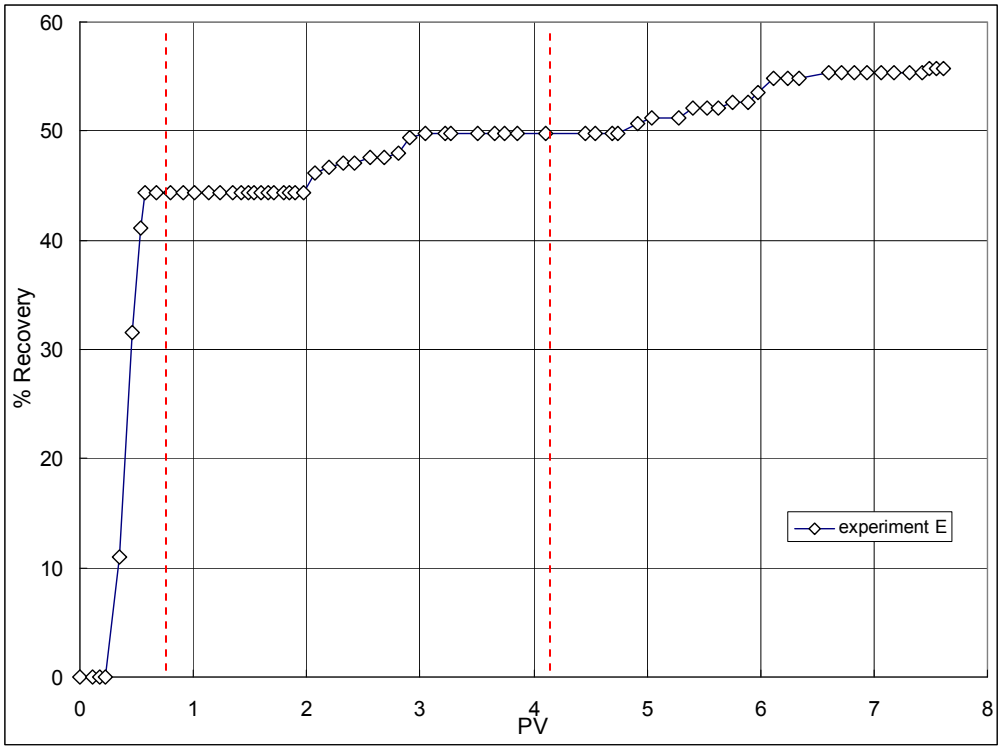

Figure 76. Percent of oil recovery versus PV of displacing fluid for Experiment E.

As one expected, a recovery of oil does not change after a breakthrough of brine solution. The ISCGT system was injected after ~1.35 PV of brine was already injected (120 min after the beginning of the injection process). However, an additional oil production starts after 2 PV total (brine + ISCGT) injection. Figures 77 and 78 represent a produced gas volume and pressure drop for the Experiment E. An instance of the first produced gas (breakthrough point) (Figure 77) coincides with the pressure drop stabilization (Figure 78). Upon completion of ISCGT system injection (~4.5 PV), a third stage of the process (ISCGT + cationic surfactant) started. An additional 11.9% oil recovery was obtained between 4.7 PV and 7.5 PV total injections.

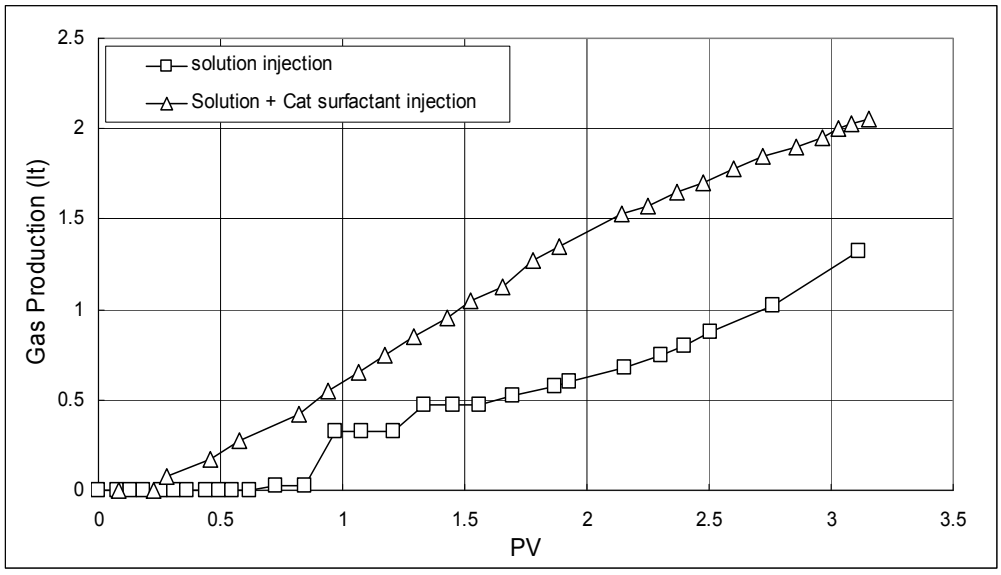

Figure 77. Generated gas volume versus PV of displacing fluids for Experiment E.

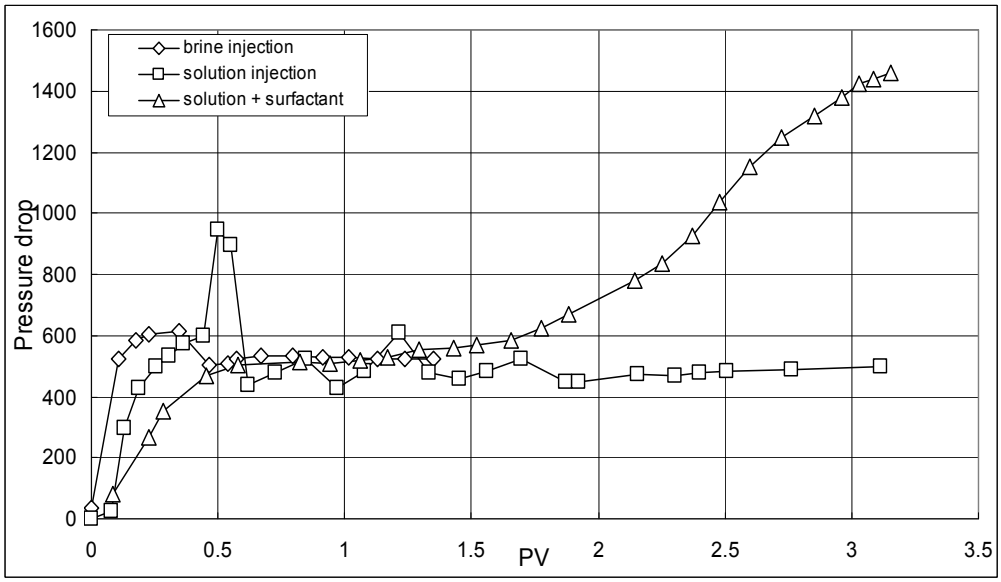

Figure 78. Pressure drop versus PV of displacing fluids for Experiment E.

As seen from Figure 78, at 0.5PV injection of ISCGT system, an abrupt increase and then decrease in pressure drop occurs. Fluctuations and then stabilization of the pressure drop was observed for this system. A pressure drop gradually increases during the ISCGT + surfactant injection up to 0.5PV. Then, it stabilizes up to 1.5PV injections. More PV injections result in significant increase of the pressure drop due to the fine structured stable foam formation. A BPR pressure was 1/3rd of that for the Experiment A, which contributed to more free CO_2 gas generation. It should be noted that an inlet pressure exceeded 1200 psi at around 2.1 PV of the third injection stage (see Table 50, Appendix F), which is equal to total 6.6 PV injection. The inlet pressure reached almost 2000 psi at the end of this experiment. At this high values of the inlet pressure CO_2 gas was dissolve in the injected system, and almost half of the core did not have enough free CO_2 gas to form the foam. Therefore, the oil recovery does not increase beyond

6.6 PV of injection. One would predict that an oil recovery would be higher if whole length of the core could be kept below 1100 psi pressure. A foam breakthrough was observed at total 6.9 PV of injection. Therefore, expected significant additional oil recovery after this point, even at pressures below 1100 psi, was not feasible.

The Experiment H also was conducted in three stages (500 ± 10 psi):
1) recovery of heavy mineral oil with brine solution,
2) recovery of residual oil with ISCGT system to the already water flooded core, and
5) recovery by ISCGT system with 1% wt. cationic surfactant added to GF component.

Tables 51-53 (Appendix F) represent the original data obtained during the first, second and third stages of the Experiment H, respectively. These data have been used to calculate a percent of the recovered oil (T = 107˚F, 14.2" long core, 18.1% porosity, 1PV = 74.2 ml). A brine solution flow rate at the first stage of the Experiment H was 25 ml/hr (IOIP = 48.4 ml in a core, S_{oi} = 65.3%). 38.4% oil recovery was obtained after the first stage of the recovery process. Flow rates of GY and GF components in the second stage of the experiment were 14 ml/hr and 12.5 ml/hr, respectively (OIP = 29.8 ml in a core, S_{oi} =40.2%). Additionally 5% of the residual oil was recovered. GY and GF flow rates during a third stage of the Experiment H were 14 ml/hr and 12.5 ml/hr, respectively (OIP = 28.3 ml, S_{oi} = 38.2%). After the third stage of the recovery process 13.4% of the residual oil was additionally recovered.

Figure 79 presents the percent oil recovery versus PV of the displacing fluids during the Experiment H. The dashed lines indicate the commencements of second and third stages. As expected, second and third injection stages had lower recovery percentages in comparison to the first stage. Injection of the ISCGT system provides 4% additional oil recovery. Cationic surfactant addition to the GF component provides another 8% additional recovery.

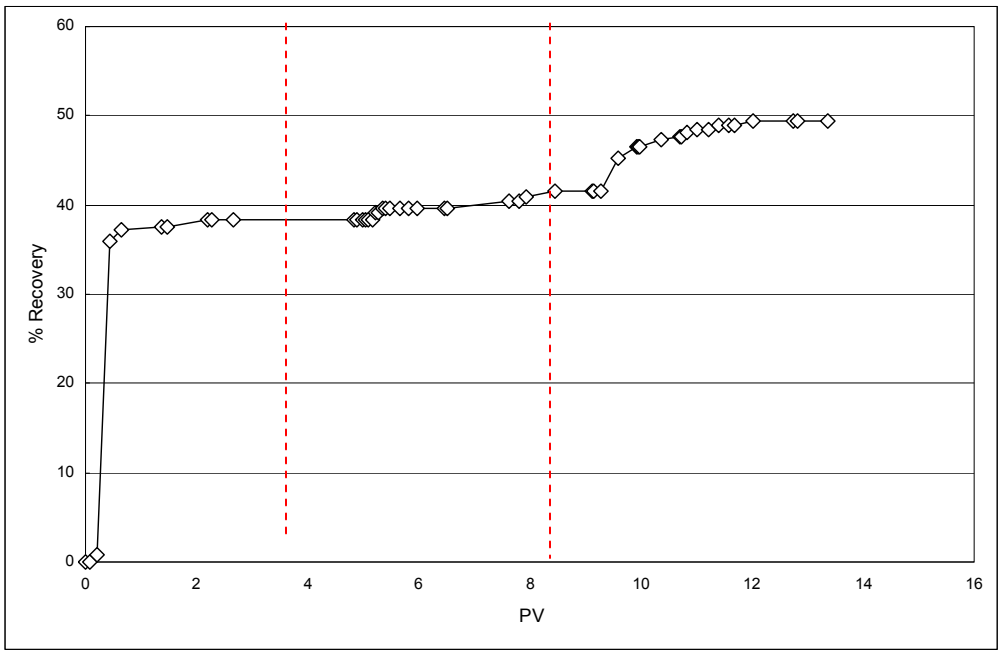

Figure 79. Percent of oil recovery versus PV of displacing fluid for Experiment H.

Figures 80 and 81 represent variations of pressure drop and generated gas volume versus injected PVs, respectively. At the first stage of the experiment, brine breakthrough is observed at around 0.5 PV of injection. Flat recovery profile continues after breakthrough as expected. Around 4.8 total PV (t = 865 minutes) injection, a second stage of the recovery process commences. An additional oil production starts at ~0.39 PV (or 5.23 PV of total injection) with simultaneous gas production (breakthrough) (Figure 81). A 5% additional oil recovery was obtained from 0.39 PV to 3.61 PV of ISCGT system injection.

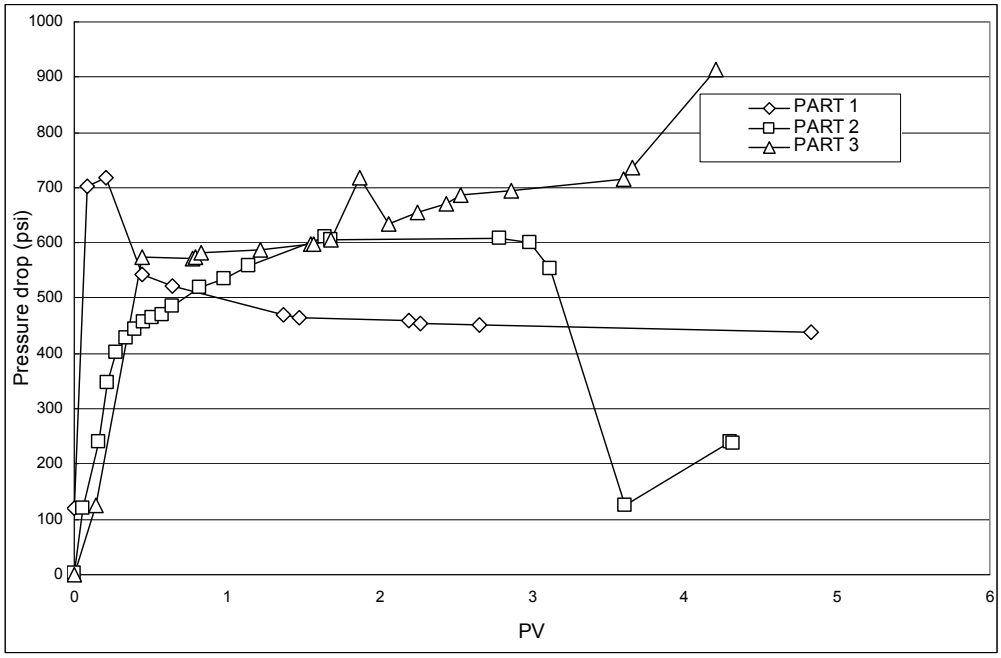

Figure 80. Pressure drop versus PV of displacing fluids for Experiment H.

Upon completion of ISCGT system injection (total 9.15 PV injection), a third stage of the recovery process started. Approximately 0.71 PV of ISCGT + cationic surfactant was injected without additional oil recovery. An additional 13.41% oil recovery was obtained between 9.6 PV and 12.02 PV injections.

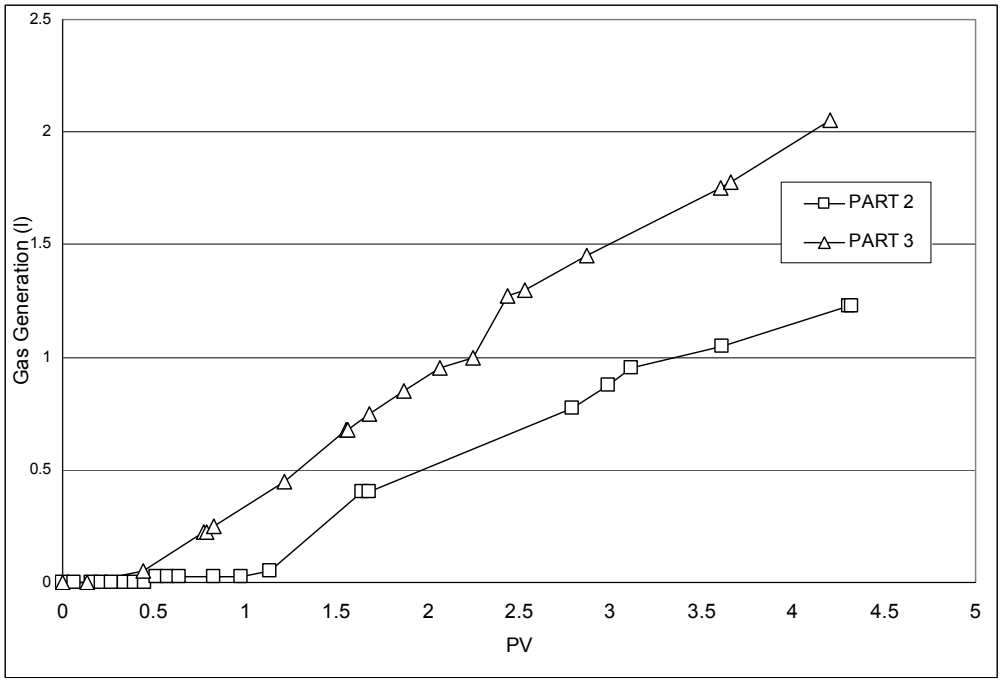

Figure 81. Generated gas volume versus PV of displacing fluids for Experiment H.

Figure 82 compares percent of oil recovery versus PV of displacing fluid for the Experiments A, E and H. In spite the identical pressures and temperatures during the Experiments E and H, the discrepancies in the oil recovery data can be explained using the data obtained from experiments described in Chapter 3.3.1. Upon observing the results of the studies conducted before H, one would suggest that the oil recovery with the ISCGT system, which can generally be evaluated as inferior to the brine recovery, is due to the delayed commencement of CO_2 gas generation at high pH environment. A basic GY component reaches the mixing point of the test system before acidic GF component if they are injected at flow rates calculated according to the stoichiometric ratio. In this case the reactants of the ISCGT system pass through most of the core without sufficient CO_2 gas generation due to the chemical equilibrium, and some portion of the oil which could be recovered with ISCGT system remains intact and recovery efficiency does not increase. To avoid this undesirable effect, we decided to start injection with acidic GF and then start providing basic GY to mixing section, so that we could take advantage of a gas generation behavior similar to the one shown in Figure 53. As was calculated before, the distance between GF accumulator and a mixing point was 2.29 times longer than that between GY and mixing point. In other words, when injection starts simultaneously, the basic GY component reaches mixing point 29.8 seconds earlier with a flow rate of 28 ml/hr. Therefore, for the second stages of the recovery process it was decided to start GY injection 150 seconds after commencement of GF injection. This manipulation resulted in 0.52 ml of excess GF component with flow rate of 12.5 ml/hr, meanwhile a GY component flow rate was 14 ml/hr.

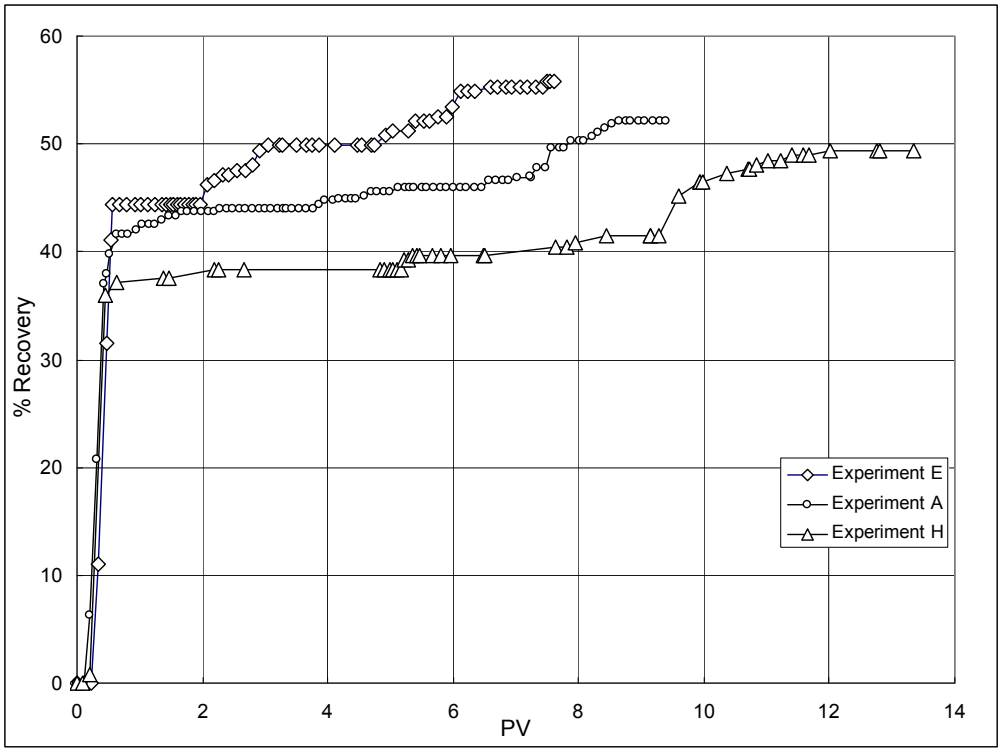

Figure 82. Percent of oil recovery versus PV of displacing fluid for experiments A, E and H.

There could be several reasons for a poor oil recovery in Experiment H compared to the Experiment E. Insufficient volume of excess acidic GY agent might be one of the reasons, which had to be tested. Another factor could be an early gas breakthrough in second stage of Experiment H if compared to Experiment E. As one knows, due to the early breakthrough a displacing agent has a free flow path through the core, and it starts bypassing the oil to be recovered. As seen from Figure 83, a gas breakthrough in a second stage of the Experiment H occurs 0.17 PV earlier than that during the second stage of the Experiment E.

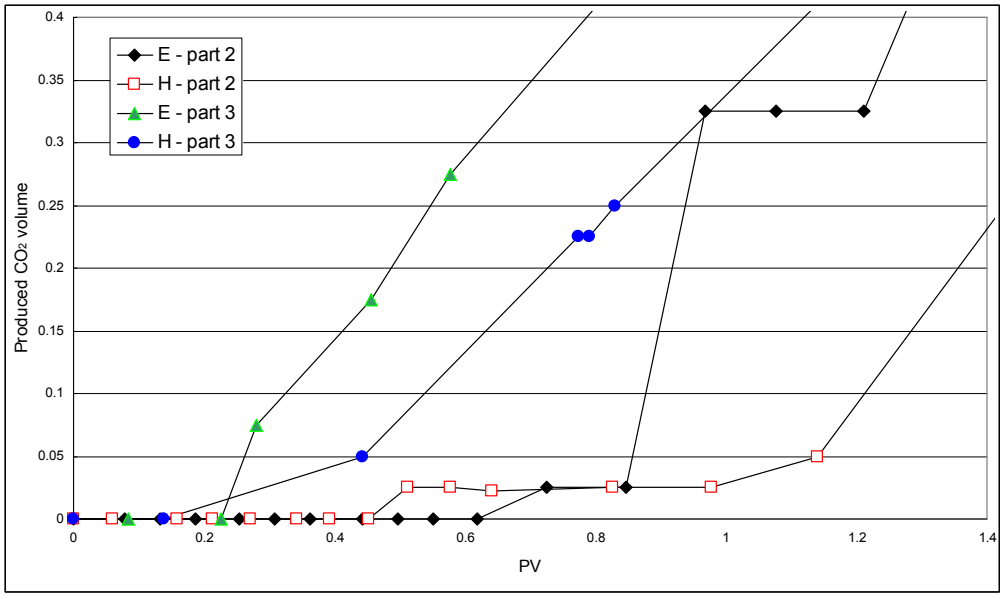

Figure 83. Generated gas volumes versus PV of displacing fluids for 2nd and 3rd stages of experiments E and H.

Considering these facts, during the third stage of Experiment H, which includes injection of ISCGT + cationic surfactant, it was decided to increase the excess volume of the acidic component GF. According to the calculations, 4 min between commencements of injections of basic GY and acidic GF components were specified. It would result in 0.83 ml excess of GF component. This maneuver allowed achieving better oil recovery results. 13.4 % additional oil recovery was obtained in third stage of Experiment H, compared to 11.9 % oil recovery value obtained during the Experiment E at equal experimental conditions. Again, early gas breakthrough in the Experiment H compared to the Experiment E should be taken into the account. It also should be underlined that 4 sets of experiments were conducted between the third stages of the Experiments E and H, among which three are ISCGT system injections. The results of our permeability measurements are shown in Tables 53 and 54 (Appendix F). Figure 89 compares two Berea sandstone core test samples: (1) unused fresh test sample, and (2) a sample soaked in 9% acidic GF solution for 24 hours. As seen from the Tables 53 and 54, the permeability increases 2-3 times due to the exposure of the core samples to GF solution. Therefore, one can assume that during these four experiments an increase in the permeability of the sandstone core led to an early breakthrough. Finally, it can be concluded that an injection of the excess GF component during the Experiment H results in a better oil recovery compared to the Experiment E. Unfortunately, the option to inject more excess GF component can create more corrosions and a special care must be taken to prevent it.

Table 53 (Appendix F) summarizes all core flood experiments conducted in this study. As seen from these data, the ISCGT system is useful when used as a tertiary oil recovery technique. A decreasing a system operation pressure significantly improves recovery performances. An initial oil recovery with brine solution in the Experiment A is higher than that of the Experiment H, whereas 18.4% additional oil recovery with ISCGT system during the Experiment H is higher compared to 14.9% additional oil recovery during the Experiment A. Beneficial effects of the decreased pressure is also can be proved with 21.7 % additional oil recovery in the Experiment E (P = 500 psi), compared to 14.9% additional oil recovery in the Experiment A (P = 1,500 psi).

CONCLUSIONS

1. The slim tube experiments conducted at 176°F temperature and pressures above 1,000 psi with the mineral oil showed that a quantity of the generated CO_2 gas during ISCGT oil recovery process is not enough to have a free CO_2 gas phase within the system because the MMP of oil and CO_2 at this temperature is above 3500 psi. Therefore, the miscibility can not be achieved in ISCGT technique due to the immiscible flood.
2. During the ISCGT process used as a secondary recovery method at 500 psi pressure, a recovery efficiency E_R is lower than that in the brine flooding. At 1000 psi pressure, the oil recovery efficiency for the ISCGT process surpasses that for the brine flooding by more than 2%. Hence, the presence of the free CO_2 (without surfactant) reduces the recovery efficiency due to (i) the increased mobility of the displacing front and (ii) the decreased amount of the dissolved CO_2 in the oil.

3. Increasing the operating pressure from 500 psi to 1,000 psi enhances a recovery efficiency E_R ~10% due to the increased quantity of dissolved CO_2 in the oil. Further increase of pressure up to 1,500 psi doesn't yield more oil recovery since all the generated CO_2 is already dissolved in the liquids system.
4. ISCGT system flood with surfactant additives at 500 psi improves recovery efficiency E_R ~5%, which is comparable to the recovery during the brine flooding at this pressure. The generated foam improves the mobility, and hence, the recovery efficiency is increased at this pressure. At 1,000 psi, the addition of the surfactant can only improve recovery efficiency E_R only by 2% which is due to the lack of foam at this pressure. Decrease in brine/oil IFT is the only factor that contributes to the recovery improvement by surfactant additives at 1,000 psi.
5. During the ISCGT process used as a tertiary recovery method, the oil recovery is improved ~4% over the brine flood technique (or 12% of residual oil in place) and an additional 1% (or 3.5% of residual oil in place) oil recovery will be achieved when surfactant additives are used.
6. The slim tube experiments demonstrated that a co-injection is a more efficient injection method than a slug injection. Moreover, a slug injection technique is very corrosive even a high concentration of the acid inhibitor is used.
7. An acid inhibitor was proved to be effective in minimizing the corrosion effects. But still corrosion can be a problem of concern during the field applications. The suggestion is that to adjust the injection flowrate of GY solution slightly more than the one calculated by chemical reaction stoichiometry ratio in order to decrease the corrosive impact of the chemical reaction products.
8. Injection sequence of the chemicals affects the reaction characteristics, but the total amount of the generated CO_2 gas does not vary significantly. Injection sequence can be determined according to the operational requirements during the field applications.
9. Regardless of the first injected solution (GF or GY), the maximum attainable pressures are less than the calculated pressures as a result of chemical equilibrium in the system and solubility of the CO_2 gas in the brine. This difference should be considered when calculating the amount of the slug during the field applications.
10. Both a brine concentration (salinity) and a system pressure have an impact on CO_2 solubility in aqueous phase and, hence, on the CO_2 pressure. Because of this impact, brine concentration of formation waters, in addition to the brine which is introduced to the system by the reaction, and the reservoir pressure should be considered during the process simulations.
11. As a result of CO_3^{-2} equilibrium, pH of the solution has an important effect on the CO_2 pressure in the system. A pH level of the system should be kept below 7 (in the acidic environment pH ≈ 5.
12. Corroding effects of the liquid components on the metal equipment should be carefully observed. The technology has a good potential when applied in the low pH zone, due to its detrimental effects on metal oil field equipment. An application of proper inhibitors will significantly reduce or eliminate the corrosion effects.
13. The most beneficial use of this technology can be (i) at remotely located and/or shallow reservoirs where the pressures are below 1,100 psi, (ii) where pipeline construction and installation of large scale compressors are costly investments, with relatively low

reservoir pressures, because the system does not have a capability to generate sufficient free CO_2 at elevated pressures.

REFERENCES (Activity 1)

1- "International Energy Annual 2004", Energy Information Administration, 14 July, 2006 (http://www.eia.doe.gov/pub/international/iealf/tablee2.xls)
2- International Energy Outlook 2008 (http://www.eia.doe.gov/oiaf/ieo/highlights.html)
3- Enhanced oil Recovery Process, CANO Petroleum (http://www.canopetro.com/default.asp?page=3)
4- Latil M. "Enhanced Oil Recovery", Gulf Publishing, 1980
5- A. Amarnath, "Enhanced oil recovery scoping study", EPRI
6- http://www.doe.gov
7- H. Y. Chen, "Engineering Reservoir", January 2007
8- F. M. Llave, and D. K. Olsen "Use of Mixed Surfactants To Generate Foams for Mobility Control in Chemical Flooding", NIPER/BDM-Oklahoma Inc., 1993
9- S. Maudgalya, "Microbial enhanced oil recovery technologies: A review of the past, present and future", SPE, Anadarko petroleum corp.
10- A. A. M. Yassin, U. Teknologi, "Enhanced Oil Recovery in Malaysia", Malaysia
11- B. Williams, "Progress in IOR Technology, Economics deemed Critical to Staving off World's Oil Production Peak", OGJ, 2003
12- P. M. Jarrell, C. E. Fox, M. H. Stein, and S. L. Webb, " Practical aspects of CO_2 flooding", SPE monograph
13- Y. Liu, R. B. Grigg, and R. K. Svec, " CO_2 foam behavior: Influence of temperature, pressure and concentration of surfactant", 2005
14- Mungan N., "Carbon Dioxide Flooding—Fundamentals", J. Cdn. Pet. Tech. (January-March 1981) 87-92
15- R. J. Pawar, N. R. Warpinsky, R. D. Benson, and R. B. Grigg, " Geologic sequestration of CO_2 in a depleted oil reservoir : and overview of a field demonstration project", 2004
16- Chang, Y. B., Coats, B. K., and Nolen, J.S., "A compositional model for CO_2 solubility in water", 1996
17- A. M. Elsharkawy, " Measuring CO_2 Minimum Miscibility Pressures: Slim-Tube or Rising-Bubble Method", 1995
18- D. N. Rao, " A new technique of vanishing interfacial tension for miscibility determination", 1997
19- H. Yongmao, W. Zenggui, J. Binshan and C. Yueming, " Laboratory Investigation of CO_2 flooding", 2004
20- L. W. Holm, " CO_2 flooding: Its time has come"
21- G. A. Rojas, and F. Ali, " Dynamics of subcritical CO_2/Brine floods for heavy-oil recovery"
22- S. A. Shedid, R. A. Almehaideb and A. Y. Zekri, "Microscopic rock characterization and influence of slug size on oil recovery by CO_2 miscible flooding in carbonate oil reservoir", UAE University, 2005
23- L. W. Holm and L. J. O'Brien, "Factors to consider when designing a CO_2 flood", Unocal Corp., 1986

24- G. C. Wang, “A laboratory study of CO_2 foam properties and displacement mechanism”, University of Alabama and University of Petroleum and Minerals, 1984
25- Kane, A. V., "Performance Review of a Large Scale $C0_2$-WAG Project, SACROC Unit-Kelly Snyder Field", J. Pet. Tech., Feb. 1979, 217-31.
26- G. G. Bernard, L.W. Holm, and C. P. Harvey, “Use of surfactant to reduce CO_2 mobility in oil displacement”, SPE, Union Oil Co. of California
27- H. Murtada, and B. Hofling, “Carbon dioxide- A mobilizing agent for heavy-oil recovery”, Veba- Oel AG
28- M. Dong, S. Huang, S. B. Dyer, and F. M. Mourits, “A comparison of CO_2 minimum miscibility pressure determinations for Weyburn crude oil”, Journal of Petroleum Science and Engineering, 32, 2001, pp. 13-22.
29- R. B. Grigg, “Improving CO_2 efficiency for recovering oil in heterogeneous reservoirs”, Annual technical progress report, New Mexico Recovery Research Center
30- Chopra, A. K., Stein, M. H., and Dismuke, C. T., “Prediction of performance of miscible-gas pilots”, JPT, December 1990
31- Patel, P. D., Christman, P. G., and Gardner, J. W., “Investigation of unexpectedly low field-observed fluid mobilities during some CO_2 tertiary floods”, SPERE, November 1987, 507
32- Schneider F. N. and Owens, W. W., “Relative permeability studies of gas-water flow following solvent injection in carbonate rocks”, SPEJ, February 1976, 23

REFERENCES (Activity 2)

1- http://www.wtrg.com/oil_graphs/oilprice1947.gif
2- http://www.wtrg.com/daily/clfclose.gif
3- http://www.grist.org/news/maindish/2005/11/03/simmons/index.html?source=weekly Interview with Matthew Simmons by Amanda Griscom Little, 3 November, 2005
4- http://www.eia.doe.gov/oiaf/ieo/figure_27.html
5- http://www.iea.org, fact sheet
6- Lake W. L., Enhanced Oil Recovery, Chapter 1, Prentice Hall, 1989.
7- http://seca.doe.gov/technologies/oil-gas/publications/eordrawings/BW/bwp.PDF
8- 2002 worldwide EOR survey, Oil & Gas Journal, 71-83, April 15, 2002
9- Moritis, G., “EOR Oil production Up slightly,” Oil & Gas Journal, (1998) 96, No. 16, 49.
10- Basnieva I. K., Zolotukhin A. B., Eremin N. A., and Udovina E. F., “Comparative Analysis of Successful Application of EOR in Russia and CIS” SPE 28002, August 1994.
11- Monger T. G., and Coma J. M., “Laboratory and field evaluation of the CO_2 Huff ’n’ Puff process for light oil recovery”, *SPE Reservoir Engineering*, November 1988.
12- Goodrich J. H., “Review and Analysis of Past and Ongoing Carbon dioxide Injection Field Tests”, 6th Biennial SPE-DOE Symposium on Improved Oil Recovery, April 1980.
13- Jarrel P. M., Fox C. E., Stein M. H., and Webb S. L., “ Practical Aspects of CO2 Flooding”, SPE Monograph Series, Volume 22, Chapters 1, 2, Texas, 2002.
14- Grigg R. B., and Svec R. K., “CO_2 Transport Mechanisms in CO_2/Brine Core flooding”, SPE 103228, September 2006.
15- L. Schramm, “Foams, Fundamentals and Applications in the Petroleum Industry”, ACS Advances in Chemistry Series, Washington, DC, 1994
16- Yuan H., Johns R.T, “Simplified Method for Calculation of Minimum Miscibility Pressure or Enrichment”, SPE 77381, 2005.

17- Grigg R. B., Gregory M. D., and Purkaple J. D., "Effect of Pressure on Improved Oil flood Recovery From Tertiary Gas Injection", SPE 35426, April 1997.
18- Shelton, J. L., and Yarborough, L., "Multiple Phase Behavior in Porous Media during CO_2 or Rich-Gas Flooding", paper SPE 5827, presented at SPE-AIME Fourth symposium on improved oil recovery, March 1976.
19- Bond, D. C., and Holbrook, O. C., "Gas Drive Oil Recovery Process", U.S. Patent 2866507, December 1958.
20- Chang S. H., Grigg R. B., "Effects of Foam Quality and Flow Rate on CO_2-Foam Behavior at Reservoir Temperature and Pressure", *SPE Reservoir Evaluation and Engineering* 2 (3), June 1999.
21- Aronson A. S., Bergeron V., Pagan M. E., and Radke C. J., " The influence of disjoining pressure on foam stability and flow in porous media", *Colloids and Surfaces A: Physicochemical and Engineering Aspects*, 83 (1994) 109-120
22- Gauglitz P. A., Friedmann F., Kam S. I., and Rossen W. R., "Foam Generation in porous media", paper SPE 75177, presented at SPE/DOE Improved Oil Recovery Symposium, Tulsa, Oklahoma, April 2002.
23- Yang S. H. and Reed R. L., "Mobility control using CO_2 foams", SPE 19689, October, 1989.
24- Siddiqui S., Talabani S., Saleh S. T., and Islam M. R, "Foam flow in low-permeability Berea Sandstone cores: a laboratory investigation", *Journal of Petroleum Science and Engineering*, 36, 2002, 133-148.
25- Kovscek A. R., Patzek T. W., and Radke C. J., "Mechanistic Foam Flow Simulation in Heterogeneous and Multidimensional Porous Media", SPE 39102, 1997.
26- Fergui O., Bertin H., Quintard M., "Transient aqueous foam flow in porous media: experiments and modeling", *Journal of Petroleum Science and Engineering*, 20, 1998, 9-29.
27- Hirasaki G. J., and Lawson J. B., "Mechanism of Foam Flow velocity in Porous media: Apparent Viscosity in Smooth Capillaries. SPE, 1985.
28- Suffridge F. E., Raterman K. T., and Russell G. C., "Foam Performance under Reservoir Conditions", SPE 19691, presented at 64^{th} annual conference of SPE in San Antonio, TX, October, 1989.
29- Mannhardt K. and Svorstøl I., "Surfactant concentration for foam formation and propagation in Snorre reservoir core", *Journal of Petroleum Science and Engineering* 30, 2001.
30- Bernard G. G., Holm L. W., and Harvey C. P., "Use of Surfactant to Reduce CO_2 Mobility in Oil Displacement", SPE 8370, 1980.
31- Liu Y., and Grigg R. B., "Salinity, pH, and Surfactant Concentration Effects on CO_2 Foam", SPE 93095, February 2005.
32- Liu Y., Grigg R. B., and Svec R. K., "CO_2 Foam Behavior: Influence of Temperature, Pressure and Concentration of Surfactant", SPE 94307, April, 2005.
33- Apaydin O. G., and Kovscek A. R., "Transient Foam Flow in Homogeneous Porous Media: Surfactant Concentration and Capillary End Effects", SPE 59286, April 2000.
34- Beneventi D., Pugh R. J., Carre B., and Gandini A., "Surface rheology and foaming properties of sodium oleate and $C_{12}(EO)_6$ aqueous solutions", *Journal of Colloid and Interface Sciences*, 268, 2003, 211-229.
35- Chou, S. I., "Conditions for Generating Foam in Porous Media," paper SPE 22628 presented at the 1991 SPE Annual Technical Conference and Exhibition, Dallas, TX, 6-9 Oct.
36- Akin S., and Kovscek A. R., "Imbibition Studies of Low-Permeability Porous Media", SPE 54590, May 1999.

37- Gharbi R., "Application of an expert system to optimize reservoir performance", *Journal of Petroleum Science and Engineering*, 2005.
38- Jessen K., Sam-Olibale L. C., Kovscek A. R., and Orr F.M., "Increasing CO_2 Storage in Oil Recovery".
39- Alizadeh N., "Enhanced Productivity in a Heavy Oil Reservoir as a Result of Immiscible Gas and Foam Injection."
40- Khatib, A. K., Earlougher R. C., and Kantar, K., "CO_2 Injections as an Immiscible Application for Enhanced Recovery in Heavy Oil Reservoirs.", paper SPE 9928, March 1981.
41- http://www.bereasandstonecores.com/
42- J. N. Butler, Carbon Dioxide Equilibria and Their Applications, Chapter 2, pp. 15-23, Addison-Wesley Publishing Company, 1982.
43- Duan, Z., and Sun, R., 2003, "An Improved Model Calculating CO_2 Solubility in Pure Water and Aqueous NaCl Solutions from 273 to 533 K and from 0 to 2000 Bar", *Chemical Geology*, **193**, pp. 257-271.
44- Y. B. Chang, B. K. Coats, and J. S. Nolen, Western Atlas Software, 1998, "A Compositional Model for CO_2 Floods Including CO_2 Solubility in Water", *SPE Reservoir Evaluation & Engineering*, pp. 155-160.
45- Masoudi R., Tohidi B., and Danesh A., "Modelling Gas Solubility in Saline Solutions and its Importance to IOR Gas Injection", Institute of Petroleum Engineering, Heriot-Watt University.
46- http://www.pttc.org/solutions/sol_2006/553.htm
47- Crolet, J. L., "Acid Corrosion in Wells (C02, H2S): Metallurgical Aspects", *Journal of Petroleum Technology*, August 1983, pp. 1553-1558.
48- Muller, N., Elshahawi, H., Dong, C., Mullins, O. C., Flannery, M., Ardila, M., and Weinheber, P., "Quantification of Carbon Dioxide Using Downhole Wireline Formation Tester Measurements", SPE 100739, September 2006.
49- Piccolo, E. L., and Nice, P. I., "Corrosion and Environmental Cracking Evaluation of High Density Brines for Use in HPHT Fields", SPE 97593, May 2005.
50- Grinsven, R. V., Jackson, L., Suarez, I., and Bouts, M., "Corrosion in High Gas Wells – A Case History", SPE 94795-MS, May 2005.
51- Gunaltun, Y., "Carbon Dioxide corrosion in Oil Wells", SPE 21330, November 1991.
52- Chitwood, G. B., Eisinger, N. C., and Puckett, B. C., "Corrosion Resistance and Long-Term Reliability of Super-Austenitic Alloy 27-7MO for Use as Expandable Pipe." SPE 95094, May 2005.
53- Coskun, O., Grigg, R., Svec, R., Siginer, D. A. and Bakhtiyarov, S. I., 2006, "The Effect of Salinity on In-Situ Generated CO_2 Gas: Simulations and Experiments", Symposium on "Advances in Materials Processing Science", ASME International Mechanical Engineering Congress and Exposition, Chicago, IL, November 5-10, 2006, Paper # IMECE2006-15703.

APPENDIX A
DENSITY AND SYSTEM PARAMETERS MEASURMENTS

Appendix A-1- Measuring density

Densitometer output is in the unit of τ (period). In order to convert it to regular units, densitometer should be calibrated by the following procedure:

1. τ of two fluids with known densities was measured by densitometer at the desired temperature and pressure.

2. ρ of these fluids was found by the use of Supertrap ^{TM} software at the same thermobaric conditions.
3. The equation of ($\rho = A\tau^2 + B$) was solved by substituting ρ and τ of the two fluids and therefore, A and B constants were calculated.
4. By substituting A and B in the above equation, density can be calculated for each specific τ.

It should be mentioned that for each set of pressure and temperature densitometer should be calibrated again and a new pair of A and B should be calculated. Nitrogen and distilled water was used to calibrate the densitometer inside the system. Densitometer in the room condition was calibrated by the use of distilled water and air.

Appendix A-2- Measuring system volume and slim-tube pore volume

To determine system and slim-tube PV, following procedure was followed:

1. System was cleaned thoroughly with THF.
2. System was dried by injection of nitrogen gas.
3. A vacuum pump was used to vacuum the system.
4. All the valves inside the system were closed
5. Distilled water was injected with constant pressure of 1000 psi by pump 1.
6. System valves were opened one by one from the point of injection and in each instance we waited until the pump pressure reached 1000 psi and then the injected volume at each step was recorded (which was equal to the pore volume of the portion of the system between the valves).

Table 13. Volume of system components

System sections	Volume, ml
From injection point to inlet filter	0.98
Inlet filter	2.35
Slim-tube	106.04
Outlet filter and densitometer	19.95
Outlet BPR	0.50
From outlet BPR to production point	7.17
System Total	136.99

It should be mentioned that system volume is considered from the point of first contact between injecting fluid and oil. Therefore, it doesn't include inlet BPR volume and this makes volumes of setups A and B similar. Table 13 shows the measured volume of different sections of system including pore volume of slim-tube.

Appendix A-3- Measuring slim-tube porosity

Porosity is defined by the following ratio:

$$\phi = \frac{V_{Void}}{V_{Total}}$$

V_{Void} is the same as pore volume of slim-tube and total volume of slim-tube can be calculated by knowing slim-tube inner diameter and length (slim-tube V_{Total} = 385.87ml). Thus, slim-tube porosity is:

106.04/385.78 = 0.2748 = 27.48%

Appendix A-

ΔP, psi	Q, ml/hr	κ, darcy
70	40	5.98
181	100	5.79
367	200	5.71
927	500	5.65

4- Measuring slim-tube permeability

Permeability of the slim-tube was measured by the following procedure:

1. System was cleaned thoroughly.
2. System was filled out with distilled water.
3. Distilled water was injected by a constant flowrate into the system.
4. ΔP across the slim-tube and flowrate was recorded.
5. Viscosity of distilled water at the same pressure and temperature was found by the help of Supertrap ^{TM} software.
6. Permeability was calculated by the use of Darcy's law:

$$\kappa(darcy) = \frac{Q(ml/hr) \times L(cm) \times \mu(cp)}{A(cm^2) \times \Delta P(psi)} \times 4.083 \times 10^{-3}$$

L and A are the length and inner area of slim-tube. τ is the viscosity of distilled water at the same thermobaric conditions. ΔP and κ are pressure across slim-tube and permeability of slim-tube respectively.

Table 14 demonstrates permeability of slim-tube calculated for different distilled water flowrates. As can be seen there is a slight decrease in calculated permeability by increasing the flowrate. This difference is because pressure drop in components of the system other than slim-tube doesn't conform to Darcy's law (like the pressure drop in the valves and plumping).

APPENDIX B
MINERAL OIL COMPOSITION

Table 14. Permeability of slim-tube measured with different flowrates of distilled water at 176°F

Pseudocomponents	Mole fraction	Molecular weight
C5	0.0180	72
C7	0.0920	91
C10	0.0920	134
C15	0.0430	206
C20	0.0092	261

C22	0.1186	288
C24	0.1718	314
C26	0.1373	342
C28	0.0989	372
C30	0.0816	402
C32	0.0757	430
C34	0.0539	450
C36	0.0465	480
C38	0.0247	510
C42	0.0003	540

Table 15. Gas chromatography results of mineral oil

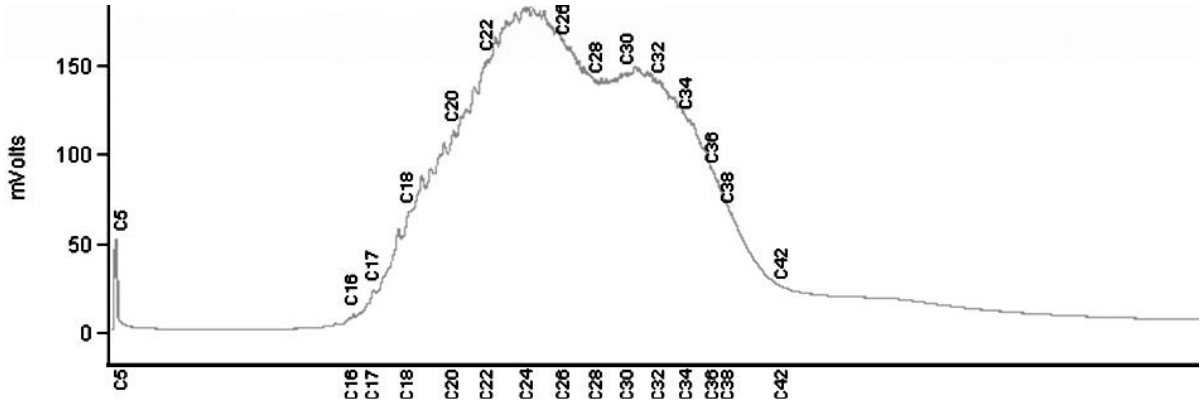

Figure 84. Gas chromatography results of mineral oil used in the tests 3-20

APPENDIX C
EXPERIMENTAL DATA

Table 16. Experimental data of test 1 (displacement of decane by distilled water at 122°F and 1000 psi)

Time, min	Q_{inj}-water, ml/hr	P_{in}, psig	P_{out}, psig	$P_{dome-out}$, psig	T, ºF	ρ, g/ml	V_P-liquid, ml	V_P-water, ml	V_P-oil, ml	E_R^*, %
5	60	1113	1008	987	123	0.712	0.0	0.0	0.0	0.00
10	60	1100	1002	979	123	0.712	6.0	0.0	6.0	0.00
15	60	1101	1002	977	121	0.712	4.6	0.0	4.6	4.38
20	60	1101	1002	978	123	0.712	4.4	0.0	4.4	7.74
25	60	1102	1002	978	122	0.712	5.1	0.0	5.1	10.95
30	60	1100	1002	977	122	0.712	5.1	0.0	5.1	14.67
35	60	1101	1002	977	123	0.712	5.1	0.0	5.1	18.39
40	60	1099	1002	977	122	0.712	5.1	0.0	5.1	22.12
45	60	1100	1002	978	123	0.712	5.1	0.0	5.1	25.84
50	60	1099	1002	978	122	0.712	5.0	0.0	5.0	29.56
55	60	1101	1002	978	123	0.712	5.1	0.0	5.1	33.21
60	60	1098	1002	977	122	0.712	5.0	0.0	5.0	36.93
65	60	1099	1002	978	123	0.712	5.1	0.0	5.1	40.58
70	60	1097	1002	977	121	0.712	5.1	0.0	5.1	44.31
75	60	1097	1002	977	124	0.712	5.1	0.0	5.1	48.03
80	60	1096	1002	976	121	0.712	4.9	0.0	4.9	51.75
85	60	1097	1002	977	124	0.720	5.1	0.0	5.1	55.33
90	60	1096	1002	977	121	0.726	5.1	0.0	5.1	59.05
95	60	1096	1002	977	124	0.715	5.1	0.0	5.1	62.77
100	60	1095	1002	977	121	0.715	4.7	0.0	4.7	66.50
105	60	1096	1002	978	123	0.715	5.1	0.0	5.1	69.93
110	60	1095	1002	977	121	0.715	4.0	0.0	4.0	73.65
115	60	1095	1002	978	123	0.715	6.2	0.0	6.2	76.57
120	60	1094	1002	977	120	0.715	5.0	0.0	5.0	81.09
125	60	1095	1002	978	123	0.715	5.1	0.0	5.1	84.74
130	60	1094	1002	977	120	0.717	5.0	0.0	5.0	88.47
135	60	1093	1002	976	123	0.980	5.1	0.0	5.1	92.12
140	60	1093	1002	976	120	0.977	4.8	0.0	4.8	95.84

145	60	1093	1002	976	123	0.972	5.1	4.5	0.6	99.34
150	60	1094	1002	976	120	0.977	4.9	4.9	0.0	99.78
155	60	1094	1002	975	123	0.977	5.2	5.2	0.0	99.78
160	60	1094	1002	975	120	0.980	5.1	5.1	0.0	99.78
165	60	1094	1002	976	123	0.980	5.0	5.0	0.0	99.78
170	60	1094	1002	976	120	0.980	5.1	5.2	0.0	99.78

Table 17. Experimental data of test 2 (displacement of crude oil by distilled water at 176°F and 1000 psi)

Time, min	Q_{inj}-water, ml/hr	P_{in}, psig	P_{out}, psig	$P_{dome-out}$, psig	T, ºF	ρ, g/ml	V_P-liquid, ml	V_P-water, ml	V_P-oil, ml	E_R^*, %
0	0	427	436	971	177	0.862	0.0	0.0	0.0	0.00
10	40	1804	1000	978	177	0.868	3.1	0.0	3.1	2.26
20	40	1804	1000	978	177	0.845	2.9	0.0	2.9	4.38
30	40	1591	1000	988	176	0.857	0.0	0.0	0.0	4.38
40	40	1714	1000	976	178	0.857	6.9	0.0	6.9	9.42
50	40	1552	1000	976	178	0.859	6.9	0.0	6.9	14.45
60	40	1345	1000	976	177	0.859	7.2	0.0	7.2	19.71
70	40	1284	1002	975	175	0.907	7.1	0.0	7.1	24.89
80	40	1253	1002	976	175	0.933	7.7	1.7	6.0	29.27
90	40	1228	1002	977	175	0.933	6.9	3.9	3.0	31.46
100	40	1205	996	974	175	0.933	7.0	4.7	2.3	33.14
110	40	1196	1002	974	177	0.941	7.0	4.8	2.2	34.74
120	40	1183	1002	975	177	0.947	7.0	4.6	2.4	36.50
130	40	1173	1002	978	177	0.947	6.9	5.0	1.9	37.88
140	40	1163	1002	976	178	0.947	7.2	5.3	1.9	39.27
150	40	1153	1002	976	177	0.947	7.2	5.3	1.9	40.66
160	40	1148	1002	978	178	0.950	7.2	5.5	1.7	41.90
170	40	1142	1002	977	177	0.950	7.2	5.8	1.4	42.92
180	40	1138	1002	981	178	0.953	7.3	5.7	1.6	44.09
190	40	1131	1002	978	175	0.950	6.8	5.4	1.4	45.11
200	40	1124	1002	977	175	0.953	7.1	5.7	1.4	46.13
210	40	1118	1002	978	174	0.953	7.0	5.6	1.4	47.15
220	40	1114	1002	977	174	0.956	7.1	5.7	1.4	48.18
230	40	1111	1002	977	174	0.956	6.9	5.5	1.4	49.20
240	40	1109	1002	978	174	0.958	6.9	5.6	1.3	50.15
250	40	1104	1002	977	177	0.956	7.1	5.8	1.3	51.09

260	40	1101	1002	977	178	0.956	6.9	5.8	1.1	51.90
270	40	1097	1002	977	179	0.958	7.2	6.0	1.2	52.77
280	40	1093	1002	976	179	0.958	7.4	6.2	1.2	53.65
290	40	1092	1002	977	179	0.964	6.8	5.8	1.0	54.38
300	40	1090	1002	977	180	0.961	7.0	6.0	1.0	55.11
310	40	1089	1002	979	180	0.961	7.4	6.3	1.1	55.91
320	40	1087	1002	977	176	0.961	7.0	5.8	1.2	56.79
330	40	1092	1002	977	178	0.956	7.7	7.0	0.7	57.30
340	40	1089	1004	977	177	0.953	7.2	5.8	1.2	58.32
350	40	1087	1002	977	178	0.956	7.5	6.5	1.0	59.05
360	40	1086	1002	977	178	0.958	6.4	5.3	1.1	59.85
370	40	1084	1002	979	178	0.956	7.6	6.6	1.0	60.58
380	40	1083	1002	976	179	0.964	7.8	7.1	0.7	61.09
390	40	1084	1002	978	178	0.967	7.1	6.3	0.8	61.68
400	40	1083	1002	977	178	0.967	6.2	5.5	0.7	62.19
410	40	1081	1002	978	178	0.964	8.3	7.4	0.9	62.85
420	40	1082	1002	979	176	0.961	6.7	6.1	0.6	63.28
430	40	1080	1002	978	177	0.970	6.8	6.4	0.4	63.58
440	40	1081	1002	978	176	0.964	7.4	6.6	0.8	64.16
450	40	1079	1002	977	176	0.961	7.3	6.6	0.7	64.67
460	40	1079	1002	978	174	0.967	7.4	6.9	0.5	65.04
470	40	1079	1002	978	174	0.973	6.6	6.1	0.5	65.40
480	40	1078	1002	976	174	0.970	8.1	7.6	0.5	65.77

Table 18. Experimental data of test 3 (displacement of mineral oil by distilled water at 176°F and 1000 psi)

Time, min	Q_{inj}-water, ml/hr	P_{in}, psig	P_{out}, psig	$P_{dome-out}$, psig	T, ºF	ρ, g/ml	V_P-liquid, ml	V_P-water, ml	V_P-oil, ml	E_R^*, %
0	0	515	520	972	175	0.820	0.0	0.0	0.0	0.00
15	40	1412	1002	982	179	0.823	8.1	0.0	8.1	5.91
30	40	1361	1002	979	177	0.823	10.1	0.0	10.1	13.28
45	40	1295	1002	983	175	0.823	9.9	0.0	9.9	20.51
60	40	1237	1002	980	177	0.823	10.1	0.0	10.1	27.88
75	40	1180	1002	984	174	0.823	9.9	0.0	9.9	35.11
90	40	1151	1002	978	174	0.882	11.9	0.0	11.9	43.80
105	40	1138	1002	978	177	0.902	11.0	3.7	7.3	49.12
120	40	1120	1002	977	177	0.922	10.1	6.1	4.0	52.04
135	40	1107	1002	977	175	0.924	10.1	6.1	4.0	54.96
150	40	1095	1002	979	176	0.922	10.2	6.4	3.8	57.74
165	40	1089	1002	983	177	0.922	10.1	6.6	3.5	60.29
180	40	1077	1002	986	175	0.919	10.0	6.7	3.3	62.70
195	40	1074	1002	983	175	0.927	10.2	7.1	3.1	64.96
210	40	1068	1002	983	177	0.924	10.0	7.2	2.8	67.01
225	40	1059	1002	983	174	0.958	10.6	7.6	3.0	69.20
240	40	1064	1002	984	175	0.922	10.0	7.7	2.3	70.88
255	40	1059	1002	984	176	0.944	10.7	9.0	1.7	72.12
270	40	1060	1002	984	174	0.950	9.9	9.9	1.7	73.36
285	40	1055	1002	985	178	0.973	10.2	10.2	0.9	74.01
300	40	1055	1002	984	176	0.975	9.3	9.3	0.4	74.31
315	40	1055	1002	982	173	0.975	9.0	9.0	0.4	74.60
330	40	1054	1002	984	177	0.975	9.6	9.6	0.2	74.74
345	40	1057	1002	980	175	0.950	10.0	10.0	0.3	74.96
360	40	1057	1002	980	174	0.970	10.0	10.0	0.2	75.11
375	40	1056	1002	980	177	0.973	11.2	11.2	0.2	75.26

Table 19. Experimental data of test 4 (displacement of mineral oil by brine at 176°F and 1000 psi)

Time, min	Q_{inj}-brine, ml/hr	P_{in}, psig	P_{out}, psig	$P_{dome-out}$, psig	T, ºF	ρ, g/ml	V_P-liquid, ml	V_P-brine, ml	V_P-oil, ml	E_R^*, %
0	0	15	30	960	176	0.815	0.0	0.0	0.0	0.00
15	40	1436	1000	980	177	0.823	4.1	0.0	4.1	2.99
30	40	1372	1000	982	176	0.823	9.8	0.0	9.8	10.15
45	40	1328	1000	982	176	0.823	10.1	0.0	10.1	17.52
60	40	1267	1000	984	176	0.823	10.1	0.0	10.1	24.89
75	40	1216	1000	983	176	0.823	9.9	0.0	9.9	32.12
90	40	1185	1000	981	177	0.919	10.1	0.0	10.1	39.49
105	40	1172	1000	977	176	0.902	11.9	2.6	9.3	46.28
120	40	1150	1002	978	177	0.902	10.4	4.8	5.6	50.36
135	40	1136	1002	978	176	0.913	10.1	4.8	5.3	54.23
150	40	1116	1002	986	177	0.916	9.9	5.2	4.7	57.66
165	40	1110	1002	976	175	0.919	10.2	5.3	4.9	61.24
180	40	1093	1002	978	176	0.916	10.0	5.6	4.4	64.45
195	40	1088	1002	977	177	0.927	10.0	5.3	4.7	67.88
210	40	1076	1002	978	176	0.941	10.4	6.2	4.2	70.95
225	40	1072	1002	978	176	0.941	10.2	6.4	3.8	73.72
240	40	1066	1002	980	177	0.950	10.3	6.9	3.4	76.20
255	40	1063	1002	979	174	0.964	10.2	7.3	2.9	78.32
270	40	1061	1002	980	177	0.978	10.2	7.7	2.5	80.15
285	40	1060	1002	978	174	1.012	10.3	8.4	1.9	81.53
300	40	1059	1002	976	177	1.021	9.3	8.4	0.9	82.19
315	40	1059	1002	977	175	1.018	8.3	8.0	0.3	82.41
330	40	1060	1002	978	177	1.024	10.4	10.3	0.1	82.48
345	40	1060	1002	978	174	1.024	9.9	9.8	0.1	82.55
360	40	1060	1002	979	178	1.021	12.8	12.7	0.1	82.63

Table 20. Experimental data of test 5 (displacement of mineral oil by GY+ GF co-injection at 176°F and 1000 psi)

Time, min	Q_{inj}-GF, ml/hr	Q_{inj}-GY, ml/hr	P_{in}, psig	P_{out}, psig	$P_{dome-out}$, psig	T, ºF	ρ, g/ml	V_P-liquid, ml	V_P-brine, ml	V_P-oil, ml	V_P-gas, L	E_R^*, %
0	0	0	2	28	985	176	0.859	0.0	0.0	0.0	0.000	0.00
15	20	20	24	28	984	177	0.857	0.0	0.0	0.0	0.000	0.00
30	20	20	1365	996	990	180	0.823	0.0	0.0	0.0	0.000	0.00
45	20	20	1533	1000	979	177	0.820	8.7	0.0	8.7	0.000	6.35
60	20	20	1455	1000	979	177	0.823	10.3	0.0	10.3	0.000	13.87

75	20	20	1395	1000	978	176	0.823	10.2	0.0	10.2	0.000	21.31
90	20	20	1362	1000	978	175	0.823	10.4	0.0	10.4	0.000	28.91
105	20	20	1322	1000	975	177	0.823	10.4	0.0	10.4	0.000	36.50
120	20	20	1279	1000	974	176	0.823	10.5	0.0	10.5	0.000	44.16
135	20	20	1266	1000	974	178	0.953	11.0	0.0	11.0	0.000	52.19
150	20	20	1258	1000	971	175	0.953	10.1	6.0	4.1	0.000	55.18
165	20	20	1260	1000	975	178	0.956	10.7	7.6	3.1	0.000	57.45
180	20	20	1251	1000	967	175	0.984	10.2	7.2	3.0	0.000	59.64
195	20	20	1240	1000	970	176	0.973	10.9	8.0	2.9	0.000	61.75
210	20	20	1198	1000	975	177	0.936	11.1	7.6	3.5	0.000	64.31
225	20	20	1170	1000	981	176	0.964	11.3	6.2	5.1	0.000	68.03
240	20	20	1151	1000	982	178	0.978	11.2	7.4	3.8	0.000	70.80
255	20	20	1137	1002	975	176	0.978	10.8	7.8	3.0	0.000	72.99
270	20	20	1130	1002	977	175	0.984	12.9	9.9	3.0	0.000	75.18
285	20	20	1120	1002	974	177	0.987	12.8	10.4	2.4	0.000	76.93
300	20	20	1116	1002	979	174	0.995	11.5	9.9	1.6	0.388	78.10
315	20	20	1118	1002	981	177	0.995	12.0	11.3	0.7	1.164	78.61
330	20	20	1120	1002	983	174	1.001	11.1	10.9	0.2	1.164	78.76
345	20	20	1122	1002	976	177	0.990	11.0	10.9	0.1	1.552	78.83
360	20	20	1122	1002	979	176	0.995	14.7	14.0	0.7	1.940	79.34

Table 21. Experimental data of test 6 (displacement of mineral oil by GY + GF co-injection at 176°F and 1000 psi)

Time, min	Q_{inj}-GF, ml/hr	Q_{inj}-GY, ml/hr	P_{in}, psig	P_{out}, psig	$P_{dome\text{-}out}$, psig	T, ºF	ρ, g/ml	V_P-liquid, ml	V_P-brine, ml	V_P-oil, ml	V_P-gas, L	E_R^*, %
0	0	0	7	232	977	176	0.837	0.0	0.0	0.0	0.000	0.00
15	18.5	21.5	1040	940	977	180	0.854	0.0	0.0	0.0	0.000	0.00
30	18.5	21.5	1543	1000	979	179	0.848	7.8	0.0	7.8	0.000	5.69
45	18.5	21.5	1508	1000	980	176	0.840	10.0	0.0	10.0	0.000	12.99
60	18.5	21.5	1484	1000	979	177	0.834	10.2	0.0	10.2	0.000	20.44
75	18.5	21.5	1426	1000	979	179	0.834	10.2	0.0	10.2	0.000	27.88
90	18.5	21.5	1369	1000	978	175	0.834	10.7	0.0	10.7	0.000	35.69
105	18.5	21.5	1315	1000	980	177	0.834	10.0	0.0	10.0	0.000	42.99

120	18.5	21.5	1254	1000	980	178	0.834	10.4	0.0	10.4	0.000	50.58
135	18.5	21.5	1209	1000	980	176	1.010	10.3	0.0	10.3	0.000	58.10
150	18.5	21.5	1190	1000	978	179	0.995	11.1	2.7	8.4	0.000	64.23
165	18.5	21.5	1180	1000	981	177	0.961	10.0	8.0	2.0	0.000	65.69
180	18.5	21.5	1194	1000	991	175	0.967	9.7	8.8	0.9	0.000	66.35
195	18.5	21.5	1195	1000	984	174	0.967	9.8	9.0	0.8	0.000	66.93
210	18.5	21.5	1179	1000	978	179	0.961	11.1	9.9	1.2	0.000	67.81
225	18.5	21.5	1173	1000	980	177	0.944	10.4	9.4	1.0	0.000	68.54
240	18.5	21.5	1154	1000	979	180	0.958	11.2	8.6	2.6	0.000	70.44
255	18.5	21.5	1137	1000	973	178	0.956	10.7	7.9	2.8	0.000	72.48
270	18.5	21.5	1112	1000	976	175	0.967	10.3	8.4	1.9	0.000	73.87
285	18.5	21.5	1103	1000	975	174	0.961	9.2	7.6	1.6	0.000	75.04
300	18.5	21.5	1104	1000	973	178	0.975	10.1	8.0	2.1	0.000	76.57
315	18.5	21.5	1106	1000	973	176	0.947	10.9	9.3	1.6	0.388	77.74
330	18.5	21.5	1102	1000	971	175	0.964	10.1	8.8	1.3	0.776	78.69
345	18.5	21.5	1104	1000	971	177	0.981	10.3	8.9	1.4	1.164	79.71
360	18.5	21.5	1101	1000	967	178	0.958	10.0	8.9	1.1	1.552	80.51
375	18.5	21.5	1099	1000	966	175	0.981	10.3	9.3	1.0	1.164	81.24
390	18.5	21.5	1097	1000	963	175	0.975	10.1	9.3	0.8	1.552	81.82
405	18.5	21.5	1095	1000	964	179	0.990	10.2	9.4	0.8	1.940	82.41
420	18.5	21.5	1097	1000	971	177	0.987	9.0	8.7	0.3	1.164	82.63
435	18.5	21.5	1097	1000	970	178	0.987	10.0	9.8	0.2	2.328	82.77
450	18.5	21.5	1094	1000	970	175	0.907	10.1	10.0	0.1	1.940	82.85
465	18.5	21.5	1096	1000	968	178	0.936	10.1	10.0	0.1	1.940	82.92

Table 22. Experimental data of test 7 (displacement of mineral oil by GY + GF + surfactant co-injection at 176°F and 1000 psi)

Time, min	Q_{inj}-GF, ml/hr	Q_{inj}-GY, ml/hr	P_{in}, psig	P_{out}, psig	$P_{dome\text{-}out}$, psig	T, ºF	ρ, g/ml	V_P-liquid, ml	V_P-brine, ml	V_P-oil, ml	V_P-gas, L	E_R^*, %
0	0	0	166	200	946	177	0.817	0.0	0.0	0.0	0.000	0.00
15	19	21	1589	1000	972	176	0.823	4.2	0.0	4.2	0.000	3.07
30	19	21	1519	1000	973	176	0.823	10.1	0.0	10.1	0.000	10.44
45	19	21	1540	1000	978	172	0.820	10.0	0.0	10.0	0.000	17.74
60	19	21	1470	1000	983	175	0.820	10.7	0.0	10.7	0.000	25.55
75	19	21	1409	1000	984	175	0.820	10.3	0.0	10.3	0.000	33.07
90	19	21	1354	1000	984	176	0.820	10.4	0.0	10.4	0.000	40.66

105	19	21	1300	1000	984	175	0.820	10.5	0.0	10.5	0.000	48.32
120	19	21	1262	1000	984	176	0.820	10.7	0.0	10.7	0.000	56.13
135	19	21	1248	1000	984	176	0.964	11.7	2.3	9.4	0.000	62.99
150	19	21	1250	1000	989	176	0.913	9.7	7.8	1.9	0.000	64.38
165	19	21	1229	1000	992	176	0.973	12.8	10.0	2.8	0.000	66.42
180	19	21	1215	1000	975	176	0.958	9.5	8.1	1.4	0.000	67.45
195	19	21	1203	1000	989	176	0.939	10.6	9.0	1.6	0.000	68.61
210	19	21	1190	1000	983	176	0.956	10.4	7.7	2.7	0.000	70.58
225	19	21	1180	1000	974	176	0.944	11.9	9.3	2.6	0.000	72.48
240	19	21	1166	1000	989	176	0.973	12.1	9.6	2.5	0.000	74.31
255	19	21	1154	1000	978	176	0.956	11.7	9.5	2.2	0.000	75.91
270	19	21	1140	1000	981	176	0.961	12.6	10.3	2.3	0.388	77.59
285	19	21	1139	1000	989	176	0.967	11.1	9.2	1.9	1.164	78.98
300	19	21	1134	1000	973	175	0.964	10.7	9.1	1.6	1.552	80.15
315	19	21	1121	1000	972	176	0.975	11.3	9.8	1.5	1.552	81.24
330	19	21	1128	1000	972	176	0.975	10.2	9.2	1.0	1.940	81.97
345	19	21	1127	1000	972	176	0.995	10.7	10.0	0.7	1.164	82.48
360	19	21				176	0.967	11.3	10.7	0.6		82.92

Table 23. Experimental data of test 8 (displacement of mineral oil by distilled water at 176°F and 1000 psi)

Time, min	Q_{inj}-water, ml/hr	P_{in}, psig	P_{out}, psig	$P_{dome-out}$, psig	T, ºF	ρ, g/ml	V_P-liquid, ml	V_P-water, ml	V_P-oil, ml	E_R^*, %
0	0	147	134	941	176	0.815	0.0	0.0	0.0	0.00
15	40	1592	1000	967	178	0.817	6.3	0.0	6.3	4.60
30	40	1552	1000	967	178	0.820	7.9	0.0	7.9	10.36
45	40	1505	1000	968	177	0.820	10.0	0.0	10.0	17.66
60	40	1443	1000	967	178	0.820	10.1	0.0	10.1	25.04
75	40	1388	1000	967	175	0.820	9.9	0.0	9.9	32.26
90	40	1323	1000	967	178	0.820	10.2	0.0	10.2	39.71
105	40	1271	1000	967	177	0.820	10.1	0.0	10.1	47.08
120	40	1219	1000	966	177	0.820	10.1	0.0	10.1	54.45
135	40	1195	1000	966	177	0.905	12.3	1.6	10.7	62.26
150	40	1181	1000	965	176	0.905	9.8	7.6	2.2	63.87
165	40	1164	1000	962	177	0.902	9.1	7.2	1.9	65.26
180	40	1148	1000	960	176	0.916	9.4	7.6	1.8	66.57

195	40	1139	1000	960	176	0.907	9.6	8.2	1.4	67.59
210	40	1133	1000	960	176	0.893	10.2	8.8	1.4	68.61
225	40	1125	1000	960	176	0.916	10.3	9.0	1.3	69.56
240	40	1121	1000	963	175	0.919	10.6	9.4	1.2	70.44
255	40	1122	1000	968	175	0.922	10.3	9.3	1.0	71.17
270	40	1117	1000	962	176	0.919	9.8	9.4	0.4	71.46
285	40	1116	1000	964	176	0.924	10.1	9.8	0.3	71.68
300	40	1116	1000	962	176	0.896	10.0	9.7	0.3	71.90
315	40	1115	1000	964	176	0.922	10.3	9.8	0.5	72.26
330	40	1115	1000	973	176	0.913	10.0	9.7	0.3	72.48
345	40	1110	1000	970	175	0.913	10.2	10.0	0.2	72.63
360	40	1110	1000	970	176	0.902	9.9	9.5	0.4	72.92
375	40	1110	1000	969	175	0.899	9.9	9.6	0.3	73.14
390	40	1107	1000	961	176	0.905	10.2	10.0	0.2	73.28
405	40	1106	1000	968	176	0.922	9.6	9.5	0.1	73.36
420	40	1105	1000	964	176	0.910	10.7	10.6	0.1	73.43

Table 24. Experimental data of test 9 (displacement of mineral oil by GY + GF co-injection at 176°F and 1500 psi)

Time, min	Q_{inj}-GF, ml/hr	Q_{inj}-GY, ml/hr	P_{in}, psig	P_{out}, psig	$P_{dome\text{-}out}$, psig	T, ºF	ρ, g/ml	V_P-liquid, ml	V_P-brine, ml	V_P-oil, ml	V_P-gas, L	E_R^*, %
0	0	0	797	800	1463	178	0.818	0.0	0.0	0.0	0.000	0.00
15	19	21	2187	1500	1461	161	0.821	1.3	0.0	1.3	0.000	0.95
30	19	21	2167	1500	1460	182	0.821	10.5	0.0	10.5	0.000	8.61
45	19	21	2071	1500	1461	179	0.821	10.3	0.0	10.3	0.000	16.13
60	19	21	2011	1500	1461	177	0.821	10.1	0.0	10.1	0.000	23.50
75	19	21	1943	1500	1461	177	0.824	10.3	0.0	10.3	0.000	31.02
90	19	21	1877	1500	1460	177	0.824	10.5	0.0	10.5	0.000	38.69
105	19	21	1805	1500	1460	177	0.824	10.5	0.0	10.5	0.000	46.35
120	19	21	1745	1500	1460	177	0.824	10.6	0.0	10.6	0.000	54.09
135	19	21	1701	1500	1460	176	1.073	10.5	0.0	10.5	0.000	61.75
150	19	21	1693	1500	1455	177	0.948	11.0	3.3	7.7	0.000	67.37
165	19	21	1693	1502	1455	177	0.948	10.3	9.7	0.6	0.000	67.81
180	19	21	1702	1510	1452	177	0.922	10.3	9.3	1.0	0.000	68.54
195	19	21	1690	1496	1450	176	0.936	10.4	9.4	1.0	0.000	69.27
210	19	21	1696	1508	1453	176	0.945	10.2	9.6	0.6	0.000	69.71

225	19	21	1670	1482	1455	177	0.931	11.0	10.1	0.9	0.000	70.36
240	19	21	1666	1508	1456	177	0.939	11.3	10.5	0.8	0.000	70.95
255	19	21	1642	1496	1457	177	0.945	11.5	8.5	3.0	0.000	73.14
270	19	21	1637	1502	1454	176	0.933	10.9	8.7	2.2	0.000	74.74
285	19	21	1630	1504	1454	176	0.939	11.5	9.6	1.9	0.000	76.13
300	19	21	1609	1488	1453	176	0.936	12.0	10.6	1.4	0.000	77.15
315	19	21	1611	1496	1452	176	0.950	10.6	9.7	0.9	0.776	77.81
330	19	21	1614	1502	1457	175	0.962	10.7	9.8	0.9	1.552	78.47
345	19	21	1620	1508	1456	175	0.950	10.3	9.8	0.5	1.358	78.83
360	19	21	1610	1498	1463	175	0.942	10.1	9.6	0.5	1.358	79.20
375	19	21	1618	1506	1464	175	0.945	10.3	10.1	0.2	1.552	79.34
390	19	21	1613	1502	1458	175	0.942	10.4	10.2	0.2	1.552	79.49
405	19	21	1616	1504	1458	175	0.942	10.5	10.4	0.1	1.940	79.56
420	19	21	1619	1508	1474	174	0.956	10.6	10.5	0.1	1.940	79.64

Table 25. Experimental data of test 10 (displacement of mineral oil by brine at 176°F and 1000 psi)

Time, min	Q_{inj}-brine, ml/hr	P_{in}, psig	P_{out}, psig	$P_{dome\text{-}out}$, psig	T, ºF	ρ, g/ml	V_P-liquid, ml	V_P-brine, ml	V_P-oil, ml	E_R^*, %
0	0	95	130	962	182	0.815	0.0	0.0	0.0	0.00
15	40	1638	1000	989	169	0.817	4.1	0.0	4.1	2.99
30	40	1561	1000	991	179	0.820	10.2	0.0	10.2	10.44
45	40	1522	1000	990	179	0.820	10.1	0.0	10.1	17.81
60	40	1448	1000	988	167	0.820	10.0	0.0	10.0	25.11
75	40	1393	1000	992	176	0.820	10.2	0.0	10.2	32.55
90	40	1340	1000	994	177	0.820	10.1	0.0	10.1	39.93
105	40	1288	1000	994	177	0.820	10.0	0.0	10.0	47.23
120	40	1237	1000	995	177	0.820	10.2	0.0	10.2	54.67
135	40	1210	1000	989	176	0.927	10.1	0.0	10.1	62.04
150	40	1198	1008	994	176	0.922	9.8	5.6	4.2	65.11
165	40	1182	1002	993	176	0.922	10.1	8.2	1.9	66.50
180	40	1176	1008	993	176	0.910	9.9	8.2	1.7	67.74
195	40	1158	998	983	176	0.913	9.8	8.3	1.5	68.83
210	40	1153	1002	982	175	0.916	10.1	8.8	1.3	69.78
225	40	1144	1000	977	175	0.919	10.3	9.1	1.2	70.66
240	40	1135	996	977	176	0.930	10.4	9.2	1.2	71.53

255	40	1136	1004	984	176	0.913	10.2	9.4	0.8	72.12
270	40	1131	1002	984	176	0.927	10.3	9.3	1.0	72.85
285	40	1118	992	983	176	0.919	10.5	9.7	0.8	73.43
300	40	1118	996	989	176	0.924	10.4	9.6	0.8	74.01
315	40	1127	1006	990	176	0.919	9.0	8.5	0.5	74.38
330	40	1122	1002	983	176	0.936	10.1	9.9	0.2	74.53
345	40	1123	1004	988	176	0.930	10.2	9.9	0.3	74.74
360	40	1118	1000	988	176	0.939	10.0	9.7	0.3	74.96
375	40	1114	998	983	176	0.916	10.3	10.1	0.2	75.11
390	40	1111	996	986	176	0.930	11.0	10.8	0.2	75.26
405	40	1112	998	995	176	0.939	10.4	10.3	0.1	75.33
420	40	1114	1002	990	176	0.941	10.6	10.3	0.3	75.55
435	40	1113	1002	994	176	0.961	10.0	9.7	0.3	75.77
450	40	1106	996	992	176	0.927	11.0	10.9	0.1	75.84
465	40	1109	1000	994	176	0.944	10.1	10.0	0.1	75.91

Table 26. Experimental data of test 11 (displacement of mineral oil by GY + GF slug injection at 176°F and 1000 psi)

Time, min	Q_{inj}-GF, ml/hr	Q_{inj}-GY, ml/hr	P_{in}, psig	P_{out}, psig	$P_{dome\text{-}out}$, psig	T, ºF	ρ, g/ml	V_P-liquid, ml	V_P-brine, ml	V_P-oil, ml	V_P-gas, L	E_R^*, %
0		0	18	172	972	174	0.826	0.0	0.0	0.0	0.000	0.00
15		40	1618	1000	986	177	0.829	4.4	0.0	4.4	0.000	3.21
30		40	1570	1000	986	180	0.829	9.6	0.0	9.6	0.000	10.22
45		40	1522	1000	987	174	0.831	10.0	0.0	10.0	0.000	17.52
60		40	1494	1000	988	182	0.829	9.9	0.0	9.9	0.000	24.74
75		40	1436	1000	987	177	0.829	9.8	0.0	9.8	0.000	31.90
90		40	1385	1000	987	175	0.829	10.1	0.0	10.1	0.000	39.27
105		40	1333	1000	987	174	0.831	10.1	0.0	10.1	0.000	46.64
120		40	1289	1000	989	175	0.831	10.2	0.0	10.2	0.000	54.09
135		40	1247	1000	989	175	0.831	10.1	0.0	10.1	0.000	61.46
150		40	1215	1000	989	175	1.225	10.0	0.0	10.0	0.000	68.76
165		40	1207	1000	992	176	1.081	11.0	4.5	6.5	0.000	73.50
180		40	1205	998	990	176	1.050	9.0	8.8	0.2	0.000	73.65
195		40	1194	998	991	176	0.978	10.3	10.2	0.1	0.000	73.72
210		40	1184	1000	978	176	0.984	9.8	9.7	0.1	0.000	73.76

225		40	1168	988	979	176	0.984	10.6	9.4	1.2	0.000	74.64
240		40	1176	1002	993	176	0.970	10.2	9.4	0.8	0.000	75.22
255		40	1170	1000	987	176	0.987	9.9	9.5	0.4	0.000	75.51
270		40	1170	1002	988	176	0.964	10.2	9.7	0.5	0.000	75.88
285		40	1170	1002	991	176	0.973	10.2	9.9	0.3	0.000	76.09
300		40	1170	1002	992	176	0.987	10.1	9.9	0.2	0.000	76.24
315		40	1170	1004	992	176	0.998	10.4	10.2	0.2	0.000	76.39
330		40	1165	1000	990	176	0.987	10.5	10.4	0.1	0.000	76.46
345		40	1166	1002	985	176	0.998	9.9	9.9	0.1	0.000	76.50
360		40	1164	1000	990	176	0.984	10.9	10.9	0.0	1.164	76.50
375	40		1164	1000	990	176	0.992	10.2	10.1	0.1	0.776	76.57
390	40		1161	1002	991	176	0.992	10.5	10.5	0.1	0.388	76.61
405	40		1151	998	991	176	0.992	10.5	10.5	0.1	0.000	76.64
420	40		1146	998	989	176	0.987	9.9	9.9	0.0	0.194	76.64
435	40		1142	1000	989	176	0.992	10.0	9.9	0.1	0.194	76.72
450	40		1139	1002	989	176	0.995	10.1	10.1	0.0	0.000	76.72
465	40		1129	998	989	176	0.987	10.2	10.1	0.1	0.388	76.79
480	40		1125	998	988	176	0.987	9.9	9.9	0.0	0.000	76.79
495	40		1119	998	988	176	0.973	10.1	10.1	0.0	0.000	76.79
510	40		1118	1000	988	176	0.998	9.8	9.8	0.0	0.000	76.79
525	40		1117	1000	988	176	0.922	10.4	10.4	0.0	0.000	76.79
540	40		1115	998	990	176	0.975	10.8	10.3	0.5	0.000	77.15
555	40		1115	998	991	176	0.970	11.7	11.6	0.1	0.000	77.23
570	40		1121	1002	992	176	0.964	10.4	10.4	0.0	0.000	77.23
585	40		1125	1006	991	176	0.899	10.5	10.5	0.0	0.028	77.23
600	40		1118	1000	986	176	0.924	10.7	10.5	0.2	0.028	77.37
615	40		1122	1006	992	176	0.933	10.6	10.2	0.4	0.042	77.66
630	40		1122	1006	984	176	0.922	9.7	9.5	0.2	0.042	77.81
645		40	1120	1002	984	176	1.021	9.2	8.6	0.6	0.000	78.25
660		40	1128	1006	985	176	1.021	9.6	9.6	0.0	0.000	78.25
675		40	1129	1002	985	176	1.021	10.2	10.2	0.0	0.000	78.25
690		40	1134	1006	981	176	1.021	9.5	9.5	0.0	0.000	78.25
705		40	1136	1002	981	176	1.018	10.1	10.1	0.0	0.000	78.25
720		40	1140	1004	981	176	1.021	9.5	9.5	0.0	0.028	78.25
735		40	1140	1002	990	176	1.021	6.1	6.1	0.0	0.000	78.25

750		40	1147	1004	993	176	1.018	8.7	8.7	0.0	0.028	78.25
765		40	1159	1012	1000	179	1.018	7.9	7.9	0.0	0.000	78.25
780		40	1172	1020	1005	177	1.018	7.4	7.4	0.0	0.000	78.25
795		60			1163	178	1.078	8.0	8.0	0.0	0.000	78.25

Table 27. Experimental data of test 12 (displacement of mineral oil by brine at 176°F and 500 psi)

Time, min	Q_{inj}-brine, ml/hr	P_{in}, psig	P_{out}, psig	$P_{dome-out}$, psig	T, ºF	ρ, g/ml	V_P-liquid, ml	V_P-brine, ml	V_P-oil, ml	E_R^*, %
0	0	21	272	957	180	0.814	0.0	0.0	0.0	0.00
15	40	1543	1000	985	176	0.817	4.4	0.0	4.4	3.21
30	40	1468	1000	986	174	0.820	9.8	0.0	9.8	10.36
45	40	1422	1000	987	175	0.820	9.7	0.0	9.7	17.45
60	40	1389	1000	984	182	0.817	9.9	0.0	9.9	24.67
75	40	1340	1000	986	175	0.820	9.9	0.0	9.9	31.90
90	40	1292	1000	986	176	0.820	10.1	0.0	10.1	39.27
105	40	1248	1000	986	176	0.820	10.0	0.0	10.0	46.57
120	40	1205	1000	986	176	0.820	10.1	0.0	10.1	53.94
135	40	1163	1000	986	176	0.820	10.1	0.0	10.1	61.31
150	40	1124	1000	986	176	0.820	10.0	0.0	10.0	68.61
165	40	1105	1004	989	176	0.898	12.5	0.0	12.5	77.74
180	40	1090	1012	987	176	0.920	10.2	6.0	4.2	80.80
195	40	1077	1002	986	176	0.959	9.9	7.4	2.5	82.63
210	40	1076	1006	987	176	0.962	10.1	8.5	1.6	83.80
225	40	1070	1002	982	177	0.990	10.3	9.3	1.0	84.53
240	40	1070	1002	982	176	0.990	10.0	9.7	0.3	84.74
255	40	1072	1006	982	177	0.973	10.2	10.0	0.2	84.89
270	40	1072	1008	982	177	0.990	10.2	10.1	0.1	84.96
285	40	1068	1004	978	177	0.995	10.4	10.4	0.0	84.96
300	40	1067	1004	978	177	1.001	9.4	9.4	0.0	84.96
315	40	1068	1004	979	177	1.004	8.3	8.3	0.0	84.96

Table 28. Experimental data of test 13 (displacement of mineral oil by GY + GF co-injection at 176°F and 500 psi)

Time, min	Q_{inj}-GF, ml/hr	Q_{inj}-GY, ml/hr	P_{in}, psig	P_{out}, psig	$P_{dome-out}$, psig	T, ºF	ρ, g/ml	V_P-liquid, ml	V_P-brine, ml	V_P-oil, ml	V_P-gas, L	E_R^*, %
0	0	0	6	6	483	179	0.040	0.0	0.0	0.0	0.000	0.00
15	19	21	563	6	482	170	0.812	0.0	0.0	0.0	0.000	0.00
30	19	21	1009	500	492	177	0.817	4.4	0.0	4.4	0.000	3.21
45	19	21	984	500	492	179	0.817	10.3	0.0	10.3	0.000	10.73
60	19	21	964	500	492	178	0.817	10.6	0.0	10.6	0.000	18.47
75	19	21	901	500	491	176	0.817	11.0	0.0	11.0	0.000	26.50
90	19	21	863	500	492	176	0.817	11.0	0.0	11.0	0.000	34.53
105	19	21	818	500	492	176	0.817	11.3	0.0	11.3	0.000	42.77
120	19	21	777	500	492	176	0.817	11.7	0.0	11.7	0.000	51.31
135	19	21	759	492	492	177	1.046	12.8	0.0	12.8	0.000	60.66
150	19	21	757	502	499	177	0.973	9.7	6.2	3.5	0.000	63.21
165	19	21	760	506	500	177	0.973	11.3	11.0	0.3	0.000	63.43
180	19	21	746	502	494	177	0.950	12.0	11.8	0.2	0.000	63.58
195	19	21	741	500	492	177	0.967	11.8	9.3	2.5	0.000	65.40
210	19	21	743	502	492	176	0.956	12.3	10.3	2.0	0.000	66.86
225	19	21	747	500	492	176	0.973	13.4	11.8	1.6	0.000	68.03
240	19	21	750	500	492	176	0.970	15.2	13.9	1.3	0.000	68.98
255	19	21	761	500	492	177	0.697	12.5	10.8	1.7	0.388	70.22
270	19	21	770	500	492	176	0.884	10.9	10.2	0.7	0.000	70.73
285	19	21	777	498	494	176	0.848	11.1	10.9	0.2	0.194	70.88
300	19	21	785	504	494	176	0.599	10.1	9.9	0.2	0.000	71.02
315	19	21	797	502	493	176	0.732	10.6	10.4	0.2	0.582	71.17
330	19	21	803	502	493	176	0.572	10.7	10.6	0.1	1.940	71.24
345	19	21	807	502	493	176	0.984	10.5	10.4	0.1	1.940	71.31
360	19	21	815	502	490	176	0.817	9.5	9.4	0.1	1.552	71.39
375	19	21	827	500	490	176	1.021	10.7	10.6	0.1	1.552	71.46
390	19	21	820	502	491	176	0.677	11.2	11.2	0.0	2.328	71.46
405	19	21	815	498	496	176	0.776	10.0	10.0	0.0	2.522	71.46
420	19	21	814	502	490	176	0.978	10.7	10.4	0.3	2.328	71.68

435	19	21	810	500	491	176	0.572	10.6	10.3	0.3	2.134	71.90
450	19	21	806	500	490	176	0.839	10.4	10.0	0.4	2.716	72.19
465	19	21	800	498	490	176	0.817	10.8	10.6	0.2	2.328	72.34
480	19	21	796	500	490	176	0.735	10.2	9.8	0.4	2.716	72.63
495	19	21	792	502	490	176	0.637	10.6	10.3	0.3	2.328	72.85
510	19	21	792	502	491	176	0.848	10.4	10.3	0.1	2.329	72.92
525	19	21	790	496	490	176	0.686	10.9	10.7	0.2	2.134	73.07
540	19	21	787	500	496	176	0.798	10.1	9.8	0.3	2.134	73.28
555	19	21	791	502	491	176	0.837	10.2	9.9	0.3	1.940	73.50
570	19	21	787	502	491	176	0.776	10.5	10.4	0.1	2.134	73.58
585	19	21	788	502	491	176	0.738	10.4	10.3	0.1	0.970	73.65

Table 29. Experimental data of test 14 (displacement of mineral oil by GY + GF + surfactant co-injection at 176°F and 500 psi)

Time, min	Q_{inj}-GF, ml/hr	Q_{inj}-GY, ml/hr	P_{in}, psig	P_{out}, psig	$P_{dome-out}$, psig	T, ºF	ρ, g/ml	V_P-liquid, ml	V_P-brine, ml	V_P-oil, ml	V_P-gas, L	E_R^*, %
0	0	0	9	32	484	174	0.809	0.0	0.0	0.0	0.000	0.00
15	19	21	913	500	491	176	0.812	3.6	0.0	3.6	0.000	2.63
30	19	21	1055	500	492	174	0.812	7.5	0.0	7.5	0.000	8.10
45	19	21	992	500	493	175	0.812	9.1	0.0	9.1	0.000	14.74
60	19	21	937	500	493	175	0.812	10.4	0.0	10.4	0.000	22.34
75	19	21	898	500	492	176	0.812	10.5	0.0	10.5	0.000	30.00
90	19	21	864	500	492	176	0.812	10.4	0.0	10.4	0.000	37.59
105	19	21	835	500	492	176	0.812	10.8	0.0	10.8	0.000	45.47
120	19	21	819	500	493	176	0.812	10.8	0.0	10.8	0.000	53.36
135	19	21	795	500	492	176	0.812	11.2	0.0	11.2	0.000	61.53
150	19	21	775	500	492	176	1.054	11.2	0.0	11.2	0.000	69.71
165	19	21	795	500	490	176	0.973	13.5	8.2	5.3	0.000	73.58
180	19	21	809	500	490	176	0.976	11.1	10.3	0.8	0.000	74.16
195	19	21	840	498	490	177	1.012	10.3	9.7	0.6	0.000	74.60
210	19	21	846	500	490	176	1.012	11.3	11.1	0.2	0.000	74.74
225	19	21	869	500	490	176	1.012	11.3	11.0	0.3	0.000	74.96
240	19	21	884	500	490	176	1.012	11.5	11.3	0.2	0.000	75.11
255	19	21	902	500	490	176	1.012	11.2	11.0	0.2	0.000	75.26
270	19	21	916	500	490	176	1.012	11.2	11.1	0.1	0.000	75.33

285	19	21	927	500	490	176	1.009	11.1	11.0	0.1	0.000	75.40
300	19	21	940	500	490	176	1.009	11.2	11.0	0.2	0.000	75.55
315	19	21	955	500	491	176	1.012	11.3	11.2	0.1	0.000	75.62
330	19	21	970	500	491	176	1.015	12.0	11.9	0.1	0.000	75.69
345	19	21	984	500	492	176	1.015	11.2	11.1	0.1	0.582	75.77
360	19	21	1000	500	493	176	1.004	0.0	0.0	0.0	0.970	75.77
375	19	21	1016	502	493	176	1.015	0.0	0.0	0.0	1.164	75.77
390	19	21	1032	502	493	176	1.015	9.9	9.8	0.1	1.164	75.84
405	19	21	1048	496	492	176	1.015	10.3	10.2	0.1	1.164	75.91
420	19	21	1063	500	496	176	1.015	10.1	10.0	0.1	1.164	75.99
435	19	21	1080	500	494	176	1.015	9.9	9.8	0.1	1.164	76.06
450	19	21	1096	500	495	176	1.015	9.8	9.7	0.1	0.970	76.13
465	19	21	1113	502	495	176	1.015	9.9	9.8	0.1	0.970	76.20
480	19	21	1127	500	494	176	1.015	9.5	9.4	0.1	0.970	76.28
495	19	21	1143	500	495	176	1.015	10.0	9.9	0.1	1.164	76.35
510	19	21	1159	502	495	176	1.015	9.7	9.6	0.1	1.164	76.42
525	19	21	1174	502	496	176	1.015	9.6	9.5	0.1	1.164	76.50
540	19	21	1188	500	490	176	1.015	9.3	9.3	0.0	1.164	76.50
555	19	21	1201	500	496	176	1.018	9.7	9.6	0.1	1.552	76.57
570	19	21	1215	500	495	176	1.018	9.6	9.5	0.1	1.164	76.64
680	19	21	1268	500	495	176	1.012	83.0	83.0	0.0		76.64
690	19	21	1271	500	495	176	1.018	7.0	7.0	0.0		76.64
705	19	21	1277	502	496	176	0.973	10.0	10.0	0.0		76.64

Table 30. Experimental data of test 15 (displacement of mineral oil by brine at 176°F and 500 psi)

Time, min	Q_{inj}-brine, ml/hr	P_{in}, psig	P_{out}, psig	$P_{dome\text{-}out}$, psig	T, ºF	ρ, g/ml	V_P-liquid, ml	V_P-brine, ml	V_P-oil, ml	E_R^*, %
0	0	70	49	483	176	0.812	0.0	0.0	0.0	0.00
15	40	1015	500	489	176	0.814	5.0	0.0	5.0	3.65
30	40	983	500	489	183	0.812	10.0	0.0	10.0	10.95
45	40	932	500	489	174	0.812	10.0	0.0	10.0	18.25
60	40	885	500	492	180	0.812	10.1	0.0	10.1	25.62
75	40	848	500	492	177	0.812	9.8	0.0	9.8	32.77
90	40	808	500	492	176	0.812	10.1	0.0	10.1	40.15
105	40	764	500	492	175	0.812	10.0	0.0	10.0	47.45

120	40	719	500	492	176	0.814	10.1	0.0	10.1	54.82
135	40	698	500	492	177	0.976	10.0	0.0	10.0	62.12
150	40	684	502	492	177	0.906	12.0	4.8	7.2	67.37
165	40	668	500	489	177	0.981	8.6	7.1	1.5	68.47
180	40	653	502	489	177	0.978	10.1	8.0	2.1	70.00
195	40	642	500	490	177	0.959	10.1	7.8	2.3	71.68
210	40	633	500	493	177	0.987	10.3	8.7	1.6	72.85
225	40	631	502	493	177	1.004	10.5	9.4	1.1	73.65
240	40	621	500	492	177	0.976	11.5	9.9	1.6	74.82
255	40	614	496	494	177	1.001	10.7	9.7	1.0	75.55
270	40	616	498	493	177	1.009	10.6	9.5	1.1	76.35
285	40	611	498	493	177	1.009	10.6	9.7	0.9	77.01
300	40	613	502	494	176	1.012	7.5	6.8	0.7	77.52
315	40	613	502	494	180	1.012	10.0	9.6	0.4	77.81
330	40	615	502	495	177	1.009	10.1	9.8	0.3	78.03
345	40	611	500	494	175	1.012	10.0	9.7	0.3	78.25
360	40	614	502	495	176	1.012	9.6	9.3	0.3	78.47
375	40	613	502	494	176	1.012	10.2	10.1	0.1	78.54

Table 31. Experimental data of test 16A (displacement of mineral oil by brine at 176°F and 500 psi)

Time, min	Q_{inj}-brine, ml/hr	P_{in}, psig	P_{out}, psig	$P_{dome-out}$, psig	T, ºF	ρ, g/ml	V_P-liquid, ml	V_P-brine, ml	V_P-oil, ml	E_R^*, %
0	0	63	54	485	181	0.809	0.0	0.0	0.0	0.00
15	40	1065	500	489	181	0.812	5.1	0.0	5.1	3.72
30	40	1022	500	489	174	0.812	10.0	0.0	10.0	11.02
45	40	972	500	489	174	0.812	10.2	0.0	10.2	18.47
60	40	925	500	489	175	0.812	10.2	0.0	10.2	25.91
75	40	879	500	489	175	0.812	9.7	0.0	9.7	32.99
90	40	835	500	489	175	0.812	10.0	0.0	10.0	40.29
105	40	789	500	489	175	0.812	10.1	0.0	10.1	47.66
120	40	745	500	489	175	0.812	10.1	0.0	10.1	55.04
135	40	722	500	489	175	0.945	9.9	0.0	9.9	62.26
150	40	707	500	488	175	0.948	9.9	5.6	4.3	65.40
165	40	687	500	487	176	0.964	10.2	8.7	1.5	66.50
180	40	676	500	487	176	0.978	10.0	7.7	2.3	68.18

195	40	667	500	487	176	0.978	10.3	9.0	1.3	69.12
210	40	658	500	487	176	0.990	10.1	9.0	1.1	69.93
225	40	652	500	487	177	0.990	10.4	9.3	1.1	70.73
240	40	647	500	487	176	0.984	10.3	9.2	1.1	71.53
255	40	641	500	486	176	1.001	10.2	9.2	1.0	72.26
270	40	635	500	485	176	1.001	10.3	9.3	1.0	72.99
285	40	633	500	486	176	1.001	10.2	9.3	0.9	73.65
300	40	631	500	486	176	0.953	9.9	9.1	0.8	74.23
315	40	628	500	486	176	1.001	10.1	9.7	0.4	74.53
330	40	627	500	487	176	1.001	10.0	9.7	0.3	74.74
345	40	626	500	486	176	1.001	10.0	9.5	0.5	75.11
360	40	625	500	487	176	0.970	9.6	9.3	0.3	75.33
375	40	623	500	486	176	1.001	10.2	10.1	0.1	75.40

Table 32. Experimental data of test 16B (displacement of mineral oil by GY + GF co-injection at 176°F and 500 psi)

Time, min	Q_{inj}-GF, ml/hr	Q_{inj}-GY, ml/hr	P_{in}, psig	P_{out}, psig	$P_{dome-out}$, psig	T, ºF	ρ, g/ml	V_P-liquid, ml	V_P-brine, ml	V_P-oil, ml	V_P-gas, L	E_R^*, %
0	19	21	627	500	487	176	1.004	4.6	4.4	0.2	0.000	75.55
15	19	21	624	500	488	173	1.001	10.4	10.3	0.1	0.000	75.62
30	19	21	639	500	488	174	0.981	11.2	11.0	0.2	0.000	75.77
45	19	21	641	500	488	175	1.001	11.5	11.2	0.3	0.000	75.99
60	19	21	632	500	489	175	1.001	10.9	10.6	0.3	0.000	76.20
75	19	21	640	500	489	176	1.001	11.0	10.7	0.3	0.000	76.42
90	19	21	638	500	489	176	1.001	11.1	10.9	0.2	0.000	76.57
105	19	21	641	500	489	175	1.001	11.0	10.7	0.3	0.000	76.79
120	19	21	645	500	489	175	1.001	11.2	11.0	0.2	0.000	76.93
135	19	21	652	500	490	176	0.995	11.1	10.8	0.3	0.000	77.15
150	19	21	656	500	490	176	1.015	11.0	11.0	0.1	0.000	77.19
165	19	21	659	500	490	176	0.984	11.0	11.0	0.0	0.000	77.19
180	19	21	664	500	490	176	1.004	11.2	11.1	0.1	0.000	77.26
195	19	21	667	500	490	176	1.004	11.7	11.7	0.0	0.000	77.26
210	19	21	670	500	490	176	0.962	15.9	15.9	0.0	0.000	77.26
225	19	21	674	500	489	176	0.945	13.3	11.9	1.4	0.000	78.28
240	19	21	673	500	489	176	0.615	10.9	10.8	0.1	0.000	78.36
255	19	21	675	500	489	176	0.499	11.0	11.0	0.0	0.000	78.36

270	19	21	675	500	489	176	0.569	8.5	8.5	0.0	0.000	78.36
285	19	21	677	500	489	176	0.596	10.4	10.4	0.0	1.164	78.36
300	19	21	678	500	489	176	0.564	10.3	10.3	0.0	2.328	78.36
315	19	21	678	500	489	176	0.669	10.4	10.4	0.0	0.388	78.36
330	19	21	677	500	489	176	0.718	10.3	10.3	0.0	0.000	78.36

Table 33. Experimental data of test 16C (displacement of mineral oil by GY + GF + surfactant co-injection at 176°F and 500 psi)

Time, min	Q_{inj}-GF, ml/hr	Q_{inj}-GY, ml/hr	P_{in}, psig	P_{out}, psig	$P_{dome-out}$, psig	T, ºF	ρ, g/ml	V_P-liquid, ml	V_P-brine, ml	V_P-oil, ml	V_P-gas, L	E_R^*, %
0	19	21	572	500	489	172	0.454	0.3	0.3	0.0	0.000	78.36
15	19	21	636	500	491	174	0.518	3.7	3.6	0.1	0.000	78.43
30	19	21	672	500	490	175	0.911	7.5	7.5	0.0	0.000	78.43
45	19	21	678	500	490	176	0.931	11.4	11.4	0.0	0.000	78.43
60	19	21	673	500	490	175	0.973	11.6	11.6	0.0	0.388	78.43
75	19	21	682	500	490	175	1.012	10.9	10.9	0.0	0.000	78.43
90	19	21	692	500	489	175	0.959	10.8	10.8	0.0	0.000	78.43
105	19	21	690	500	489	175	0.936	11.5	11.5	0.0	0.000	78.43
120	19	21	699	500	489	175	0.770	11.1	11.1	0.0	0.000	78.43
135	19	21	693	500	489	175	0.688	10.8	10.7	0.1	0.000	78.47
150	19	21	700	500	488	177	1.021	10.3	10.2	0.1	0.000	78.50
165	19	21	688	500	487	178	0.699	11.6	11.5	0.0	0.000	78.54
180	19	21	701	500	487	178	0.806	8.9	8.8	0.1	0.000	78.58
195	19	21	704	500	488	177	1.018	10.9	10.9	0.0	0.000	78.58
210	19	21	707	500	488	177	0.716	10.3	10.3	0.0	0.000	78.61
225	19	21	713	500	488	177	0.936	10.7	10.6	0.1	0.000	78.65
240	19	21	705	500	487	176	0.738	11.2	11.2	0.0	0.000	78.65
255	19	21	715	500	487	177	0.928	10.3	10.3	0.1	0.000	78.69
270	19	21	712	500	487	176	0.642	11.4	11.4	0.0	0.000	78.72
285	19	21	716	500	486	177	0.621	9.6	9.5	0.1	0.388	78.76
300	19	21	721	500	488	176	0.931	10.7	10.6	0.0	0.000	78.80
315	19	21	720	500	488	176	0.853	10.4	10.3	0.0	0.000	78.83
330	19	21	725	500	487	176	0.881	10.3	10.3	0.0	0.000	78.87
345	19	21	727	500	487	176	0.850	10.0	9.9	0.1	0.776	78.91
360	19	21	731	500	487	176	0.790	10.3	10.2	0.0	1.940	78.94
375	19	21	730	500	486	176	0.697	10.9	10.8	0.1	1.940	78.98

390	19	21	732	500	487	176	0.839	9.8	9.7	0.1	1.164	79.05
405	19	21	733	500	487	176	0.748	11.1	11.0	0.1	1.940	79.12

Table 34. Experimental data of test 17 (displacement of mineral oil by CO_2 at 176°F and 1000 psi)

Time, min	Injected CO_2[1], PV	P_{CO2}, psig	P_{in}, psig	P_{out}, psig	$P_{dome-in}$, psig	$P_{dome-out}$, psig	T, ºF	ρ, g/ml	V_P-oil, ml	V_P-gas, L	E_R^*, %
0	0.00	1583	186	196	1969	979	170	0.812	0.0	0.000	0.00
0	0.00	2082	1272	986	2007	982	176	0.817	0.0	0.000	0.00
15	0.27	2075	1156	1002	2008	979	174	0.817	4.0	0.000	2.92
30	0.54	2085	1147	1002	2009	979	174	0.817	2.4	0.000	4.67
45	1.07	2099	1188	1000	2007	978	174	0.817	3.0	0.000	6.86
60	1.48	2118	1207	1002	2009	979	177	0.817	3.9	0.000	9.71
75	1.74	2127	1207	1002	2008	979	179	0.817	4.9	0.000	13.28
90	1.91	2131	1174	1002	2007	980	177	0.817	5.7	0.000	17.45
105	2.07	2132	1126	1002	2008	980	176	0.817	6.4	0.000	22.12
120	2.23	2134	1053	1002	2009	980	175	0.817	9.2	0.000	28.83
135	2.39	2136	1038	1002	2010	980	176	0.224	10.7	0.793	36.64
150	2.55	2138	1040	1002	2011	979	177	0.203	1.3	1.954	37.59
165	2.71	2142	1041	1004	2010	979	179	0.216	1.0	3.115	38.32
195	3.03	2148	1032	1004	2008	976	177	0.182	2.1	5.295	39.85
225	3.36	2153	1032	1004	2008	976	175	0.209	1.6	7.419	41.02
255	3.68	2159	1033	1004	2009	976	178	0.193	1.4	9.543	42.04
285	4.00	2168	1027	1000	2010	972	178	0.280	1.5	11.751	43.14
345	4.64	2178	1026	998	2009	971	177	0.195	2.4	16.226	44.89
405	5.29	2193	1026	1000	2009	972	176	0.206	2.2	20.870	46.50
465	5.93	2204	1026	1004	2010	972	179	0.211	2.0	24.579	47.96
525	6.58	2215	1025	1000	2008	972	176	0.201	1.9	29.563	49.34
645	7.87	2225	1024	1000	2010	972	178	0.188	3.5	42.957	51.90
765	9.15	2240	1024	1000	2010	972	179	0.203	2.8	53.575	53.94
1170	13.50	2083	1008	1000	2005	971	177	0.190	10.6	108.284	61.68

[1] Accumulative volume of injected CO_2 in slim-tube thermobaric conditions

Table 35. Experimental data of test 18 (displacement of mineral oil by CO_2 at 176°F and 2000 psi)

Time, min	Injected CO_2[1], PV	P_{CO2}, psig	P_{in}, psig	P_{out}, psig	$P_{dome\text{-}in}$, psig	$P_{dome\text{-}out}$, psig	T, ºF	ρ, g/ml	V_P-oil, ml	V_P-gas, L	E_R^*, %
0	0.00	2354	22	18	2870	1978	170	0.806	0.0	0.000	0.00
0	0.00	2714	2464	2040	2900	2005	180	0.821	0.0	0.000	4.96
15	0.14	2760	2770	2008	2900	1988	174	0.821	4.0	0.000	11.09
30	0.23	2741	2195	1996	2900	1982	174	0.821	2.4	0.000	11.24
45	0.79	2799	2011	1974	2900	1970	179	0.821	3.0	0.000	20.95
60	0.93	2746	2484	1982	2900	1982	179	0.821	3.9	0.000	23.28
75	1.15	2779	2002	1983	2900	1983	178	0.821	4.9	0.000	27.52
90	1.32	2750	2759	2014	2900	1985	175	0.821	5.7	0.000	39.34
105	1.46	2766	1992	1992	2900	1978	176	0.821	6.4	0.000	39.34
120	1.60	2787	1927	1926	2900	1958	177	0.821	9.2	0.000	40.88
135	1.74	2796	2061	2006	2900	1982	179	0.821	10.7	0.000	50.80
150	1.88	2794	2040	2004	2900	1975	176	0.448	1.3	0.934	51.90
165	2.02	2792	2033	2006	2910	1978	174	0.396	1.0	3.568	52.63
180	2.17	2790	2024	2000	2910	1976	175	0.410	2.1	6.230	53.43
195	2.31	2793	2015	2000	2910	1976	179	0.391	1.6	8.637	54.73
225	2.59	2793	2025	1998	2910	1975	176	0.375	1.4	14.385	55.82
255	2.87	2792	2016	2000	2900	1979	179	0.424	1.5	19.482	57.65
315	3.44	2791	2022	2000	2910	1981	174	0.410	2.4	31.205	59.26
375	4.01	2792	2024	2002	2920	1981	175	0.402	2.2	42.560	60.64
435	4.57	2794	2022	2000	2915	1980	176	0.361	2.0	52.726	61.88
495	5.14	2794	2019	2000	2915	1979	179	0.388	1.9	64.308	63.71
615	6.27	2794	2018	2002	2915	1980	179	0.369	3.5	86.819	65.90
795	7.97	2795	2014	2002	2910	1980	179	0.421	2.8	121.451	69.84

[1] Accumulative volume of injected CO_2 in slim-tube thermobaric conditions

Table 36. Experimental data of test 19 (displacement of mineral oil by CO_2 at 176°F and 2000 psi)

Time, min	Injected CO_2[1], PV	P_{CO2}, psig	P_{in}, psig	P_{out}, psig	$P_{dome\text{-}in}$, psig	$P_{dome\text{-}out}$, psig	T, ºF	ρ, g/ml	V_P-oil, ml	V_P-gas, L	E_R^*, %
0	0.00	1829	156	152	2870	1984	173	0.806	0.0	0.000	0.00
0	0.00	2823	2832	2002	2950	1986	176	0.821	0.0	0.000	0.00
15	0.14	2798	2805	2000	2950	1979	176	0.821	12.6	0.057	9.20
30	0.25	2759	2764	2006	2910	1980	176	0.821	14.8	0.057	20.00
45	0.37	2758	2163	1998	2900	1978	175	0.821	12.9	0.057	29.42
60	0.48	2770	2060	2000	2900	1978	176	0.821	5.0	0.085	33.07
75	0.62	2784	2054	1998	2910	1979	176	0.821	4.5	0.085	36.35
90	0.76	2784	2044	2006	2910	1981	176	0.464	16.2	0.085	48.18
105	0.91	2784	2036	2002	2910	1980	176	0.388	4.0	3.200	51.09
120	1.05	2783	2032	2000	2910	1979	176	0.421	1.6	6.654	52.26
150	1.33	2781	2030	2000	2910	1978	176	0.415	2.8	13.932	54.31
180	1.61	2780	2025	1998	2910	1977	176	0.407	2.1	20.841	55.84
240	2.18	2781	2021	1998	2910	1984	176	0.377	3.8	31.573	58.61
300	2.75	2780	2020	1998	2910	1979	176	0.391	3.2	46.581	60.95
360	3.31	2781	2028	2004	2910	1982	176	0.366	2.4	61.533	62.70
420	3.88	2781	2023	2002	2910	1978	176	0.415	2.4	73.879	64.45
480	4.44	2781	2011	1990	2910	1980	176	0.364	2.0	89.595	65.91
600	5.58	2780	2020	2002	2910	1983	176	0.402	3.2	121.055	68.25
720	6.71	2779	2019	2002	2910	1983	176	0.366	2.5	140.083	70.07
1012	9.46	2562	1669	1668	2900	1962	176	0.278	5.1	212.405	73.80

Table 37. Experimental data of test 20 (displacement of mineral oil by CO_2 at 176°F and 2000 psi)

Time, min	Injected CO_2[2], PV	P_{CO2}, psig	P_{in}, psig	P_{out}, psig	$P_{dome\text{-}in}$, psig	$P_{dome\text{-}out}$, psig	T, ºF	ρ, g/ml	V_P-oil, ml	V_P-gas, L	E_R^*, %
0	0.00	2468	534	534	4100	2968	173	0.806	0.0	0.000	0.00
0	0.00	3956	3961	3066	4100	3008	151	0.823	0.0	0.000	0.00
15	0.11	3912	3902	3042	4100	2987	181	0.820	12.2	0.000	8.91
30	0.21	3904	3301	3038	4100	2986	176	0.820	10.7	0.000	16.72
45	0.32	3950	3386	3012	4100	2955	175	0.823	4.4	0.000	19.93

[1] Accumulative volume of injected CO_2 in slim-tube thermobaric conditions

[2] Accumulative volume of injected CO_2 in slim-tube thermobaric conditions

60	0.43	3939	3461	3010	4100	2957	174	0.823	10.4	0.000	27.52
75	0.53	3933	3277	3002	4100	2949	175	0.823	11.5	0.000	35.91
90	0.64	3931	3042	2996	4100	2948	175	0.823	10.4	0.000	43.50
105	0.75	3922	2980	2982	4100	2945	176	0.823	1.0	0.000	44.23
120	0.85	3963	3060	3004	4100	2951	176	0.823	3.9	0.000	47.08
135	0.96	3962	3034	3004	4100	2951	176	0.652	15.8	0.850	58.61
150	1.07	3960	3025	2996	4100	2948	176	0.633	2.2	5.493	60.22
165	1.17	3958	3025	3000	4100	2951	175	0.630	1.6	9.430	61.39
195	1.39	3957	3027	3002	4100	2951	175	0.624	2.9	17.641	63.50
225	1.60	3955	3022	3000	4100	2948	175	0.624	2.6	27.297	65.40
285	2.02	3962	3019	2998	4100	2947	175	0.619	4.2	45.732	68.47
345	2.45	3958	3015	2998	4100	2945	176	0.616	3.6	65.922	71.09
405	2.88	3964	3007	2992	4100	2945	176	0.594	2.6	78.862	72.99
465	3.30	3960	3008	2992	4100	2944	175	0.608	2.5	99.477	74.82
585	4.16	3959	3006	2992	4100	2944	176	0.610	3.9	140.395	77.66
705	5.01	3960	3004	2992	4100	2943	175	0.613	3.2	152.628	80.00
825	5.86	3959	3010	3002	4100	2950	176	0.613	3.1	194.961	82.26
1108	7.87	3645	2838	2840	4100	2906	175	0.733	5.2	289.426	86.06

APPENDIX D
EXPERIMENTAL SETUP PICTURES

Figure 85. Image of Slim-tube

Figure 86. Image of temperature bath exterior

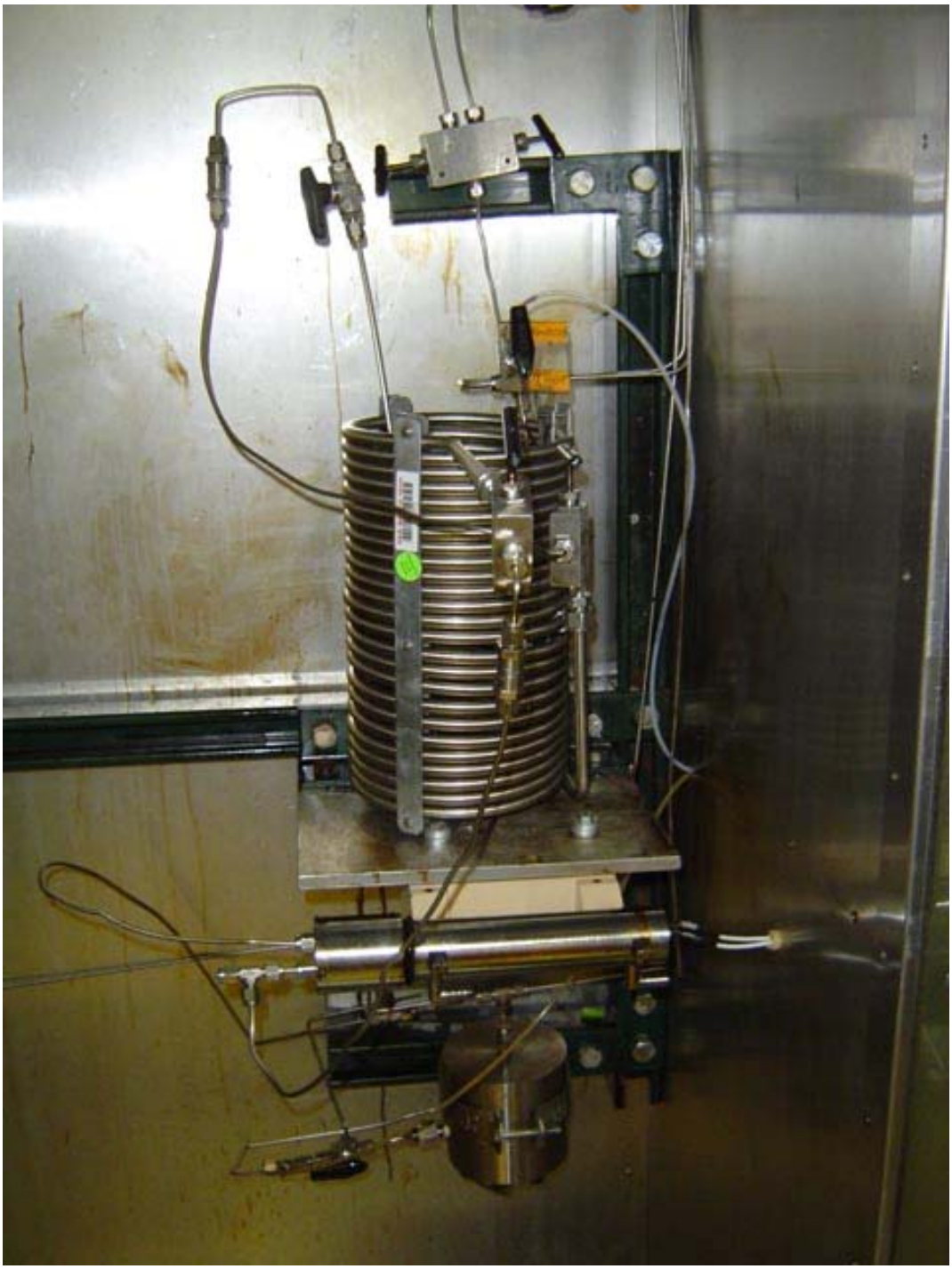

Figure 87. Image of part of experimental setup A inside the temperature bath (from top to bottom: Slim-tube, densitometer and outlet BPR)

Figure 88. Image of part of experimental setup B inside the temperature bath

APPENDIX E. CO_2 Pressure and Volume Measurements.

Table 38. CO_2 pressure data

Total GF injected ml.	Experimental CO_2 pressure (psia)	Theoretical CO_2 pressure (psia) *	% Prod. CO2 dissolved in Brine	Salt molarity
0	0	0.00	0.00	0.00

* Ideal mixing, 100% conversion, no solubility of CO_2 in brine assumed

3.98	0	4.27	4.47	0.12
9.01	0	9.98	2.51	0.27
14.04	0	15.87	1.71	0.39
19.04	1	21.76	1.77	0.51
24.01	1	27.86	1.48	0.61
29.03	9	33.23	4.01	0.70
34.01	9	39.59	3.59	0.78
39.01	9	46.13	3.27	0.86
44.06	14	52.25	4.23	0.93
49	16	58.75	4.41	1.00
54.03	23	64.78	5.65	1.06
59.55	30	71.68	6.66	1.12
64	39	76.72	8.14	1.17
69	48	82.69	9.41	1.22
74.02	57	88.67	10.69	1.27
78.45	67	93.89	11.87	1.30
0	0	0.00	0.00	0.00
5.02	0	5.61	0.72	0.16
10.01	0	11.36	0.38	0.29
15	2	17.06	1.35	0.41
20.01	2	23.09	1.06	0.53
25	3	29.09	1.43	0.63
29.99	4	35.28	1.57	0.72
35.03	6	41.56	1.97	0.80
40.02	8	47.92	2.31	0.88
45.04	8	54.72	2.14	0.95
50.02	10	61.36	2.45	1.01
58.61	14	73.09	3.05	1.11
63.99	22	79.78	4.46	1.17
69.02	30	86.13	5.68	1.22
74.02	39	92.33	7.00	1.27
78.45	48	97.71	8.29	1.30
0	0	0.00	0.00	0.00
5.04	1	5.08	9.53	0.13
10.01	1	10.71	5.04	0.24
14.97	1	16.47	3.53	0.35
20.02	1	22.49	2.76	0.45
25.05	2	28.45	2.93	0.54
29.98	2	34.63	2.55	0.62
34.99	2	41.06	2.27	0.69
40.11	2	47.82	2.06	0.76
44.99	3	54.20	2.31	0.83
50.08	4	61.04	2.53	0.89
55.03	5	67.84	2.74	0.95
60.04	12	73.35	4.97	1.00
65.01	20	78.55	7.33	1.05
70.14	30	83.52	10.01	1.10
75.01	40	88.17	12.42	1.14

80	49	93.29	14.39	1.18
80.62	50	93.94	14.62	1.19
84.99	59	98.08	16.54	1.22
90.04	69	103.17	18.40	1.26
95.91	80	109.23	20.36	1.30

Table 39. CO_2 pressure data.

Total GY injected (ml.)	**Experimental CO_2 pressure (psia)**	**Theoretical CO_2 pressure (psia)** *	**% Prod. CO2 dissolved in Brine**	**Salt molarity**
0	4	4.00	0.00	0.00
5.01	9	8.95	11.19	0.16
10.04	14	14.12	10.42	0.30
15.04	19	19.36	10.29	0.42
20.04	25	24.62	10.69	0.54
25.04	30	30.10	10.61	0.64
30.04	36	35.51	11.16	0.73
35.03	42	41.02	11.58	0.81
40.02	47	46.74	11.77	0.88
45.05	53	52.48	12.23	0.95
50.04	59	58.32	12.60	1.01
55.04	65	64.27	12.99	1.07
60.05	71	70.33	13.39	1.13
65.03	78	76.30	13.99	1.18
70.02	84	82.62	14.31	1.22
74.84	83	89.89	13.58	1.26
77.34	80	94.15	12.83	1.28
79.87	77	98.54	12.11	1.30
0	4	4.00	0.00	0.00
5.06	9	8.88	12.48	0.16
10.07	13	14.11	10.03	0.30
15.08	19	20.40	3.69	0.43
20.05	25	24.32	11.32	0.54
25.07	30	29.66	11.50	0.64
30.06	36	34.99	11.95	0.73
35.12	41	40.53	12.28	0.81
40.01	47	45.88	12.81	0.88
45.13	53	51.65	13.19	0.95
50.07	58	57.35	13.52	1.01
55.09	64	63.17	13.96	1.07
60.05	70	69.01	14.42	1.13
65.1	76	75.14	14.78	1.18
70.07	82	81.18	15.26	1.22
74.99	79	88.86	14.13	1.26
79.99	74	97.28	12.74	1.31

* Ideal mixing, 100% conversion, no solubility of CO_2 in brine assumed

0	0	0.00	0.00	0.00
5.06	4	5.04	10.37	0.16
10.05	8	10.30	8.90	0.30
15.05	13	15.55	9.21	0.43
20.1	19	20.84	10.01	0.54
25.03	24	26.20	10.24	0.64
30.03	29	31.66	10.69	0.73
35.07	35	37.19	11.28	0.81
40.08	41	42.82	11.75	0.88
45.01	46	48.49	12.11	0.95
50.08	52	54.37	12.59	1.02
55.06	58	60.22	13.09	1.07
60.01	64	66.12	13.59	1.13
68.15	74	76.12	14.32	1.21
69.56	75	77.96	14.36	1.22
70.18	76	78.67	14.48	1.23
74.6	76	85.27	13.87	1.26
79.58	73	93.34	12.83	1.30
0	0	0.00	0.00	0.00
5.03	3	5.20	6.95	0.16
10.04	9	10.29	8.91	0.30
15.02	13	15.61	8.69	0.42
20.07	18	21.00	9.19	0.54
25.05	24	26.32	9.88	0.64
30.04	30	31.67	10.69	0.73
35.05	35	37.28	11.01	0.81
40.06	41	42.92	11.50	0.88
45.04	46	48.66	11.87	0.95
50.05	52	54.47	12.37	1.02
55.03	58	60.33	12.88	1.07
60.06	64	66.34	13.38	1.13
65.05	71	72.32	13.99	1.18
70.04	77	78.47	14.49	1.22
75.11	77	86.02	13.82	1.27
79.58	74	93.34	12.83	1.30
0	0	0.00	0.00	0.00
5.02	4	4.92	11.84	0.16
10.06	7	10.31	8.89	0.30
14.99	13	15.40	9.76	0.42
20.01	18	20.74	10.05	0.54
25.01	24	26.03	10.78	0.64
29.98	30	31.39	11.32	0.73
35.02	35	37.03	11.57	0.81
40.08	42	42.53	12.39	0.88
45.07	47	48.33	12.58	0.95
49.99	53	54.00	13.05	1.02
55.02	58	60.05	13.31	1.07
60.04	64	66.04	13.79	1.13

65.01	70	72.13	14.19	1.18
70.13	75	78.64	14.48	1.22
75	76	85.71	14.01	1.27
79.82	68	94.41	12.20	1.31
0	0	0.00	0.00	0.00
5.01	5	5.10	8.37	0.16
9.99	10	10.23	8.95	0.30
15.02	14	15.60	8.69	0.42
19.99	20	20.80	9.64	0.54
24.96	25	26.21	9.91	0.64
29.97	31	31.58	10.70	0.73
35.01	36	37.22	11.02	0.81
39.98	40	43.05	11.00	0.88
44.98	46	48.70	11.64	0.95
49.98	52	54.50	12.16	1.01
55.06	58	60.49	12.67	1.07
60.11	63	66.70	12.97	1.13
64.96	70	72.49	13.61	1.18
69.99	76	78.72	14.12	1.22
75	78	85.82	13.83	1.27
79.22	74	92.86	12.77	1.30

APPENDIX F. Core Flood Experiments Data.

Table 40. Data set for experiment B

TIME (min)	Pin (psia)	Pout (psia)	ΔP (psia)	Vpump reading 1	Vpump reading 2	Voil (ml)	Vbrine (ml)	Vgas (l)	% recovery
0	813	814	-1	220.03	495	0	0	0	0.00
10	1880	1503	377	215	491	0	0	0.025	0.00
20	2420	1530	890	209	486	0	2	0.025	0.00
30	2482	1519	963	205	483	0.6	11.2	0.025	1.02
40	2596	1536	1060	200	478	8.2	19	0.025	14.01
50	2500	1500	1000	196	474	15.6	22.8	0.075	26.65
60	2530	1535	995	191	470	19.8	24.6	0.075	33.82
70	2527	1500	1027	186	465	21.4	32.6	0.1	36.55
80	2530	1522	1008	182	462	22	36.8	0.1	37.58
90	2540	1512	1028	177	457	22.2	41.8	0.1	37.92
100	2560	1533	1027	171	452	22.8	52	0.125	38.95
110	2570	1525	1045	168	449	22.8	58	0.4	38.95
120	2579	1515	1064	163	445	22.8	67	0.4	38.95
130	2505	1523	982	158	440	22.8	76.2	0.4	38.95
140	2564	1538	1026	153	436	22.8	86	0.425	38.95
150	2588	1518	1070	148	432	23.2	95	0.425	39.63
160	2582	1400	1182	144	428	23.2	107.4	0.425	39.63
170	2593	1528	1065	140	424	23.4	119	0.45	39.97
180	2584	1340	1244	135	420	23.6	129	0.55	40.31
190	2590	1530	1060	130	416	23.8	140	0.55	40.65

200	2486	1529	957	124	411	23.8	149	0.6	40.65
210	2545	1500	1045	120	406	23.8	156	0.625	40.65
220	2613	1512	1101	116	403	24	164	0.7	40.99
230	2647	1467	1180	112	399	24	173	0.75	40.99
240	2665	1506	1159	107	395	24	181	0.8	40.99
250	2695	1530	1165	102	390	24	190	0.875	40.99
260	2720	1490	1230	98	387	24.2	199	0.95	41.34
270	2638	1531	1107	93	382	24.2	206.8	0.975	41.34
280	2724	1507	1217	88	378	24.2	215	1.025	41.34
290	2792	1522	1270	84	374	24.4	222.6	1.1	41.68
300	2850	1505	1345	79	369	24.4	231	1.175	41.68
310	2882	1522	1360	74	365	24.6	239	1.25	42.02
320	2895	1506	1389	69	361	24.6	248	1.325	42.02
330	2920	1502	1418	64	356	24.6	257	1.4	42.02
340	2860	1523	1337	59	352	24.6	265	1.425	42.02
350	2936	1512	1424	55	348	24.8	273.4	1.5	42.36
360	2986	1517	1469	50	344	25	280	1.575	42.70
370	3022	1537	1485	45	340	25	289	1.65	42.70
380	3042	1490	1552	41	336	25	298	1.725	42.70
390	3015	1409	1606	35	331	25.2	307	1.825	43.04
400	3016	1370	1646	32	328	25.2	314	1.875	43.04
410	3015	1500	1515	27	323	25.2	323	1.95	43.04
420	2767	1510	1257	25	317	25.2	332.4	2.05	43.04
430	3100	1533	1567	19	312	25.2	339	2.1	43.04
440	3114	1514	1600	15	308	25.2	346	2.175	43.04
450	3130	1512	1618	10	304	25.2	354.5	2.25	43.04
460	3144	1493	1651	6	300	25.2	363	2.325	43.04
473	3135	1500	1635	0	295	25.2	373	2.425	43.04

Table 41. Data set for experiment C

TIME (min)	Pin (psia)	Pout (psia)	ΔP (psia)	Vpump 1	Vpump 2	Voil (ml)	Vbrine (ml)	Vgas (l)	% recovery	PV
0	826	852	-26	266.14	507.77	0	0	0	0.00	0.00
10	1660	1490	170	261.3	503.62	0	0	0	0.00	0.11
20	2250	1545	705	255.75	498.7	0	1.8	0.025	0.00	0.24
30	2436	1538	898	251.65	495	4	2	0.05	7.07	0.33
40	2465	1540	925	247.2	491.06	6.8	3.8	0.05	12.03	0.44
50	2537	1508	1029	242.3	486.67	17.8	5	0.075	31.48	0.55
60	2640	1497	1143	238.12	482.88	19.6	10	0.125	34.66	0.65
70	2714	1498	1216	233.25	478.53	19.8	22	0.15	35.02	0.76
80	2785	1510	1275	227.64	473.54	20.6	30	0.175	36.43	0.89
90	2820	1520	1300	224.25	470.5	20.6	36	0.2	36.43	0.97
100	2856	1510	1346	219.34	466.19	20.6	46	0.325	36.43	1.08
110	2884	1514	1370	214.77	462.1	20.6	56	0.375	36.43	1.19
120	2914	1502	1412	209.61	457.57	20.6	64	0.425	36.43	1.31
130	2943	1511	1432	204.73	453.08	20.6	74	0.475	36.43	1.42
140	2964	1528	1436	201	449.8	20.6	81	0.525	36.43	1.51
150	2987	1528	1459	195.96	445.3	20.6	92	0.575	36.43	1.62
160	2757	1508	1249	193.15	442.8	20.6	99	0.625	36.43	1.69
170	2705	1497	1208	191.17	440.99	20.6	103.5	0.65	36.43	1.74
180	2685	1531	1154	189.01	439.1	20.6	107	0.675	36.43	1.78
190	2680	1502	1178	186.35	436.7	20.6	111.2	0.7	36.43	1.85
200	2688	1488	1200	184.33	434.84	20.6	115.4	0.7	36.43	1.89
215	2709	1500	1209	180.74	431.72	20.6	125.4	0.725	36.43	1.98
230	2728	1494	1234	177.3	428.71	20.6	132.4	0.725	36.43	2.06
245	2743	1497	1246	173.54	425.28	20.6	138.4	0.75	36.43	2.14
260	2723	1500	1223	170.311	422.4	20.6	144.4	0.775	36.43	2.22
275	2765	1495	1270	166.85	419.28	20.6	150.4	0.775	36.43	2.30
290	2810	1505	1305	162.93	415.81	20.6	157.4	0.8	36.43	2.39
305	2837	1535	1302	159.45	412.78	20.6	163.4	0.8	36.43	2.47
310	2847	1497	1350	156.34	409.89	20.6	169.4	0.825	36.43	2.54
325	2855	1480	1375	152.82	406.78	20.6	176.4	0.85	36.43	2.62
355	2870	1505	1365	148.06	402.53	20.6	185.6	0.875	36.43	2.73
360	2880	1498	1382	144.62	399.46	20.6	192.4	0.9	36.43	2.81
380	2890	1512	1378	142.12	397.2	20.6	197	0.925	36.43	2.87
400	2912	1520	1392	137.66	393.26	20.6	204.4	0.95	36.43	2.97
420	2932	1537	1395	132.76	388.87	20.7	212.4	0.975	36.61	3.09
440	2960	1520	1440	128.5	385.07	20.7	220.6	1	36.61	3.19
460	2985	1530	1455	123.27	380.37	20.7	229.2	1.05	36.61	3.31
470	2995	1525	1470	121.47	378.8	20.7	232.4	1.05	36.61	3.35
480	2845	1490	1355	120.21	377.66	20.7	237.4	1.075	36.61	3.38
500	2681	1518	1163	117.93	375.62	20.7	243.4	1.1	36.61	3.43

Table 42. Data set for experiment D

TIME (min)	Pin (psia)	Pout (psia)	ΔP (psia)	Vpump reading	Voil (ml)	Vbrine (ml)	Vgas (l)	% recovery	PV
0	713	713	0	507.7	0	0	0	0.00	0.00
15	2330	1505	825	494.6	0	3.6	0	0.00	0.18
30	2335	1525	810	481.85	0.6	15.4	0	1.15	0.35
45	2145	1492	653	469.71	10.4	19.2	0	19.87	0.51
60	2133	1533	600	456.81	18	22.8	0	34.39	0.69
75	2090	1490	600	444.02	19.4	35	0	37.06	0.86
90	2130	1535	595	431.63	19.4	46.6	0	37.06	1.03
105	2135	1535	600	420.31	19.4	58.8	0.025	37.06	1.18
120	2140	1535	605	407.27	19.4	70.6	0.05	37.06	1.35
135	2143	1535	608	393.95	19.4	84	0.075	37.06	1.53
150	2130	1530	600	381.22	19.4	96.8	0.1	37.06	1.71
158	2145	1532	613	366.9	19.8	112	0.1	37.83	1.90
180	2146	1535	611	356.27	19.8	124	0.1	37.83	2.04
195	2150	1535	615	344.72	19.8	133.6	0.1	37.83	2.20
210	2150	1530	620	331.99	20	146.2	0.1	38.21	2.37
225	2155	1535	620	319.17	20	159.4	0.1	38.21	2.54
240	2143	1525	618	307.01	20	171.6	0.125	38.21	2.71
255	2160	1535	625	294.57	20	184	0.125	38.21	2.87

Table 43. Data set for experiment F

TIME (min)	Pin (psia)	Pout (psia)	ΔP (psia)	Vpump 1	Vpump 2	Voil (ml)	Vbrine (ml)	Vgas (l)	% recovery	PV
0	485	478	7	263.33	504.69	0	0	0	0.00	0.00
5	870	490	380	257.64	491.8	0	0	0	0.00	0.25
10	1215	495	720	255.02	486.46	0	1.6	0	0.00	0.36
15	1435	498	937	252.7	487.4	0	3.4	0	0.00	0.38
20	1620	500	1120	250.59	485.51	0	5.2	0	0.00	0.43
25	1800	500	1300	248.15	483.33	0.6	7.4	0	1.12	0.49
30	1935	500	1435	246	481.5	0.8	10	0	1.49	0.55
35	2040	500	1540	243.42	479.11	0.8	13.6	0	1.49	0.61
40	2095	498	1597	241.25	477.17	2.8	14	0	5.21	0.67
45	2130	500	1630	238.91	475.03	6.4	14	0	11.91	0.73
50	2155	490	1665	236.55	472.97	10.4	14	0.05	19.35	0.79
55	2167	492	1675	234.02	470.71	14.8	14	0.05	27.54	0.85
60	2168	490	1678	231.95	468.97	18	14.4	0.05	33.49	0.90
65	2155	490	1665	228.94	466.18	20	18	0.05	37.21	0.98
70	2140	488	1652	226.55	464.05	20.4	22	0.05	37.96	1.04
80	2111	485	1626	222.48	460.41	20.8	29.2	0.125	38.70	1.15
90	2105	490	1615	217.77	456.2	20.8	37	0.125	38.70	1.27
100	2115	490	1625	213.3	452.2	20.8	46	0.125	38.70	1.38
110	2155	490	1665	208.3	447.75	20.8	54	0.125	38.70	1.51
120	2200	490	1710	204.95	444.87	20.8	61	0.125	38.70	1.59
140	2327	490	1837	194.67	435.5	20.8	77	0.125	38.70	1.86

150	2385	488	1897	189.77	431.2	20.8	87	0.125	38.70	1.98
170	2450	490	1960	180.5	422.95	21	110.4	0.55	39.07	2.22
190	2515	489	2026	170.62	414.11	21	129.4	0.6	39.07	2.47
210	2550	490	2060	161.6	406.11	21.4	144	0.675	39.82	2.70
230	2590	490	2100	152.67	398.08	21.6	161.4	1.15	40.19	2.93
252	2650	480	2170	141.28	387.87	21.6	177.2	1.275	40.19	3.22
270	2710	490	2220	133.37	380.8	21.6	194.2	1.4	40.19	3.42
300	1233	490	743	265.94	503.6	21.7	194.8	2.1	40.38	3.43
310	1070	482	588	264.61	502.37	21.8	197.8	2.1	40.56	3.48
320	1005	488	517	263.38	501.23	21.8	199.6	2.1	40.56	3.56
350	955	482	473	260.09	498.17	22	204.2	2.125	40.93	3.72
370	959	492	467	257.79	496.03	22	206	2.15	40.93	3.94
390	970	490	480	255.32	493.74	22	210.2	2.15	40.93	4.23
455	1076	490	586	247.76	486.7	22	220.2	2.225	40.93	4.71
525	1025	493	532	241.39	480.89	22	230.8	2.3	40.93	5.36
635	1050	495	555	231.92	472.22	22	250.2	2.4	40.93	6.25
705	1035	493	542	225.63	466.47	22	257.2	2.55	40.93	7.30
1300	816	490	326	199.4	442.55	22.4	306.2	2.75	41.68	9.04

Table 44. Data set for experiment G

Time (min)	**Pin (psia)**	**Pout (psia)**	**Vpump 1 (psia)**	**Vpump 2 (psia)**	**Voil (psia)**	**Vbrine (psia)**	**Vgas (l)**	**ΔP (psia)**	**PV**	**% Recovery**
0	10	20	266	507	0	0	0	-10	0.00	0.00
5	590	435	262.65	502	0	0	0	155	0.11	0.00
12	1120	490	259.4	499.1	0.2	0.2	0	630	0.20	0.38
20	1615	495	255.6	495.7	0.2	2.4	0	1120	0.29	0.38
25	1918	495	252.62	493.05	0.2	4.6	0	1423	0.37	0.38
30	2070	497	250.69	491.23	0.4	6	0	1573	0.42	0.76
35	2225	499	248.68	490.47	0.4	8.4	0	1726	0.46	0.76
40	2235	500	247.5	487.4	0.5	11.5	0	1735	0.51	0.94
45	2125	500	246.28	486.31	0.5	10.6	0	1625	0.54	0.94
50	2020	495	245.1	485.3	3.4	15.2	0	1525	0.57	6.42
55	1920	495	244	484.28	6.2	15.2	0	1425	0.60	11.71
60	1815	490	242.81	483.22	9.4	15.2	0	1325	0.63	17.75
70	1660	493	240.51	481.16	14.6	15.6	0.025	1167	0.69	27.58
80	1550	480	237.88	478.8	18.4	17	0.025	1070	0.76	34.75
90	1500	480	235.79	476.96	19	21	0.025	1020	0.81	35.89
100	1465	480	233.3	474.3	19.4	25.4	0.025	985	0.88	36.64
110	1445	480	231.28	472.92	19.8	29.8	0.025	965	0.93	37.40
120	1445	483	228.76	470.67	20	34	0.025	962	0.99	37.78
130	1450	480	226.53	468.68	20	38	0.025	970	1.05	37.78
140	1460	482	224.14	466.55	20	42	0.025	978	1.11	37.78
150	1475	490	221.73	464.44	20	45.6	0.025	985	1.17	37.78
160	1493	477	219.16	462.1	20.4	50	0.05	1016	1.24	38.53
170	1504	480	217.13	460.29	20.4	53.2	0.05	1024	1.29	38.53
180	1518	488	214.64	458.06	20.4	56.8	0.05	1030	1.35	38.53
190	1520	488	212.47	456.13	20.4	60	0.05	1032	1.41	38.53
200	1535	485	209.87	453.8	20.4	54	0.05	1050	1.47	38.53

225	1533	490	204.1	448.7	20.4	73	0.075	1043	1.62	38.53
240	1515	480	200.8	445.7	20.4	78.9	0.075	1035	1.71	38.53
260	1495	483	196.2	441.6	20.6	86.2	0.075	1012	1.82	38.91
285	1360	490	190.38	436.41	21	95.6	0.075	870	1.97	39.66
315	1230	480	183.33	430.11	21.2	108	0.15	750	2.15	40.04
382	1070	475	167.64	416.11	21.4	132.6	0.175	595	2.55	40.42
395	1040	485	164.65	413.41	21.4	137	0.175	555	2.63	40.42
410	1035	490	161.23	410.38	21.6	141	0.2	545	2.72	40.80
430	1015	490	156.55	406.21	21.8	147	0.225	525	2.83	41.18
455	1007	483	150.67	400.35	22.4	153	0.25	524	2.99	42.31
470	1000	485	146.95	397.65	22.6	159	0.275	515	3.08	42.69
495	999	492	141.36	392.64	23.2	165.6	0.3	507	3.22	43.82
515	1000	483	136.71	388.49	23.2	162.2	0.325	517	3.34	43.82
535	985	490	132.04	384.32	23.8	179	0.375	495	3.46	44.95
550	968	486	128.47	381.13	24	183	0.4	482	3.55	45.33
570	960	480	123.87	377.02	24.4	189.2	0.425	480	3.67	46.09
591	965	493	118.78	372.48	24.6	196	0.475	472	3.80	46.46
605	970	482	115.95	369.95	24.6	200.4	0.525	488	3.87	46.46

Table 45. Data set for experiment A (stage 1)

Time (min)	**Pin (psia)**	**Pout (psia)**	**ΔP (psia)**	**Vpump (ml)**	**Voil (ml)**	**Vbrine (ml)**	**Vgas (l)**	**% recovery**	**PV**
8	1750	1520	230	500.25	0	0.5	0	0.00	0.00
10	1830	1525	305	500	0	0.8	0	0.00	0.00
20	1830	1530	300	491	0	10.4	0.475	0.00	0.11
30	1820	1550	270	483	3.4	15.8	0.475	6.29	0.21
40	1738	1525	213	474	11.2	15.8	0.5	20.72	0.32
50	1705	1505	200	466	20	16.5	0.5	37.01	0.42
55	1705	1515	190	461	20.5	19	0.5	37.93	0.48
60	1705	1520	185	458	21.5	22	0.5	39.78	0.52
70	1697	1510	187	449	22.5	29	0.5	41.63	0.63
80	1697	1525	172	442	22.5	37	0.525	41.63	0.71
90	1685	1510	175	433	22.5	45	0.525	41.63	0.82
100	1685	1525	160	423	22.7	54.4	0.525	42.00	0.95
110	1700	1530	170	416	23	62	0.525	42.56	1.03
120	1675	1510	165	406	23	8	0.55	42.56	1.15
130	1690	1530	160	398	23	16	0.55	42.56	1.25
140	1695	1527	168	389	23.2	24	0.55	42.93	1.36
150	1700	1532	168	381	23.4	32	0.55	43.30	1.46
160	1705	1535	170	372	23.4	40	0.55	43.30	1.57
170	1690	1525	165	364	23.6	49	0.55	43.67	1.67
180	1700	1535	165	356	23.6	58	0.55	43.67	1.77
190	1700	1540	160	348	23.6	66	0.575	43.67	1.86
200	1720	1555	165	337	23.6	9	0.575	43.67	2.00
210	1700	1540	160	329	23.6	17	0.575	43.67	2.10
220	1705	1540	165	322	23.6	23	0.575	43.67	2.18
230	1711	1542	169	313	23.8	32	0.575	44.04	2.29
240	1710	1550	160	304	23.8	41.2	0.575	44.04	2.40

250	1718	1546	172	297	23.8	49	0.575	44.04	2.49
260	1690	1515	175	288	23.8	58	0.575	44.04	2.60
270	1720	1550	170	281	23.8	67	0.6	44.04	2.68
280	1712	1543	169	271	23.8	6	0.6	44.04	2.81
290	1710	1542	168	263	23.8	14	0.6	44.04	2.90
300	1715	1547	168	255	23.8	22	0.6	44.04	3.00
310	1718	1550	168	247	23.8	32	0.6	44.04	3.10
320	1720	1550	170	238	23.8	42	0.6	44.04	3.21

Table 46. Data set for experiment A (stage 2)

Time (min)	Pin (psia)	Pout (psia)	ΔP (psia)	Vpump 1 (ml)	Vpump 2 (ml)	Voil (ml)	Vbrine (ml)	Vgas (l)	% recovery	PV
10	1535	1500	35	259	499	0	0	0	0.00	0.00
12	1647	1505	142	255	495	0	1.6	0	0.00	0.10
20	1688	1530	158	254	494	0	7.5	0.3	0.00	0.12
30	1700	1529	171	250	490	0	16.2	0.3	0.00	0.22
40	1702	1505	197	245	486	0	25.2	0.3	0.00	0.33
50	1685	1508	177	240	482	0	34.8	0.3	0.00	0.44
60	1710	1517	193	235	477	0	43.8	0.3	0.00	0.56
70	1708	1514	194	231	473	0.2	52	0.325	0.66	0.66
80	1729	1540	189	227	470	0.4	60.4	0.325	1.32	0.75
90	1729	1521	208	221	465	0.4	70	0.325	1.32	0.88
100	1735	1545	190	217	462	0.5	78.4	0.325	1.65	0.97
110	1725	1520	205	213	457	0.5	89.3	0.325	1.65	1.08
120	1732	1546	186	209	454	0.5	3.6	0.4	1.65	1.16
130	1740	1531	209	205	451	0.5	11.6	0.4	1.65	1.25
140	1736	1525	211	200	446	0.6	23.6	0.4	1.98	1.37
150	1730	1515	215	195	442	0.8	36	0.4	2.65	1.48
160	1731	1541	190	191	438	0.8	45.8	0.425	2.65	1.58
170	1730	1515	215	186	434	0.8	56.8	0.45	2.65	1.69
180	1743	1539	204	182	430	0.8	66	0.475	2.65	1.79
190	1735	1525	210	177	425	1	76	0.525	3.31	1.91
200	1752	1533	219	171	421	1	85	0.55	3.31	2.03
210	1746	1523	223	168	418	1	96	0.625	3.31	2.11
213	1679	1541	138	166	416	1	0.8	0.65	3.31	2.15
220	1755	1529	226	160	411	1	10	0.675	3.31	2.29
240	1757	1535	222	157	408	1	18	0.725	3.31	2.36
230	1753	1516	237	152	403	1	27	0.8	3.31	2.48

Table 47. Data set for experiment A (stage 3)

Time (min)	Pin (psia)	Pout (psia)	ΔP (psia)	Vpump 1 (ml)	Vpump 2 (ml)	Voil (ml)	Vbrine (ml)	Vgas (l)	% recovery	PV
0	970	970	0	251	497	0	0	0	0.00	0.00
10	1659	1515	144	246	493	0	0	0	0.00	0.11
20	1721	1530	191	242	489	0	4.5	0	0.00	0.21
30	1775	1530	245	237	485	0	13.1	0.025	0.00	0.32
40	1832	1540	292	232	481	0	21.2	0.05	0.00	0.43
50	1873	1543	330	228	477	0	30	0.075	0.00	0.53

60	1905	1550	355	223	472	0	39.2	0.1	0.00	0.65
70	1930	1540	390	218	468	0	48.2	0.125	0.00	0.76
80	1935	1550	385	213	463	0.4	57	0.15	1.37	0.88
90	1944	1508	436	208	459	0.4	67	0.175	1.37	0.99
100	1945	1533	412	203	455	0.4	77.6	0.2	1.37	1.10
110	1950	1540	410	199	451	0.4	86	0.225	1.37	1.20
120	1952	1541	411	194	446	0.5	7.6	0.25	1.71	1.32
130	2000	1530	470	179	442	0.5	16	0.275	1.71	1.55
140	1997	1535	462	184	438	0.6	26	0.3	2.05	1.54
150	1996	1544	452	180	434	1	36	0.375	3.42	1.64
160	1990	1515	475	174	429	1	46	0.425	3.42	1.77
170	1940	1500	440	170	425	2	54	0.475	6.84	1.87
180	1989	1542	447	165	420	2	63	0.55	6.84	2.00
190	2000	1515	485	161	417	2	71	0.6	6.84	2.08
200	2019	1537	482	156	413	2.4	79	0.675	8.21	2.19
210	2020	1545	475	151	408	2.4	8	0.725	8.21	2.31
220	2013	1545	468	147	405	2.4	15	0.8	8.21	2.40
230	1952	1557	395	142	400	2.6	26	0.875	8.89	2.52
240	1970	1498	472	138	396	2.8	34	0.925	9.57	2.62
250	2009	1543	466	133	392	3	42	1.05	10.26	2.73
260	2000	1493	507	128	388	3.2	52	1.1	0.00	0.00
270	1970	1451	519	123	383	3.4	61.2	1.2	0.00	0.11
280	2003	1517	486	119	379	3.4	69	1.25	0.00	0.21
290	2013	1527	486	115	376	3.4	77	1.325	0.00	0.32
300	1983	1491	492	110	371	3.4	87	1.425	0.00	0.43
310	1970	1481	489	106	368	3.4	95.4	1.5	0.00	0.53
320	1990	1503	487	100	362	3.4	105.4	1.6	0.00	0.65
330	1973	1420	553	95	358	3.4	109.5	1.875	0.00	0.76
340	1986	1490	496	91	354	3.4	123.5	1.925	1.37	0.88

Table 48. Data set for experiment E (stage 1)

Time (min)	**Pin (psia)**	**Pout (psia)**	**Vpump (ml)**	**Voil (ml)**	**Vbrine (ml)**	**Vgas (l)**	**ΔP (psia)**	**% recovery**	**PV**
0	91	55	507.94	0	0	0	36	0.00	0.00
10	1025	500	500	0	3.6	0.3	525	0.00	0.11
15	1080	497	495	0	7.6	0.3	583	0.00	0.17
20	1105	500	491.05	0	11.2	0.3	605	0.00	0.23
30	1110	495	482.35	4.8	15.6	0.325	615	10.97	0.35
40	980	475	473.35	13.8	15.6	0.35	505	31.55	0.47
46	990	483	468	18	17	0.35	507	41.15	0.54
50	1010	485	465.6	19.4	18	0.35	525	44.35	0.57
60	1025	490	458.1	19.4	26	0.35	535	44.35	0.67
70	1023	490	449.05	19.4	34	0.375	533	44.35	0.79
81	1020	490	440.01	19.4	44	0.375	530	44.35	0.92
90	1020	490	432.61	19.4	51	0.375	530	44.35	1.02
100	1010	485	424.06	19.4	60	0.625	525	44.35	1.13
110	1015	490	416.13	19.4	68	0.625	525	44.35	1.24
120	1015	490	407.9	19.4	76	0.95	525	44.35	1.35

Table 49. Data set for experiment E (stage 2)

Time (min)	Pin (psia)	Pout (psia)	Vpump 1 (ml)	Vpump 2 (ml)	Voil (ml)	Vbrine (ml)	Vgas (l)	ΔP (psia)	% recovery	PV
0	45	44	265.19	506.64	0	0	0	1	0.00	0.00
5	432	405	262	504	0	0	0	27	0.00	0.08
10	777	480	260	502	0	2.2	0	297	0.00	0.13
15	900	470	258	500	0	4.4	0	430	0.00	0.19
20	977	477	255	498	0	8.2	0	500	0.00	0.25
25	1025	490	253	496	0	11.4	0	535	0.00	0.31
30	1060	485	251	494	0	15.6	0	575	0.00	0.36
35	1088	490	248	491	0	20	0	598	0.00	0.44
40	1035	90	246	489	0	26	0	945	0.00	0.50
45	950	55	244	487	0	31	0	895	0.00	0.55
50	915	475	241	485	0	35.8	0	440	0.00	0.62
60	970	490	237	481	0.8	43.4	0.025	480	3.29	0.73
70	1015	490	232	477	1	51	0.025	525	4.11	0.85
80	905	475	227	473	1.2	62	0.325	430	4.93	0.97
90	975	490	223	469	1.2	70	0.325	485	4.93	1.08
100	925	315	218	464	1.4	80	0.325	610	5.75	1.21
110	970	490	213	460	1.4	88	0.475	480	5.75	1.33
120	950	490	208	456	1.6	97	0.475	460	6.57	1.45
130	965	480	204	452	2.2	117	0.475	485	9.04	1.56
140	751	226	199	447	2.4	129	0.525	525	9.86	1.70
155	850	400	192	441	2.4	141	0.575	450	9.86	1.87
160	880	430	190	439	2.4	146	0.6	450	9.86	1.93
180	955	480	181	431	2.4	165.2	0.675	475	9.86	2.15
191	950	480	175	426	2.4	173	0.75	470	9.86	2.30
200	966	486	171	423	2.4	182.5	0.8	480	9.86	2.40
210	970	485	167	419	2.4	191	0.875	485	9.86	2.51
230	975	485	157	410	2.4	208.6	1.025	490	9.86	2.76
260	990	490	143	398	2.4	241.2	1.325	500	9.86	3.11

Table 50. Data set for experiment E (stage 3).

Time (min)	Pin (psia)	Pout (psia)	Vpump 1 (ml)	Vpump 2 (ml)	Voil (ml)	Vbrine (ml)	Vgas (l)	ΔP (psia)	% recovery	PV
0	435	355	263.47	502.1	0	0	0	80	0.00	0.08
10	690	425	258	497	0	0	0	265	0.00	0.23
15.66	843	492	256	495	0	1.8	0.075	351	0.00	0.28
30	965	495	249	489	0.4	12.6	0.175	470	1.82	0.46
40	980	475	244	485	0.6	21.4	0.275	505	2.73	0.58
60	1005	490	235	476	0.6	38.6	0.42	515	2.73	0.82
70	996	490	230	472	1	47	0.55	506	4.56	0.94
80	1010	490	225	468	1	56	0.65	520	4.56	1.06
90	1020	490	221	464	1	65	0.75	530	4.56	1.17
100	1050	495	216	460	1.2	73	0.85	555	5.47	1.29
110	1056	495	211	455	1.2	81	0.95	561	5.47	1.43
120	1060	491	207	452	1.6	90	1.05	569	7.29	1.52

130	1062	480	202	447	2.2	98	1.125	582	10.03	1.66
140	1115	490	197	443	2.2	106.6	1.275	625	10.03	1.78
150	1150	480	193	439	2.2	114	1.35	670	10.03	1.89
170	1266	485	183	430	2.4	131	1.525	781	10.94	2.14
180	1330	495	179	426	2.4	139	1.575	835	10.94	2.25
190	1420	495	174	422	2.4	147	1.65	925	10.94	2.37
200	1525	490	170	418	2.4	154	1.7	1035	10.94	2.48
210	1630	480	165	414	2.4	161.4	1.775	1150	10.94	2.60
220	1730	480	160	410	2.4	169	1.85	1250	10.94	2.72
230	1805	488	155	405	2.4	176	1.9	1317	10.94	2.86
240	1870	490	151	401	2.4	183	1.95	1380	10.94	2.96
245	1900	477	148	399	2.6	186	2	1423	11.85	3.03
250	1930	490	146	397	2.6	189.2	2.025	1440	11.85	3.09
256	1940	483	143	395	2.6	194	2.05	1457	11.85	3.15

Table 51. Data set for experiment H (stage 1).

Time (min)	Pin (psia)	Pout (psia)	Vpump (ml)	Voil (ml)	Vbrine (ml)	Vgas (l)	ΔP (psia)	PV	% Recovery
0	600	480	505.96	0	0	0	120	0.00	0.00
20	1190	488	499.48	0	5.4	0	702	0.09	0.00
40	1202	485	490.58	0.4	13.6	0	717	0.21	0.83
80	1024	481	473.28	17.4	14.2	0	543	0.44	35.92
120	1000	477	458.47	18	28	0	523	0.64	37.16
250	954	483	404.45	18.2	80	0.025	471	1.37	37.57
270	950	485	396.57	18.2	87.4	0.05	465	1.47	37.57
395	940	480	343.6	18.6	139.6	0.075	460	2.19	38.39
410	937	483	337.7	18.6	144.2	0.1	454	2.27	38.39
480	934	481	308.73	18.6	173.8	0.1	453	2.66	38.39
865	923	484	147.5	18.6	323.8	0.1	439	4.83	38.39

Table 52. Data set for experiment H (stage 2).

Time (min)	Pin (psia)	Pout (psia)	Vpump 1 (ml)	Vpump 2 (ml)	Voil (ml)	Vbrine (ml)	Vgas (l)	ΔP (psia)	PV	% recovery
0	446	443	266.35	507.93	0	0	0	3	0.00	0.00
10	595	475	262.37	507.47	0	0	0	120	0.06	0.00
15	715	475	261.13	501.35	0	1.2	0	240	0.16	0.00
25	830	484	258.99	499.44	0	4	0	346	0.21	0.00
35	885	484	256.78	497.46	0	7.6	0	401	0.27	0.00
45	910	483	254.45	494.4	0	12	0	427	0.34	0.00
55	925	480	251.97	493.17	0.4	16.2	0	445	0.39	1.34
65	937	480	249.63	491.08	0.4	20.6	0	457	0.45	1.34
75	944	480	247.27	489	0.6	24.6	0.025	464	0.51	2.01
85	951	480	244.7	486.7	0.6	29.6	0.025	471	0.58	2.01
95	965	480	242.24	484.5	0.6	34.2	0.0225	485	0.64	2.01
127	1000	480	235.03	478.04	0.6	47.6	0.025	520	0.83	2.01
150	1015	480	228.56	473.16	0.6	57.8	0.025	535	0.98	2.01
180	1045	485	222.72	467.05	0.6	70	0.05	560	1.14	2.01

265	1087	476	203.07	449.51	0.6	101	0.4	611	1.64	2.01
270	1090	485	201.61	448.21	0.6	105.8	0.4	605	1.68	2.01
457	1090	482	158.11	409.35	1	195.2	0.775	608	2.79	3.35
490	1085	485	150.39	402.49	1	199.8	0.875	600	2.99	3.35
510	1030	477	145.2	398.03	1.2	218.2	0.95	553	3.12	4.02
595	605	480	125.86	380.58	1.5	232.6	1.05	125	3.61	5.03
710	725	485	98.74	356.37	1.5	258.2	1.225	240	4.30	5.03
715	724	486	98.07	355.77	1.5	259.2	1.225	238	4.32	5.03

Table 53. Data set for experiment H (stage 3).

Time (min)	**Pin (psia)**	**Pout (psia)**	**Vpump 1 (ml)**	**Vpump 2 (ml)**	**Voil (ml)**	**Vbrine (ml)**	**Vgas (l)**	**ΔP (psia)**	**PV**	**% recovery**
0	340	340	265.95	507.98	0	0	0	0	0.00	0.00
10	460	335	261.9	501.83	0	0	0	125	0.14	0.00
60	1068	493	249.9	491.11	1.8	9.2	0.05	575	0.44	6.35
115	1056	485	237	479.6	2.4	32.4	0.225	571	0.77	8.47
120	1060	485	236.33	479	2.4	34	0.225	575	0.79	8.47
125	1063	480	234.78	477.6	2.4	37	0.25	583	0.83	8.47
190	1070	482	219.67	464.12	2.8	65	0.45	588	1.22	9.88
247	1082	483	206.43	452.3	3	88.8	0.675	599	1.55	10.58
250	1083	485	205.98	451.88	3	90.4	0.675	598	1.56	10.58
270	1090	483	201.4	447.8	3.2	100.4	0.75	607	1.68	11.29
300	1199	482	194.03	441.21	3.4	112	0.85	717	1.87	12.00
330	1120	485	186.94	434.87	3.4	124.8	0.95	635	2.06	12.00
360	1140	485	179.65	428.35	3.6	137	1	655	2.25	12.70
390	1155	485	172.45	421.95	3.6	150.8	1.275	670	2.43	12.70
410	1173	487	168.71	418.71	3.6	156.8	1.3	686	2.53	12.70
466	1180	485	155.46	406.79	3.8	179.8	1.45	695	2.87	13.41
590	1203	488	126.71	381.12	3.8	228.8	1.75	715	3.60	13.41
600	1222	485	124.46	379.11	3.8	379.11	1.775	737	3.66	13.41
690	1400	485	103.21	360.14	3.8	360.14	2.05	915	4.20	13.41

Table 54. Permeability of fresh core

Average Perm	X Samples\Increments		Leak Test Value	Minimum
99.8674598	17	0.0625	289.5616451	71.8338
Time to Complete	Y Samples\Increments		Standard Deviation	Maximum
3499.053726	9	0.0625	16.62963759	146.2811

Table 55. Permeability of soaked core

Average Perm	X Samples\Increments		Leak Test Value	Minimum
278.5614189	17	0.0625	304.9134198	149.3639

Time to Complete	Y Samples\Increments		Standard Deviation	Maximum
7551.043875	9	0.0625	168.4103574	800

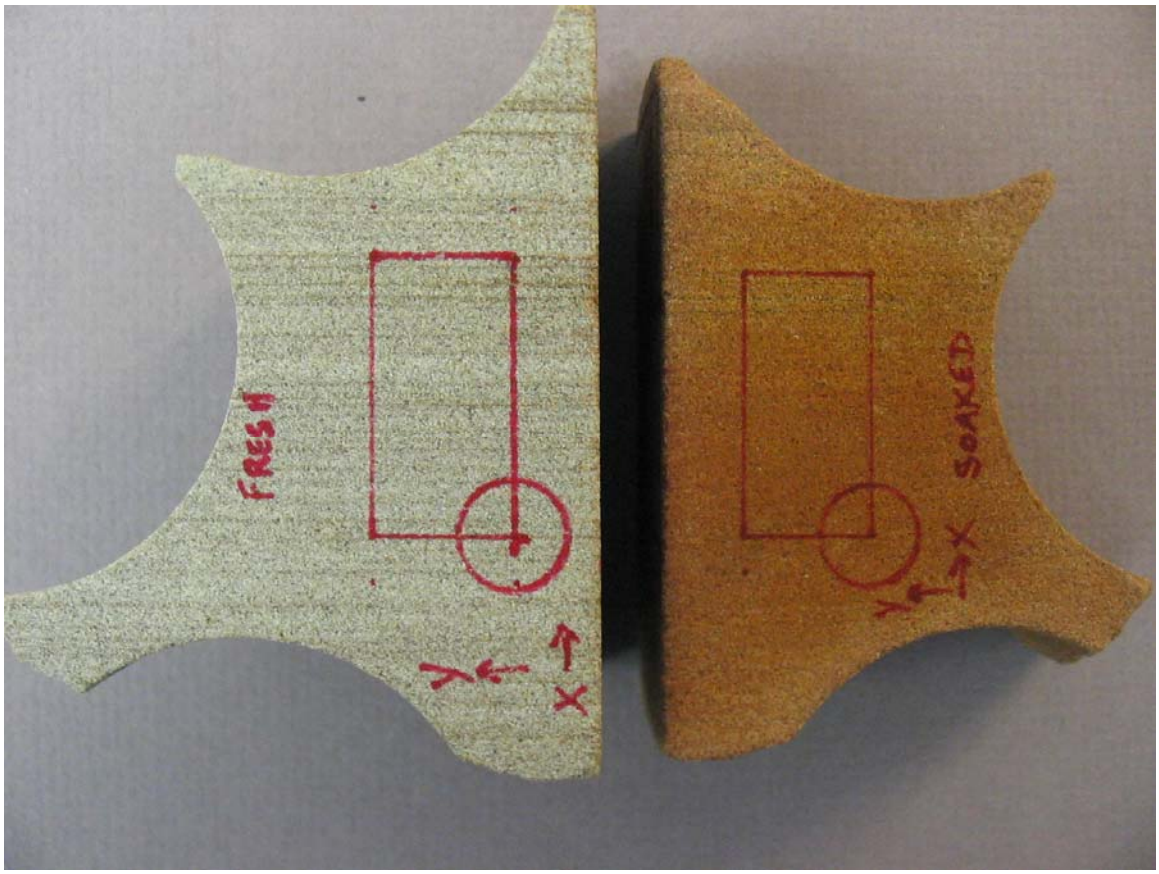

Figure 89. Core before (left) and after (right) tests.

Table 56. Core flood experiments.

Experiment	Displaced Fluid	Displacing Fluid 1	Displacing Fluid 2	Flow rate 1 (ml/hr)	Flow rate 2 (ml/hr)	Pressure (psi)	Excess material and volume (ml)	Recovery (%)
A-1	Oil	Brine	N/A	50	N/A	1500	N/A	44.04%
A-2	Oil	Na2CO3	HCl	28	25	1500	GY - 0.23 ml	3.31%
A-3	Oil	Na2CO3	HCl + Cat. Surfactant	28	25	1500	GY - 0.23 ml	11.63%
B	Oil	Na2CO3	HCl	28	25	1500	GY - 0.23 ml	43.05%
C	Oil	Na2CO3	HCl + Cat. Surfactant	28	25	1500	GY - 0.23 ml	36.61%
D	Oil	Brine	N/A	50	N/A	1500	N/A	38.21%
E-1	Oil	Brine	N/A	50	N/A	500	N/A	44.35%
E-2	Oil	Na2CO3	HCl	28	25	500	GY - 0.23 ml	9.86%
E-3	Oil	Na2CO3	HCl + Cat. Surfactant	28	25	500	GY - 0.23 ml	11.85%
F	Oil	Na2CO3	HCl	28	25	500	GY - 0.23 ml	41.68%
G	Oil	Na2CO3	HCl + Cat. Surfactant	28	25	500	GY - 0.23 ml	46.46%
H-1	Oil	Brine	N/A	25	N/A	500	N/A	38.40%
H-2	Oil	Na2CO3	HCl	14	12.5	500	GF - 0.52 ml	5.03%
H-3	Oil	Na2CO3	HCl + Cat. Surfactant	14	12.5	500	GF - 0.83 ml	13.41%